



University  
of Glasgow

Mustapa, Marami binti (2018) *Calretinin-expressing interneurons in the mouse spinal cord*. PhD thesis.

<https://theses.gla.ac.uk/41204/>

Copyright and moral rights for this work are retained by the author

A copy can be downloaded for personal non-commercial research or study, without prior permission or charge

This work cannot be reproduced or quoted extensively from without first obtaining permission in writing from the author

The content must not be changed in any way or sold commercially in any format or medium without the formal permission of the author

When referring to this work, full bibliographic details including the author, title, awarding institution and date of the thesis must be given

Enlighten: Theses

<https://theses.gla.ac.uk/>  
[research-enlighten@glasgow.ac.uk](mailto:research-enlighten@glasgow.ac.uk)

# **Calretinin-expressing interneurons in the mouse spinal cord**

Marami binti Mustapa

MSc Human Anatomy (University of Dundee)

MBBS (University of Malaya)

November 2018

Submitted in fulfilment of the requirements for the Degree of Doctor of  
Philosophy

Institute of Neuroscience and Psychology

College of Medical, Veterinary and Life Sciences

University of Glasgow

## Summary

Skin and organs in the body are innervated by primary afferents that respond to both noxious and non-noxious stimuli. The sensory information from the surrounding structures is transmitted into the dorsal horn by these afferents following their sensory modality and the region of the body that they innervate. The information is interpreted by neuronal circuits involving excitatory and inhibitory interneurons that lie in the dorsal horn of the spinal cord.

This current study involves characterisation of a specific population of inhibitory neurons that are presumably involved in presynaptic inhibition towards central terminal of non-peptidergic C fibres that terminate in a complex known as synaptic glomeruli (type I) in the middle of lamina II of the dorsal horn. The inhibition is formed through axoaxonic synapses on the central axons of these primary afferent fibres. A preliminary work carried out by Dr David I Hughes using CR::eGFP mouse line found that calcium binding protein, calretinin (CR) is expressed mostly by excitatory interneurons and a small percentage by inhibitory interneurons. Electron microscopic study was performed in these animals and he found that axonal boutons originated from dorsal horn calretinin cells were presynaptic to the central axon of type I glomeruli, which belong to C<sup>MrgD</sup> afferents. He also found that these cells have islet morphology which suggested that they are inhibitory cells.

The main objective of the project was to characterize a population of inhibitory CR interneurons in the superficial dorsal horn (SDH) and their synaptic connection with C<sup>MrgD</sup> primary afferent fibres. To achieve this several transgenic mouse lines that labelled inhibitory interneurons in the dorsal horn were used including lines in which Nociceptin and RorB transgenes were either expressed under the control of the regulatory elements of the Nociceptin gene or knocked into the RorB locus, respectively. Using Nociceptin::eGFP mice it was found that 93% of the cells that expressed eGFP were positive for Pax2 thus showed that these animals labelled inhibitory interneurons in the dorsal horn. In this mouse lines it was found that inhibitory CR cells in lamina II formed a band of dendrites and axons that perfectly overlapped with non-peptidergic C fibres plexus that were labelled with Isolectin B4 (IB4). The great majority of inhibitory interneurons (78%) in the SDH of Nociceptin::eGFP mice were immunoreactive

for eGFP. Based on this result, Nociceptin::eGFP mice were then crossed with CR<sup>Cre</sup> and Ai9 mice to allow reconstructions of individual neurons. It was found that inhibitory CR interneurons resemble islet cells and had dendrites projecting extensively in the rostrocaudal axis with a limited dorsoventral extent that arborized within lamina II. Due to a few limitations with Nociceptin::eGFP mice, this project was then continued with a knock-in mouse line, RorB<sup>eGFP</sup> mouse that also labelled inhibitory interneurons in the dorsal horn. It was found that more of lamina II inhibitory CR-immunoreactive cells were labelled in RorB<sup>eGFP</sup> mouse line than the Nociceptin::eGFP mouse, thus showed that RorB<sup>eGFP</sup> mice appeared to be a better choice for investigating the inhibitory CR cells than Nociceptin::eGFP mice.

In this study it was found that inhibitory CR cells do not co-express other neurochemical markers of the inhibitory interneurons such as galanin, nNOS, NPY and PV. This showed that CR represent another neurochemically distinct group of inhibitory interneurons in the dorsal horn. To investigate the synaptic connection between CR islet cells with C<sup>MrgD</sup> afferents, the third part of the study was carried out using the RorB<sup>CreERT2</sup> mouse line with tamoxifen induction. In this study, it was found that intraperitoneal injection of tamoxifen in early stage of postnatal life resulted in more labelling of cells, meanwhile less cells were labelled if tamoxifen were given at the later stage of postnatal life. Surprisingly, under optimal conditions, only a quarter of the inhibitory CR cells in lamina II were immunoreactive for tdTomato. However, the majority of tdTomato cells in the SDH are inhibitory interneurons and immunoreactive for CR, thus showed that this mouse line was highly selective for inhibitory CR cells. Using this mouse line, it was found that most of C<sup>MrgD</sup> afferents central terminals were in contact with axonal boutons of inhibitory CR cells and the excitatory synapses on the dendritic trees of inhibitory CR cells were derived from C<sup>MrgD</sup> afferents. About 40% of the inhibitory CR axonal boutons are in contact with non-peptidergic C-nociceptors and electron microscopic revealed that the axons belonged to the inhibitory CR cells formed axoaxonic synapses with C<sup>MrgD</sup> afferents. A few studies claimed there is a loss of these cells after peripheral nerve injury. However, in this study there were no loss of cells seen following sciatic nerve transection with no alteration on the rostrocaudal and dorsoventral extent of inhibitory CR cells in the affected area on RorB<sup>CreERT2</sup>; Ai9 mice.

The results from this study suggest that a subset of lamina II inhibitory interneurons that express CR form axoaxonic synapses on the central boutons of type I synaptic glomeruli which belong to C<sup>MrgD</sup> afferents and they also receive excitatory inputs from these primary afferents. As a conclusion, results from this study are in parallel with the recommendation that different neurochemical populations of inhibitory neurons have distinct functional roles and also emphasize the important of presynaptic inhibition on central terminals of C<sup>MrgD</sup> primary afferents in maintaining normal somatosensation.

## Acknowledgement

بِسْمِ اللَّهِ الرَّحْمَنِ الرَّحِيمِ

*In the name of God, the Most Compassionate, Most Merciful.*

I would like to express my gratitude to God for sending me the best supervisor that anyone can have, Professor Andrew Todd for his endless encouragement and support. He is indeed a very hardworking person that I have ever meet in my life, and because of this, he inspired me to always learn and do well. Thank you, Professor Andrew, for this great opportunity to be able to do PhD project under your supervision. I would also like to thank Dr David Hughes, my second supervisor for his assistance and constant advice throughout the time I am here.

This work would not be completed without Drs Allen Dickie and Noboru Iwagaki great contribution for carried out the whole-cell patch-clamp recordings. I would like to thank Mrs Christine Watt and Mr Robert Kerr for their superb technical support. I am grateful to all members of the Spinal Cord Group whom I have had the pleasure to work during this project. Each of you has given of your time, energy and expertise: Dr Erika Polgár, Dr John Riddell, Dr Maria Gutierrez-Mecinas, Dr Robert Ganley, Dr Kieran Boyle, Dr Patricia del-Rio, Dr Andrew Bell and Olivia Davis. To Dr Anne Bannatyne and Dr Nur Aishah binti Che Roos, thank you for your supportive words throughout my time in Glasgow.

Nobody has been more important to me in the pursuit of this project than the members of my family. To my parents, thank you for your positive words and encouragement throughout my life. To my caring and beloved husband, Wan Khairul Akmal, no words can describe the sacrifices you have made for your children and me, only God can pay you back. To my beautiful children, Muizzuddin and Nusaibah, thank you for being there with me...you are the love of my life!

I would also like to thank all my friends for listening, offering me advice and encouraging me to strive towards my goal. Finally, a special thanks to the Ministry of Higher Education Malaysia for providing the funds and support for this study.

## **Author's Declaration**

I declare that the work presented in the thesis is my own work, except where explicit reference is made to the contribution of others. Drs Allen Dickie and Noboru Iwagaki performed the whole-cell patch-clamp recordings, and Dr David Hughes performed the sciatic nerve transection. This thesis has not been submitted in any previous application for any other degree in the University of Glasgow or any other institution.

Marami binti Mustapa

November 2018

## List of Abbreviations

AAV	adeno-associated virus
AMHs	A-fibre mechano-heat-sensitive
CCI	chronic constriction injury
CGRP	calcitonin gene related peptide
CMHs	C-fibre mechano-heat-sensitive
CR	calretinin
Cre	cre-recombinase
CTb	cholera toxin B subunit
DAB	3,3' diaminobenzidine
DH	dorsal horn
DRG	dorsal root ganglia
DV	dorsoventral
eGFP	enhanced green fluorescence protein
EM	electron microscope or electron microscopy
GABA	gamma-aminobutyric acid
Gal	galanin
GFP	green fluorescent protein
HRP	horseradish peroxidase

IB4	<i>Bandeiraea simplicifolia</i> isolectin IB4
LTMR	low threshold mechanoreceptor
LTP	long term potentiation
MrgprD	mas-related G protein coupled receptor D
NK1r	neurokinin-1 receptor
nNOS	neuronal nitric acid synthase
NPY	neuropeptide Y
PB	phosphate buffer
PBS	phosphate-buffered saline
PV	parvalbumin
RC	rostrocaudal
SDH	superficial dorsal horn
SNI	spared nerve injury
SNT	sciatic nerve transection
sst <sub>2A</sub>	somatostatin receptor 2 <sub>A</sub>
TRPM8	transient receptor potential receptor melastatin 8
TRPV1	transient receptor potential receptor vanilloid 1
VGAT	vesicular GABA transporter
VGLUT3	vesicular glutamate transporter 3

# Table of Contents

<b>1</b>	<b>Introduction</b>	<b>1</b>
1.1	Spinal cord .....	2
1.1.1	Anatomy of the spinal cord	2
1.1.2	Spinal grey matter organization	2
1.2	Primary afferent fibres .....	5
1.2.1	Myelinated nociceptors	7
1.2.2	Unmyelinated nociceptors	8
1.2.3	Low threshold mechanoreceptors	10
1.2.4	Neurochemical properties and receptors of primary afferents	12
1.2.5	Synaptic glomeruli	15
1.2.5.1	Type I and type II glomeruli	16
1.3	Projection neurons.....	20
1.4	Excitatory and inhibitory interneurons of the dorsal horn .....	28
1.4.1	Interneuron classification	30
1.4.1.1	Morphology	30
1.4.1.2	Firing pattern	37
1.4.1.3	Neurochemical markers	37
1.5	Aims of the project .....	49
<b>2</b>	<b>General Methods</b>	<b>51</b>
2.1	Transgenic mouse lines and crosses .....	52
2.3	Perfusion fixation .....	56
2.3	Tissue processing and immunocytochemistry .....	56
2.4	Antibody characterization .....	57
2.5	Confocal microscopy and analysis .....	58
2.6	Statistical analysis .....	58
<b>3</b>	<b>Morphological features of CR islet cells within dorsal horn</b>	<b>60</b>
3.1	Introduction.....	61
3.2	Materials and methods .....	63
3.2.1	Morphology and analysis of recorded neurons	63
3.2.2	Animals and tissue processing for other anatomical parts of the study	65
3.2.3	CR and eGFP expression in Nociceptin::eGFP mouse	65
3.2.4	Distribution of inhibitory CR interneurons in laminae I-III of Nociceptin::eGFP and RorB <sup>eGFP</sup> mice	66
3.3	Results .....	67
3.3.1	Morphology of the cells in the Nociceptin::eGFP; CR <sup>Cre</sup> ; Ai9 mice	67
3.3.2	The proportion of dorsal horns neurons that are labelled with CR <sup>+</sup> /eGFP <sup>+</sup> in Nociceptin::eGFP mice	74
3.3.3	Quantitative analysis of inhibitory CR <sup>+</sup> /eGFP <sup>+</sup> cells in Nociceptin::eGFP and RorB <sup>eGFP</sup> mice	79
3.4	Discussion .....	85

3.4.1	Morphological features of recorded cells	85
3.4.2	CR <sup>+</sup> /eGFP <sup>+</sup> cells in Nociceptin::eGFP mice	86
3.4.3	Comparison between Nociceptin::eGFP and RorB <sup>eGFP</sup> mouse lines	89
<b>4</b>	<b>Expression of neurochemical markers of inhibitory interneuron populations in CR<sup>+</sup>/eGFP<sup>+</sup> cells in Nociceptin::eGFP and RorB<sup>eGFP</sup> mice</b>	<b>91</b>
4.1	Introduction.....	92
4.2	Materials and method .....	93
4.2.1	Animals and tissue processing	93
4.2.2	Expression of 4 distinct inhibitory markers and sst <sub>2A</sub> in CR <sup>+</sup> /eGFP <sup>+</sup> in Nociceptin::eGFP mice	93
4.2.3	Assessment of co-localisation of the 4 distinct inhibitory markers in CR <sup>+</sup> /eGFP <sup>+</sup> in RorB <sup>eGFP</sup> mice	94
4.3	Results .....	95
4.3.1	Expression of galanin, nNOS, NPY, PV and sst <sub>2A</sub> among CR <sup>+</sup> /eGFP <sup>+</sup> cells in Nociceptin::eGFP mice	95
4.3.2	Neurochemical markers in RorB <sup>eGFP</sup> and their expression by CR <sup>+</sup> /eGFP <sup>+</sup> and CR <sup>-</sup> /eGFP <sup>+</sup> cells	105
4.4	Discussion .....	108
4.4.1	Expression of neurochemical markers for inhibitory neurons in CR <sup>+</sup> /eGFP <sup>+</sup> cells in Nociceptin::eGFP and RorB <sup>eGFP</sup>	108
4.4.2	Expression of the sst <sub>2A</sub> receptor in CR <sup>+</sup> /eGFP <sup>+</sup> neurons in Nociceptin::eGFP mice	110
4.4.3	Association of other inhibitory neurochemical markers with CR <sup>-</sup> /eGFP <sup>+</sup> cells in RorB <sup>eGFP</sup> mice	112
<b>5</b>	<b>Synaptic connections between tdTomato<sup>+</sup> cells in RorB<sup>CreERT2</sup>; Ai9 and RorB<sup>CreERT2</sup>; Ai34 mice and non-peptidergic C-fibres</b>	<b>113</b>
5.1	Introduction.....	114
5.2	Materials and methods .....	116
5.2.1	Tamoxifen optimization in RorB <sup>CreERT2</sup> ; Ai9	116
5.2.2	Animals and tissue processing for confocal microscopy	117
5.2.2.1	Proportion of tdTomato cells that are CR- and Pax2-immunoreactive in the RorB <sup>CreERT2</sup> ; Ai9 mouse	118
5.2.2.2	Contacts between IB4-binding primary afferents and tdTomato-axonal boutons in RorB <sup>CreERT2</sup> ; Ai34 mice	118
5.2.2.3	Contacts between non-peptidergic primary afferents and tdTomato-positive axons and dendrites in RorB <sup>CreERT2</sup> ; Ai9 mice	119
5.2.3	Animals and tissue processing for electron microscopy	120
5.3	Results .....	123
5.3.1	Effects on tamoxifen dosage on tdTomato expression in RorB <sup>CreERT2</sup> ; Ai9 mice	123
5.3.2	Inhibitory CR cells in RorB <sup>CreERT2</sup> ; Ai9 mice	123
5.3.3	Contacts between IB4-labelled primary afferents and RorB axonal boutons in RorB <sup>CreERT2</sup> ; Ai34 mice	127
5.3.4	Contacts between non-peptidergic C-nociceptors and tdTomato cells in RorB <sup>CreERT2</sup> ; Ai9 mice	130
5.3.4	Electron microscopy findings	136
5.4	Discussion .....	140

5.4.1 Tamoxifen-induced tdTomato in RorB <sup>CreERT2</sup> ; Ai9 mice	140
5.4.2 The RorB <sup>CreERT2</sup> mouse line	143
5.4.3 Contacts between tdTomato-axonal boutons and non-peptidergic C-nociceptors in RorB <sup>CreERT2</sup> ; Ai9 and RorB <sup>CreERT2</sup> ; Ai34 mice	145
5.4.4 Discovery from EM study	148
<b>6 The effect of sciatic nerve transection on inhibitory CR islet cells in RorB<sup>CreERT2</sup>; Ai9 mice</b>	<b>151</b>
6.1 Introduction.....	152
6.2 Materials and methods .....	157
6.2.1 Animals and operative procedures	157
6.2.2 Tissue processing of RorB <sup>CreERT2</sup> ; Ai9 mice	157
6.2.3 The number of inhibitory CR <sup>+</sup> /tdTomato <sup>+</sup> cells on the injured and intact side of the spinal cords	158
6.2.4 Proportion of inhibitory CR <sup>+</sup> cells among all neurons in lamina II	164
6.2.5 Morphology of CR <sup>+</sup> /tdTomato <sup>+</sup> cells after SNT	165
6.3 Results .....	166
6.3.1 Quantitative analysis of the inhibitory CR <sup>+</sup> /tdTomato <sup>+</sup> cells following SNT	166
6.3.2 Quantitative analysis of the inhibitory CR cells following SNT	167
6.3.3 Morphological analysis of CR <sup>+</sup> /tdTomato <sup>+</sup> cells	168
6.4 Discussion .....	175
6.4.1 No loss of cells after PNI	175
6.4.2 No change in the morphology of the cells	177
<b>7 Concluding remarks</b>	<b>179</b>
<b>8 References</b>	<b>187</b>
<b>9 Publication</b>	<b>223</b>

## List of Figures

Figure 1-1 Rexed's laminae and the termination of primary afferents in different laminae of the spinal cord. ....	19
Figure 1-2 Anterior and lateral spinothalamic tract (Anterolateral system) ....	25
Figure 1-3 Dorsal column-medial lemniscus pathway (DCML).....	27
Figure 1-4 Four main morphological classes of interneurons in lamina II of dorsal spinal cord .....	36
Figure 3-1 Morphology of the CR <sup>+</sup> /eGFP <sup>+</sup> recorded cells in Nociceptin::eGFP;CR <sup>Cre</sup> ;Ai9 mice .....	70
Figure 3-2 Neurobiotin filled cell from Nociceptin::eGFP;CR <sup>Cre</sup> ;Ai9 mouse.....	72
Figure 3-3 CR and Noc::eGFP cells immunostaining in the dorsal horn .....	76
Figure 3-4 Lamina II CR-Noc::eGFP cells form a tight band in the middle of lamina II .....	78
Figure 3-5 CR and RorB <sup>eGFP</sup> cells immunostaining in the dorsal horn.....	84
Figure 4-1 Lack of co-localisation of CR-Noc::eGFP, nNOS and galanin in laminae I-III.....	99
Figure 4-2 Lack of co-localisation of CR-Noc::eGFP, NPY and PV in laminae I-III. ....	101
Figure 4-3 CR-Noc::eGFP and sst2A in the superficial dorsal horn .....	104
Figure 5-1 Tissue processing for Electron microscopy .....	122
Figure 5-2 tdTomato, CR and Pax2 immunostaining from the dorsal horn of RorB <sup>CreERT2</sup> ; Ai9 that have the high numbers of tdTomato cells labelling ...	126
Figure 5-3 IB4-labelled central terminals contacting tdTomato axonal boutons	129
Figure 5-4 IB4 labelled primary afferents synaptic inputs to RorB cells.....	133
Figure 5-5 Axoaxonic contacts formed by RorB cells.....	135
Figure 5-6 Electron microscopic images of axoaxonic synapse on central bouton of type I glomeruli from tamoxifen treated RorB <sup>CreERT2</sup> ; Ai9 mice .....	139
Figure 6-1 Transverse section of RorB <sup>CreERT2</sup> ; Ai9 mice that had undergone SNT on the left side.....	161
Figure 6-2 The effect of sciatic nerve transection on the SDH neurons in RorB <sup>CreERT2</sup> ; Ai9 mice .....	163
Figure 6-3 A typical islet cell morphology of RorB cell found in the middle of lamina II on the side ipsilateral to the nerve injury .....	174
Figure 7-1 Neuronal circuits in the dorsal horn of the spinal cord. ....	186

## List of Tables

Table 2-1 Summary of the different mouse lines and crosses used in various chapter of this study .....	55
Table 2-2 Primary antibodies used in this study .....	59
Table 3-1 Dendritic dimensions of reconstructed eGFP <sup>+</sup> /tdTomato <sup>+</sup> .....	73
Table 3-2 Percentages of neurons in laminae I-III that were CR <sup>+</sup> /eGFP <sup>+</sup> in Noc:: <sup>+</sup> eGFP mice .....	81
Table 3-3 The numbers of neurons that were eGFP, Pax2- and/or CR- immunoreactive in Nociceptin:: <sup>+</sup> eGFP and RorB <sup>eGFP</sup> mice .....	82
Table 4-1 Expression of other neurochemical markers with CR and eGFP in Nociceptin:: <sup>+</sup> eGFP mice .....	102
Table 4-2 Colocalization of neurochemical markers with CR and eGFP in RorB <sup>eGFP</sup> mice .....	107
Table 6-1 Number of tdTomato cells counted on the side ipsilateral and contralateral to the nerve injury .....	170
Table 6-2 Numbers of NeuN, Pax2 and inhibitory CR <sup>+</sup> cells in laminae I- II on the side ipsilateral and contralateral to the nerve injury .....	171
Table 6-3 CR <sup>+</sup> /tdTomato <sup>+</sup> cells dendritic dimensions on the side ipsilateral and contralateral to the nerve injury .....	172

# 1 Introduction

## **1.1 Spinal cord**

### **1.1.1 Anatomy of the spinal cord**

The spinal cord is part of the central nervous system and contained within the vertebral canal. It extends from the base of the skull to the level of the first lumbar vertebra in human and third lumbar vertebra in the rat. The spinal cord is enlarged in cervical and lumbar regions, which corresponds to increased innervation of upper and lower extremities respectively. The spinal cord is protected by surrounding vertebral column and meninges. The meninges also protect the brain, and are composed of dura, arachnoid and pia mater. In the human, there are 31 spinal nerves that emerge from both side of the spinal cord and are divided into 8 cervical, 12 thoracic, 5 lumbar and 1 coccygeal nerve on each side. In the rat, the spinal cord comprises 34 pairs of spinal nerves: 8 cervical, 13 thoracic, 6 lumbar, 4 sacral and 3 coccygeal. The lumbar and sacral nerves extend as long roots called the cauda equina.

The internal structure of spinal cord comprises surrounding white matter and inner grey matter. The grey matter contains nerve cell bodies and glial cells. On transverse section, it appears H-shaped. The butterfly or H-shaped grey matter is further divided into a smaller dorsal and larger ventral horn. The neurons of the dorsal horns receive sensory information through 'pseudounipolar' neurons situated in dorsal root ganglia (DRG) that enters the spinal cord via the dorsal roots of the spinal nerves. The ventral horns contain cell bodies of motor neurons that send axons via the ventral roots of the spinal nerves to terminate on striated muscles.

### **1.1.2 Spinal grey matter organization**

Estimation using a stereological method, found about 4 million neurons in the spinal grey matter of the mouse (Bjugn, 1993). The highest number of neurons was found in the thoracic region, followed by cervical and lumbar region and the least is in sacro-coccygeal region with 1.4 million, 1.2 million, 0.9 million and 0.4 million neurons respectively. These numbers showed that we need a proper classification or organization of the grey matter to enhance our understanding on the functions of the cells that are present in the grey matter of the spinal

cord. Usually, the grey matter of the spinal cord is classified into a dorsal horn, intermediolateral horn, ventral horn and intermediate zone (Afifi and Bergman, 1986) before a laminar scheme was introduced by Bror Rexed in the 1950s. Since then, the Rexed laminae are widely used by many neuroanatomists to describe the organization of the grey matter.

A study by Rexed (1952) proposed that the spinal grey matter can be divided into 10 laminae (layers) which were first identified in transverse sections of the spinal cord of the cat. Later, this classification was extended to other species such as human, monkey, dog, mouse and rat (Liu and Chambers, 1964, Buxton and Goodman, 1967, Sidman et al., 1971, Molander et al., 1989, Schoenen and Faull, 2004). However, only studies involving rodent and human have a complete description of the cytoarchitectural organization of the grey matter (Schoenen and Faull, 2004, Sidman et al., 1971). The Rexed laminae were divided based on neuronal size, shape, cytological features and density. The laminae were arranged in the dorso-ventral axis (laminae I-IX) with lamina X (substantia grisea centralis) being located around the central canal. The dorsal horn consists of laminae I-VI, lamina VII is the intermediate grey matter and laminae VIII-IX are part of the ventral horn. In each lamina, the neurons within have distinct functions, dendritic shape, chemoarchitecture and connection arrangements (Rexed, 1952). According to Rexed (1952), the basic principles of the layering of the grey matter are comparable across species. Below is a description of each lamina of the spinal grey matter based on finding in various species (Rexed, 1952, Schoenen and Faull, 2004, Sengul and Watson, 2012).

The thinnest layer lamina I, also known as the marginal layer is located at the most dorsal region of Rexed's laminae, and curves around the lateral edge of the dorsal horn. It appeared reticulated due to the penetration of several small and large nerve fibres. It consists of neurons of variable sizes and is loosely organized. Large elongated and smaller triangular, multipolar and fusiform neurons have been identified. The boundary between lamina I and the white matter is less visible due to penetration of small and large nerve fibres. Lamina I cells include excitatory and inhibitory interneurons. Projection neurons constitute 5% of all the cells in this region (Todd et al., 2002, Spike et al., 2003).

Lamina II is also known as substantia gelatinosa of Rolandi because it looks more gelatinous than the rest of grey matter, due to the lack of myelinated fibres. Lamina II can be subdivided into outer (dorsal) lamina II<sub>o</sub> and inner (ventral) lamina II<sub>i</sub> based on the density and distribution of cells. The lamina II cells are generally small. It is closely packed apart from the medial side, where it is broken up by the crossing of many large fibres from dorsal funiculus. The outer lamina II has more closely packed cells, whereas lamina II inner has a lighter appearance due to fewer cells. Lamina II contains large numbers of excitatory and inhibitory interneurons. Among these interneurons, the excitatory stalked (vertical) cells and inhibitory islet cells are commonly found in lamina II (Gobel, 1975, Gobel, 1978). These will be discussed in detail below. Laminae I-II, also known as the superficial dorsal horn (SDH), is a major termination site for A $\delta$  and C fibres (Light and Perl, 1979, Zylka et al., 2005).

Lamina III lies parallel to laminae I-II, broader than the first two laminae with lighter appearance because the neurons are less densely packed than in lamina II. However, the cells in lamina III are larger with a wider distribution of cell sizes. Myelinated afferent fibres are more numerous here than lamina II. Apart from that, projection neurons are also frequently found here (Burstein et al., 1990). Lamina III and IV are collectively known as nucleus proprius.

Lamina IV is larger than laminae I-III, extends straight across the dorsal horn with the same thickness without a ventral bend. It consists of loosely packed cells with various sizes. A distinct characteristic of lamina IV is the presence of large and small cells side by side.

Lamina V is the widest layer and extends across the narrowest part of the dorsal horn. It has a reticulated appearance laterally due to many longitudinally running fibre bundles. It is divided into lateral and medial part by the presence of thick bundles of nerve fibres on the lateral side. The neurons in lamina V vary in shape and size.

Lamina VI forms the base of the dorsal horn. It has a straight dorsal border and a convex ventral border with the broadest part lying near the medial side. Similar to lamina V, lamina VI too can be divided into lateral and medial zone. The cells in the medial part are smaller and tightly packed than the cells in lateral zone

part. Lamina III-VI consist of interneurons and projection neurons and serve as the termination sites for large myelinated A $\beta$  and small myelinated A $\delta$  primary afferent fibres (Light and Perl, 1979, Woodbury et al., 2008). The deeper lamina cells also consist of excitatory and inhibitory interneurons that use glutamate and GABA/glycine as neurotransmitters, respectively (Todd and Sullivan, 1990).

The intermediate zone of spinal grey is formed by lamina VII. The shapes of the cells vary, including multipolar, triangular and fusiform and these are evenly distributed, thus giving the lamina a homogeneous appearance. It has a concave dorsal border and medially it has an unclear border with area X. Ventrally, lamina VII is adjacent to lamina VIII and motor nuclei of lamina IX on the medial and lateral side, respectively. Lamina VIII is confined to the medial side of the ventral horn and consists of small and large cells. Both laminae VII and VIII do not contain any motor neurons. Meanwhile lamina IX is in the ventral horn and several motor nuclei that innervate skeletal muscle lie within the area. The largest nerve cells across all laminae can be found in lamina IX. Lamina X is the grey matter surrounding the central canal and consists of small interneurons.

## 1.2 Primary afferent fibres

The primary somatosensory afferent axons transmit information from the peripheral tissue to the dorsal horn of the spinal cord. These fibres respond to various types of stimuli such as noxious, thermal, itch and innocuous tactile, received by the peripheral terminals. The primary afferents encode stimuli into electrical signals and transmit those signals to the central nervous system. Primary afferents are pseudo-unipolar neurons with their somata located in the trigeminal ganglion and dorsal root ganglia (DRG). The axons of these afferent fibres have a peripheral process that innervates the skin, muscles, joint capsules or viscera and contain receptors specialized for each type of innocuous or noxious stimulus. The central branches terminate in the spinal cord or trigeminal nuclei by making axodendritic and axosomatic synapses with second order neurons, before this information is transmitted to higher centres in the brain. Most primary afferents axons enter the dorsal horn near their level of origin with a few fibres ascending or descending one or two spinal segments before they penetrate the dorsal horn (Traub et al., 1986). Primary afferent fibres terminate in the dorsal horn depending on their sensory modalities (Figure 1-1), with

nociceptive and thermoreceptive A $\delta$  and C fibres terminating in the superficial laminae of the dorsal horn, while A $\delta$  and AB mechanoreceptors innervate the deeper part of the dorsal horn (Todd, 2010). Non-nociceptive C fibres such as transient receptor potential receptor melastatin 8 (TRPM8) expressing C-thermoreceptors were found to terminate in lamina I (Dhaka et al., 2008). In addition, C-LTMR (low threshold mechanoreceptor), which express vesicular glutamate transporter 3 (VGLUT3), terminate in lamina III of the dorsal horn of the spinal cord (Seal et al., 2009).

According to anatomical and functional criteria, primary afferents can be categorized into AB, A $\delta$  and C fibres depending on their cell body sizes, axon diameter, degree of myelination and axonal conduction velocities. It is known that, the larger the diameter of primary afferent fibres and the thicker the myelin sheath, the faster the conduction speed. For example, myelinated AB and A $\delta$  fibres have medium and large soma sizes with conduction velocities of 35-75 m/s and 5-30 m/s respectively. Meanwhile, unmyelinated C fibres are the smallest and slowest, with conduction velocities of 0.5-2 m/s. In addition, muscle afferents fibres can be divided into group IV, III, II and I fibres based on their conduction velocity.

Some of the subset of thinly myelinated A $\delta$  and slow conducting unmyelinated C fibres such as A $\delta$ -LTMRs (also known as D-hair afferents) and C-LTMRs exhibit thresholds below the nociceptive range. However, most of these primary afferent fibres are nociceptors and thermoreceptors, and based on their response to noxious mechanical, thermal or chemical stimuli, many are considered to be polymodal nociceptors (Abraira and Ginty, 2013). The nociceptors are a specialized primary afferent nerve fibre type that respond to intense (noxious) stimuli, thus providing protection from potential injury by conveying information to the central nervous system on the location and intensity of noxious stimuli. They are not activated by innocuous stimuli such as warming or touch (Burgess and Perl, 1967). Nociceptors comprise both myelinated A-fibres and unmyelinated C primary afferent fibres.

### 1.2.1 Myelinated nociceptors

The A-fibre nociceptors include most of thinly myelinated A $\delta$  and a few fast conducting cutaneous AB fibres (Burgess and Perl, 1967, Djouhri and Lawson, 2004). A-fibre nociceptors conduct fast pricking and sharp pain with more discrete information regarding stimulus (Slugg et al., 2000). A-fibre nociceptor receptive fields are small; thus they provide precise localization of pain. The strongest response by noxious-stimulated A-fibre primary afferent is generated following damaging of the tissue in the contact area by pinching of the skin using serrated forceps (Perl, 1968). The A-fibre nociceptors can be subdivided into those with high (type I) and low (type II) thresholds to heat (Treede et al., 1998). Type I are A-fibre mechano-heat-sensitive (AMHs) nociceptors, also known as polymodal nociceptors, which respond to heat, mechanical and chemical stimuli. These type I A-fibre nociceptors were previously identified as high threshold mechanoreceptors, due to their high heat threshold following short duration stimuli (Burgess and Perl, 1967). Their conduction velocity is between that of A $\delta$  (5-30 m/s) and AB fibres (35-75 m/s). These type I AMHs can be found in the hairy and glabrous skin. Meanwhile, type II A-fibre nociceptors, found only on a hairy skin, and have a slower conduction velocity compared to type I AMHs. Furthermore, type I fibres show a gradual increase in response to heat, whereas type II fibres have a slow adapting response to heat, and this pattern is similar to that of C-fibre mechano-heat-sensitive nociceptors (CMHs) (Treede et al., 1995). Type I fibres are activated by burn and chemical injury and thus may play a role in the development of hyperalgesia, while type II fibres probably initiate the first pain sensation from heat, and contribute to pain due to the application of capsaicin to the skin (Ringkamp et al., 2001).

In the spinal cord, A $\delta$  nociceptors innervate lamina I, II<sub>o</sub> and V and some of these fibres project in the Lissauer's tract or the dorsal column upon entering the spinal cord (Light and Perl, 1979). Light and Perl also found that some of the nociceptive A $\delta$  fibres passing ventrally before terminating in lamina V and some had collateral branches that project to the ventral part of lamina IV by penetrating deeply to the dorsal horn before making a dorsal turn. Meanwhile, large diameter AB nociceptors projected throughout lamina I-V with flame-shaped central arbors (Woodbury et al., 2008). We have little knowledge on the neurochemical properties of A-fibres nociceptors. Studies using guinea pig have

shown that some A $\delta$ -afferents that carry nociceptive information contain neuropeptides such as substance P and calcitonin gene-related peptide (CGRP) (Lawson et al., 1997, Lawson et al., 2002).

Injection of Cholera toxin B subunit (CTb) into the intact peripheral nerves allows visualisation of the central termination of myelinated afferent fibres in the dorsal horn of the spinal cord. The CTb protein binds to the GM1 ganglioside and is taken up and transported mostly by A-fibres after injection into the nerves (Shehab and Hughes, 2011). This protein labelled axonal boutons in lamina I as well as in deeper laminae. The central terminals in lamina I presumably belong to A $\delta$  nociceptors, whereas those in the deeper laminae, mainly belongs to A $\delta$  and A $\beta$  low threshold mechanoreceptors (Light and Perl, 1979, Lamotte et al., 1991).

### **1.2.2 Unmyelinated nociceptors**

Most C-fibre nociceptors are polymodal fibres which respond to noxious mechanical, chemical and thermal stimuli (Perl, 1996, Cain et al., 2001). They give rise to unpleasant, poorly localized and burning sensations and they greatly outnumber A $\delta$  nociceptors. C-nociceptive fibres can be divided into broadly two major subclasses depending on their expression of neuropeptides and on their growth factor dependence (Snider and McMahon, 1998, Julius and Basbaum, 2001). The neuropeptides calcitonin gene related protein (CGRP), substance P/Neurokinin A (NKA), somatostatin and galanin are expressed by peptidergic nociceptors, while non-peptidergic C nociceptive fibres lack these peptides (Hökfelt et al., 1975, Bennett et al., 1996). Furthermore, these two distinct C primary afferent fibres that are involved in nociceptive pathways depend on different protein signalling for their survival. Nerve growth factor (NGF)/Tropomyosin receptor kinase A (TrkA) signalling is needed by peptidergic nociceptive fibres, whereas non-peptidergic neurons depend on glial cell line-derived neurotrophic factor (GDNF) and receptor tyrosine kinase (c-Ret) signalling. In addition, non-peptidergic C fibres binds Griffonia simplicifolia isolectin IB4 and possess the purinergic receptor P2X3 (Snider and McMahon, 1998, Bennett et al., 1998, Zylka et al., 2005). Non-peptidergic and peptidergic primary afferents differ in response to nerve injury. Using an animal model of constriction neuropathy, Bailey and Ribeiro-da-Silva (2006) found a transient loss of axonal boutons that bind to IB4 following nerve injury, with normal

immunoreactivity of CGRP-labelled axons . This study also used electron microscopy and found degenerative changes of central terminal of type I glomeruli, which originate from non-peptidergic unmyelinated primary afferents. These finding suggest that there is loss of these non-peptidergic fibres, and not only loss of IB4 binding.

A study by Zylka et al. (2003) showed that Mas related G protein-coupled receptors (Mrgprs including MrgprAs, MrgprBs, MrgprC and MrgprD) are expressed in small diameter neurons, which presumably include nociceptors. This is further supported by electrophysiological evidence showing that MrgprD neurons have some properties typical of nociceptors such as prolonged action potentials, tetrodotoxin resistant Na<sup>+</sup> current and Ca<sup>2+</sup> currents that are inhibited by mu opioids (Dussor et al., 2008). Expression of Mrgprd is restricted to non-peptidergic neurons that innervate the specific layer of epidermis, stratum granulosum and this termination site is distinct from that of peptidergic neurons (Zylka et al., 2005). Mrgprd-expressing cells in the mouse contain the ATP-gated ion channel receptor P2X3 and only a small subset (9%) expressed TRPV1 receptor (the capsaicin and noxious heat-gated receptor), whereas all Mrgprd positive cells in the rat contain the TRVP1 receptor (Zylka et al., 2003). In addition, most of Mrgprd afferents do not contain substance P or CGRP, and MrgprD is confined to the subset of nociceptors that express GDNF, and these represent ~75% of IB4 binding neurons (Dong et al., 2001, Zylka et al., 2003, Zylka et al., 2005). Almost all (99.6%) Mrgprd expressing neurons are labelled with IB4, however, IB4 binding was not specific for non-peptidergic C fibres, as it can overlap with peptides such as CGRP (Dong et al., 2001, Wang and Zylka, 2009, McCoy et al., 2013). These finding show that Mrgprd is a specific marker for non-peptidergic C nociceptors and for that reason, they will be referred to as C<sup>MrgD</sup> afferents. In order to determine the two major classes of C-fibres, the peptidergic and non-peptidergic that express MrgprD, Cavanaugh et al. (2009) tested the behavioural response by pharmacological and genetic ablation each populations respectively. Cavanaugh and colleagues found that ablation of MrgprD expressing neurons only affected behavioural response to noxious mechanical stimuli (the effect on peptidergic population will be discuss below), although it was found that MrgprD-expressing neurons respond to thermal and mechanical stimuli (Rau et al., 2009). A later study found that mechanical

stimulation to the skin by pinching but not gentle stroke of a brush causes activation of Mrgprd-positive fibres (Vrontou et al., 2013).

After rhizotomy, the CGRP immunoreactivity in the dorsal horn will disappear, thus showing its primary afferent origin (Noguchi et al., 1990, Hökfelt et al., 1994). CGRP labelled primary afferents contain noxious heat receptor TRPV1 and pharmacological ablation of the central terminals of TRPV1-positive neurons leads to selective deficits in behavioural response to noxious thermal stimuli (Cavanaugh et al., 2009). A study by McCoy et al. (2013) using mice lacking CGRP $\alpha$ -expressing neurons revealed that these fibres contribute to perception of noxious heat and itch but are not needed to sense noxious mechanical or  $\beta$ -alanine itch stimuli. Moreover, these mice become more sensitive to cold and prefer warmer temperatures.

Centrally, unmyelinated C-nociceptors terminate in different laminae with peptidergic fibres innervating mainly lamina I and II<sub>o</sub>, while C<sup>MrgD</sup> primary afferent fibres arborize in the middle of lamina II of the SDH with little overlap between these two fibre types (Plenderleith et al., 1990, Averill et al., 1995, Snider and McMahon, 1998, Woodbury et al., 2000, Zylka et al., 2005). The peripheral axons of the non-peptidergic fibres innervate the skin, meanwhile the peptidergic fibres terminate within joints, viscera and skin (Taylor et al., 2009).

### **1.2.3 Low threshold mechanoreceptors**

Neurons that respond to innocuous touch of the skin are called low threshold mechanoreceptors (LTMRs), and these include A and C fibres. These LTMRs will be classified as A $\beta$ , A $\delta$  or C fibres depending on their action potential conduction velocities (Horch et al., 1977). LTMRs are stimulated by non-noxious weak mechanical force including vibration, stretch of the skin, movement or bend of hair follicles and indentation on the skin. However, some fibres are also activated by phasic cooling or thermal stimuli (Abraira and Ginty, 2013). LTMRs can be classified as slowly adapting (SA), intermediate (IA) or rapidly adapting (RA), based on their firing pattern to sustained mechanical stimuli (Burgess et al., 1968). Most of A $\beta$ -fibres are LTMRs, and these were shown to terminate within laminae III-V of the cat dorsal horn, with some giving branches to the gracile and cuneate nuclei (Rexed, 1952, Willis and Coggeshall, 2004). Meanwhile, in the rat, low-threshold A $\beta$  mechanoreceptive afferents can extend

into lamina II<sub>i</sub> (Woolf, 1987). They can be divided into rapidly adapting and slowly adapting fibres, referring to the response of these fibres to skin indentation. The SA-fibres will continuously discharge action potential throughout the stimulus and are associated with Merkel cells and Ruffini endings, whereas RA only fire on the onset and offset of indentation of the skin and are associated with Pacinian and Meissner corpuscles (Willis and Coggeshall, 2004). AB RA- and SA-LTMRs bifurcate into branches that extend rostrally and caudally with collateral axons that terminate deep in the dorsal horn (Brown et al., 1981). Some of the rostral branches of these fibres form a direct connection from the periphery to the brain without terminating in the spinal cord. They extend straight through the dorsal column and form synapses with the dorsal column nuclei neurons (Brown and Fyffe, 1981). The central projection of the SA-fibres terminates in the more superficial part of the dorsal horn and also the deeper part of the dorsal horn, meanwhile the RA-fibres have a flame shaped axonal arborisation which innervate the deeper regions (Woodbury et al., 2001, Woodbury and Koerber, 2007).

The A $\delta$  D-hair afferents are located in hairy skin and are found to be sensitive to the slow movement of hairs (Light et al., 1982). Unlike AB-fibres, A $\delta$ -LTMRs project via the dorsal column to the dorsal horn without giving long rostral or caudal branches (Traub and Mendell, 1988). The central terminals of these fibres terminate in the inner part of lamina II and in lamina III (Light and Perl, 1979) and are found to be part of the type II synaptic glomeruli (see below) (Light et al., 1982).

C-LTMRs were first described by Zotterman (1939). He mentioned that these fibres are believe to be related to tickling and itching sensations. In the cat, a subset of C-fibres is found to be activated by low threshold mechanical and thermal stimulation but not by noxious stimuli (Bessou and Perl, 1969, Bessou et al., 1971). Meanwhile, in the human, these fibres are reported to be involved with pleasant touch sensations (Löken et al., 2009). Olausson et al. (2002) found that the human insular cortex is activated by stimulation of these fibres, suggesting that they are required in developing positive emotions. C-LTMRs fibres are more numerous than A-LTMRs and are very sensitive to indentation of the skin, similar to A-fibres, except that they are activated by stimuli that move slowly across their receptive field (Li et al., 2011). Apart from using VGLUT3,

tyrosine hydroxylase (TH) can be used to specifically label C-LTMRs in the dorsal root ganglia (Seal et al., 2009, Li et al., 2011). More than 80% of TH-immunoreactive neurons co-express VGLUT3 mRNA and they do not express CGRP, TrkA or TRPV1, which are markers for peptidergic nociceptors and do not bind to IB4 or express MrgprA1, MrgprA3, MrgprA4, MrgprB4, MrgprC11 or MrgprD, which are markers for non-peptidergic nociceptors (Li et al., 2011). These fibres are only found in hairy skin and their central boutons are absent from the medial part of the dorsal horn in the lumbar and cervical enlargement which are innervated from glabrous skin. Study done recently in human, found that stimulation of C-LTMRs causes reduce in heat pain but this was not seen in patients with impaired C-LTMRs, as in small fibre neuropathy (Habig et al., 2017). Another distinct subset of non-peptidergic C-fibres that express Mas-related G protein coupled receptor B4 (MrgprB4) are found to innervate hairy skin alone and are also associated with pleasant touch (Liu et al., 2007). Massage-like stroking of hairy skin but not pinching of the skin causes activation of these fibres (Vrontou et al., 2013).

#### **1.2.4 Neurochemical properties and receptors of primary afferents**

The neurotransmitter glutamate is very important in maintaining spinal excitatory synaptic transmission in normal or pathological pain conditions through activation of glutamate receptors. Primary afferents use glutamate as their fast neurotransmitter, thus they will have excitatory effect on their synaptic targets (Broman et al., 1993). They act via glutamate receptors, including *N*-methyl-D-aspartate (NMDA),  $\alpha$ -amino-3-hydroxy-5-methyl-4-isoxazolepropionic acid (AMPA)/kainate and metabotropic glutamate receptors (mGlu) (Tao et al., 2005, Bardoni, 2013). Glutamate is packed into synaptic vesicles by vesicular glutamate transporters (VGLUTs) before its release. There are three VGLUTs that have been discovered, namely VGLUT1, VGLUT2 and VGLUT3 (Takamori, 2006, Fremeau et al., 2002). Likewise, VGLUTs have been widely used as a marker for glutamatergic axons and were mainly expressed by excitatory interneurons in the dorsal horn (Todd et al., 2003). However, these glutamatergic neuronal markers are also found to be expressed by primary afferents that terminate in the dorsal horn. Central terminals of low threshold mechanoreceptors in laminae III-VI contain VGLUT1, whereas a low level of

VGLUT2 is found in many unmyelinated primary afferents in the rodents, and they do not express VGLUT1 (Todd et al., 2003, Brumovsky et al., 2007). However, VGLUT1 is also expressed by descending neurons from the pyramidal cells of neocortex and corticospinal fibres (Du Beau et al., 2012). VGLUT3 is expressed by unmyelinated low threshold mechanoreceptor C fibres that innervate the inner layer of lamina II (Seal et al., 2009). Seal et al also found that VGLUT3-immunoreactivity do not overlap with the IB4 band but lies exclusively among cells that express protein kinase C gamma (PKC $\gamma$ ). Each of the VGLUTs is expressed by different population of primary afferents suggesting that they have distinct functions in transmitting different stimuli from the periphery to the brain.

Substance P is found in the dorsal ganglia, dorsal roots of the spinal nerves and primary afferent central terminals in the superficial part of the dorsal horn, consistent with its role as a sensory neurotransmitter involved with the perception of pain (Cuello et al., 1977, Douglas and Leeman, 2011). In the dorsal horn, substance P is also expressed by local neurons and descending serotonergic pathways (Hökfelt et al., 1978, Gilbert et al., 1982). It is a member of tachykinin family of neuropeptides, which act through the neurokinin-1 receptor (NK1r), a seven transmembrane domain G-protein coupled receptor. Other members of tachykinin family are neurokinin A and B, which act on the neurokinin 2 and 3 receptors respectively (Maggi, 1995). Substance P and neurokinin A are expressed by both primary afferent and interneurons, meanwhile neurokinin B is only present in SDH interneurons (Ogawa et al., 1985). Substance P is expressed by A $\delta$ -fibres and unmyelinated C fibres that terminate in lamina I-II of the dorsal horn, which are involved in transmitting noxious stimuli to the spinal cord dorsal horn (Cao et al., 1998, Lawson et al., 1997, Kantner et al., 1985). There have been several reports that most of SP-containing primary afferents also co-express CGRP (Wiesenfeld-Hallin et al., 1984, Lee et al., 1985, Gibbins et al., 1985). Substance P is thought to contribute to nociceptive transmission through central hyperexcitability, thus increasing the sensitivity to pain (Salter and Henry, 1991). Substance P was thought to be upregulated by AB fibres after nerve injury or inflammation (Fukuoka et al., 1998, Marchand et al., 1994, Neumann et al., 1996), however, a study using three nerve injury models: sciatic nerve transection (SNT), spinal

nerve ligation (SNL) and chronic constriction injury (CCI) disputed this (Hughes et al., 2007). Hughes et al did not see any expression of substance P in A $\beta$  fibres in those models. In addition, they also found that no internalization of NK1r in the spinal dorsal horn after electrical stimulation of A $\beta$  primary afferent are seen in the SNL and CCI models, suggesting that substance P was not released from afferents in significant amounts.

Transient receptor potential (TRP) channels were first identified in *Drosophila* (Minke, 1977). TRPs are ion channels that have six protein families; the vanilloid receptor TRPs (TRPVs), the melastatin or long TRPs (TRPMs), the mucolipins (TRPMLs), the polycystins (TRPPs), the classical TRPs (TRPCs) and ankyrin transmembrane protein 1 (ANKTM1) (Clapham, 2003, Montell et al., 2002). In the nervous system, TRPs are involved in the response towards various stimuli received from the periphery, neuron outgrowth and receptor signalling (Moran et al., 2004). The vanilloid receptor, now known as TRPV1, is important in processing heat sensation and is mostly expressed by A $\delta$ - and C-nociceptors (Caterina and Julius, 2001). TRPV1 is activated specifically by capsaicin, the main pungent ingredient in chili peppers of the genus capsicum (Caterina et al., 1997). TRPV1 is also activated by noxious heat (>43°C), low pH and lipids such as anandamide (Caterina et al., 1997, Tominaga et al., 1998, Caterina and Julius, 2001). Activation of TRPV1 by binding of capsaicin causes influx of Na<sup>+</sup> and Ca<sup>2+</sup>, leading to firing of action potentials, and is associated with the burning sensation related with spicy food (Holzer, 1991). Ablation of TRPV1 in knockout mice resulted in decreased reactions to noxious heat and vanilloid induced pain without any changes in response to noxious mechanical stimuli (Caterina et al., 2000). Cavanaugh et al. (2011) reported that, in the DRG of adult mice, TRPV1 is expressed selectively by peptidergic C primary afferent fibres.

TRPM8 and TRPA1 are another two family members of TRPs, which that are activated by cold stimuli. TRPM8 responds to cooling (<26-28°C) and cooling compounds such as menthol and icilin. Meanwhile, TRPA1 is stimulated by noxious cold (<18 °C) and icilin with response menthol (McKemy et al., 2002, Peier et al., 2002, Story et al., 2003). In rat DRG, TRPA1-expressing neurons do not show immunoreactivity for neurofilament 200 (NF200), a neurochemical marker for A-fibres, and this receptor is observed only in C-fibres that express

TRPV1 mRNA, whereas TRPM8-positive cells do not co-express TRPV1, and can have either A- or C- fibres (Kobayashi et al., 2005). This studies also observed that TRPA1 and TRPM8 are rarely co-expressed. Peier et al. (2002) reported that in mouse, TRPM8-immunoreactive cells in DRG do not contain TRPV1 or CGRP, or IB4. This finding strongly suggests that TRPM8 is express by distinct group of thermoreceptive neurons. A TRPM8<sup>-/-</sup> mouse showed abnormal behaviour towards cool thermosensation, thus further support that this receptor is responsible for detection of innocuous cold (Dhaka et al., 2007).

### **1.2.5 Synaptic glomeruli**

Most primary afferents terminate in the dorsal horn of the spinal cord in simple synaptic arrangements, but some have a more complex form involving several synapses, known as the synaptic glomerulus. Electron microscopy is the best method to explore this synaptic arrangement in detail. These complex structures consist of a central primary afferent bouton that forms synapses with surrounding profiles. Coimbra and colleagues have shown that 70% of the central terminals of the glomeruli in lamina II of the rat degenerated 5 days after dorsal rhizotomy, thus providing that most of these are formed by primary afferent central boutons (Coimbra et al., 1974). The surrounding profiles include presynaptic GABAergic axons from local neurons which form axoaxonic synapse onto the primary afferent boutons. Other structures are dendrites that are post-synaptic to the primary afferent boutons and some GABAergic vesicle-containing dendrites that can form reciprocal synapses with the central axon (Todd, 1996). In addition, surrounding structures can form synapses between themselves, with the central axons also forming a synapse onto one of them. This arrangement is known as the synaptic triad.

The synaptic glomeruli indicate that a complex structure is needed to interpret incoming sensory information from the periphery. Two types of synaptic glomeruli were found in the rat spinal cord by Ribeiro-Da-Silva and Coimbra (1982). The classification is based on several criteria mainly focusing on the central terminal of a glomerulus; i) electron density of the background cytoplasm and size, ii) regularity of contour, iii) number of mitochondria and iv) synaptic vesicles uniformity, compactness and diameter.

### 1.2.5.1 Type I and type II glomeruli

Type I glomeruli are located in the middle and ventral part of lamina II, at the termination site for unmyelinated C fibres. Central axons of the type I glomeruli are darker and have densely packed synaptic vesicles with variable diameter. They are thought to belong mainly to non-peptidergic unmyelinated primary afferent fibres (Ribeiro-Da-Silva and Coimbra, 1984, Ribeiro-da-silva et al., 1989).

Type II glomeruli are mainly found in the ventral part of lamina II and the dorsal part of lamina III, overlapping with the termination site of myelinated primary afferent fibres. Central axons of type II glomeruli have electron-lucent cytoplasm and vesicles of more uniform size and most probably, the central axons of the type II glomeruli are derived from myelinated primary afferent fibres (Ribeiro-Da-Silva and Coimbra, 1984). Both A $\delta$  and A $\beta$  fibres terminate in lamina II, however the central terminals of these myelinated primary afferent fibres can be differentiated by looking at the synaptic complexes that they form. The central axons of type II glomeruli are thought to belong to A $\delta$  down hairs and are found mostly in lamina II and III (Ribeiro-Da-Silva and Coimbra, 1982, Light et al., 1982). In addition, myelinated primary afferent fibres such as large A $\beta$  hair follicle afferents form non-glomerular synapses (Watson et al., 2002). Even though they terminate differently, both of them receive inhibitory axoaxonic inputs (Maxwell and Noble, 1987, Todd et al., 1991, Todd, 1996). Dendritic spines from islet cells in lamina II of the cat dorsal horn were found to be presynaptic to central boutons of lamina II glomeruli (Gobel et al., 1980).

Presynaptic inhibition of primary afferents is mediated by axoaxonic and dendroaxonic synapses in both type I and type II glomeruli. Peripheral presynaptic dendrites in type II glomeruli are less numerous compared to type I glomeruli, but the former have more peripheral axon terminals (Ribeiro-Da-Silva and Coimbra, 1982). A few studies found that peripheral axons and presynaptic dendrites in the glomeruli contain  $\gamma$ -aminobutyric acid (GABA) in the rat, cat and monkey (Barber et al., 1978, Maxwell et al., 1990, Carlton and Hayes, 1990, Todd, 1996). These GABAergic structures are believed to be derived from local inhibitory interneurons. A study of GABA and glycine using a quantitative post-embedding immunogold technique, showed that all of the peripheral axons and most of the vesicle containing dendrites are immunoreactive for GABA. However,

in type II glomeruli, most of the peripheral axons and few of the vesicle containing dendrites contained both GABA and glycine (Todd, 1996). From these finding we can conclude that different neurochemical populations of inhibitory interneurons are involved in the presynaptic inhibition of myelinated and unmyelinated primary afferent fibres. Recently, Hughes et al. (2012) showed that parvalbumin (PV) containing neurons found in lamina Ili and III form axoaxonic synapses on the central terminals of type II glomeruli and are most likely a source of presynaptic inhibition of myelinated primary afferent fibres.

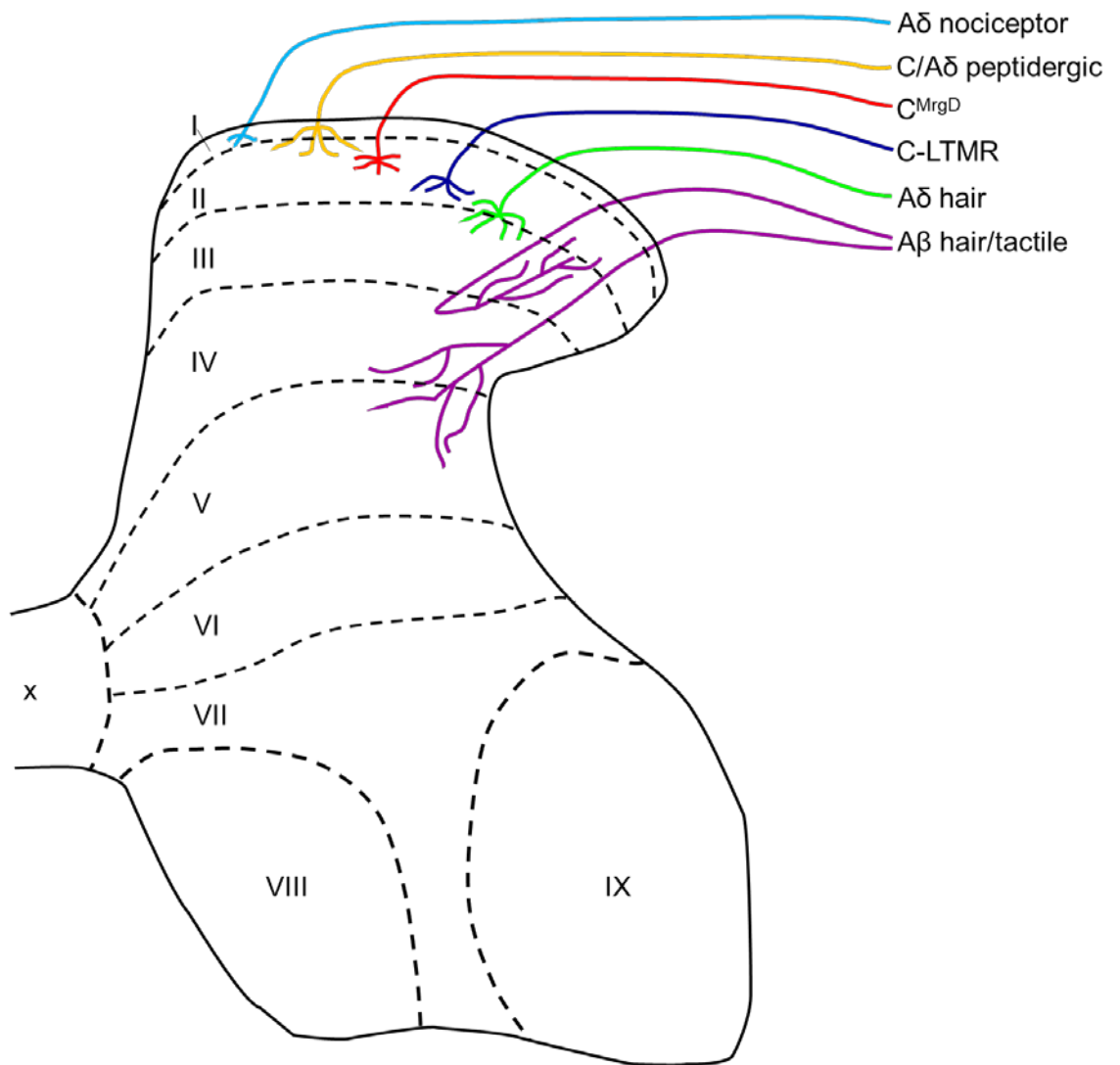


**Figure 1-1 Rexed's laminae and the termination of primary afferents in different laminae of the spinal cord.**

Rexed (1952) divided the grey matter of the cat into laminae I-X based on the cell size and packing density of neurons, and this is applicable across several other mammalian species. The dashed lines indicate laminar boundaries. This image also shows the central terminations site of the major group of primary afferents. A $\delta$  nociceptors arborize mainly in lamina I with some fibres penetrating more deeply. Peptidergic primary afferent fibres including some A $\delta$  nociceptors, innervate lamina I and II, with some fibres terminating in deeper laminae. Meanwhile, non-peptidergic C-MrgD nociceptors arborize in the middle of lamina II. A $\delta$  hair follicle afferents end at the border between laminae II and III, whereas A $\beta$  hair follicle and tactile afferents terminate in laminae III-V. Modified from Todd (2010).

### 1.3 Projection neurons

The sensory information from spinal cord dorsal horn is projected to the brain via numerous ascending tracts that are located in the ventral, lateral and dorsal funiculi. Many anatomical and electrophysiological studies have been performed in the rat to determine the potential brain targets and their origin in the spinal cord. Retrograde and anterograde tracing studies allow individual neurons to be labelled from specific brain region and their termination site in the brain can be mapped, respectively. The three main ascending tracts in the brain are the anterolateral tract (ALT), the post-synaptic dorsal column (PSDC) system and spino-cervicothalamic (SCT) pathway. This study will be focusing on ALT since these are the main ascending pathway for nociception.

The ALT (Figure 1-2) consists of two separate tracts: anterior spinothalamic tract and lateral spinothalamic tract that are located in the anterior funiculus and anterior part of the lateral funiculus, respectively. The anterior spinothalamic tract transmits crude touch and pressure sensations, meanwhile the lateral spinothalamic tract transmit pain and temperature (Martin et al., 1990). In the rat, the ALT neurons are located in lamina I, are largely absent from lamina II and are distributed throughout lamina III-VI (Todd, 2010). In lamina I, the dendritic trees of projection neurons are confined within the same lamina, meanwhile, the ALT neurons in laminae III-IV have dendrites that extent dorsally into lamina II.

In the rat, ALT neurons in laminae III-IV expressed NK1r and receive numerous contacts from GABAergic cells that contain neuropeptide Y (NPY), as well as from dynorphin-expressing excitatory neurons (Baseer et al., 2012, Polgár et al., 1999, Polgár et al., 2011). The axons of these NK1r positive projection neurons project to contralateral brainstem region and thalamus nuclei (Marshall et al., 1996, Todd et al., 2000, Al-Khater et al., 2008). However, some fibres that travel to the brain have a bilateral projection (Spike et al., 2003). These brain regions include caudal ventrolateral medulla (CVLM), the nucleus of the solitary tract (NTS), lateral parabrachial area (LPb) and the periaqueductal grey matter (PAG) (Lima and Coimbra, 1988, Hylden et al., 1989, Lima et al., 1991, Todd et al., 2000, Spike et al., 2003, Al-Khater et al., 2008, Al Ghamdi et al., 2009). The ALT neurons in laminae III-IV are thought to be wide-dynamic-range (WDR). They

are innervated mainly by substance P-containing nociceptors and receive sparse synaptic inputs from myelinated low threshold afferents (Polgár et al., 2007, Naim et al., 1998). Most of NK1r-immunoreactive cells in lamina III show pERK after noxious thermal, mechanical or chemical stimuli (Polgár et al., 2007). The morphology of the ALT neurons in lamina I includes fusiform, pyramidal and multipolar with dendritic trees confined within the same layer (Spike et al., 2003, Almarestani et al., 2007). Han et al. (1998) found that pyramidal cells are thermoreceptive, fusiform cells are nociceptive, while multipolar cells are either polymodal or nociceptive-specific. Some studies found that A retrograde labelling study showed about 5% of the total neuronal population in lamina I was constitute by projection neurons and that ~80% of projection neurons in lamina I express the main receptor for substance P, the NK1r (Spike et al., 2003, Al-Khater and Todd, 2009). Projection neurons are not the only cells that express NK1r, as some interneurons in lamina I also express this receptor. These two populations of cells can be distinguished by their soma size. Generally, most of the NK1r expressing projection neurons in lamina I have a larger soma size cross sectional area ( $>200\mu\text{m}^2$ ) in horizontal sections, whereas most NK1r-positive interneurons have a soma area that is smaller than this (Al Ghamdi et al., 2009). The ALT neurons that expressed NK1r in lamina I are densely innervated by substance P containing primary afferents and they upregulated Fos (the protein product of the immediate early gene *c-fos*) after noxious stimulation (subcutaneous injection of formalin) (Todd et al., 2002). Neurons that express NK1r in the dorsal horn can be selectively destroyed by intrathecal injection of substance P conjugated to the cytotoxin saporin (Mantyh et al., 1997, Nichols et al., 1999). In inflammatory and neuropathic pain models in rats that had been treated with the above toxin, the signs of hyperalgesia were dramatically reduced. However, in mice without NK1r or the gene coding for substance P formation (preprotachykinin), there was no change in hyperalgesia in inflammatory and neuropathic pain models (Cao et al., 1998, De Felipe et al., 1998). These findings showed, most probably glutamate released by the substance P expressing primary afferents that act on the NK1r expressing projection neurons of the ALT, is responsible for the development of hyperalgesia (De Biasi and Rustioni, 1988).

About 3% of lamina I projection neurons are very large multipolar cells that are either lack NK1r or weakly labelled with NK1r antibody (Puskár et al., 2001). A study by Baseer et al. (2014) showed about 40% of NK1r-lacking lamina I projection neurons received synaptic input from non-peptidergic type I A $\delta$  nociceptors thus strongly suggest it play an important role in perception of fast pain. These giant neurons can be distinguished by the dense inhibitory and excitatory synaptic input to the cell bodies and dendrites (Puskár et al., 2001, Polgár et al., 2008). Retrograde labelling, using injection of cholera toxin B subunit into the parabrachial area, labelled the majority of the lamina I giant cells and they expressed Fos following noxious stimulation, suggesting they are activated by nociceptors (Puskár et al., 2001). GABAergic axons that contained nitric oxide synthase (nNOS) formed numerous synapse with these giant neurons (Puskár et al., 2001).

The dorsal column tract includes the dorsal column-medial lemniscus pathway (the gracile and cuneate fasciculi) and the PSDC pathway. The dorsal column-medial lemniscus fibres carry discriminative touch, vibration, conscious muscle joint sense, tactile information and conscious information (Figure 1-3). Sensory nerve fibres in the dorsal root ganglia enter the white matter of the spinal cord and ascend ipsilaterally in the dorsal column to terminate on the cuneate and gracile nuclei. The sensory nerve fibres from upper limb enter the spinal cord and form the cuneate fasciculus and the fibres from lower limb form the gracile fasciculus. The second-order neurons, internal arcuate fibres, cross the midline and ascend as the medial lemniscus through the medulla oblongata, the pons and the midbrain. The fibres terminate by synapsing on the third-order neurons in the ventral posterolateral nucleus of the thalamus which then project to the primary somatosensory cerebral cortex.

The PSDC tract is formed by the axons of dorsal horn neurons that synapse in the dorsal column nuclei. These PSDC neurons respond to innocuous mechanical stimuli (Giesler and D. Cliffer, 1985) and noxious peripheral stimuli (Bennett et al., 1984). The PSDC neurons are mainly located in laminae III-IV and also in the deeper laminae V-VI of different mammalian species (Brown and Fyffe, 1981, Bennett et al., 1983). The axons of these neurons project through the dorsal funiculus before terminating in the junction area between the spinal cord and the medulla. The PSDC pathway is organized somatotopically in such that

cervical cells terminate in the nucleus cuneatus while neurons in the lumbosacral enlargement project to the nucleus gracilis.

The SCT pathway includes spinocervical and cervicothalamic tracts. These pathways transmit light cutaneous touch and noxious stimuli to the thalamus. Neurons of the spinocervical tracts are found in lamina I-V. The spinocervical axons project in the ipsilateral lateral funiculus and synapses in the lateral cervical nucleus. In the rat, the spinocervical tract is organized somatotopically: medially lie the sacral fibres and laterally lie the cervical fibres. Axons of the lateral cervical nucleus neurons decussate in the ventral white commissure of the upper cervical spinal cord and ascend in the medial lemniscus to reach the thalamus (cervicothalamic tract) (Berkley et al., 1980).

Todd (2010) suggested that projection neurons are functionally diverse since they have a large number of supraspinal target. For instance, ascending neurons in the dorsal horn project to the VPL indicate a feasible role in sensory discriminative aspects of pain (Gauriau and Bernard, 2004). The nociceptive input from SDH is transmitted to the LPb which then project to the amygdala or the hypothalamus. According to Gauriau and Bernard (2002), the parabrachial-amygdala connection and parabrachial-hypothalamic fibres are believed to have a role in the emotional components of pain processing and in motivational affective responses during pain states, respectively.

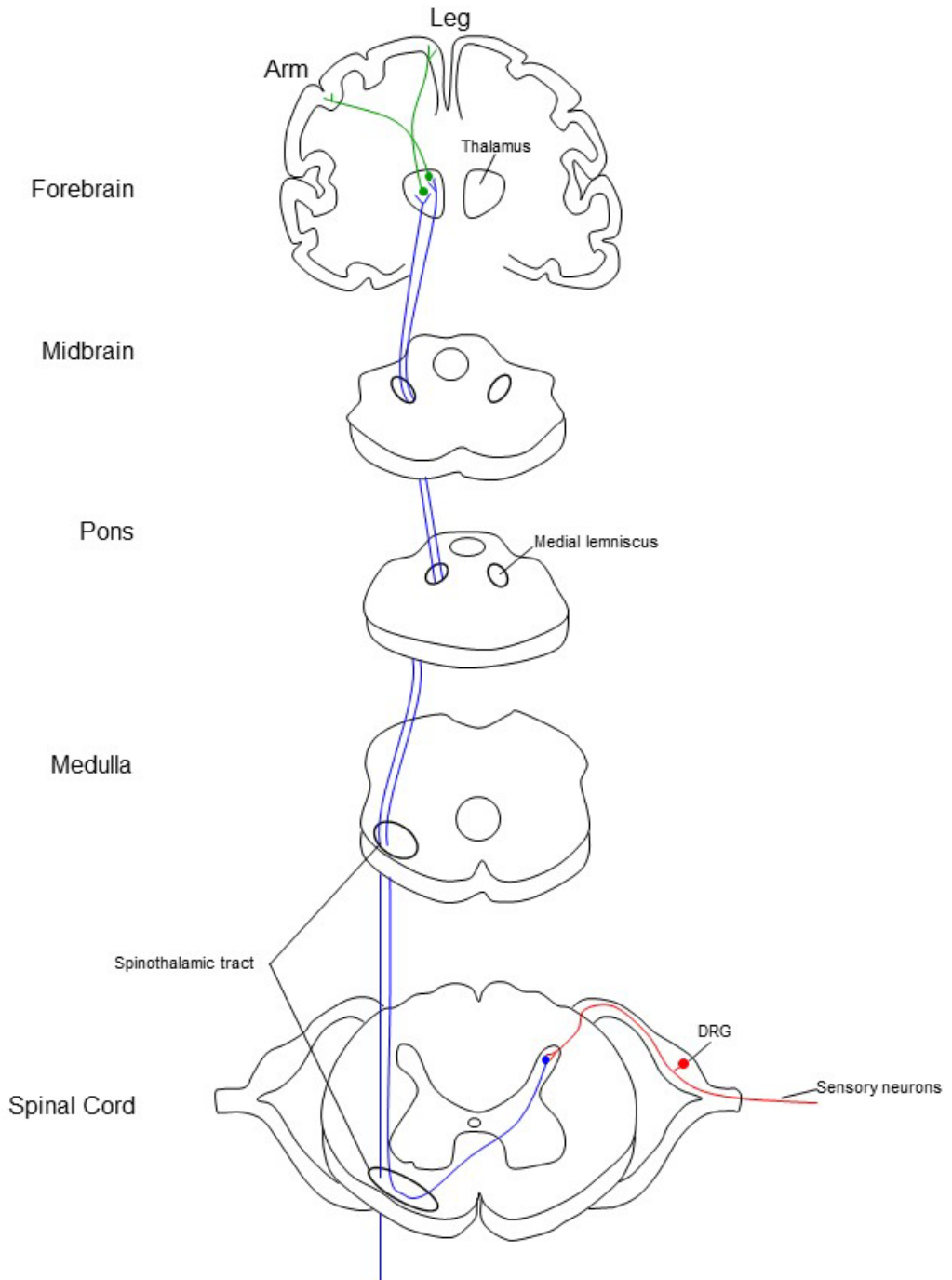


**Figure 1-2 Anterior and lateral spinothalamic tract (Anterolateral system)**

The ALT neurons convey information such as crude touch, pressure sensations, pain and temperature. The sensory nerve fibres (red) give branches to the spinal cord dorsal horn which then activate neurons in the spinal cord that belong to the spinothalamic tract (blue). Spinothalamic axons cross the midline and ascend in the white matter as the spinothalamic tract. This tract forms connection with the medial lemniscus before terminate in the thalamus. The third order neurons in the thalamus (green) project to the primary somatosensory cortex.

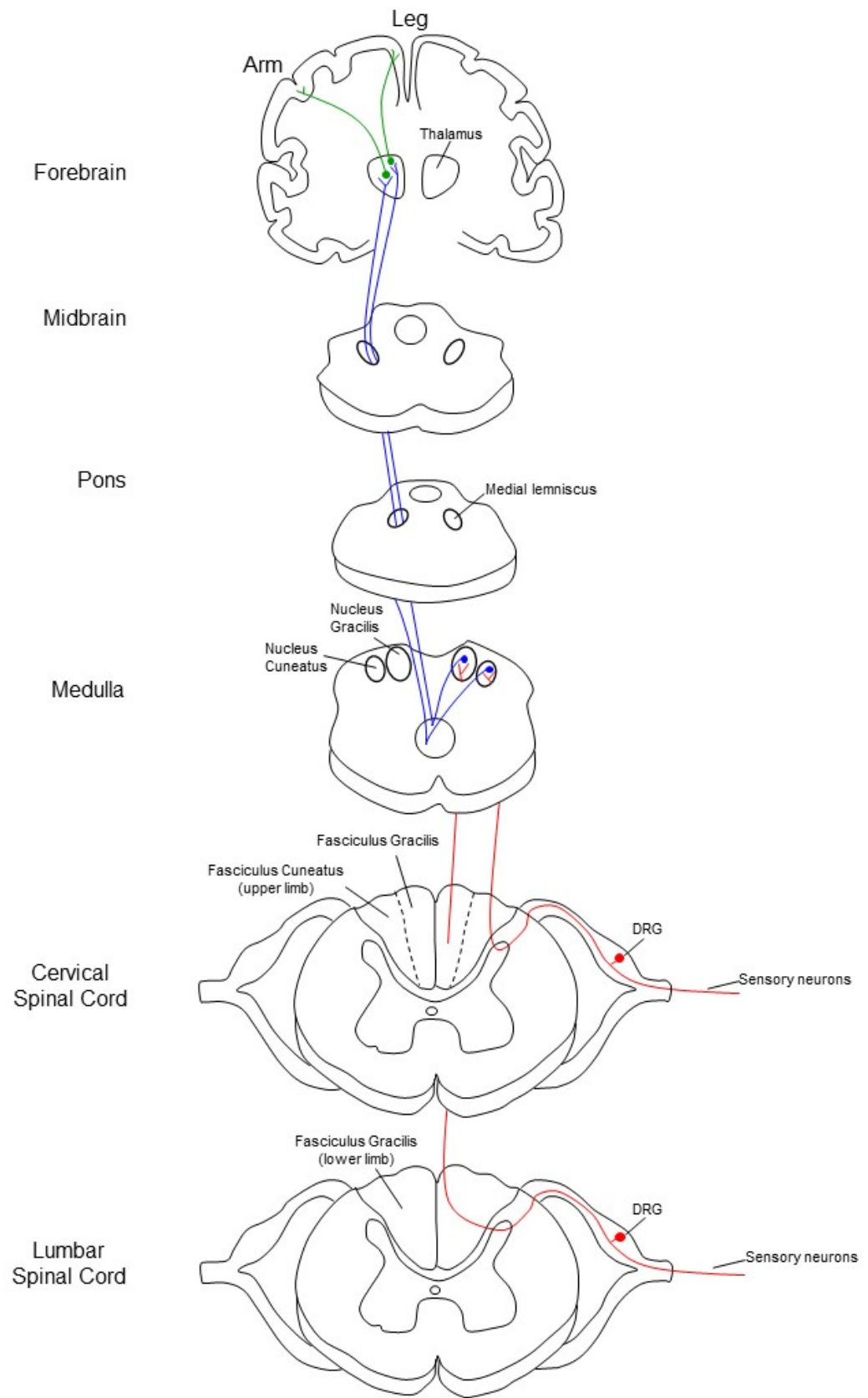


**Figure 1-3 Dorsal column-medial lemniscus pathway (DCML)**

These projection neuron carries the sensory modalities of discriminative touch, vibration, conscious muscle joint sense, tactile information and conscious information. The name arises from the two structures that form the DCML. The first order neurones (red) carry information from fasciculus cuneatus (cervical spinal cord) and fasciculus gracilis (lumbar spinal cord) which then synapse in the nucleus cuneatus and gracilis of the medulla oblongata. The second order neurons (blue) begin in the cuneate nucleus or gracilis which than synapse with the third order neurons (green) in the thalamus. These fibres decussate in the medulla oblongata and travel in the contralateral medial lemniscus fibres to reach the thalamus. The third order neurons in the thalamus then project to the primary somatosensory cortex.

## 1.4 Excitatory and inhibitory interneurons of the dorsal horn

The great majority of laminae I-III neurons have axons that only arborize within the spinal cord, and these are known as interneurons (Todd, 2010). Nearly all neurons in lamina II are interneurons, and 95% of those are in lamina I (Spike et al., 2003, Polgár et al., 2004). Lamina III contains projection neurons from several different tracts (Abraira and Ginty, 2013), thus making it difficult to estimate the percentage of interneurons in this lamina. However, it is thought that most neurons in lamina III are interneurons (Todd, 2017). Interneurons are divided into two major functional classes: excitatory and inhibitory cells. They receive input from the central terminals of the primary afferents and modify the sensory information before projecting it to various parts of the brain. In addition, they also receive synaptic inputs from the brain and from other interneurons.

Most of the neurons in laminae I-III are excitatory interneurons which use glutamate as their fast neurotransmitter, while inhibitory interneurons use GABA and/or glycine. Quantitative immunocytochemical studies in rodents have suggested that about 25-40% of neurons in laminae I-III are GABA immunoreactive with some using glycine as co-transmitter (Todd and Sullivan, 1990, Polgár et al., 2003, Polgár et al., 2013a). Inhibitory interneurons are believed to play a major role in modifying pain and itch sensation in the dorsal horn (Basbaum et al., 2009, Ross et al., 2010, Zeilhofer et al., 2012). They reduce the response to nociceptive stimuli, silence the nociceptive neurons during innocuous stimulation, prevent crosstalk between sensory modalities and keep the neuronal excitation within somatotopically defined areas of the dorsal horn (Sandkühler, 2009). Failure of these functions will lead to pathological pain states.

In the rat, 30% of neurons in lamina III are enriched with glycine and are therefore likely to be glycinergic. Glycine enrichment is found in 9% and 14% of the neurons in lamina I and II, respectively (Todd and Sullivan, 1990). All of these cells were GABA-immunoreactive. Study using *in situ* hybridization for neuronal glycine transporter 2 (GlyT2) and findings from GlyT2::eGFP mice demonstrated that glycinergic cells are more numerous in the deeper dorsal horn between laminae III-V and are thus most likely involved with tactile stimulation

(Zeilhofer et al., 2005, Hossaini et al., 2007). However, an electrophysiological study by Yasaka et al. (2007) found there are purely glycinergic synapses present in laminae I-III. It is possible that these lack of GABA<sub>A</sub> receptors or that they are derived from glycinergic neurons located in deeper lamina (Chéry and De Koninck, 1999).

GABA and glycine are taken up into vesicles at the inhibitory axon terminals by means of vesicular GABA transporter (VGAT; also known as the vesicular inhibitory amino acid transporter, VIAAT). Therefore, antibodies against this molecule can be used to identify the axons of inhibitory interneurons (Sardella et al., 2011b). In addition, antibodies against the GABA-synthesizing enzyme glutamic acid decarboxylase (GAD) and the neuronal glycine transporter (GLYT2) are alternative to labelling the inhibitory boutons (Mackie et al., 2003, Tiong et al., 2011). Immunostaining with this antibody allows us to visualise inhibitory axons in laminae I-III, which are mostly derived from local interneurons. As mentioned before, A $\delta$  and C nociceptors mainly terminate in laminae I and II and these can receive synapses from GABAergic interneurons which are thought to be located within the same laminae. This type of synapse is known as an axoaxonic synapses, and these mediate GABAergic presynaptic inhibition (Magoul et al., 1987, Todd, 1996). GABAergic neurons also form axodendritic and axosomatic synapses in lamina II and this underlie postsynaptic inhibition (Magoul et al., 1987). Blockage of GABA<sub>A</sub> receptors in rat spinal cord creates behavioural signs of tactile allodynia (Sivilotti and Woolf, 1994).

The remaining ~75% of the interneurons in laminae I-III that are not GABAergic or glycinergic are presumably glutamatergic. There are currently no reliable immunocytochemical markers for the cell bodies of glutamatergic neurons. It appears that all excitatory interneurons in laminae I-III express vesicular glutamatergic transporter 2 (VGLUT2). This means that, axons of these cells can be identified using antibody against VGLUTs (Todd et al., 2003). These axonal boutons containing VGLUT2, which are mostly derived from local excitatory interneurons, are very numerous in laminae I-III.

## 1.4.1 Interneuron classification

Various attempts have been made to identify distinct functional populations among the SDH interneurons, by using cell morphology, electrophysiology properties, expression of neurochemical markers and developmental lineage (Grudt and Perl, 2002, Maxwell et al., 2007, Yasaka et al., 2010, Heinke et al., 2004, Wildner et al., 2013, Iwagaki et al., 2013). Sadly, there is still no universally accepted classification that can be used for all dorsal horn interneurons (Todd, 2010). The most widely accepted scheme is that developed by Grudt and Perl for lamina II neurons. This relies mainly on diversity of the cells' dendritic morphology and their firing patterns during injection of depolarizing current (Grudt and Perl, 2002). Since the SDH is the first relay site for the pain pathway, it is crucial for us to characterise interneurons into different functional group. This will help us understand the spinal pain processing mechanisms and should lead to the development of new pain therapies (Graham et al., 2007).

### 1.4.1.1 Morphology

Initially, the Golgi technique was used to study the morphology of neurons in the spinal cord or spinal trigeminal nucleus in various species (Gobel, 1975, Gobel, 1978, Schoenen, 1982, Lima and Coimbra, 1986, Todd and Lewis, 1986). These studies identified two main cell type among lamina II neurons, based on dendritic and axonal characteristics: this were name islet and stalked cells (Gobel, 1975, Gobel, 1978). Nevertheless, they found many cells with different morphologies, and this could not reliably assign to specific classes. A later study by Grudt and Perl (2002) using whole-cell patch-clamp recording from spinal cord slices in vitro identified four main morphological classes: islet, vertical, central and radial cells (Figure 1-4). Vertical cells by Grudt and Perl overlapped with stalked cells described by Gobel 1975, 1978. Their classification scheme was based on the laminar location and size of the soma and dendritic tree; the size, number, branching pattern and main direction of dendritic tree and axon.

#### 1.4.1.1.1 Islet cells

Islet cells was first identified in spinal trigeminal nucleus of the cat using the Golgi method and were described as having large dendritic trees that extended in rostrocaudal axis for more than 500  $\mu\text{m}$  (Gobel, 1975). A morphometric

analysis by Yasaka et al. (2007), using quantification of dendritic parameters in rat spinal cord, found that the four group of cells, identified by Grudt and Perl could be differentiated by this method. According to this study, islet cells had a ratio of rostrocaudal to dorsoventral dendritic extent (RC:DV) of more than 3.5, and most had rostrocaudal dendritic lengths of more than 400  $\mu\text{m}$  (Figure 1-4). Some islet cells had a dendritic extension of between 300-400  $\mu\text{m}$  long, and had axons that remained within the dendritic tree. Both the dendrites and axons arborize within lamina II and dendritic trees are limited in dorsoventral and mediolateral extent (Grudt and Perl, 2002, Yasaka et al., 2007). Gobel et al. (1980) reported that, the dendritic tree had long tertiary branches that gave rise to recurrent branches that turned 180° towards the cell body. Meanwhile, the axons of these cells branch extensively within the volumes of dendritic tree and can extend beyond this in rostrocaudal axis (Grudt and Perl, 2002). The cell bodies of islet cells are small (less than 15  $\mu\text{m}$  in diameter), found throughout lamina II and rarely has axosomatic synapse (Gobel et al., 1980, Yasaka et al., 2010).

In terms of their electrophysiological properties, islet cells have a lower resting membrane potential other than lamina II neurons. they show a tonic firing pattern and have an  $I_h$  current (Melnick, 2008). The majority of the islet cells receive monosynaptic input from axons conducting at  $<1\text{ms}^{-1}$ , which therefore belongs to C-fibres (Grudt and Perl, 2002). In addition, some islet cells received monosynaptic A $\delta$  fibres input. This authors also found that EPSCs and IPSCs evoked in islet cells have greater amplitude than those in other recorded morphological cell type (Yasaka et al., 2007). More stimulating current was needed to evoke action potentials in islet cells compared to other cells that show tonic firing (Melnick, 2008).

All islet cells are immunoreactive for GABA and their axon terminals contain GAD and VGAT (Todd and McKenzie, 1989, Maxwell et al., 2007, Yasaka et al., 2010). A study using a mouse line that express enhanced green fluorescent protein (eGFP) under the control of GAD67 promoter showed that the majority of eGFP-immunoreactive neurons in lamina II were islet cells (Heinke et al., 2004). In support of the finding that all islet cells are GABAergic, a study using VGLUT2::eGFP mice showed that none of the VGLUT2::eGFP (glutamatergic) cells had islet morphology. These mice are a bacterial artificial chromosome

(BAC) transgenic mouse line, in which expression of eGFP is under the control of the vesicular glutamate transporter (VGLUT2) gene (Punnakkal et al., 2014).

#### 1.4.1.1.2 Central cells

Central cells and their dendritic arbor remain within the same lamina II<sub>i</sub> and they have the rostrocaudal extension that is shorter than that of islet cells (Figure 1-4). The dendritic tree often asymmetrical, being larger either rostral or caudal to the cell bodies. They are restricted in the mediolateral and dorsoventral planes (Grudt and Perl, 2002). The axons travelled rostrocaudally, and they can extend into lamina I and the superficial part of lamina III (Grudt and Perl, 2002, Yasaka et al., 2010). Cells that have a dendritic tree RC:DV ratio of more than 3.5 and a rostrocaudal extension of less than 300  $\mu\text{m}$  was identified as central cells (Yasaka et al., 2007). Grudt and Perl (2002) further divide these cells into two populations, based on their action potential discharge. Those that fired action potentials throughout the depolarizing current pulse were classed as tonic central cells, while those that fired action potential only at the beginning of the current pulse were called transient central cells. Transient central cells were further divided based on the presence or absence of potassium current  $I_A$ . Transient central cells in lamina II were found to form excitatory monosynaptic inputs to vertical cells in lamina II<sub>o</sub> (Lu and Perl, 2005). Dorsal root stimulation experiments showed that most of central cells received monosynaptic eEPSCs from C fibres and a few cells receive polysynaptic input from A $\delta$  fibres, similar to what were seen in islet cells (Yasaka et al., 2007). Central cells are found among both excitatory or inhibitory (Yasaka et al., 2010).

#### 1.4.1.1.3 Radial cells

Radial cells have somata that are usually found near the middle of lamina II (Grudt and Perl, 2002, Yasaka et al., 2007). They have dense dendritic trees that extend in all directions when viewed in sagittal section with restricted rostrocaudal (<275  $\mu\text{m}$ ) and dorsoventral (<160  $\mu\text{m}$ ) plane within lamina II (Yasaka et al., 2010). In addition, Grudt and Perl (2002) described that the dendritic arbors of radial cells are also very restricted in the mediolateral plane and that they had low to moderate density of dendritic spines (Figure 1-4). The axons of radial cells normally spread rostrally or caudally for more than 500  $\mu\text{m}$  from the cell body. They generally remain within lamina II, with some axons

extending into laminae I and/or III (Yasaka et al., 2010). These cells have action potential that are delayed from the onset of depolarizing current pulse injection and show irregular discharge pattern of action potentials (Grudt and Perl, 2002). Dorsal root stimulation experiments revealed that radial neurons received monosynaptic input from both C-fibres and A $\delta$ -fibres and as well as IPSCs from myelinated and unmyelinated primary afferents (Grudt and Perl, 2002, Yasaka et al., 2007). Radial cells usually exhibit a high frequency of spontaneous EPSCs and spontaneous IPSCs, thus showing that they received numerous excitatory and inhibitory synapses (Grudt and Perl, 2002). Radial cells were found to contain VGLUT2 (Yasaka et al., 2010), suggesting that they are excitatory cells. Consistent with this, radial cells were also identified in VGLUT2::eGFP mice (Punnakkal et al., 2014) but not in Gad67::eGFP (Heinke et al., 2004).

#### 1.4.1.1.4 Vertical cells

Vertical cells population described by Grudt and Perl (2002) includes stalked cells which was identified by Gobel (1975). Their dendritic trees spread in the rostrocaudal plane with limited mediolateral extension (Figure 1-4). Although some cells have many dendritic spines, others have relatively few (Grudt and Perl, 2002, Yasaka et al., 2010). The cell bodies are generally found in lamina II and they have projecting dendrites which can pass through laminae II-IV. Nevertheless sometimes the dendrites can extend dorsal to the soma (Grudt and Perl, 2002). Yasaka et al. (2007) described the vertical cells as having dendritic arbors shaped like a fan or cone with soma lying dorsal at the apex. Usually, axons of vertical cells extend rostral and caudal to the dendritic arbor, remaining within lamina II. However, they often had axons that enter lamina I and some travelled into deeper laminae (Grudt and Perl, 2002). Dorsal root stimulation experiment showed that vertical cells receive monosynaptic input from A $\delta$  primary afferent fibre and evoked IPSCs from both C-fibre and A $\delta$  fibre (Yasaka et al., 2007). Most vertical cells are excitatory however some cells with similar morphology have been showed to be inhibitory (Maxwell et al., 2007, Yasaka et al., 2010). Some lamina I neurons receive monosynaptic input from excitatory vertical cells in lamina II<sub>o</sub> (Lu and Perl, 2005). Interestingly, those inhibitory vertical cells are generally smaller and have less compact dendritic arbor (Yasaka et al., 2010).

#### 1.4.1.1.5 Minor classes and unclassified cells

Apart from the four main cell groups, Grudt and Perl (2002) identified one more class of cells in lamina II known as medial-lateral neurons. The mediolateral and dorsoventral expansion of the dendritic trees of these cells were larger than that of islet, radial or central cells. In addition, their dendrites extended from lamina I to the superficial part of lamina III in dorsoventral direction. Meanwhile, their axons spread further than the dendritic trees in the rostrocaudal plane, and extended from lamina I to the superficial part of lamina III. The medial-lateral cells exhibited  $I_A$ -like transient outward current, similar to that of transient central cells. However, they were different from transient central cells based on their tonic firing pattern and the lack of IPSC evoked by dorsal root stimulation. Only three from 157 lamina II cells recorded by Grudt and Perl (2002) belong to this group, and therefore it is not considered to be major classes. Furthermore, Punnakal et al. (2014) did not identify any cells belonging to this class.

The classification scheme by Grudt and Perl (2002) cannot be applied to ~30% of lamina II neurons (Yasaka et al., 2007, Maxwell et al., 2007, Yasaka et al., 2010). The morphology of these neurons does not fit into any of the recognize morphological classes, and they may represent more than one cell type.

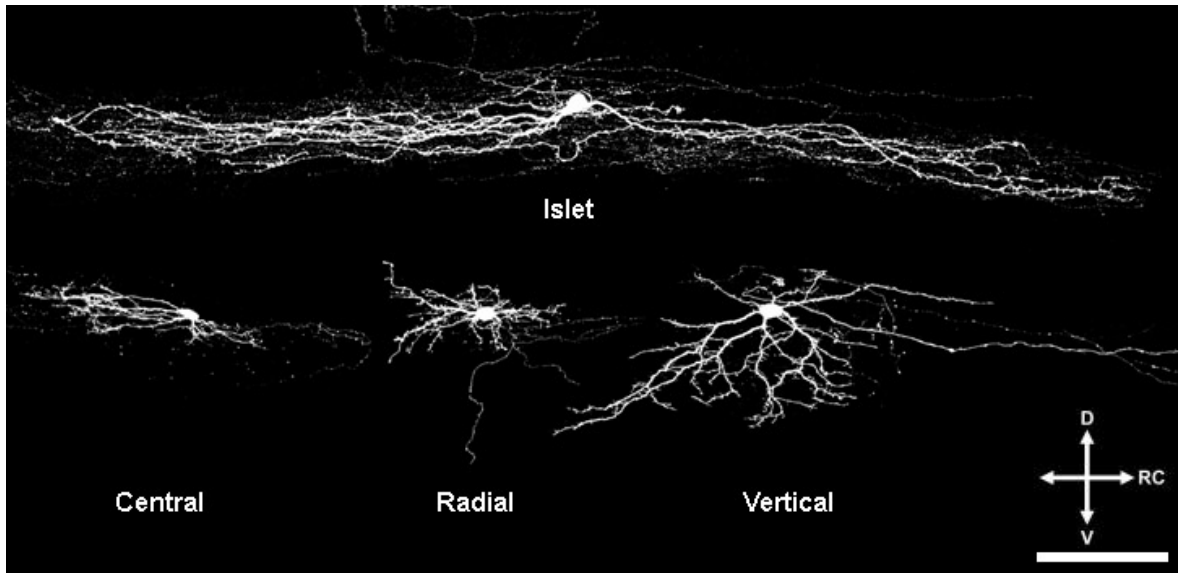


**Figure 1-4 Four main morphological classes of interneurons in lamina II of dorsal spinal cord**

Islet cells have dendritic trees spread extensively in rostrocaudal direction ( $> 400 \mu\text{m}$ ) with a limited dorsoventral extent. Central cells have less extensive rostrocaudal extension ( $< 400 \mu\text{m}$ ) that is shorter than islet cells with restricted mediolateral and dorsoventral extent. Radial cells have a short dendritic trees that extent in all directions, and vertical cells have a projecting dendrites shaped like a fan with cell bodies located dorsally. These cells are seen in sagittal section and their morphology are similar with the main classes described by Grudt and Perl (2002). D: dorsal, V: ventral, RC: rostrocaudal. Scale bar =  $100 \mu\text{m}$ . Modified from Todd (2010).

### 1.4.1.2 Firing pattern

Electrophysiological experiments have shown that interneurons can be classified according to their firing pattern, in response to injected depolarizing current. Islet, central, vertical and radial cells differ in their action potential discharge responses during depolarization current injection. They can be categorized as tonic firing, delayed firing, initial bursting, single spiking, gap and reluctant firing (Grudt and Perl, 2002, Ruscheweyh and Sandkühler, 2002, Heinke et al., 2004, Prescott and Koninck, 2002, Yasaka et al., 2010). Tonic firing pattern is defined as having action potential discharge at regular interval throughout the current pulse, meanwhile delayed firing neurons exhibit a long latency before the onset of action potential. Initial bursting firing neurons discharge action potential only at the onset of current injection. The single spiking firing pattern is defined as having only one or two action potentials discharged at the onset of current injection. The gap between the first and second action potential is long in gap firing neurons, followed by continuous, the regular firing of action potentials. No action potentials occur after depolarising current injection in reluctant firing neurons.

Gap, delayed and reluctant action potential firing patterns are probably related to the presence of  $I_A$  current, which is mediated by a voltage-gated potassium channel. These A-type firing patterns are associated with excitatory interneurons and are mostly confined within this group (Yasaka et al., 2010). In addition, tonic or initial burst firing pattern are commonly exhibited by inhibitory interneurons.

### 1.4.1.3 Neurochemical markers

As an alternative strategy, neurochemical markers have been widely used to distinguish different groups of interneurons (Todd, 2010). Some of these markers such as galanin and NPY are expressed mainly by inhibitory interneurons, meanwhile some such as somatostatin, neurotensin and neurokinin B (NKB) are exclusively found in excitatory interneurons (Rowan et al., 1993, Proudlock et al., 1993, Todd et al., 1994, Simmons et al., 1995, Polgár et al., 2006). However, others such as nNOS, dynorphin and CR are expressed by both inhibitory and excitatory interneurons (Sardella et al., 2011a, Sardella et al., 2011b, Smith et al., 2015). Interestingly, these neurochemical populations differ

in their laminar distribution within the dorsal horn. For example, parvalbumin-expressing cells are found in lamina II<sub>i</sub>-III, meanwhile NPY-immunoreactive cells are scattered throughout laminae I-III (Polgár et al., 2011, Hughes et al., 2012). This suggest that there is an association between these neurochemical classes and functional populations (Todd, 2017).

#### 1.4.1.3.1 Inhibitory interneurons

Four largely non-overlapping groups of inhibitory interneurons have been identified so far in laminae I-III of rat dorsal horn based on the expression of neuronal nitric oxide synthase (nNOS), neuropeptide Y (NPY), galanin and parvalbumin (Polgár et al., 1999, Tiong et al., 2011, Sardella et al., 2011b, Hughes et al., 2012). In addition, there is extensive overlapped between galanin and dynorphin among inhibitory interneurons (Sardella et al., 2011a). The neurochemical populations are similar in the mouse except that there is some overlapped between the populations and in addition some cells contain both galanin and NPY (Iwagaki et al., 2013, Kardon et al., 2014, Boyle et al., 2017). The cells also differ in their expression of receptors, their responses to noxious stimuli and their postsynaptic targets.

The somatostatin receptor ( $sst_{2A}$ ) is virtually restricted to inhibitory neurons, and in both rat and mouse, about half of the inhibitory interneurons express  $sst_{2A}$  receptors (Todd et al., 1998, Polgár et al., 2013a). Expression of  $sst_{2A}$  receptors differs between each of the neurochemical populations mentioned above. Almost all inhibitory cells that express nNOS and galanin have  $sst_{2A}$  receptor but the receptor is expressed by fewer of the NPY-positive cells and not in parvalbumin-immunoreactive neurons (Iwagaki et al., 2013, Polgár et al., 2013b). A recent study using mouse, estimated that more than 90% of inhibitory dynorphin cells also expressed  $sst_{2A}$ . (Boyle et al., 2017). nNOS and dynorphin are present in both excitatory and inhibitory populations, and thus immunostaining for the  $sst_{2A}$  receptor can help to distinguish between these cell types (Sardella et al., 2011a, Sardella et al., 2011b, Polgár et al., 2013b). In addition, electrophysiological experiments have shown that somatostatin acting on the  $sst_{2A}$  receptor causes hyperpolarization of inhibitory cells and thus disinhibition (Yasaka et al., 2010).

Both phosphorylated extracellular signal-regulated kinases (pERK) and transcription factor Fos are a marker for neuronal activation (Gao and Ji, 2009). After a variety of noxious stimuli including pinch, heat, capsaicin and the formalin test, cells immunoreactive for NPY and galanin show pERK. However, only a few of the nNOS cells and none of parvalbumin cells show pERK (Polgár et al., 2013b). Even though inhibitory nNOS cells did not show pERK after the above stimuli, Fos was seen in the majority of these cells following formalin and noxious heat stimulation. In addition, following a pinch stimulus, pERK is seen in lamina III NPY-immunoreactive cells (Iwagaki et al., 2016). Capsaicin causes activation of the heat sensitive channel TRPV1 (Caterina et al., 1997). However, surprisingly in the experiments described above, nNOS-expressing cells did not respond to capsaicin. This may be explained by innervation of the nNOS-immunoreactive cells by TRPV1-lacking heat nociceptors (Polgár et al., 2013b). Neurons that contain parvalbumin do not show pERK or express Fos after various types of noxious stimulation, which suggest that these cells are only involved in innocuous sensations (Polgár et al., 2013b).

Many studies have shown that, inhibitory cells that express NPY, nNOS, parvalbumin or galanin differ in their synaptic contacts. For example in rat, NPY immunoreactive boutons selectively innervate NK1r-immunoreactive lamina III ALT nociceptive projection neurons. However, this ALT neurons are not exclusively innervated by NPY-containing axonal boutons, as they also receive input from other GABAergic axons (Polgár et al., 1999). In addition, the other synaptic targets of inhibitory NPY-expressing neurons include excitatory PKC $\gamma$ -positive interneurons in lamina II<sub>i</sub> (Polgár et al., 2011). The present of gephyrin puncta as the contacts formed by NPY-expressing boutons on the PKC $\gamma$ -immunoreactive cells indicate that these are sites of GABAergic synapses. This study also found evidence that lamina III NK1r-expressing projection neurons and PKC $\gamma$ -immunoreactive cells are innervated by different group of NPY-positive neurons. The NPY-containing axonal boutons that were in contact with lamina III NK1r-expressing projection neurons were larger and had a stronger NPY-immunoreactivity compared to those axonal boutons that innervated PKC $\gamma$ -positive cells. A study using mouse found NPY-immunoreactive axons also innervate lamina III spinoparabrachial projection cells that express NK1R as well as that and those lack NK1r (Cameron et al., 2015). A recent study that involved

both electrophysiological and morphological experiments was carried out using a NPY-eGFP transgenic mouse line, to look at the cells that express NPY (Iwagaki et al., 2016). However, only 33% of the NPY-immunoreactive cells in laminae I-II were GFP positive although GFP was present in 82% of those in lamina III. Using dorsal root stimulation, they found that some NPY cells are innervated by C primary afferent neurons. These C fibre input were not affected by bath-applied capsaicin. In addition, fewer of the cells showed an increase in mEPSC frequency in response to capsaicin and none responded to icilin. This suggests that most of the NPY-expressing cells do not receive input from TRPV-1-expressing or TRPM8-expressing primary afferents. Iwagaki et al. (2016) also found most lamina III NPY-expressing cells have dendrites that project into SDH, which is consistent with a monosynaptic input. Furthermore, the recorded cells were located in the medial part of the lumbar enlargement, which lacks of C-LTMRs, since this region receives input from glabrous skin. This suggests that NPY-immunoreactive cells are innervated by C<sup>MrgD</sup> fibres that lack TRPV1. These primary afferent neurons are most probably involved in mechanical nociception (Iwagaki et al., 2016, Cavanaugh et al., 2009).

Puskár et al. (2001) found that in the rat a quarter of the GABAergic boutons synapsing on the lamina I giant projection neurons were derived from cells containing nNOS, while only 6% of the inhibitory synapses are from NPY-expressing boutons (Polgár et al., 2011). Meanwhile, only 3% of gephyrin puncta on lamina I NK1r-expressing projection cells associated with nNOS axonal boutons (Puskár et al., 2001). Most of parvalbumin-immunoreactive axons terminal form axoaxonic synapses with central boutons of A-LTMR and are postsynaptic to it, suggesting that these cells is an important source of presynaptic inhibition of myelinated (A-LTMR) primary afferent fibres and also receive monosynaptic input from these afferents (Hughes et al., 2012). Since these cells do not upregulate pERK or FOS and their major synaptic input is from A-LTMRs, Hughes et al. (2012) suggest that parvalbumin-expressing cells might have a role in inhibiting tactile input. Furthermore, they discovered that parvalbumin-positive cells never form presynaptic input on central bouton of type I glomeruli, thus supporting the idea that synaptic connections within the dorsal horn neurons are specific and well organized. In addition, Petitjean et al.

(2015) found that parvalbumin-immunoreactive cells form synapses on PKC $\gamma$  cells in lamina II<sub>i</sub>.

The distribution of NPY-immunoreactive cells distribution is similar in both mouse and rat (Rowan et al., 1993, Iwagaki et al., 2016, Boyle et al., 2017). In the rat, NPY-positive cells comprise 4-6% of the total population of neurons in laminae I-III (Polgár et al., 2011). However, a higher proportion of cells that are immunoreactive for NPY is seen in the mouse. NPY-immunoreactive cells accounted for about 8-10% of all neurons within laminae I-III (Boyle et al., 2017). All NPY-immunoreactive neurons in laminae I-III of the rat and mouse were found to be GABA-immunoreactive, and to express inhibitory marker PAX2, respectively (Rowan et al., 1993, Boyle et al., 2017). In the mouse, about 30% of the inhibitory interneurons within laminae I-II are positive for NPY, as are 25% of those in lamina III (Boyle et al., 2017). In addition, NPY is found in 15% and 5% of VGAT-positive boutons within laminae I-II, and lamina III, respectively (Polgár et al., 2011). The percentages for VGAT terminal boutons are slightly lower than the proportions of the inhibitory NPY-immunoreactive cells, probably due to the smaller number of axons arising from the NPY-positive cells (Polgár et al., 2011). In the mouse lamina II, NPY cells were morphologically heterogeneous but were never islet (Iwagaki et al., 2016). The quantitative study on the inhibitory interneurons by Boyle and colleagues found that 4-6% of NPY-immunoreactive cells in laminae I-III were also nNOS-immunoreactive (Boyle et al., 2017). NPY acts through Y1 and Y2 receptors. Both of these receptors can be found on the primary afferents, and Y1 receptors are also present on many neurons within the laminae I-III (Brumovsky et al., 2007). NPY has an analgesic effect and this may result from reducing the amount of substance P that is released by the primary afferent C-fibres and/or from an inhibitory effect on dorsal horn neurons (Duggan et al., 1991, Polgár et al., 2011).

The parvalbumin-expressing neuron cell bodies are located within laminae II-III and this finding is similar in rat, cat and mouse (Yamamoto et al., 1989, Antal et al., 1990, Anelli and Heckman, 2005, Hughes et al., 2012). The cells that expressed parvalbumin are more concentrated within laminae II<sub>i</sub> and III. However, in the mouse, about 80% of parvalbumin-immunoreactive cells are found in lamina III, whereas in the rat ~30% of the cells that expressed

parvalbumin are found within lamina II and ~60% of these are within lamina III (Antal et al., 1990, Hughes et al., 2012). Most of the parvalbumin-immunoreactive cells have dendritic trees that extend rostrocaudally, resembling islet cells. However, in the mouse, some of parvalbumin-immunoreactive neurons are found to be central-like cells (Hughes et al., 2012). Most parvalbumin cells are enriched with both GABA and glycine (Laing et al., 1994, Antal et al., 1990, Yamamoto et al., 1989, Abaira et al., 2017). Boyle et al. (2017) estimated that about 11% of the inhibitory interneurons within laminae I-II expressed parvalbumin. The axons of parvalbumin-expressing cells formed a dense plexus mainly within lamina II<sub>i</sub> and some of these axons extended into lamina III, where they formed axoaxonic synapses on central terminals of type II glomeruli. The majority of these axon terminals contain VGAT and they rarely express VGLUT1 (Hughes et al., 2012). A marker for glycine transporter, GlyT2 is also present in the axon terminals of parvalbumin-immunoreactive cells (Petitjean et al., 2015). Electrophysiological experiments revealed that after depolarizing current injection, the parvalbumin-expressing cells showed a high frequency of action potential discharge. These findings suggest that parvalbumin-positive cells provide a strong inhibitory control on the central terminals of myelinated primary afferent fibres. Parvalbumin cells also expressed the hyperpolarization activated cation current ( $I_h$ ) (Hughes et al., 2012) and this, together with a tonic firing discharge pattern are typical characteristics of islet cells (Grudt and Perl, 2002, Yasaka et al., 2010). It has been shown that the activation of parvalbumin-expressing cells reduced mechanical allodynia in a neuropathic pain model and that ablation of these cells leads to mechanical hypersensitivity (Petitjean et al., 2015). In the mouse, the majority of parvalbumin-containing cells within laminae I-III do not express with nNOS, although some of these overlap with the NPY cells (Boyle et al., 2017).

Galanin is involved in inflammatory pain where it exerts an inhibitory function (Wiesenfeld-Hallin and Xu, 1998). Among dorsal horn neurons, the peptide is restricted to GABAergic cells that do not use glycine as a co-transmitter (Simmons et al., 1995). Galanin cells are seen more within laminae I-II<sub>o</sub> than in laminae II<sub>i</sub>-III (Tiong et al., 2011). The cells in laminae I-II that are immunoreactive for galanin do not express nNOS, NPY or parvalbumin. However,

in lamina III most of the galanin-immunoreactive cells co-express nNOS. More than 90% of galanin cells in laminae I-II co-express  $\kappa$ -opioid peptide dynorphin, which can be revealed by using antibody against the dynorphin precursor preprodynorphin (PPD (Sardella et al., 2011a, Tiong et al., 2011).) The immunostaining of PPD is found mostly in the SDH and a few cells that are positive for this peptides are also seen in the deeper laminae (Sardella et al., 2011a, Boyle et al., 2017). Most of these dynorphin cells in laminae I and II are inhibitory cells and dynorphin is present in 4% of the VGAT containing boutons in these regions (Sardella et al., 2011a, Boyle et al., 2017). About 85% of inhibitory dynorphin cells are galanin-immunoreactive and this correspond to 96% of galanin cells (Boyle et al., 2017). Duan et al. (2014) showed that the ablation of inhibitory dynorphin-expressing cells in  $Pdyn^{Cre}$  mice causes mechanical allodynia with a normal response towards noxious heat and cold stimuli. They suggested that dynorphin cells are involved in gating mechanical pain. However, interpretation of this finding is complicated since dynorphin is transiently expressed during development, and thus cells that were ablated in this study might include the cells that transient expressed dynorphin (Todd, 2017).

In the dorsal horn, most of the nNOS cells are found in lamina II with some of these being located in laminae I and III (Sardella et al., 2011b). Around 30%-50% of nNOS cells within laminae II and III expressed PKC $\gamma$ , which is restricted to excitatory interneurons. This shows that nNOS is also present in the excitatory neurons (Sardella et al., 2011b). The nitric oxide (NO) produce by nNOS cells take part in the development and maintenance of hyperalgesia in inflammatory and neuropathic pain models (Lam et al., 1996, Guan et al., 2007).

A few studies using prion promoter-eGFP mouse line (PrP-eGFP) and basic helix-loop-helix transcription factor (*Bhlhb5*<sup>-/-</sup>) mice further linked the inhibitory cells that express galanin/dynorphin and nNOS (Ross et al., 2010, Iwagaki et al., 2013, Kardon et al., 2014). According to Iwagaki et al. (2013) cells that express eGFP under the control of the prion promoter (PrP) contain either nNOS, galanin or both neurochemical markers. In this study, eGFP cells accounted for 23% of neurons that express galanin, 57% of cells that contain only nNOS and 83% of those with both nNOS and galanin. Furthermore this cells did not express NPY or parvalbumin (Iwagaki et al., 2013). Iwagaki and colleagues also found that the

majority of these cells express  $sst_{2A}$  and that application of somatostatin caused PrP-eGFP cells to be hyperpolarized through the activation of G protein-gated inwardly rectifying potassium channels (GIRK). Initially, all of the PrP-eGFP cells were thought to be central cells (Hantman et al., 2004). However, a study by Ganley et al. (2015) showed that they are morphologically heterogeneous and were never islet cells. PrP-eGFP cells are innervated mostly by non-overlapping populations of unmyelinated afferents that express *Mrgprd*, TRPV1 or TRPM8 (Iwagaki et al., 2016).

A study by Ross et al. (2010) reported that in the SDH, some of the interneuron populations were found to be involved with the suppression of itch. The transcription factor *Bhlhb5* is needed for the survival of some populations of inhibitory interneurons in the dorsal horn and ablation of *Bhlhb5* causes increase respond towards pruritogen and the development of skin lesion that results from excessive scratching (Ross et al., 2010, Kardon et al., 2014). In *Bhlhb5* knockout mice, galanin/dynorphin- and nNOS-immunoreactive inhibitory interneurons are missing and these cells are called B5-I neurons. They accounted for two thirds of  $sst_{2A}$ -immunoreactive cells (Kardon et al., 2014). This study also showed that B5-I neurons that are galanin-immunoreactive expressed the endogenous  $\kappa$ -opioid receptor agonist dynorphin which suppress itch in respond to injections of various pruritogens. However, it is possible that GABA/glycine mediates the fast relief provided by counter stimuli such as scratching since *PPD*<sup>-/-</sup> and wild type mice have similar respond to intradermal pruritogens injection. Kardon and colleagues also found that B5-I neurons are innervated by capsaicin-, mustard oil- and menthol-responsive primary afferents, thus suggests that these cells inhibit itch by chemical counter stimuli.

Calretinin (CR) is one of the family members of calcium binding proteins and have a similar structure to calbindin (Camillo et al., 2014). Initially it was thought that CR is expressed only by excitatory interneurons (Todd, 2010). However, Smith et al. (2015) found that 15% of CR-immunoreactive cells in the SDH expressed *Pax2* and mostly they are islet cells. Details on inhibitory CR will be discussed further in chapter 3.

#### 1.4.1.3.2 Excitatory interneurons

Even though the excitatory interneurons accounted for 70% of the populations within laminae I-III, much less information was available on their organization. Through morphological studies, vertical and radial cells are found to be mostly glutamatergic (Grudt and Perl, 2002, Maxwell et al., 2007, Yasaka et al., 2010). Immunocytochemical markers such that the neuropeptides somatostatin (SST), neurotensin, neurokinin B (NKB) and gastrin releasing peptide (GRP) are mainly confined within excitatory interneurons and it has been shown that substance P-, neurotensin-, NKB- and GRP-expressing cells form distinct populations, which are thought to be functionally diverse (Gutierrez-Mecinas et al., 2016a, Gutierrez-Mecinas et al., 2017). Other markers that are associated with excitatory interneurons include the calcium binding proteins calbindin and CR and PKC $\gamma$  are glutamatergic neurons (Antal et al., 1991, Polgar et al., 1999, Smith et al., 2015). However, about 15% of CR cells in laminae I and II are inhibitory (Smith et al., 2015).

VGLUT-2 has been detected in excitatory interneurons, such as those cells that contain substance P, neurotensin, enkephalin and somatostatin (Todd et al., 2003). This is consistent with previous studies that have shown that none of the somatostatin- and neurotensin-immunoreactive cells in the SDH contain GABA (Todd and Spike, 1992, Proudlock et al., 1993). Todd and colleagues also found that VGLUT2 immunoreactivity was never seen in glycinergic, cholinergic, monoaminergic axons and very rarely co-labelled with GAD-immunoreactive (GABAergic) boutons within the spinal cord.

The somatostatin (SST)-positive cells are concentrated in the superficial laminae, although scattered cells are seen in lamina III (Proudlock et al., 1993). Somatostatin is never found in GABAergic or glycinergic neurons within laminae I-II and is expressed by various populations of excitatory interneurons in this region (Proudlock et al., 1993, Gutierrez-Mecinas et al., 2016a). However, some of the SST-immunoreactive cells in the deeper laminae are found to be inhibitory (Proudlock et al., 1993, Duan et al., 2014). SST is extensively co-localized with neurotensin, PPTB, GRP and other excitatory neuronal markers such as PKC $\gamma$  and CR (Gutierrez-Mecinas et al., 2016a, Polgar et al., 1999). However, Duan et al. (2014) reported that SST and CR are found in two separate populations of cells

based on their finding that SST mRNA is absent in Cre-expressing neurons in the CR<sup>Cre</sup> knock-in mice. On the contrary Gutierrez-Mecinas and colleagues found that more than half of the cells that contain SST also express CR and two thirds of CR-immunoreactive cells co-express SST (Gutierrez-Mecinas et al., 2016a). SST-expressing neurons are morphologically heterogeneous with several distinct firing patterns (Duan et al., 2014). This study reported that the ablation of SST-expressing neurons in the dorsal horn dramatically reduced the mechanical pain and this is probably due to the loss of more than one populations of excitatory interneurons, parallel to the finding that the majority of excitatory populations co-express SST (Todd, 2017).

The PKC $\gamma$ -immunoreactive neurons are mainly found in lamina II<sub>i</sub> and III (Polgar et al., 1999). However, a few of these cells can be seen dorsal and ventral to this region. The PKC $\gamma$ -immunoreactivity is seen in the cell body and extends into the dendrites which form a dense plexus within lamina II<sub>i</sub> (Gutierrez-Mecinas et al., 2016a). These cells are found to play a role in the development of mechanical allodynia in a chronic pain state since PKC $\gamma$  knock-out mice showed a normal mechanical threshold for evoking hindpaw withdrawal on the injured side to a mechanical stimulus in the partial sciatic nerve injury model (Malmberg et al., 1997). A study reported that PKC $\gamma$ -positive cells receive input from lamina III glycinergic neurons and form part of a pathway that contributed to mechanical allodynia (Lu et al., 2013). Two years later, Petitjean et al. (2015) reported that this lamina III glycinergic neurons correspond to the parvalbumin cells. This finding suggested that the feedforward inhibition of A-LTMR input to the PKC $\gamma$ -immunoreactive cells is provided by parvalbumin-positive cells, thus leading to the prevention of mechanical allodynia.

The neurotensin-immunoreactive cells are found within lamina II<sub>i</sub> and the dorsal part of lamina III. More than 90% of neurotensin axons express VGLUT2 and are enriched with glutamate (Todd et al., 1994, Todd et al., 2003). In addition, none of the cell bodies are found to be GABA-immunoreactive (Todd et al., 1992). Mostly, these cells overlap with the dense plexus of PKC $\gamma$  dendritic trees in lamina II<sub>i</sub>, and 90% of them co-express PKC $\gamma$  (Gutierrez-Mecinas et al., 2016a). This study also found that NT and GRP cells are separate, although there is some overlap with NT and preprotachykinin B (PPTB) in laminae I-II. The neurokinin B

(NKB) somata can be revealed by immunostaining for PPTB, which is a precursor for NKB (Kaneko et al., 1998, Polgár et al., 2006). PPTB immunoreactivity is concentrated in laminae II<sub>i</sub> and III of the dorsal horn (Gutierrez-Mecinas et al., 2016a). In the rat, almost all of the PPTB-immunoreactive axons also expressed VGLUT2 (Polgár et al., 2006). Meanwhile in the mouse, cells that contain PPTB mRNA within the laminae II-III are immunoreactive for Tlx3, which control the expression of VGLUT2, thus suggest that NKB is expressed mostly by excitatory interneurons within this region (Xu et al., 2008). Half of the cells that are immunoreactive for PPTB also expressed PKC $\gamma$  but none of them are overlap with GRP cells (Gutierrez-Mecinas et al., 2016a). Ablation of NKB expressing cells in the Tac2<sup>Cre</sup> mice, did not have an effect on the nerve injury-induced mechanical allodynia (Duan et al., 2014).

GRP and gastrin releasing peptide receptor (GRPR) are believed to be involved in modulating itch (Sun and Chen, 2007, Sun et al., 2009). In the spinal cord, GRP is seen in the superficial laminae of the dorsal horn and is contained within structures resemble axons (Takanami et al., 2014, Gutierrez-Mecinas et al., 2014). It has been reported that GRP is expressed by the primary afferents based on immunocytochemistry study and they did not found *GRP* mRNA expression in the SDH (Sun and Chen, 2007). However, a few groups suggested that, this is due to the cross reaction with substance P, since many studies cannot detect mRNA for GRP in the dorsal root ganglion (Gutierrez-Mecinas et al., 2014, Michael et al., 2012, Solorzano et al., 2015). The most common method to reveal GRP cells is through GRP-eGFP transgenic mouse line, in which eGFP is expressed only by the cells with GRP mRNA (Solorzano et al., 2015, Gutierrez-Mecinas et al., 2016a). Mostly GRP axonal boutons also expressed VGLUT2 but usually they are not immunoreactive for VGAT, thus support the idea that GRP are expressed in the excitatory interneurons (Gutierrez-Mecinas et al., 2014). Even though GRP neurons are part of the itch pathway, only a few of these cells express Fos or pERK following intradermal injection of chloroquine (Bell et al., 2016). GRPR is also involved in normal itch responses, since mice lacking these receptors show reduced itch behaviours after administration of histamine-independent pruritogens (eg: chloroquine), without alteration in pain threshold (Sun and Chen, 2007). Furthermore, the ablation of GRPR-expressing neurons with intrathecal saporin conjugated to bombesin reduced behavioural responses to

pruritogens (Sun et al., 2009). This authors also found increased pruritogens-evoked scratching after intrathecal administration of GRPR agonists, and less scratching after intrathecal administration of GRPR antagonists.

The substance P axonal boutons are thought to derive from primary afferents or interneurons (Ju et al., 1987, Todd et al., 2003). Recently, a newly identified population of excitatory interneurons that express substance P was found in the dorsal horn of the spinal cord. These can be identified by using immunocytochemistry to reveal the substance P precursor, preprotachykinin A (PPTA). However, more reliable methods involve the intraspinal injection of adenoassociated virus (AAV) coding for a Cre-dependent form of eGFP (AAV.flex.eGFP) in mice, which Cre was knocked into the *Tac1* locus (*Tac1<sup>Cre</sup>*) (Gutierrez-Mecinas et al., 2017). These cells are seen in laminae I-III and in the deeper parts of the dorsal horn. Surprisingly Gutierrez-Mecinas et al. found that around 20% of PPTA-immunoreactive neurons in laminae I-III are Pax2 positive, indicating that they are inhibitory cells. Injection of AAV.flex.eGFP into *Tac1<sup>Cre</sup>;Ai9* mice causes expression of eGFP near the injection sites and around 10% of the eGFP-immunoreactive cells are labelled with Pax2 (Gutierrez-Mecinas et al., 2017). Studies using rat and mouse found axonal boutons that contain SP but not CGRP with a strong expression of VGLUT2 (Todd et al., 2003, Gutierrez-Mecinas et al., 2017). These are likely to be derived from glutamatergic interneurons (Todd et al., 2003). However, although some SP cells are found to be inhibitory neurons, very few boutons that contain SP and VGAT are identified. In addition, Gutierrez-Mecinas et al. (2017) found that SP-expressing cells overlapped extensively with somatostatin, but not with GRP, neurokinin B, neurotensin or PKC $\gamma$ . Many of the SP cells responded to noxious or pruritic stimuli (Gutierrez-Mecinas et al., 2017).

CR-expressing cells in the SDH are mostly (85%) excitatory interneurons (Smith et al., 2015). In Smith et al. (2016) they calculated about 30% of neurons in laminae I and II are labelled with CR. Excitatory CR comprise 25.5% of all neurons in superficial laminae. Since 75% of all interneurons are excitatory, therefore about 34% of excitatory interneurons are CR. The excitatory CR-expressing neurons have been shown to be involved in a polysynaptic circuit that links innocuous tactile input with nociceptive circuitry by transferring information from VGLUT3-

expressing interneurons to nociceptive circuits, which causes development of mechanical hypersensitivity/allodynia (Peirs et al., 2015). Ablation of CR-positive cells causes greater threshold of hind paw withdrawal towards noxious mechanical stimuli, without changes in motor coordination, light touch, thermal, pinprick and pinch stimulation thresholds (Duan et al., 2014).

## 1.5 Aims of the project

The study was based on a preliminary work carried out by Dr David I Hughes. Using electron microscopy on Neurobiotin filled CR islet cells patched in CR::eGFP mice, he showed that axonal boutons originated from these cells were presynaptic to central axon of type I glomeruli, which belong to C<sup>MrgD</sup> afferents. The main objective of the project was to characterize a population of inhibitory CR interneurons in the SDH and their synaptic connection with C<sup>MrgD</sup> primary afferent fibres. To carry out this study, we used several transgenic mouse lines including lines in which Nociceptin and RorB transgenes were either expressed under the control of the regulatory elements of the Nociceptin gene or knocked into the RorB locus, respectively. These lines allowed identification of populations of inhibitory interneurons in the superficial laminae. The aims of this project are to expand our knowledge concerning the inhibitory interneurons that are involved in the pain pathway, by testing the following 2 initial hypotheses:

1. That inhibitory CR neurons do not overlap with four other distinct neurochemical populations of inhibitory interneurons that were identified in the rat and mouse dorsal horn. These have been defined by the expression of neuropeptide Y (NPY), galanin, neuronal nitric oxide synthase (nNOS) or parvalbumin (Tiong et al., 2011, Sardella et al., 2011a, Sardella et al., 2011b, Hughes et al., 2012). This hypothesis was tested by carrying out immunocytochemistry reactions to look at the co-expression of CR with the other four neurochemical markers mentioned above.
2. That Nociceptin and Ror $\beta$  are suitable markers to identify inhibitory CR interneurons in lamina II. Most CR-expressing cells are excitatory interneurons (Albuquerque et al., 1999). However, about 15% of the cells are inhibitory cells (Smith et al., 2015).

During the course of the study, it was found that Nociceptin and Ror $\beta$  were expressed in the majority of inhibitory CR neurons. The combination of Nociceptin::eGFP; CR<sup>Cre</sup>; Ai9 mouse crossed allowed detection of these cells. Subsequently, it was found that Ror $\beta$  was a better marker. Ror $\beta$ <sup>CreERT2</sup>; Ai9 mouse line labelled predominantly CR inhibitory interneurons in lamina II. This allowed the testing of the following additional hypotheses.

3. That the inhibitory CR neurons are mostly islet cells (Smith et al., 2015). This study was carried out using whole cell patch-clamp recordings on parasagittal slices from adult mice with Neurobiotin labelling to allow for reconstruction of the neurons.
4. That they are closely associated with non-peptidergic C<sup>MrgD</sup> primary afferents, and specifically that they are the major source of axoaxonic synapse on the C<sup>MrgD</sup> afferents. This hypothesis was tested by immunocytochemistry reactions and electron microscopic study. Electron microscopy allowed identification of the axonal boutons of CR islet cells within Ror $\beta$  cells population and their relation to type I synaptic glomeruli.
5. That inhibitory CR islet cells in Ror $\beta$ <sup>CreERT2</sup>; Ai9 mice undergo significant change following peripheral nerve injury. Previously, it has been reported that there is no loss of GABA-immunoreactive neurons after chronic constriction injury (Polgár et al., 2004). However, it is possible that inhibitory CR islet neurons are affected because boutons belonging to C<sup>MrgD</sup> afferents which are thought to form their major synaptic input are lost under this condition. This hypothesis was tested by sciatic nerve transection (SNT) experiments.

## 2 General Methods

All experiments were approved by the Ethical Review Process Applications Panel of the University of Glasgow and were performed in accordance with the UK Animals (Scientific Procedures) Act 1986. The perfusion of the mice was performed by Dr Erika Polgár. Information on specific techniques will be provided in the related chapters.

## 2.1 Transgenic mouse lines and crosses

In order to investigate these inhibitory calretinin populations in superficial laminae, we used multiple mouse lines and crosses, which are described below and summarized in Table 2-1.

**Nociceptin::eGFP** is a bacterial artificial chromosome (BAC) transgenic line in which enhanced green fluorescence protein (eGFP) is expressed in the prepronociception/orphanin FQ (ppN/OFO) positive neurons (Zeilhofer et al., 2002). eGFP was introduced into ppN/OFO gene by homologous recombination (Yang et al., 1997). Then, polymerase chain reaction (PCR) was performed to generate 5' and 3' homology arms flanking the start codon and exon 2 of ppN/OFO. Southern blot analysis was used to identify BAC clones containing the preferred recombination. Purified linearized BAC DNA was injected into the male pronuclei of fertilized oocytes. This mouse line is generated by Professor Hanns Ulrich Zeilhofer from the University of Zurich. These mice were crossed with C57BL/6 mice, and for all experiments, heterozygous animals were used.

**CR-ires-Cre (CR<sup>Cre</sup>)** mice were first used by Taniguchi et al. (2011) to genetically target GABAergic neurons in the cerebral cortex. The allele of CR-ires-Cre carries Cre recombinase and an internal ribosome entry site in the *calretinin* locus. Cre expression is directed by the endogenous *calretinin* enhancer components to calretinin interneurons in the brain and cortex. Breeding these mice that contain Cre-mediated recombination with *loxP*-flanked sequences containing mice causes the offspring to be born without the floxed sequences (The Jackson Laboratory, 2018) .

**Ai9 reporter mice** contain a loxP-flanked STOP cassette, which prevents CAG promoter-driven transcription of the red fluorescent protein variant (tdTomato). The targeted mutation was inserted into the *Gt(ROSA)26Sor* locus. Breeding the Ai9 mice with mice that express Cre recombinase, will cause the STOP cassette to be deleted in the Cre-expressing cells, which causes the offspring to express strong tdTomato fluorescence (Madisen et al., 2010). This allowed the study of the structural details of the neurons including dendritic spine and axons by confocal microscopy.

**Ror $\beta$ <sup>eGFP</sup>** is a knock-in mouse in which retinoid-related orphan nuclear receptor  $\beta$  gene (Ror $\beta$ ) positive interneuron populations are labelled (Abraira et al., 2017). Using Phusion polymerase, 5' and 3' homology arm of Rorb gene was isolated from embryonic stem (ES) cell DNA before it was inserted into a vector. The Ror $\beta$ -specific exon was replaced by an eGFP cDNA. Chimeric mice were generated using ES cell clones. Chimeras were crossed with C57BL/6J mice, then intercrossed to produce homozygous Ror $\beta$  mice (Liu et al., 2013). This mouse line was generated by Professor David Ginty from Harvard University, who provided perfusion fix tissue which was analysed in this study.

**Ror $\beta$ <sup>CreERT2</sup>** is a knock-in targeted mutant mouse, which expresses Cre recombinase-estrogen receptor (Cre-ERT<sup>2</sup>) fusion protein from the mouse Ror $\beta$  promoter and the activity of this protein depends on the administration of tamoxifen. Administration of tamoxifen causes the Cre-ERT<sup>2</sup> to enter the nucleus of the cells and induce the Cre-ERT<sup>2</sup> fusion gene activity in Ror $\beta$ <sup>CreERT2</sup> mouse line. These mice were produced by means of a targeting vector that was constructed using recombineering technology (Liu et al., 2003). Through homologous recombination, the Cre-ERT<sup>2</sup> fusion-*FRT-Neomycin-Frt-loxP* cassette was introduced to the first coding ATG of exon 1 of the Ror $\beta$  gene in embryonic stem cells (ES) and the last 4bp of Ror $\beta$  were replaced (Abraira et al., 2017). Breeding these mice with mice that expressed *loxP*-flanked structures results in deletion of the floxed sequences in the Ror $\beta$ -expressing cells of the offspring.

**Ai34 reporter mice** carry a loxP-flanked STOP cassette, which prevents the transcription of CAG promoter-driven synaptophysin-tdTomato fusion gene. This promoter was inserted to the *Gt(ROSA)26Sor* locus. After breeding the Ai34 mice

with mice that express Cre recombinase, the STOP cassette will be deleted in the Cre-expressing tissues. The offspring will express the synaptophysin-tdTomato fusion protein which can be found concentrated in the synaptic terminals of the Cre-expressing neurons (Madisen et al., 2012).

**Nociceptin::eGFP; CR<sup>Cre</sup>; Ai9 mice:** Nociceptin::eGFP mice were crossed with CR<sup>Cre</sup> mice and Ai9 mice. In these triple transgenic mice line, calretinin and nociceptin cells contain tdTomato and eGFP, respectively, while cells with both calretinin and nociceptin contain both fluorescence proteins. These mice lines were used to investigate the morphology of inhibitory calretinin cells. For all crosses and experiments, heterozygous animals were used.

**RorB<sup>CreERT2</sup>; Ai9 mice:** RorB<sup>CreERT2</sup> mice were bred with Ai9 mice. The RorB cells expressed strong tdTomato native fluorescence due to the presence of Cre-recombinase in the cells after administration of tamoxifen. This mouse line was used to study the morphology of RorB-CR interneurons and their contacts with C<sup>MrgD</sup> primary afferents. Heterozygous animals were used for RorB<sup>CreERT2</sup> mice, and either heterozygous or homozygous animals were used for Ai9 mice.

**RorB<sup>CreERT2</sup>; Ai34 mice:** RorB<sup>CreERT2</sup> mice was bred with Ai34 mice. The synaptophysin-tdTomato fusion protein was targeted to the RorB axons which expressed Cre-recombinase. They were used to analyse contact between IB4-labelled primary afferents and RorB axonal boutons. This mouse line was also generated by Professor David Ginty from Harvard University, who provided perfusion fix tissue which was analysed in this study.

**Table 2-1 Summary of the different mouse lines and crosses used in various chapter of this study**

<b>Mouse line</b>	<b>Relevant chapter(s)</b>	<b>Remarks</b>
Noc::eGFP	Chapter 3 and 4	Nociceptin and RorB transgenes were either expressed under the control of the regulatory elements of the Nociceptin gene (Zeilhofer et al., 2002) or knocked into the RorB locus (Abraira et al., 2017), respectively. Populations of inhibitory interneurons in the superficial laminae can be identify using these lines.
RorB <sup>eGFP</sup>	Chapter 3 and 4	
Noc::eGFP; CR <sup>Cre</sup> ; Ai9	Chapter 3	
RorB <sup>CreERT2</sup> ; Ai9 mice	Chapter 5 and 6	
RorB <sup>CreERT2</sup> ; Ai34 mice	Chapter 5	

## 2.3 Perfusion fixation

Adult mice of either sex (14-32g) were deeply anesthetized using pentobarbitone injected intraperitoneally (30 mg). They were then perfused transcardially with a brief rinse of Ringer's solution, followed by perfusion with 250 ml of freshly made fixative. The fixative contained 4% de-polymerised formaldehyde in 0.1 M phosphate buffer (PB) for confocal study and 4% de-polymerised formaldehyde with 0.2%, 0.5% or 1% glutaraldehyde for electron microscopic study. A laminectomy was performed to expose the spinal cord. The dura mater was removed using curved blades, and lumbar segments L1-L5 were identified based on the pattern of input from dorsal roots. A block of tissue consisting of L1-L5 were removed from the spinal cord and were divided into individual segments. The lumbar cord segments were kept in fixative for 2 hours at 4°C and then transfer to PB. Lumbar segments that were not used immediately transferred to 30% sucrose in PB solutions in a liquid nitrogen tank.

## 2.3 Tissue processing and immunocytochemistry

Lumbar spinal cord segments from L1-L5 were used in all the experiments. The lumbar segments were cut into 60µm thick sections using a vibrating blade microtome (Leica VT 1200, Leica Microsystems Ltd Milton Keynes, UK). Sections with different orientation (transverse, sagittal and horizontal) were used depending on the purpose of the experiments. For example, transverse sections were used to look at the proportion of cells in the different laminae. Meanwhile, for the morphology of the cells, sagittal/horizontal sections were used to show the rostrocaudal extension of dendritic tree and axons of calretinin islet cells. All sections were immersed in 50% ethanol for 30 minutes to enhance antibody penetration (Llewellyn-Smith and Minson, 1992). Sections were then rinsed with phosphate buffered saline that contained 0.3M NaCl three times. For sections used in the electron microscopy study, details of tissue processing will be discussed in the corresponding chapter.

Sections were incubated in primary antibodies at 4°C for five days in most experiments unless stated otherwise. The sections were rinsed three times over 30 minutes in phosphate-buffered saline (PBS) prior to incubation in secondary antibodies for one day at 4°C. All secondary antibodies obtain from Jackson

ImmunoResearch, West Grove, PA, USA were raised in donkey and were species-specific. They were conjugated to Alexa 488, Alexa 647, Pacific Blue, Rhodamine Red or Biotin. Secondary antibodies were diluted 1:500 for Alexa 488, Alexa 647 and Biotin, 1:200 for Pacific Blue and 1:100 for Rhodamine Red. Apart from the reaction that was done for electron microscopy, primary and secondary antibodies were diluted in PBS containing 0.3% Triton-X100 and 5% normal donkey serum. Details of the sources and concentrations of primary antibodies are given in Table 2-2. Following the immunocytochemistry procedure, sections were rinsed again in PBS three times over the period of 30 minutes before being mounted on glass slides in anti-fade medium (Vectashield; Vector Laboratories, Burlingame, CA, USA) and stored at -20°C. The details on antibodies combination will be discussed in relevant chapter.

## 2.4 Antibody characterization

All antibodies used in this study were previously characterised and are shown to give specific staining for the antigens that they target. The IB4 antibody was raised against the lectin from *Bandeiraea simplicifolia* and specificity is shown by the absence of immunoreactivity in tissue without lectin. For all 3 calretinin antibodies staining is absent in the cerebral cortex of mice lacking calretinin (manufacturer's specification). All 3 calretinin antibodies were raised against recombinant human calretinin. The eGFP antibody was raised against full-length recombinant eGFP, and its staining matches that of eGFP (Iwagaki et al., 2013). Galanin immunostaining is absent from the brains of galanin knock-out mice (Makwana et al., 2010) and pre-treatment with galanin abolished dorsal horn immunostaining with galanin antibody, demonstrating its specificity for the peptide (Simmons et al., 1995).

The Homer antibody was raised against amino acids 1-175 of mouse Homer 1 and labels a band at 43-45 kDa in immunoblots of mouse brain (Nakamura et al., 2004). The mCherry antibody raised against the full-length amino acid sequence and also recognizes tdTomato. The mouse monoclonal antibody NeuN reacts with a protein in cell nuclei extracted from mouse brain (Mullen et al., 1992). In the rat spinal cord, all neurons, but not glial cells are labelled by Neun (Todd et al., 1998). The nNOS antibody recognizes a single band of 155 kDa in Western blots of rat hypothalamus and immunostaining is abolished by pre-incubation with

nNOS (Herbison et al., 1996). No specific staining of NPY is present following treatment with antiserum in sections that have been incubated with NPY peptide (Rowan et al., 1993).

The PAP antibody immunoreactivity is absent in spinal cord sections from knockout mice (Zylka et al., 2008). The antibody against Pax2 was raised against amino acids 188 to 385 of the mouse protein and distinguishes bands of the appropriate size on western blots of the kidney of the mouse embryo (Dressler and Douglass, 1992). The guinea pig parvalbumin antibody was raised against mouse parvalbumin and recognizes a protein band of the appropriate size on western blot. The sst2a antibody was raised against the C terminal 15 amino acids of the mouse sst2a receptor, coupled to keyhole limpet haemocyanin. Immunostaining is abolished by incubation with the peptide antigen (manufacturer's specification). The VGAT antibody were raised against amino acids 31-112 of the mouse protein and recognized a single band of the appropriate molecular weight in blots of brain extracts (Takamori et al., 2000).

## **2.5 Confocal microscopy and analysis**

Zeiss LSM710 confocal microscope equipped with argon multi-line, 405 nm diode, 561 nm solid-state and 633 nm HeNe lasers was used to scan sections. Unless otherwise stated, sections were scan from the top to the bottom of the sections. Scans were taken through dry (5x, 10x and 20x) and oil immersion (40x and 63x) lenses (numerical apertures: 1.3 for 40x objective and 1.4 for 63x objective). The pin hole was set to one Airy unit to minimise out of focus light.

## **2.6 Statistical analysis**

The statistical tests that were used in this study include: one-way ANOVA followed by Holm-Sidak post hoc for multiple-comparisons test and a student's t test. A *p* value of less than 0.05 was considered significant.

**Table 2-2 Primary antibodies used in this study**

<b>Antibody</b>	<b>Label</b>	<b>Species</b>	<b>Dilution</b>	<b>Source</b>
BS lectin I	Non-peptidergic C fibres	Goat	1:2000	Vector
CR	Interneurons	Goat	1:1000	Swant
CR	Interneurons	Mouse	1:1000	Swant
CR	Interneurons	Rabbit	1:1000	Swant
eGFP	Interneurons	Chicken	1:1000	Abcam
Galanin	Interneurons	Rabbit	1:1000	Bachem
Homer	Glutamatergic synapses	Goat	1:1000	M Watanabe
mCherry	Interneurons	Rabbit	1:2000*/1:10,000*/1:20,000	Abcam
NeuN	Neurons	Mouse	1:1000	Millipore
nNOS	Interneurons	Rabbit	1:2000	Millipore
NPY	Interneurons	Rabbit	1:1000	Bachem
PAP	Non-peptidergic C fibres	Chicken	1:1000	Aves Labs
Pax2	Inhibitory interneurons	Rabbit	1:1000	ThermoFisher Scientific
PV	Interneurons	Guinea pig	1:2500	M Watanabe
Sst2a	Inhibitory interneurons	Guinea pig	1:2000	Gramsch laboratories
VGAT	Inhibitory interneurons	Rabbit	1:1000	Synaptic systems

Different concentrations of antibodies against mCherry were used for immunocytochemistry and electron microscopy. A high concentration (1:1000) of mCherry antibody was used in confocal microscopic studies and dilute mCherry (1:10,000/1:20,000) was used in electron microscopic study.

### **3 Morphological features of CR islet cells within dorsal horn**

### 3.1 Introduction

Calcium binding protein calretinin (CR) was first identified in 1987 by genetic cloning from the chicken retina from which the name is derived (Rogers, 1987). In the spinal dorsal horn, CR-positive cells are mainly found in SDH (Ren et al., 1993), where most nociceptive fine myelinated A $\delta$  and unmyelinated C primary afferents terminate (Light and Perl, 1979, Zylka et al., 2005). This suggests that CR-expressing cells are involved in modulating nociceptive transmission from the periphery. CR-immunoreactive neurons are also present at a lower density in other part of dorsal horn such as laminae V-VIII and X (Ren et al., 1993).

In 1999, Albuquerque et al investigated CR-expressing neurons using cultures of dorsal horn from rat embryos and they concluded that these cells are mostly excitatory interneurons based on the absence of GABA and glycine immunoreactivity from more than 90% of CR-immunoreactive cells. Since then a few studies have used CR as a neurochemical marker for excitatory interneurons in superficial dorsal horn (Huang et al., 2005, Torsney et al., 2006, Smith et al., 2015, Smith et al., 2016). Based on the finding of Albuquerque et al. (1999), CR was initially thought to be expressed only by excitatory interneurons (Todd, 2010). However, recent studies using GAD<sub>67</sub><sup>eGFP</sup> knock-in mice have revealed that 13% of the eGFP-expressing (GABAergic) neurons in lamina II are positive for CR (Huang et al., 2010). In addition, 15% of CR-immunoreactive cells in superficial dorsal horn of mouse expressed the inhibitory marker Pax2, and 25% of Pax2 cells in lamina II were CR-positive (Smith et al., 2015).

The SDH is known to be densely packed with interneurons, with excitatory cells outnumbering the inhibitory neurons by three to one (Polgár et al., 2013a, Todd, 2010). Smith et al. (2016) calculated that about 30% of neurons in laminae I and II are labelled with CR antibody and these are mostly excitatory. Since, 15% of CR-immunoreactive cells are inhibitory, these make up ~4.5% of the total neurons population in superficial dorsal horn (Smith et al., 2016). More than 95% of CR-immunoreactive cells in the SDH were found in lamina II, with the remaining ~5% being present in lamina I of the mouse dorsal horn (Smith et al., 2015). Excitatory CR-immunoreactive neurons had a diverse morphology and included central, vertical, radial. Interestingly most of inhibitory CR-

immunoreactive neurons were islet cells (Smith et al., 2015). This finding is consistent with description on CR morphology by Ren et al. (1993).

Inhibitory CR expressing cells are mainly found in lamina II, thus, they might involve in nociceptive pathways. Smith et al. (2015) also studied the responsiveness of CR cells to noxious peripheral stimulation *in vivo*. In the spinal cord, under normal conditions, pERK is not induced by innocuous stimuli, but is seen following noxious stimuli including mechanical, thermal, chemical and itch (Ji et al., 1999, Gao and Ji, 2009, Zhang et al., 2014). They found that over 50% of the neurons in laminae I and II that showed pERK following noxious mechanical stimulation (pinch) also expressed CR. In addition, 15% of the pERK cells expressed both CR and Pax2. Conversely, only 23% of cells expressing pERK after noxious chemical stimulation (capsaicin) were found to contain CR, of which only 3% of pERK cells contained both CR and Pax2. These findings suggest that both excitatory and inhibitory CR cells are preferentially activated by noxious mechanical stimuli rather than capsaicin.

Smith et al. (2015) performed targeted patch clamp recording of eGFP cells from a transgenic mouse line that expressed eGFP under the control of the CR promoter (CR::eGFP). They found that some cells showed characteristics of inhibitory neurons such as tonic and initial bursting firing patterns during depolarizing step current injection (Smith et al., 2015, Yasaka et al., 2010). Smith and colleagues described these cells as atypical. They showed that atypical CR cells exhibited either non-selective cation current ( $I_h$ ) or low threshold 'T-type' calcium current ( $I_{Ca,T}$ ). The atypical CR cells received low frequency of excitatory drive as shown by low frequency and small amplitude spontaneous EPSCs (sEPSCs) (Smith et al., 2015). Unlike the typical CR cells, the atypical CR cells expressed mu- and delta- opioid receptors. Conversely the typical CR cells but not the atypical CR neurons responded to noradrenaline and serotonin (Smith et al., 2016). The major inhibitory input to the atypical CR cells derived from glycinergic neurons. The examination of Neurobiotin atypical filled cells resembles islet morphology.

Interestingly Hughes et al. (2012) had previously identified a population of parvalbumin-expressing cells in lamina III with similar characteristic to atypical CR cells. The morphology class of parvalbumin-expressing cells is islet type. They

received weak excitatory drive and their action potential discharge profiles are mostly tonic firing and initial bursting. Parvalbumin-expressing cells similarly receive inhibition that was predominantly glycinergic but not in inhibitory CR-expressing cells (Smith et al., 2015).

The aim of this part of the study is to characterise further inhibitory CR-expressing neurons by looking at the morphology and anatomical characteristics of these cells. In this chapter, Nociceptin::eGFP;CR<sup>Cre</sup>;Ai9 mouse lines were used to allow reconstructions of individual neurons. In this mouse line, eGFP is expressed by many inhibitory cells under the controlled of Nociceptin promoter. Meanwhile, the Cre mediated removal of a stop cassette will result in tdTomato expression by CR cells. Inhibitory CR cells could be identified by co-expression of eGFP and tdTomato. In addition, Nociceptin::eGFP and RorB<sup>eGFP</sup> mice were used to look for other anatomical features.

## **3.2 Materials and methods**

### **3.2.1 Morphology and analysis of recorded neurons**

Nine Nociceptin::eGFP;CR<sup>Cre</sup>;Ai9 mice 4-6 weeks old and of either sex (17-19g) were used for the reconstruction of recorded neurons. Sagittal slices were used for electrophysiological experiments as described previously and recorded cells were labelled with Neurobiotin as in the previous studies (Ganley et al., 2015, Iwagaki et al., 2016). At the end of the electrophysiological experiments, slices were fixed overnight in 4% formaldehyde dissolved in 0.1M in PB. The slices were washed using PBS for 3 times for 10 min and incubated overnight at 4°C in avidin-Pacific blue (1:1000) diluted in PBS containing 0.3% Triton-X100. Slices were washed again with PBS before being mounted in anti-fade medium on microscope slides in a window within a 270-350 µm thick agar spacer so that the cover slip will lie flat on the slice and also to avoid the slice from being compressed. These slides containing slices were stored at -20°C.

The recorded cells in the slices were first observed using a fluorescence microscope, to examine the general morphology of the cells. If the dendritic trees of the cells were beaded or appeared to have been truncated, the cells were not analysed further. The selected cells were scanned in detail afterward

using confocal microscopy. Scanning was started with 5x lens using 405 nm laser and dark field illumination to capture the whole slice and to determine the laminar location of the cell within the slice. Laminae I-II were seen as a distinct dark band due to the lack of myelinated fibres (Yasaka et al., 2010). Then, the lens was changed to 40x oil immersion to reveal eGFP and tdTomato within the cell bodies of the recorded filled cells. The entire structure including cell body, dendritic trees and axons of the Neurobiotin labelled cells was scanned through a 63x oil immersion lens, using the 405 nm laser, at 0.5  $\mu\text{m}$  z-separation with the aperture was set to 1 Airy unit. The scans were done through the whole depth of the structures of the cells to include all parts of the cells. However, in a few cases the deepest processes could not be seen clearly through the thickness of the slice. All images taken were saved as Zeiss.lsm 5 files and were viewed using Zen 2010 software. The image stacks were used as a template to manually reconstruct the cells with the neuron-tracing feature in NeuroLucida for Confocal Software (MBF Bioscience, Williston, VT, USA). The reconstructed cell drawings were saved as NeuroLucida.DAT files. Dendrites can be distinguished from axons as they have spines and their processes will taper with increasing distance from the cell soma. Meanwhile, axons are thinner than dendrites and they have varicosities, which were seen as irregularly spaced swellings along the process. All the parameters from individual neuron were acquired from the NeuroLucida Explorer output.

After the initial analysis, the slice was resectioned by embedding it in 3% agar (dissolved in distilled water). The agar was cut into a small block containing the slice and the bottom right corner of the agar was notched to reveal the correct orientation of the sections when mounted on the slide. The slice was cut into 60  $\mu\text{m}$  sections using a vibrating blade microtome, and these were then mounted on the microscope slides in sequential order with a similar orientation. The cells were rescanned using the confocal microscope as described above, in order to reveal parts of the dendritic trees and axons that were present deep within the slices and were difficult to resolve in the initial scans (Ganley et al., 2015). The scanned images were added to the original reconstruction drawing.

Apart from using dark field illumination to determine the laminar location of these cells, sections that contained the recorded cells were also incubated with

IB4 to locate the cells relative to the IB4 plexus, which is found in the middle of lamina II. The sections containing recorded filled cells were incubated overnight in unconjugated IB4 (1:1000) at 4°C followed by incubation in the primary antibody, goat anti-IB4 (1:2000) for 3 days. Following that, sections were incubated in secondary antibodies conjugated to Alexa 647 (1:500) for 24 hours. Sections were mounted in anti-fade medium and rescanned using the confocal microscope to reveal Pacific blue and Alexa 647.

### **3.2.2 Animals and tissue processing for other anatomical parts of the study**

Six Nociceptin::eGFP male adult mice, weighing between 17-28g were deeply anaesthetised with pentobarbitone and perfused through the left ventricle with freshly made 4% formaldehyde. The lumbar spinal cord segments (L1-L5) were dissected out from all animals and post-fixed for 2 hours with the same solution at 4°C before being transferred to PB. The L4 segments were cut into 60 µm thick transverse sections using a vibrating blade microtome followed by immersion in 50% ethanol for 30 minutes to enhance antibody penetration (Llewellyn-Smith and Minson, 1992). The segments were cut serially into 4 bottles and these were processed for further analysis. Perfusion fixed spinal cords from 3 juvenile RorB<sup>eGFP</sup> mice of either sex were received from Professor David Ginty from Harvard University and were processed in a similar way. All of these sections were then processed for multiple immunolabelling as described below.

### **3.2.3 CR and eGFP expression in Nociceptin::eGFP mouse**

To quantify the eGFP-positive cells and CR-positive cells in the Nociceptin::eGFP mouse, transverse sections from the L4 segments of 3 Nociceptin::eGFP mice were incubated with chicken anti-eGFP, rabbit anti-CR, mouse anti-Neun. These primary antibodies were revealed with Alexa 488, Rhodamine Red and Alexa A647, respectively. Following the immunocytochemical reaction, the sections were incubated in DAPI for 10 min for nuclear staining. Three sections from each mouse were randomly selected and scanned using confocal microscope. These were scanned with a Zeiss LSM 710 confocal microscope with a 40x oil immersion lens (numerical aperture 1.3), 1 µm z-step and the aperture set to 1 Airy unit.

Those sections were scanned to produce a z-stack of 30 optical sections. Tile scans were used to capture the whole width of laminae I-III. Scanned sections were analysed offline using Neurolucida for Confocal Software. The outline of the dorsal horn and the boundaries between laminae I-III were drawn. The lamina I/II boundary was drawn 20  $\mu\text{m}$  below the dorsal white matter and the ventral extend of the CR-immunoreactive cells was used to determine lamina II/III border. The ventral border of lamina III was taken as 100  $\mu\text{m}$  from lamina II.

Those sections were analysed using Neurolucida software. The outline of the dorsal horn and border between laminae I, II and III were drawn as described above. A modified optical disector method was used to obtain an unbiased sample of neurons in laminae I-II and lamina III of the scanned sections (Gutierrez-Mecinas et al., 2016a, Smith et al., 2016, Tiong et al., 2011). All cell nuclei (identified by both Neun and DAPI) that had their bottom surface between reference and look up sections (5th and 25th optical sections respectively) were plotted onto the Neurolucida drawing and neurons with nuclei present in the look-up section were then excluded. Then, the channel corresponding to eGFP and CR were then viewed, and the presence or absence of each type of staining was documented.

### **3.2.4 Distribution of inhibitory CR interneurons in laminae I-III of Nociceptin::eGFP and RorB<sup>eGFP</sup> mice**

To define the population of CR<sup>+</sup>/eGFP<sup>+</sup> cells that were inhibitory in the Nociceptin::eGFP and RorB<sup>eGFP</sup> mice, 3 transverse sections each from L4 segments of 3 Nociceptin::eGFP and 3 RorB<sup>eGFP</sup> mice were incubated with chicken anti-eGFP, goat or mouse anti-CR and rabbit anti Pax2. Following that, primary antibodies that were used in Nociceptin::eGFP mice were revealed with Alexa 488, Pacific Blue and Rhodamine Red, respectively. Meanwhile, primary antibodies that were used in RorB<sup>eGFP</sup> mice were revealed with Alexa 488, Rhodamine Red and Pacific Blue, respectively. Three sections from each mouse were selected randomly and scanned with confocal microscope and analysed using Neurolucida for Confocal Software as described before. For the Nociceptin::eGFP mice, the 5th optical section was used as the reference section and the 25th as the look up section. Meanwhile, in the RorB<sup>eGFP</sup> mice, the 5th and 20th optical sections were used instead as reference and look up

sections. The size of the disector in the RorB<sup>eGFP</sup> mice was reduced because the immunostaining with the CR antibody was strongest within the first 20<sup>th</sup> optical sections. Therefore, cell bodies that were located deep in the sections could not be analysed due to incomplete antibody penetration. All cell bodies of eGFP positive neurons in both animals that had their bottom surface of their nucleus between the reference and look up sections were plotted onto the drawing. Then, the channel for CR and Pax2 were then viewed and the presence or absence of both type of staining was documented for each of the selected eGFP immunoreactive neurons.

### 3.3 Results

#### 3.3.1 Morphology of the cells in the Nociceptin::eGFP; CR<sup>Cre</sup>; Ai9 mice

Eleven of the eGFP<sup>+</sup>/tdTomato<sup>+</sup> cells that were recorded from 9 Nociceptin::eGFP;CR<sup>Cre</sup>;Ai9 mice that had undergone whole cell recordings and been labelled with Neurobiotin were reconstructed manually using NeuroLucida Confocal software for morphological analysis. Examples of 3 reconstructed cells are shown in Figure 3-1. Some of the slices contained more than 1 cell with a maximum of 3 cells contained in a slice. When more than one cells present in a slice, the cells were sufficiently far apart to allow them to be differentiated and reconstructed. The cell bodies of all 11 eGFP<sup>+</sup>/tdTomato<sup>+</sup> neurons were located in lamina II and in each case, eGFP and tdTomato were detected in the cell bodies. Dendrites of each cells were completely filled with Neurobiotin since the labelling was consistent throughout the dendritic length and did not fade at the distal ends. All neurons had dendrites projecting extensively in the rostrocaudal axis (mean  $\pm$  SD; 257.65  $\mu$ m  $\pm$  47.35) and confined within lamina II. In most cases, the dendritic arborisations of these cells were very complex and numerous spines were presented on the whole dendritic length. Even though all cells had rostrocaudally extensive dendrites, in 1 case, the cell had dendrites that arborized mainly to one side of the cell body (Figure 3-1 a). The cell had a limited dorsoventral dendritic spread of 51.10  $\mu$ m  $\pm$  13.60 (mean  $\pm$  SD). In rat, the dendritic rostrocaudal and dorsoventral spread of individual neurons were measured to determine morphological classes, as defined by Yasaka et al.

(2007). Information on the dendritic dimensions with RC:DV ratio of all cells is shown in Table 3-1.

The axonal arborisations could be followed for considerable distances, thus suggesting that the labelling of axons was relatively complete in all cells. In 3 cases, axons were truncated at the surface of the slices. For the remaining 8 cells, the axons extended further rostrally and/or caudally than the dendrites and were limited to lamina II. All the cells have very fine axons with small boutons that were evenly distributed along the axons. Sagittal sections containing the cells bodies and dendritic trees of Neurobiotin labelled cells were reacted with IB<sub>4</sub> and the dendritic and axonal branches were found to be largely restricted within the IB<sub>4</sub> plexus (). The IB<sub>4</sub> plexus was confined to lamina II, with the most intense labelling in the middle of lamina and the pattern was identical to that reported in previous studies (Cavanaugh et al., 2011).

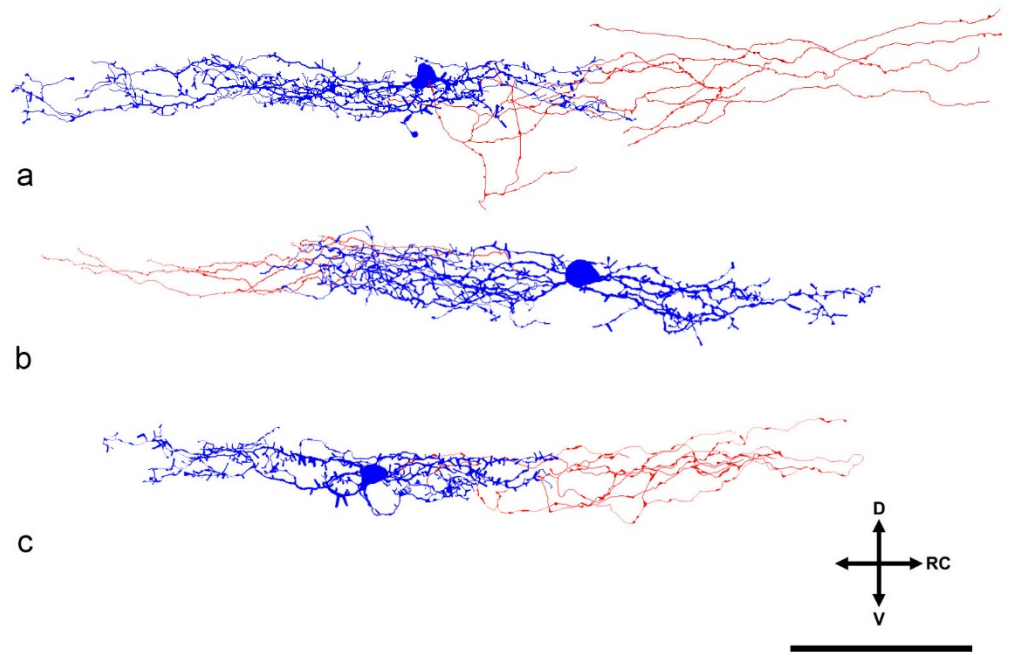


**Figure 3-1 Morphology of the CR<sup>+</sup>/eGFP<sup>+</sup> recorded cells in Nociceptin::eGFP;CR<sup>Cre</sup>;Ai9 mice**

Three examples (**a-c**) of Neurolucida reconstructions of recorded neurons. Cell bodies and dendritic trees are shown in blue and axons in red. These drawings show that CR<sup>+</sup>/eGFP<sup>+</sup> cells appear to be islet type. D: dorsal, V: ventral, RC: rostrocaudal. Scale bar = 100  $\mu$ m.

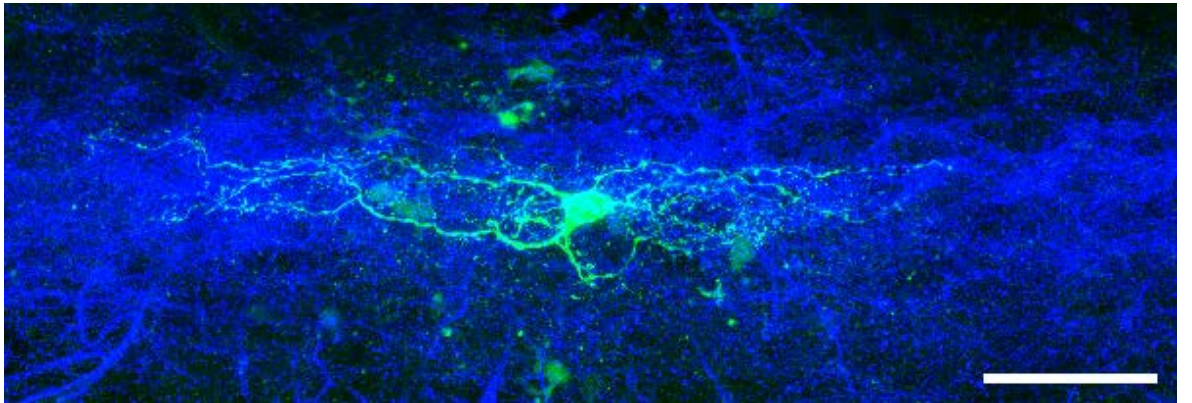


**Figure 3-2 Neurobiotin filled cell from Nociceptin::eGFP;CR<sup>Cre</sup>;Ai9 mouse.** Parasagittal section is showing 1 neurobiotin filled cell (green) and the dendritic and axonal branches were found to be largely restricted within the Isolectin B<sub>4</sub> (blue) in the middle of lamina II. All of the reconstructed cells resemble islet cell morphology. Scale bar = 50  $\mu$ m.

**Table 3-1 Dendritic dimensions of reconstructed eGFP<sup>+</sup>/tdTomato<sup>+</sup> recorded cells in Nociceptin::eGFP; CR<sup>Cre</sup>; Ai9 mice**

Cells	RC extent ( $\mu\text{m}$ )	DV extent ( $\mu\text{m}$ )	RC:DV ratio
1	193.50	62.80	3.08
2	211.10	35.60	5.93
3	221.60	50.80	4.36
4	229.30	45.00	5.10
5	241.40	72.60	3.33
6	246.40	39.30	6.27
7	263.80	64.80	4.07
8	264.40	35.50	7.45
9	288.50	54.90	5.26
10	337.20	64.30	5.24
11	342.80	36.50	9.39

### 3.3.2 The proportion of dorsal horns neurons that are labelled with CR<sup>+</sup>/eGFP<sup>+</sup> in Nociceptin::eGFP mice

The cell bodies and dendritic plexus of CR-immunoreactive neurons were located mostly in lamina II, although occasionally cells were seen in laminae I and III (Figure 3-3). This finding was similar to those of previous studies performed in mouse and rat (Smith et al., 2015, Ren et al., 1993). Meanwhile, the somata of eGFP-positive cells were scattered throughout laminae I-III and throughout the deeper laminae. In addition, a dense plexus of eGFP dendrites was seen in the middle of lamina II (Figure 3-4). Most of the cells that were double labelled with CR and eGFP were found in lamina II and the dendrites and axons forming a tight band in the middle of lamina II. Occasionally these CR<sup>+</sup>/eGFP<sup>+</sup> cells were seen in laminae I and III (Figure 3-3). The examination of confocal image stacks revealed that those cells that were located in laminae I and III also contributed to the band in the middle of lamina II. All CR<sup>+</sup>/eGFP<sup>+</sup> cells were NeuN-positive and this showed that they are neurons. The immunostaining of all antibodies used in this part of the study could be seen throughout the full thickness of the optical sections. Quantitative data obtain using disector method on this part of the study are shown in Table 3-2. A total of 2173 (mean 724) and 1578 (mean 526.2) neurons was analysed in laminae I-II and lamina III of 3 mice, respectively. Of this, 949 (mean 316.2) and 191 (mean 63.4) were CR-immunoreactive cells in laminae I-II and lamina III, respectively. The results were consistent across the three sets of sections. The total numbers of eGFP-positive cells identified in this part of the study were 477 (mean 159.1) in laminae I-II and 370 (mean 123.2) in lamina III. eGFP-immunoreactive cells accounted for 21.9% (range 20.9-22.7%) of all neurons in laminae I-II and 23.4% (range 21.7-26.3%) of those in lamina III. There were 126 (mean 42.3) and 38 (mean 12.8) CR<sup>+</sup>/eGFP<sup>+</sup> cells were found in laminae I-II and lamina III, respectively. Quantitative analysis revealed that, CR<sup>+</sup>/eGFP<sup>+</sup> cells constituted 5.8% (range 4.6%-6.7%) of neuronal populations in laminae I-II and 2.4% (range 1.3%-3.9%) of those in lamina III (Table 3-2).

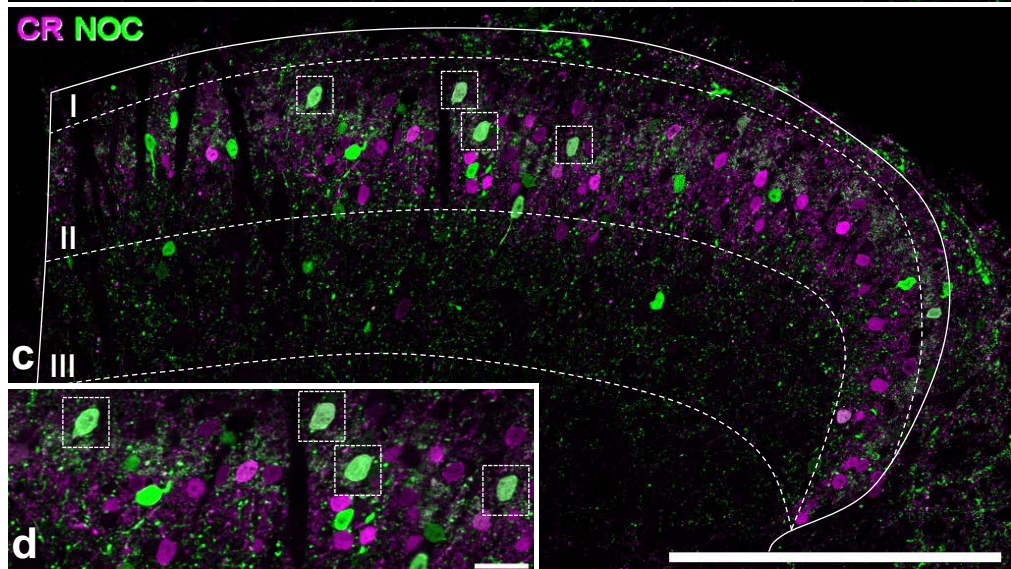
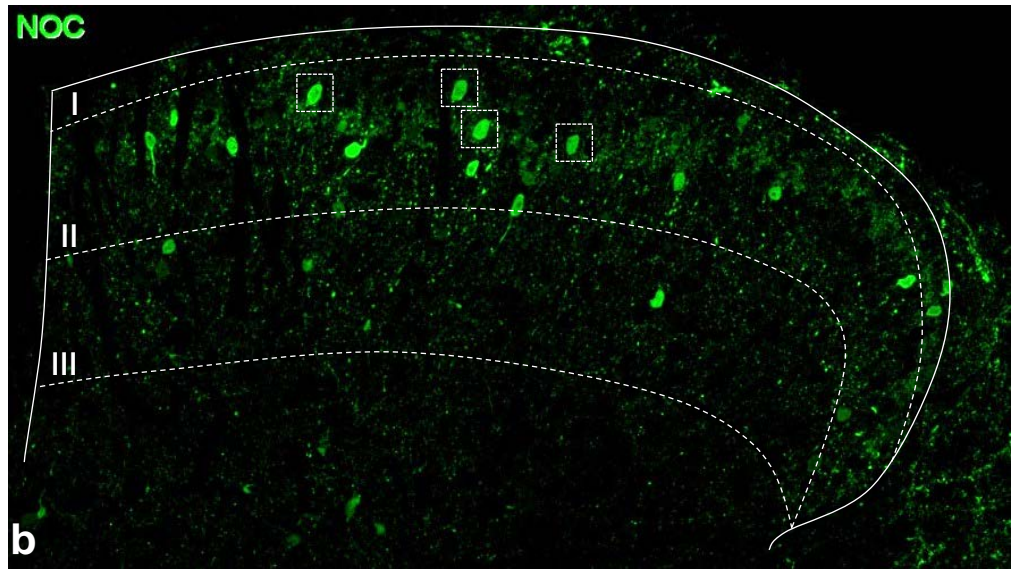
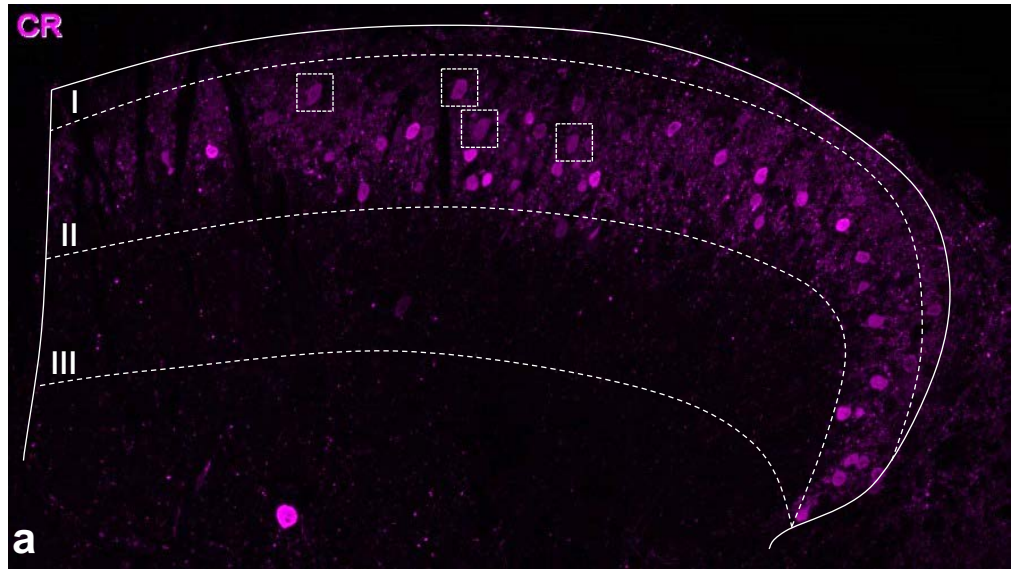


**Figure 3-3 CR and Noc::eGFP cells immunostaining in the dorsal horn.** **a, b** show a confocal image taken from a transverse section of lumbar 4 that had been immunostained to reveal calretinin (CR) and enhanced green fluorescence protein (eGFP). Calretinin immunoreactivity is numerous in lamina II with some staining in a deeper lamina. Noc::eGFP cells are present throughout laminae I-III. **c** a merged image. **a-c** four small boxes contain cells immunoreactive for both CR and eGFP. **d** Insert show a higher magnification view of four lamina II CR-Noc::eGFP cells. These neurons form a band of dendrites in the middle of lamina II. The dashed lines represents the borders between laminae I-III. Scale bar for main image = 200  $\mu\text{m}$ , scale bar for inset = 20  $\mu\text{m}$ .

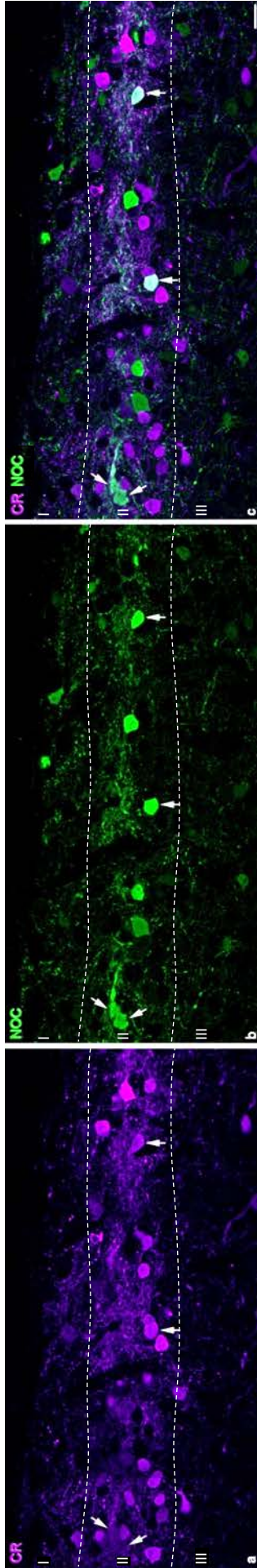


**Figure 3-4 Lamina II CR-Noc::eGFP cells form a tight band in the middle of lamina II.** **a, b** show a confocal scan of a sagittal section from a Noc::eGFP mouse that had been immunostained for calretinin (CR) and enhanced green fluorescence protein (eGFP). CR and eGFP immunostaining is present in lamina II. **c** a merged image. Four cells (arrows) are immunoreactive for both CR and eGFP. The dashed lines represents the dorsal and ventral borders of lamina II. Scale bar = 20  $\mu$ m

### 3.3.3 Quantitative analysis of inhibitory CR<sup>+</sup>/eGFP<sup>+</sup> cells in Nociceptin::eGFP and RorB<sup>eGFP</sup> mice

For this part of the study, two transgenic mouse lines were used to compare which line captures most of the inhibitory CR-immunoreactive cells in laminae I-III and also the extent to which they preferentially labelled these cells. Nine sections each from 3 Nociceptin::eGFP and 3 RorB<sup>eGFP</sup> mice were analysed. Tissue from Nociceptin::eGFP mice showed that the distribution of cells that were eGFP, CR, and CR<sup>+</sup>/eGFP<sup>+</sup> cells were similar to that described above. In the RorB<sup>eGFP</sup> mice, the distribution of CR-immunoreactive cells were similar to that in Nociceptin::eGFP but the penetration of CR antibody was less complete. The eGFP cell bodies and dendrites were found in laminae II-III and less frequently seen in lamina I. As seen in the Nociceptin::eGFP (see above), the eGFP dendrites were found in the middle of lamina II. The double labelled CR and eGFP cell bodies and dendrites were located in lamina II and occasional cells seen in laminae I and III of RorB<sup>eGFP</sup> mice.

Quantitative data for this part of the study is shown in Table 3-3. In Nociceptin::eGFP mice, 504 (mean 168.2, n=3) eGFP-positive cells were counted in laminae I-II and 374 (mean 124.7) of those were in lamina III. In SDH, 92.6% (range 89.1-96.3%) of the cells that expressed eGFP were positive for Pax2. Meanwhile, in RorB<sup>eGFP</sup> mice, 253 (mean 84.2, n=3) eGFP immunoreactive cells were counted in laminae I-II and 165 (mean 54.9) of those cells were counted in lamina III. Of this, 91.8% (range 90-93.1%) of eGFP cells were labelled with Pax2 in laminae I-II. In lamina II of both transgenic strains, 93% of eGFP positive cells were Pax2 positive. A total of 1094 (mean 364.6) and 811 (mean 270.3) CR-immunoreactive cells were counted in laminae I-III of Nociceptin::eGFP and RorB<sup>eGFP</sup> mice, respectively. In lamina I-II of Nociceptin::eGFP mice, 15% (range 13.8%-16.4%) of CR-immunoreactive cells co-expressed Pax2, whereas 15.8% (range 15%-17.2%) of the CR-immunoreactive cells were Pax2 positive in RorB<sup>eGFP</sup> mice. Analysis of the expression of the inhibitory neuron marker Pax2 among CR-immunoreactive neurons showed that in laminae I-II, 24.2% (range 20.4-29.7%) of Pax2 expressing cells were immunoreactive for CR.

Comparison between the two transgenic mouse lines indicated that there was a difference in the proportion of inhibitory CR-immunoreactive cells in lamina II that were labelled with eGFP. In the Nociceptin::eGFP mouse line, 75% (range

69.8%-78.9%) of inhibitory CR-immunoreactive cells were positive for eGFP, whereas the proportion for the RorB<sup>eGFP</sup> line was 90% (range 85.2%-95.8%). In addition, the proportion of lamina II eGFP-immunoreactive cells that were positive for CR and Pax2 were also different. In the Nociceptin::eGFP mouse line, 19% (range 13.7%-22.7%) of these cells were labelled with CR and Pax2 in, while the corresponding percentage for the RorB<sup>eGFP</sup> line was 45% (range 39.5%-49%).

**Table 3-2 Percentages of neurons in laminae I-III that were CR+/eGFP+ in Noc::eGFP mice**

<b>Lamina</b>	<b>Number of neurons counted</b>	<b>CR cells</b>	<b>eGFP cells</b>	<b>CR+/eGFP+ cells</b>	<b>% of neurons that were CR+/eGFP+</b>
I	100.8 (90-113)	16.7 (15-19)	25.7 (19-35)	1.8 (1-3)	1.8 (0.9-2.5)
II	623.2 (586-697)	299.5 (287-323)	133.4 (118-162)	40.5 (30-53)	6.4 (5.1-7.5)
I-II	724 (677-797)	316.2 (303-342)	159.1 (141-181)	42.3 (31-53)	5.8 (4.6-6.7)
III	526.2 (498-541)	63.4 (55-70)	123.2 (108-142)	12.8 (6-21)	2.4 (1.3-3.9)

Numbers of cells counted or percentages of cells are shown in the table. Values are the mean cell counts for 3 mice with ranges in parentheses.

**Table 3-3 The numbers of neurons that were eGFP, Pax2- and/or CR-immunoreactive in Nociceptin::eGFP and RorB<sup>eGFP</sup> mice**

	eGFP cells	CR cells	CR <sup>+</sup> Pax2 <sup>+</sup> cells	eGFP <sup>+</sup> Pax2 <sup>+</sup> cells	CR <sup>+</sup> eGFP <sup>+</sup> Pax2 <sup>+</sup> cells	% eGFP that were Pax2	% CR that were Pax2	% eGFP that were CR <sup>+</sup> /Pax2 <sup>+</sup>	% CR <sup>+</sup> /Pax2 <sup>+</sup> that were eGFP
<b>Nociceptin::eGFP mice</b>									
I	25.6 (21-32)	14.6 (9-21)	4.7 (3-7)	22.9 (19-30)	4.4 (3-7)	89.1 (81.9-93)	31.2 (27.8-35)	16.6 (13.7-21)	96.5 (89.6-100)
II	142.5 (115-167)	303.2 (283-338)	43.4 (37-54)	132.3 (112-157)	32.4 (26-41)	93 (88.4-96.9)	14.2 (13.2-16)	19.1 (13.7-22.7)	74.7 (69.8-78.9)
I-II	168.2 (136-177)	317.8 (292-352)	48 (40-58)	155.2 (131-177)	36.8 (29-44)	92.6 (89.1-96.3)	15 (13.8-16.4)	21.8 (21-23.2)	76.5 (71.9-80.6)
III	124.7 (102-154)	46.7 (45-49)	18.6 (17-20)	89.7 (74-106)	9.2 (7-11)	72.2 (69.2-75.1)	39.9 (37-42)	7.5 (5.6-9.6)	49.5 (34.9-57.9)
I-III	292.8 (238-345)	364.6 (338-401)	66.7 (57-78)	244.8 (205-283)	56.7 (39-55)	83.9 (82-86)	18.2 (16.9-19.4)	15.7 (14.9-16.3)	67.4 (67.2-67.7)
<b>RorB<sup>eGFP</sup> mice</b>									
I	6.9 (2-11)	8 (4-10)	1.9 (1-3)	5.7 (2-9)	0.3 (0-1)	86.4 (74.8-100)	25.7 (18.4-33.3)	2.5 (0-7.4)	10.6 (0-31.8)
II	77.2 (70-84)	250.2 (235-264)	38.9 (35-43)	71.6 (63-80)	35 (30-41)	92.6 (89.7-94.7)	15.6 (14.8-17.1)	45.2 (39.5-49)	89.6 (85.2-95.8)
I-II	84.2 (73-92)	258.2 (245-267)	40.8 (37-45)	77.4 (65-85)	35.2 (31-41)	91.8 (90-93.1)	15.8 (15-17.2)	42.1 (35.4-45.7)	86.1 (82.7-91.8)
III	54.9 (51-61)	12.1 (6-17)	7.3 (4-11)	36 (34-40)	1.4 (0-2)	65.7 (63.5-69.1)	59.7 (56.9-62.7)	2.7 (0-4.7)	15.9 (0-31)
I-III	139.1 (123-150)	270.3 (252-280)	48.1 (41-56)	113.4 (100-121)	36.6 (31-43)	81.5 (80.9-82.3)	17.8 (16.3-20)	26.5 (20.9-29.8)	76.1 (74.5-77.2)

Numbers of cells counted or percentages of cells are shown in the table. Values are the mean cell counts for 3 mice with ranges in parentheses

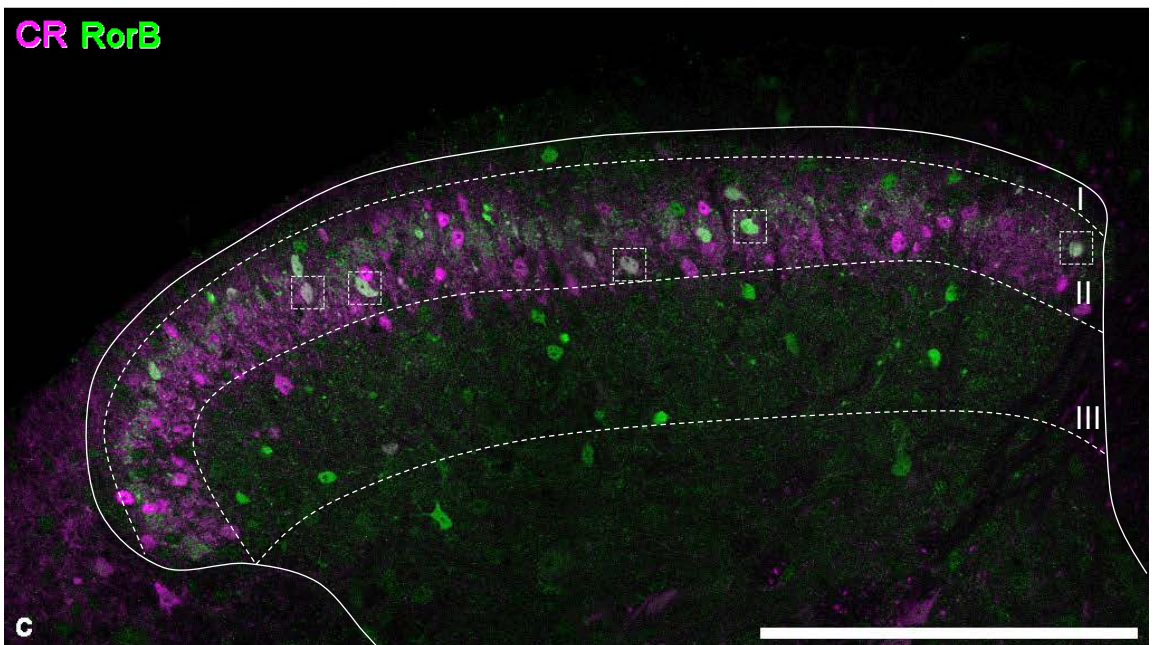
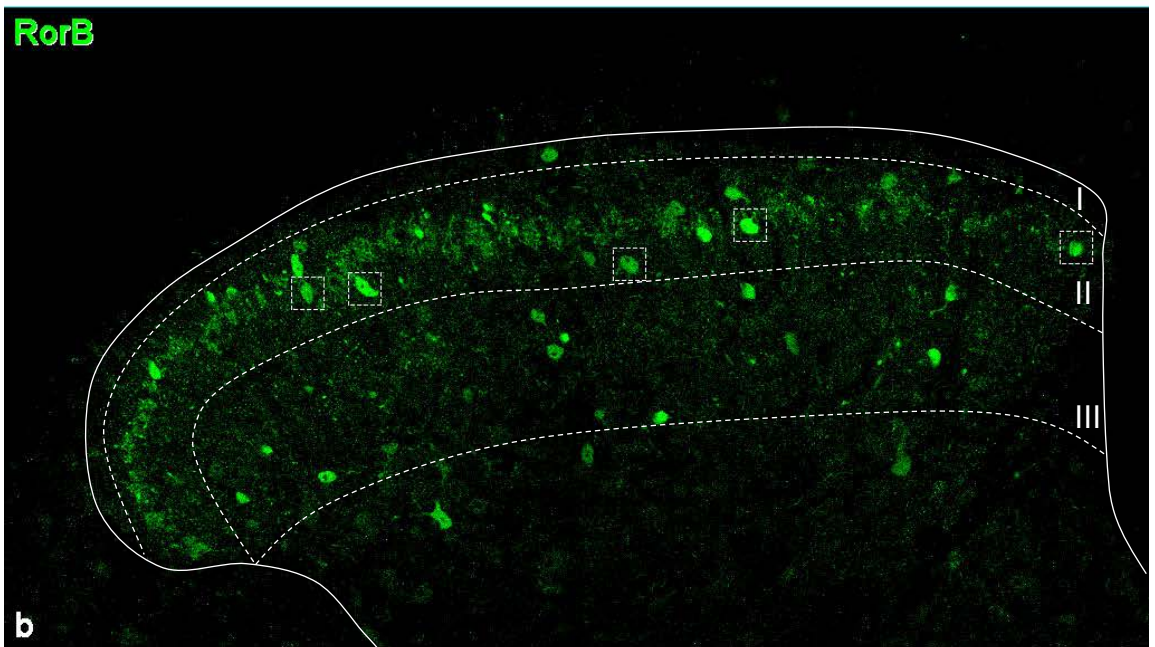
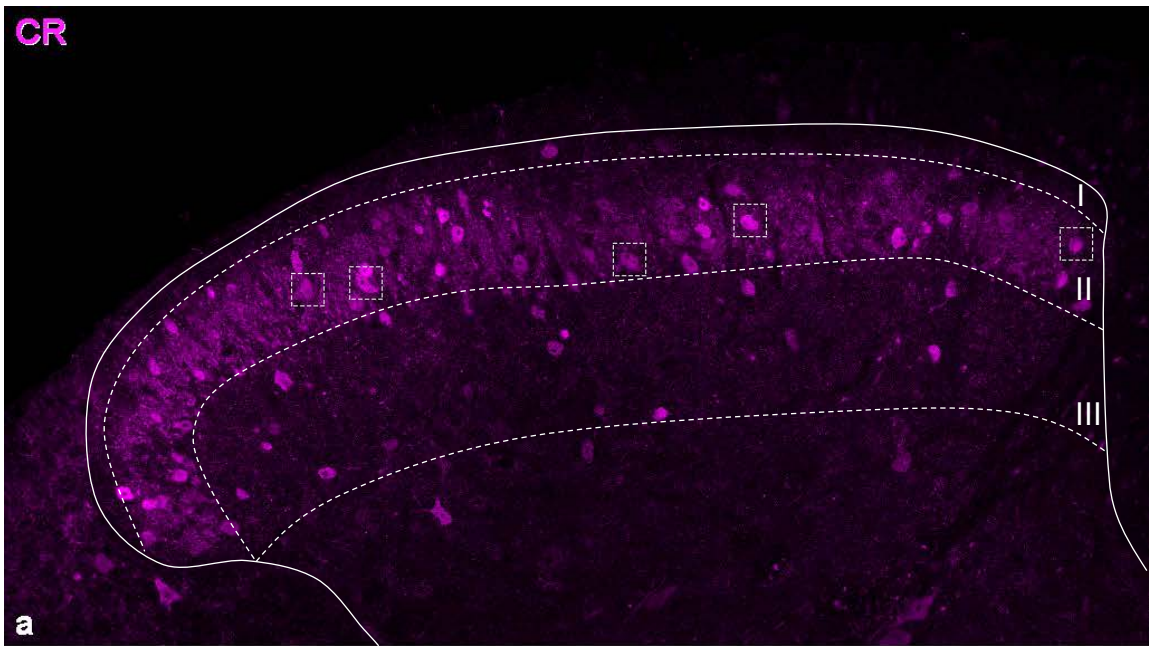


**Figure 3-5 CR and RorB<sup>eGFP</sup> cells immunostaining in the dorsal horn.** **a, b** show a confocal image taken from a RorB<sup>eGFP</sup> mouse that had been immunostained to reveal calretinin (CR) and enhanced green fluorescence protein (eGFP). CR immunoreactivity is numerous in lamina II and occasionally present in lamina III and in a deeper laminae. eGFP cells are present throughout laminae I-III. **c** a merged image. **a-c** five small boxes contain cells immunoreactive for both CR and eGFP. These neurons form a band of dendrites in the middle of lamina II. The dashed lines represents the borders between laminae I-III. Scale bar = 200  $\mu$ m.

### 3.4 Discussion

The main findings for this part of the study are: (1) that all reconstructed CR<sup>+</sup>/eGFP<sup>+</sup> neurons from Nociceptin::eGFP;CR<sup>Cre</sup>;Ai9 mice; are islet cells; (2) that Nociceptin::eGFP and RorB<sup>eGFP</sup> mouse lines are useful tools for investigating inhibitory CR cells in the SDH; (3) that 90% of lamina II inhibitory CR-immunoreactive cells are positive for eGFP in RorB<sup>eGFP</sup> mouse line while the corresponding percentage for the Nociceptin::eGFP mouse was 75%; and (4) that the RorB<sup>eGFP</sup> mouse line is more suitable than Nociceptin::eGFP for studying the inhibitory CR cells in SDH.

#### 3.4.1 Morphological features of recorded cells

From the observations of the 11 eGFP<sup>+</sup> and tdTomato<sup>+</sup> cells that were reconstructed in Nociceptin::eGFP;CR<sup>Cre</sup>;Ai9 mice, it was found that all of the neurons resembled islet cells. They had dendritic trees that extended mainly in the rostrocaudal axis and often had recurrent branches that turned 180° towards the cell body (Figure 3-1). In addition, the cells also had limited dorsoventral extension. Eight of these cells also have axons that arborized within the volume occupied by the dendritic trees and usually, the axons extended further than the dendrites either rostrally and/or caudally (Figure 3-1). According to Grudt and Perl (2002), islet cells had rostrocaudal dendritic spread > 400 μm long with axons that were restricted to the volume of their dendritic arbors. Following these criteria for characterizing islet cells, Yasaka et al. (2007) concluded that neurons with dendritic trees between 300-400 μm will be classified as islet cells if their axons arborize within the volume of the dendritic tree. In addition to the above criteria, islet cells were required to have ratio of RC/DV more than 3.5. Based on these criteria, only 2 of the reconstructed cells (cell 10 and 11 from Table 3-1) in this study would be classified as islet cells. The other 9 cells had shorter rostrocaudal dendritic extension between 193.50 - 288.50 μm (mean ± SD; 240.00 μm ± 29.60) and 2 of these cells (cell 1 and 5 from Table 3-1) had RC/DV ratios of less than 3.5. However, the study by Yasaka et al. (2007) was carried out on cells from the rat and it is likely that there are differences in the size of the cells between the species. Polgár et al. (2013a) reported that the length of the L4 segment in mouse was 1.45 mm, meanwhile the corresponding value was 2.45 mm in rat (Polgár et al., 2004). Given that islet cells had

rostrocaudal dendritic extension of more than 300  $\mu\text{m}$  in rat, then the equivalent length in mouse would be  $\sim 177 \mu\text{m}$  since the mouse L4 segment was 59% of the length of the corresponding rat segment. However, although the dorsoventral extent of the SDH in the mouse ( $\sim 80 \mu\text{m}$ ) is also smaller than that of the rat ( $\sim 100 \mu\text{m}$ ), this difference is smaller (80%) (A.J. Todd unpublished observations). A RC:DV ratio of 3.5 in the rat would therefore correspond to  $\sim 2.6$  in the mouse. Based on this adjusted criteria, all the eGFP<sup>+</sup>/tdTomato<sup>+</sup> reconstructed cells in the present study would be classified as islet cells.

Morphological study done on Neurobiotin filled atypical CR cells in lamina II of CR::eGFP mice showed that all of the recorded cells ( $n = 10$ ) had rostrocaudal extent between 350-600  $\mu\text{m}$  and RC:DV ratio between 6-14 (Smith et al., 2016). Smith and colleagues therefore classified these as islet cells following the scheme developed for hamster and rat by Grudt and Perl (2002) and Yasaka et al. (2007), respectively. The atypical CR cells that they recorded had dendritic trees that were considerably larger in the rostrocaudal axis than those of the 11 reconstructed cells in this study and this might reflect a selection bias in the study by Smith et al. (2016), who may have selected only larger cells for patch clamp recording. In a study using mouse to investigate physiological properties of GABAergic dorsal horn neurons, Heinke et al. (2004) found Neurobiotin filled lamina II cells with elongated dendritic trees that extended between 150-650  $\mu\text{m}$ . However, they could not separate the cells into 'islet' or 'central' based on the rostrocaudal dendritic extent. Therefore, they classified their sample as islet cells even though some of the cells had relatively short rostrocaudal dendritic extent. These findings indicated that it was difficult to apply the classification scheme used by previous studies that were carried out in other species (Grudt and Perl, 2002, Yasaka et al., 2007).

### **3.4.2 CR<sup>+</sup>/eGFP<sup>+</sup> cells in Nociceptin::eGFP mice**

The Nociceptin::eGFP mouse line is a bacterial artificial chromosome (BAC transgenic) line that expresses enhanced green fluorescent protein (eGFP) in ppN/OFC neurons. The neuropeptide Nociceptin is also known as orphanin FQ (N/OFC) because the peptide activated a receptor previously known as an orphan receptor, whereas the letters F (phenylalanine) and Q (glutamine) derived from the first and last amino acid of this peptide (Meunier et al., 1995,

Reinscheid et al., 1995). N/OFQ is derived from a larger precursor protein called ppN/OFQ (Ikeda et al., 1998). It was named nociceptin due to the pronociceptive effect (hyperalgesia) that was seen after the peptide was injected intracerebroventricularly (Meunier et al., 1995). However, N/OFQ has antinociceptive effects at the spinal level by hyperpolarising the membrane of the primary afferents and inhibiting glutamate release at their central terminals (Zeilhofer et al., 2002, Zeilhofer and Calò, 2003).

To establish whether the Nociceptin::eGFP mouse line provides a reliable way of defining inhibitory CR cells, the transcription factor Pax2 was used to confirm that eGFP<sup>+</sup> cells visualized in this mouse line were inhibitory neurons. Pax2 was first used to identify inhibitory neurons in the brain. In the cerebellum, it was found that developing GABAergic neurons expressed Pax2 (Maricich and Herrup, 1999). A few years later, Cheng et al. (2004) showed in the embryonic (E12.5) dorsal horn, double staining of Gad1 mRNA and Pax2 protein indicated that 98% of Pax2 cells co-expressed Gad1, a gene coding for glutamic acid decarboxylase GAD67, an enzyme that synthesis GABA (Cheng et al., 2004). Since then, Pax2 has been widely used to define inhibitory neurons, as it has been shown to be a reliable marker for these cells in the dorsal horn (Huang et al., 2008). Furthermore, in SDH of adult rat, 99% of Pax2 positive cells were found to be immunoreactive for GABA and effectively all GABA positive cells contained Pax2 (Larsson, 2017b). Pax2 is commonly used in preference to GABA as a marker for inhibitory neurons since there are technical difficulties associated with immunostaining for GABA. Glutaraldehyde fixed tissue is required for good retention of amino acid and this has a detrimental effect on many types of immunostaining. In addition, GABA immunostaining is often restricted to the surface of thick tissue sections (Sloviter et al., 2001, Sardella et al., 2011b). Multiple antibody labelling for immunocytochemistry was used to examine the cells throughout the various depth of the sections in this study, than the used of glutaraldehyde tissue fixation was not a favourable choice due to reduction in antibody binding (Van Ewijk et al., 1980).

In lamina I-II of Nociceptin::eGFP mice, it was found that 93% (89.1%-96.3%) of eGFP-immunoreactive cells were Pax2 positive and that 75% of inhibitory CR (Pax2<sup>+</sup>) cells were positive for eGFP. This suggest that the Nociceptin::eGFP

mouse line is a reliable method that is used for capturing most of inhibitory CR neurons. Previously, Albuquerque et al. (1999) suggested that CR-expressing cells in SDH used glutamate as fast neurotransmitters despite the fact that they found 12% and 7% of CR-expressing neurons were GABA- and glycine-immunoreactive, respectively. Subsequently, Smith et al. (2015) found 15% of the CR-immunoreactive cells in laminae I-II were labelled with Pax2, and their finding is very similar with this study as the corresponding value in this study was that 15% of CR-expressing cells in laminae I-II of Nociceptin::eGFP mice were Pax2 positive. These observations were also consistent with the finding by Albuquerque et al. (1999), that 12% of CR-positive cells were GABA<sup>+</sup>. However, in a recent study that was carried out in rat, Larsson (2017a) found that only 8% of the lamina II CR-immunoreactive cells were labelled with Pax2. However, Larsson reported that the staining with Pax2 antibody was relatively weak, and this might contribute to the lower number of inhibitory CR cells in his study.

In the present study, quantitative analysis showed that CR-immunoreactive cells accounted for 24% of the inhibitory interneurons in laminae I-II, and this result was similar (~25%) to what was found by Smith et al. (2015). On the contrary, Huang et al. (2010) reported that CR cells constitute 13% of inhibitory (eGFP<sup>+</sup> cells) in lamina II of GAD<sub>67</sub><sup>eGFP</sup> mice. This finding was much lower than what was found in a present study. This might be due to a technical issue, for example the poor penetration of CR antibodies or alternatively because not all GABAergic neurons were labelled with eGFP in this mouse line. In addition, Boyle et al. (2017) reported that in laminae I-II of the mouse dorsal horn, galanin, nNOS, NPY and PV make up about 75% of inhibitory neurons (GABAergic) in these laminae and they suggested that the remaining 25% of Pax2-immunoreactive cells belonged to the inhibitory CR cell population (Smith et al., 2015).

In the Nociceptin::eGFP mice, eGFP-positive cells constitute 22% of all neurons in SDH and 93% of these cells are inhibitory (Pax2). A previous quantitative study of inhibitory interneurons in the mouse spinal cord indicated that GABA-immunoreactive cells account for 25.8% of all neurons in laminae I-II (Polgár et al., 2013a) and therefore the proportion of the inhibitory neurons that were eGFP-immunoreactive neurons among all inhibitory neurons in laminae I-II is estimated to be 78%. These suggest that the majority of inhibitory cells

contained Nociceptin and this is consistent with the finding of Neal et al. (1999) who showed that both Nociceptin mRNA and its precursor, ppN/OFQ were highly expressed in the superficial laminae of the spinal cord dorsal horn. The Nociceptin opioid peptide receptor (NOP) immunoreactivity was also seen in the same regions. The expression of the Nociceptin by inhibitory interneurons is also consistent with the finding that the Nociceptin selectively inhibits the release of glutamate from nociceptive C- and A $\delta$ - fibres without interfering with GABAergic or glycinergic neurotransmission at the spinal cord level (Luo et al., 2002). Although the Nociceptin::eGFP mice captured most of inhibitory cells, this mouse line was not selective of inhibitory CR cells, since it captures around ~80% of all inhibitory interneurons in the SDH.

### **3.4.3 Comparison between Nociceptin::eGFP and RorB<sup>eGFP</sup> mouse lines**

During the earlier part of the study, observations on the transverse sections from the Nociceptin::eGFP mouse line showed that eGFP labelled many inhibitory neurons in the SDH. These cells formed a dendritic plexus in the middle of lamina II and this could correspond to CR islet cells, which have a narrow dorsoventral extent. Immunostaining the sections with CR antibody revealed that some of the cells in lamina II were double labelled with CR and eGFP and that the dendritic and axonal band seen in the middle of lamina II was also CR-immunoreactive. The Nociceptin::eGFP mouse could therefore be crossed with CR<sup>Cre</sup>; Ai9 (which causes the CR cells to express tdTomato) to allow identification of CR/Pax2 cells in spinal cord slices used for electrophysiology experiment. For this reason, it is important to validate the Nociceptin::eGFP mouse line. As described above, the analysis revealed that the Nociceptin::eGFP mouse line captured most of inhibitory CR but also many other inhibitory neurons. These results showed that Nociceptin::eGFP mouse line crossed with CR<sup>Cre</sup>; Ai9 was suitable for electrophysiology experiments such as to look at the firing patterns and synaptic input, and to carry out pharmacological study on the inhibitory CR cells. However, there were 2 disadvantages of this approach: (1) Nociceptin::eGFP mouse line only captures 75% of inhibitory CR cells; (2) Nociceptin::eGFP mouse line labelled most of inhibitory neurons which made it more difficult to identify inhibitory CR cells in electrophysiological experiments. During the course of this study, spinal cords from RorB<sup>eGFP</sup> mice were received

from Professor David Ginty. Earlier observations on the transverse sections of the RorB<sup>eGFP</sup> mice suggested that fewer eGFP<sup>+</sup> cells were seen in the SDH, compared to the Nociceptin::<sup>eGFP</sup> mice and these cells also formed a prominent dendritic and axonal band in the middle of lamina II that corresponded to CR immunostaining.

To understand the functions of inhibitory CR cells in the SDH, it is important to determine which mouse line would capture most of these cells. In this part of the study, a comparison between Nociceptin::<sup>eGFP</sup> and RorB<sup>eGFP</sup> mouse line was done by doing quantitative analysis on the numbers of inhibitory CR that were eGFP in SDH. In addition, the specificity of labelling for inhibitory CR cells was also important.

Quantitative analysis in Nociceptin::<sup>eGFP</sup> and RorB<sup>eGFP</sup> mouse lines showed that more than 90% of laminae I-II eGFP cells in both animals were labelled with Pax2, thus showing that these mouse lines were reliable tools to investigate inhibitory CR cells in the SDH. In lamina II of RorB<sup>eGFP</sup> mice, 90% of inhibitory CR-labelled cells were immunoreactive for eGFP, whereas only 75% of the same cells were stained for eGFP in Nociceptin::<sup>eGFP</sup> mice. Furthermore, in lamina II of RorB<sup>eGFP</sup> mice, 45% of eGFP-immunoreactive cells were labelled with both CR and Pax2, meanwhile the corresponding percentage for Nociceptin::<sup>eGFP</sup> mice was 19%.

As a conclusion from this part of the study, the results showed that RorB<sup>eGFP</sup> mouse line is more effective than Nociceptin::<sup>eGFP</sup> mouse for investigating inhibitory CR cells in the SDH since: (1) 90% of eGFP cells in SDH were Pax2 positive; (2) 90% of inhibitory CR-labelled cells were immunoreactive for eGFP in lamina II; and (3) the RorB<sup>eGFP</sup> mouse was more selective than the Nociceptin::<sup>eGFP</sup> mouse since a higher proportion of eGFP-immunoreactive cells were labelled with CR and Pax2 antibodies. Interestingly, Wildner et al. (2013) reported that the expression of RorB was specific to the subset of inhibitory dorsal horn neurons, thus making it as a marker of choice for defining inhibitory subpopulations.

#### **4 Expression of neurochemical markers of inhibitory interneuron populations in CR<sup>+</sup>/eGFP<sup>+</sup> cells in Nociceptin::**eGFP** and RorB<sup>eGFP</sup> mice**

## 4.1 Introduction

Abraira and Ginty (2013) reported that, around 99% of the neurons within the dorsal horn are local interneurons, the majority of which are excitatory. A quantitative study carried out in mouse found that about one quarter of the neurons in laminae I-II and ~ 40% of those in lamina III are inhibitory interneurons that are GABA and/or glycine immunoreactive (Polgár et al., 2013a). It has been suggested that pathological pain states arise due to the loss of function of inhibitory cells, which normally suppress pain and itch (Sandkühler, 2009, Kardon et al., 2014, Petitjean et al., 2015).

As noted above, nNOS, NPY, galanin/dynorphin and PV are found to be expressed by distinct populations of inhibitory interneurons in the dorsal horn of the rat spinal cord (Sardella et al., 2011b, Polgár et al., 2011, Tiong et al., 2011, Hughes et al., 2012, Sardella et al., 2011a). Boyle et al. (2017) reported that in the mouse, ~75% of the inhibitory interneurons in lamina I-II are accounted for by cells immunoreactive for these four distinct neuronal markers. In addition, it appears that, *sst<sub>2A</sub>* is virtually restricted to inhibitory neurons (Todd et al., 1998, Polgár et al., 2013a, Cameron et al., 2015).

The quantitative analysis carried out in chapter 3 showed that in laminae I-II, 15% of CR cells are inhibitory. Meanwhile, CR-positive neurons account for 24% of the inhibitory cells. Both findings are similar to those reported by Smith et al. (2015). In addition, Smith and colleagues reported that 50% of Pax2 CR-immunoreactive neurons in laminae I-II are positive for the *sst<sub>2A</sub>* receptor. They also found that none of the galanin-immunoreactive cells were positive for CR, whereas there was minimal expression of CR in NPY and inhibitory nNOS populations. However, they did not determine the percentage of inhibitory CR cells that expressed galanin, nNOS or NPY. In addition, Smith et al. (2015) did not verify the expression of another distinct inhibitory neuronal marker, PV, among inhibitory CR cells.

The aims of this part of the study are to determine: 1) the extent to which CR<sup>+</sup>/eGFP<sup>+</sup> cells express four (galanin, nNOS, NPY and PV) other neurochemical markers of the inhibitory interneurons in laminae I-II of Nociceptin::eGFP and Rorβ<sup>eGFP</sup> mice; 2) the proportion of CR<sup>+</sup>/eGFP<sup>+</sup> neurons that express *sst<sub>2A</sub>* receptor

in Nociceptin::eGFP mice; and 3) expression of the various peptides (galanin, nNOS, NPY and PV) by CR<sup>-</sup>/eGFP<sup>+</sup> cells in RorB<sup>eGFP</sup> mice.

## 4.2 Materials and method

### 4.2.1 Animals and tissue processing

Three Nociceptin::eGFP adult mice of male sex, weighing between 28-32g were deeply anaesthetised with pentobarbitone and perfused through the left ventricle with freshly made 4% de-polymerised formaldehyde. Lumbar spinal cord segments were dissected out from all animals and post-fixed for 2 hours with the same solution at 4°C before being transferred to PB. The L4 segments were cut into 60 µm thick transverse sections using a vibrating blade microtome followed by immersion in 50% ethanol for 30 minutes to enhance antibody penetration (Llewellyn-Smith and Minson, 1992). The segments were cut serially into 4 bottles and these were processed according to different immunocytochemical protocols. In addition, perfusion fixed spinal cords from 3 RorB<sup>eGFP</sup> young adult mice were received from Professor David Ginty from Harvard University and were processed in a similar way. Sections were then processed for multiple immunolabelling as described in 4.2.2 and 4.2.3.

### 4.2.2 Expression of 4 distinct inhibitory markers and sst<sub>2A</sub> in CR<sup>+</sup>/eGFP<sup>+</sup> in Nociceptin::eGFP mice

To determine the extent to which galanin, nNOS, NPY, PV and sst<sub>2A</sub> were expressed by CR<sup>+</sup>/eGFP<sup>+</sup> cells, sections from L4 segments of 3 Nociceptin::eGFP mice were incubated with the following antibodies: chicken anti-eGFP, mouse anti-CR, rabbit anti-galanin, rabbit anti-nNOS, rabbit anti-NPY, guinea pig anti-PV and guinea pig anti-sst<sub>2A</sub>. The reactions were performed in 3 different sets of immunocytochemical protocols: (i) eGFP, CR, galanin and sst<sub>2A</sub>, (ii) eGFP, CR, nNOS and sst<sub>2A</sub>, (iii) eGFP, CR, NPY and PV. The primary antibodies were revealed with appropriate fluorescent secondary antibodies.

For each immunocytochemical reactions, 4 sections from each Nociceptin::eGFP mouse and 3 sections from each RorB<sup>eGFP</sup> mouse were selected randomly before immunostaining for the corresponding peptide was viewed. These sections were scanned with a Zeiss LSM 710 confocal microscope with a 40x oil immersion lens

(numerical aperture 1.3), 1  $\mu\text{m}$  z-step and the aperture set to 1 Airy unit. These sections were scanned to produce a z-stack of 30 optical sections. Tile scans were used to capture the whole width of laminae I-III. Confocal scans were analysed offline using Neurolucida for Confocal Software. The outline of the dorsal horn and the boundaries between laminae I-III were drawn. The lamina I/II boundary was drawn 20  $\mu\text{m}$  below the dorsal white matter and the ventral extent of the CR-immunoreactive cells was used to determine lamina II/III border. The ventral border of lamina III was taken as 100  $\mu\text{m}$  below the lamina II-III border.

A modified optical disector method was used to obtain an unbiased sample of neurons in laminae I-III of the scanned sections (Gutierrez-Mecinas et al., 2016a, Tiong et al., 2011). All cell bodies of eGFP-positive neurons in laminae I-III that had their bottom surface between reference and look up sections (10th and 25th optical sections, respectively) were plotted onto the Neurolucida drawing. Then, the CR channel was viewed to determine the proportion of eGFP-immunoreactive cells that were positive for CR. Following that, the channel corresponding to either galanin, nNOS, NPY, PV or *sst*<sub>2A</sub> was then viewed. The presence or absence of each type of staining was documented for each of the selected CR<sup>+</sup>/eGFP<sup>+</sup> neurons.

Since the reference and look-up sections were reasonably far apart, every optical sections between them were carefully examined to ensure that all neurons with nuclei presented between these two planes were included in the sample.

#### **4.2.3 Assessment of co-localisation of the 4 distinct inhibitory markers in CR<sup>+</sup>/eGFP<sup>+</sup> in RorB<sup>eGFP</sup> mice**

To define the co-localization between CR<sup>+</sup>/eGFP<sup>+</sup> neurons with galanin, NPY, nNOS and PV, 3 sections from L4 segments of 3 RorB<sup>eGFP</sup> mice were immunoreacted with mouse anti-NeuN, chicken anti-eGFP, rabbit anti-galanin, rabbit anti-NPY, rabbit anti-nNOS, guinea pig anti-PV and goat anti-CR. NeuN was used to help to distinguish the outline of cells that expressed galanin and NPY which were found in patches in the perikaryal cytoplasm (Mullen et al., 1992, Todd et al., 1998). The reactions were performed in four different sets of

immunocytochemical reactions: (i) eGFP, CR, galanin and NeuN, (ii) eGFP, CR, nNOS and NeuN, (iii) eGFP, CR, NPY and NeuN, (iv) eGFP, CR, and PV. These were revealed with appropriate fluorescent secondary antibodies. For all four different immunoreactions, 3 sections from each mouse were selected and scanned using the confocal microscope and analysed as described earlier.

For all the immunoreactions, cell bodies of eGFP cells in laminae I and II with the bottom of the nucleus located between 10th and 25th optical sections were initially plotted onto the NeuroLucida drawing. Then the channel corresponding to CR was viewed and CR<sup>+</sup>/eGFP<sup>+</sup> and CR<sup>-</sup>/eGFP<sup>+</sup> cells were identified. Following this, the remaining channels were then observed and the presence or absence of each type of immunostaining was documented for each of the selected neurons.

All of the analyses in this part of the study were carried out in laminae I-II only because the majority of CR<sup>+</sup>/eGFP<sup>+</sup> cells were seen here. In addition, the RorB<sup>eGFP</sup> spinal cords were not properly fixed and this will give rise to poor immunostaining of sst<sub>2A</sub> antibody. Therefore, the analysis on the expression of somatostatin receptor in CR<sup>+</sup>/eGFP<sup>+</sup> cells was not carried out in RorB<sup>eGFP</sup> mice.

## 4.3 Results

### 4.3.1 Expression of galanin, nNOS, NPY, PV and sst<sub>2A</sub> among CR<sup>+</sup>/eGFP<sup>+</sup> cells in Nociceptin::eGFP mice

In all 3 set of immunoreactions from the Nociceptin::eGFP mice, the distribution of cell bodies and dendrites that were eGFP<sup>+</sup>, CR<sup>+</sup> and double labelled CR<sup>+</sup>/eGFP<sup>+</sup> neurons was similar to previous findings reported in chapter 3. To look at the relationship between CR<sup>+</sup>/eGFP<sup>+</sup> and galanin-immunoreactive neurons, sections reacted against CR, eGFP, and galanin antibodies were analysed. Quantitative data obtain using the disector method on this part of the study is shown in Table 4-1. A total of 921 (mean 307) eGFP-positive cells and 101 (mean 33.7) CR<sup>+</sup>/eGFP<sup>+</sup> neurons were identified in laminae I-III. Of the CR<sup>+</sup>/eGFP<sup>+</sup> cells, 87% (range 80-90.3%) were in lamina II. The pattern of galanin-immunoreactive cells was similar to what has been reported in previous studies (Todd and Spike, 1993, Tiong et al., 2011). The galanin immunoreactivity was seen in the perikaryal cytoplasm, and the cell bodies were found in laminae I-III with a dense axonal

plexus in laminae I and II<sub>o</sub>. Furthermore, 172 (mean 57.3) galanin-positive cells were counted in laminae I-III with 93% (range 92.5-94.5%) of these cells being found in lamina II. The quantitative analysis showed that none of the CR<sup>+</sup>/eGFP<sup>+</sup> cells were galanin-immunoreactive in laminae I-III (Figure 4-1).

To determine the relationship between CR<sup>+</sup>/eGFP<sup>+</sup> cells and nNOS, sections reacted against CR, eGFP, and nNOS were analysed. In laminae I-III, a total of 826 (mean 275.3) eGFP-positive neurons and 108 (mean 36) CR<sup>+</sup>/eGFP<sup>+</sup> cells were counted. About 90% (range 85.7-94.3%) CR<sup>+</sup>/eGFP<sup>+</sup> neurons were found in lamina II. The nNOS-immunoreactive cell bodies were found mainly in laminae I-II with fewer cells seen in lamina III. The nNOS immunostaining was mainly seen in perikaryal cytoplasm with extension into the proximal dendrites. However, there was variability in the intensity of the immunostaining between nNOS-immunoreactive cells. Some cells showed very intense immunostaining and some have a weaker labelling. A dense plexus of dendrites and axons of the nNOS-immunoreactive neurons was seen in laminae I-II. The distribution of cells was the same as that reported previously (Sardella et al., 2011b). A total of 633 (mean 211) nNOS-immunoreactive cells were counted in laminae I-III. Of these, 81% (range 77.9-82.5%) cells were found in lamina II. Analysis performed on all sections showed that, there was no nNOS expression in CR<sup>+</sup>/eGFP<sup>+</sup> cells in Nociceptin::eGFP mice (Figure 4-1).

To look at the extent of overlap between NPY and PV with CR and eGFP, sections reacted to reveals CR, eGFP, NPY and PV were analysed (Figure 4-2). A total of 956 (mean 318.7) eGFP-immunoreactive cells were counted in laminae I-III. Meanwhile, 97 (mean 32.3) CR<sup>+</sup>/eGFP<sup>+</sup> cells were counted in lamina I-III with 86% (range 82.8-92.3%) of these cells being in lamina II. The somata of NPY-immunoreactive cells were found more in laminae I-II and were more sparsely distributed in lamina III. The immunostaining for NPY was seen in the perikaryal cytoplasm and a dense plexus of NPY-immunoreactive axons was found in laminae I-II with scattered axons seen in deeper laminae. The distribution of these cells was comparable with previous studies carried out in both mouse and rat (Rowan et al., 1993, Polgár et al., 2011, Iwagaki et al., 2016). In laminae I-III, 479 (mean 159.7) NPY-immunoreactive cells were counted. Observations in all sections from 3 Nociceptin::eGFP mice showed that 8% (range 3.4-11.9%) of the CR<sup>+</sup>/eGFP<sup>+</sup> cells were immunoreactive for NPY (Figure 4-2). A total of 645

(mean 215) PV-immunoreactive cells were counted in laminae I-III and a similar pattern was seen to that described in a previous study in mouse (Hughes et al., 2012). The cell bodies of PV-positive neurons were distributed mainly in lamina II<sub>i</sub>-III and were absent from lamina I. The immunoreactivity for PV was seen in the cytoplasm and nucleus of the cells. Most (91%, range 87.9-93.2%) of these cells were found in lamina III. Quantitative analysis revealed that none of the PV-immunoreactive cells in laminae I-III were CR<sup>+</sup>/eGFP<sup>+</sup> cells (Figure 4-2).

The analysis of sst<sub>2A</sub> labelling on CR<sup>+</sup>/eGFP<sup>+</sup> cells was carried out using the same sections that were used to look at the relations to galanin and nNOS. The distribution of sst<sub>2A</sub> was similar to that seen in previous studies (Todd et al., 1998, Polgár et al., 2013a, Shi et al., 2014). The immunostaining of sst<sub>2A</sub> immunoreactivity was observed as a dense band in laminae I-II and the immunostaining was rarely seen in lamina III. At high magnification, the immunostaining was associated with neuronal cell membranes with minimal reactivity in the cytoplasm. In laminae I-II from 8 sections per animal, 184 (25-35 per mouse) CR<sup>+</sup>/eGFP<sup>+</sup> cells were counted and of these, 90 (13-16 per mouse) cells were labelled with sst<sub>2A</sub> which correspond to 49% (range 42.9-55.2%). In lamina II, 48% (range 41.2-53.6%) of the CR<sup>+</sup>/eGFP<sup>+</sup> cells were sst<sub>2A</sub>-immunoreactive (Figure 4-3).

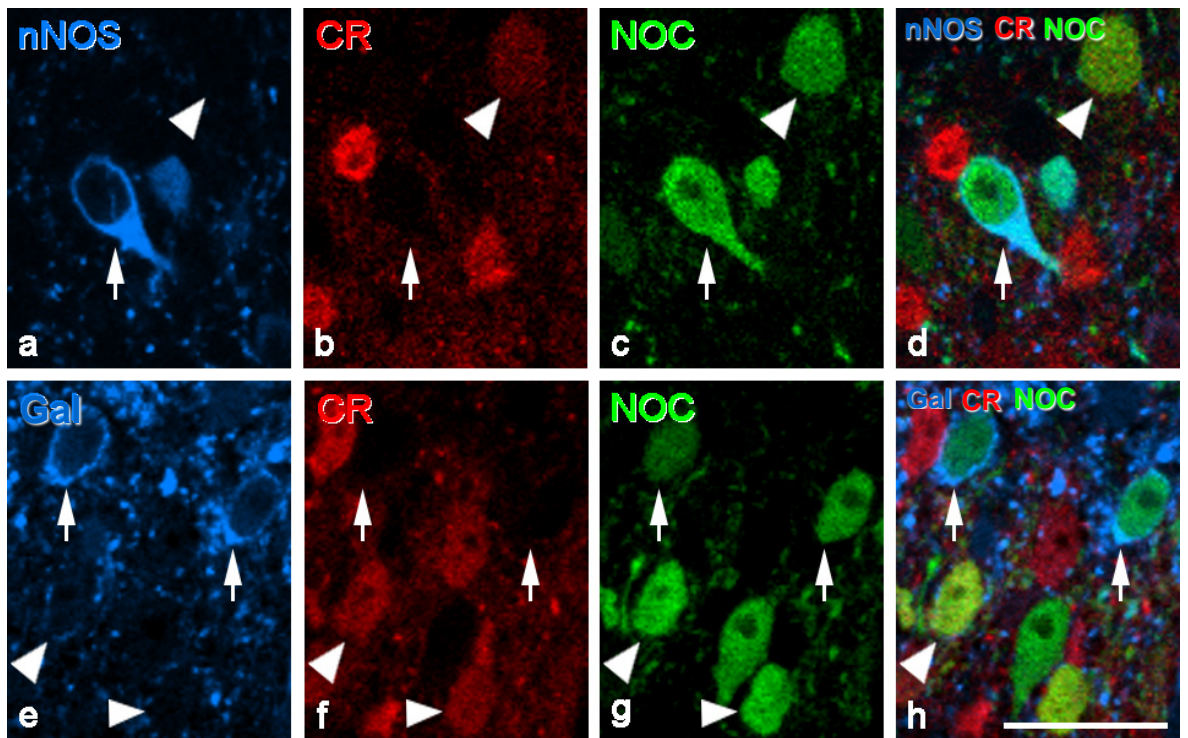


**Figure 4-1 Lack of co-localisation of CR-Noc::eGFP, nNOS and galanin in laminae I-III.**

Confocal images of a transverse section from lamina II of Noc::eGFP mouse that had been immunostained for nNOS (blue), CR (red), eGFP (green) and galanin (Gal) (blue). **a-c** shows nNOS containing cell body (arrow) is not immunoreactive for CR but is labelled with eGFP. **b, c** show CR-Noc::eGFP cell (arrow head) is lack of nNOS. **e-g** shows two galanin-immunoreactive cells (arrows) are lack of CR but are labelled with eGFP. **f, g** show neurons immunoreactive for both CR and eGFP (arrow heads) are not labelled with galanin. **d,h** a merged images. **a-h** are from a single optical section. Scale bar = 20  $\mu$ m.

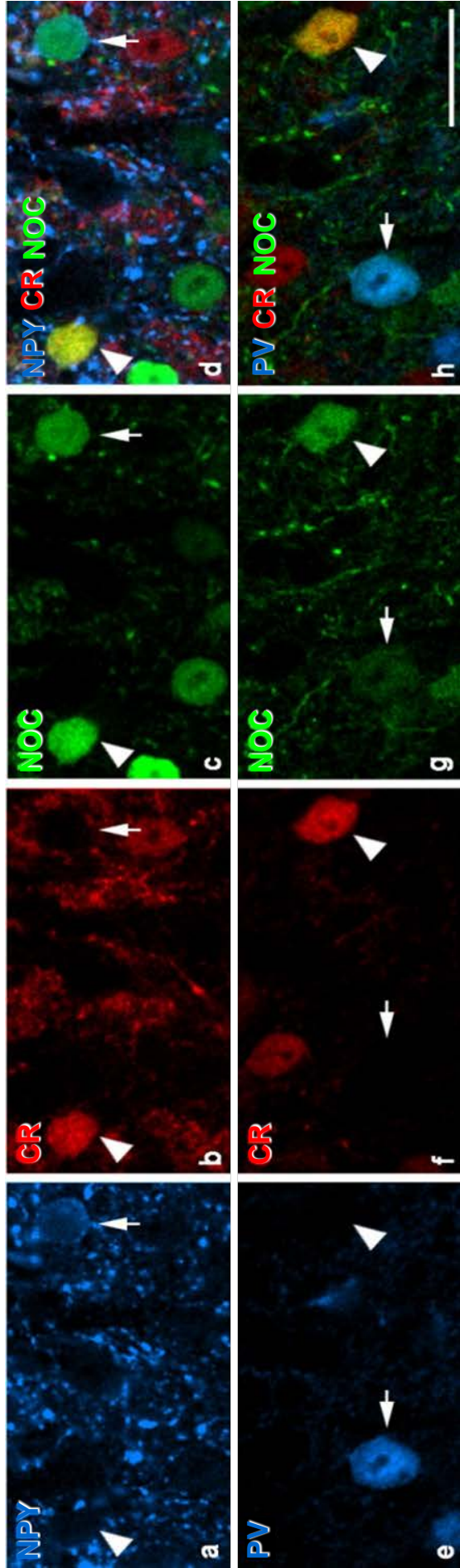


**Figure 4-2 Lack of co-localisation of CR-Noc::eGFP, NPY and PV in laminae I-III.** Confocal images of a transverse section from Noc::eGFP mouse that had been immunostained for NPY (blue), CR (red), Noc::eGFP (green) and PV (blue). **a-c** shows NPY containing cell body (arrow) in lamina II is lack of CR but are labelled with eGFP and CR-Noc::eGFP cell (arrow head) is immunoreactive for NPY (weakly labelled). **e-g** show PV-immunoreactive cell (arrow) in lamina Iii is lack of CR but are labelled with eGFP. **f, g** show neurons immunoreactive for both CR and Noc::eGFP (arrow head) is not labelled with PV. **d,h** a merged images. **a-h** are from a single optical section. Scale bar = 20  $\mu$ m.

**Table 4-1 Expression of other neurochemical markers with CR and eGFP in Nociceptin::eGFP mice**

	Lamina	GFP+	CR+/GFP+	Galanin+	CR+/GFP+/Galanin+
<b>Galanin</b>	I	20.7 (19-22)	1 (1)	3.7 (2-6)	0
	II	162.3 (156-175)	27.7 (24-31)	52 (49-55)	0
	III	124 (108-149)	5 (2-8)	1.7 (1-3)	0
	I-III	307 (293-324)	33.7 (30-40)	57.3 (53-64)	0
	Lamina	GFP+	CR+/GFP+	nNOS+	CR+/GFP+/nNOS+
<b>nNOS</b>	I	17 (14-19)	0.3 (0-1)	7.3 (5-9)	0
	II	156.7 (143-169)	32.3 (30-34)	170 (165-176)	0
	III	101.7 (78-119)	3.3 (2-5)	33.7 (30-41)	0
	I-III	275.3 (255-302)	36 (35-38)	211 (200-226)	0
	Lamina	GFP+	CR+/GFP+	NPY+	CR+/GFP+/NPY+
<b>NPY</b>	I	18 (14-21)	1.3 (1-2)	6.7 (4-9)	0
	II	166.7 (145-206)	28.7 (24-38)	95 (90-102)	2.7 (1-5)
	III	134 (113-160)	2.3 (1-4)	58.3 (49-71)	0
	I-III	318.7 (283-385)	32.3 (26-42)	159.7 (154-170)	2.7 (1-5)
	Lamina	GFP+	CR+/GFP+	PV+	CR+/GFP+/PV+
<b>PV</b>	I	18 (14-21)	1.3 (1-2)	0 (0)	0
	II	166.7 (145-206)	28.7 (24-38)	18.7 (15-24)	0
	III	134 (113-160)	2.3 (1-4)	196.3 (174-210)	0
	I-III	318.7 (283-385)	32.3 (26-42)	215 (198-227)	0

In each case, the mean values for 3 Nociceptin::eGFP mice are shown, with the range in brackets.

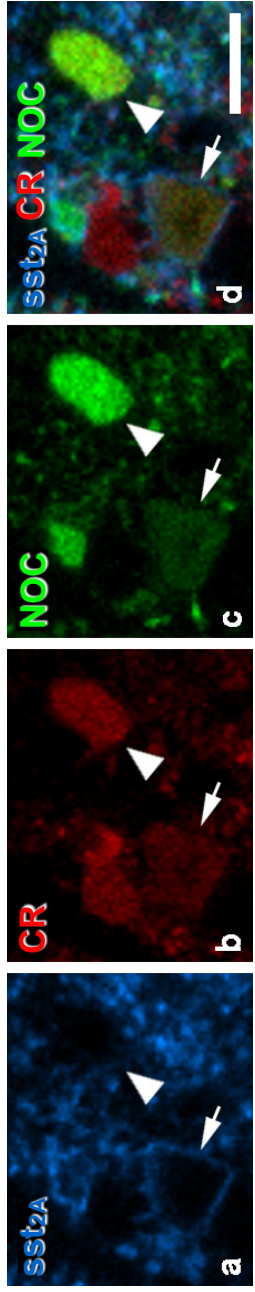


**Figure 4-3 CR-Noc::eGFP and sst2A in the superficial dorsal horn.** Confocal image showing a single optical section of Noc::eGFP mouse to reveal sst2A (blue), CR (red) and eGFP (green). **a-d** show a neuron that is immunoreactive for sst2a (arrow) is also labelled with CR and eGFP. Not all CR-Noc::eGFP cell (arrow head) immunoreactive for sst2A. Scale bar = 10  $\mu$ m.

### 4.3.2 Neurochemical markers in RorB<sup>eGFP</sup> and their expression by CR<sup>+</sup>/eGFP<sup>+</sup> and CR<sup>-</sup>/eGFP<sup>+</sup> cells

In this part of the study, similar arrangement of cell bodies and dendritic plexus of eGFP, CR and CR<sup>+</sup>/eGFP<sup>+</sup> neurons was seen as described in chapter 3. The distribution of neurons and the immunoreactivity of galanin, nNOS, NPY and PV in RorB<sup>eGFP</sup> mice was similar to what has been reported in previous studies and in present study using Nociceptin::eGFP mice (Tiong et al., 2011, Sardella et al., 2011b, Polgár et al., 2011, Hughes et al., 2012).

To determine the relationship between CR<sup>+</sup>/eGFP<sup>+</sup> cells and galanin, sections from 3 animals reacted with eGFP, CR, galanin and NeuN were analysed. Quantitative data obtain using the disector method on this part of the study is shown in Table 4-2. A total of 319 (mean 106.3) and 136 (mean 45.3) eGFP-positive cells and CR<sup>+</sup>/eGFP<sup>+</sup> neurons were counted in laminae I-II, respectively. Of this, 94% (range 91.2-95.2%) of the CR<sup>+</sup>/eGFP<sup>+</sup> cells were counted in lamina II. In the SDH, 154 (mean 51.3) galanin-immunoreactive cells were counted and none of the CR<sup>+</sup>/eGFP<sup>+</sup> cells were associated with galanin. However, 59% (range 49.2-69.4%) of the CR<sup>-</sup>/eGFP<sup>+</sup> neurons were labelled with galanin, and this accounted for 70% (range 62-77.8%) of the galanin-immunoreactive cells in SDH.

To look at the presence of nNOS immunostaining in CR<sup>+</sup>/eGFP<sup>+</sup> cells, the sections reacted with eGFP, CR, nNOS and NeuN were analysed. In laminae I-II, 339 (mean 113) eGFP-immunoreactive cells were counted. A total of 142 (mean 47.3) CR<sup>+</sup>/eGFP<sup>+</sup> neurons in SDH were calculated and 93% (range 87.2-95.8%) of these being in lamina II. A total of 437 (mean 145.7) nNOS-IR cells were counted and nNOS immunoreactivity was seen in only 2% (range 0-5.1%) of the CR<sup>+</sup>/eGFP<sup>+</sup> cells. On the other hand, 17% (range 15.4-18.8%) of the CR<sup>-</sup>/eGFP<sup>+</sup> cells were immunoreactive for nNOS in SDH. In addition, 7% (range 6.5-7.8%) of the nNOS-immunoreactive neurons were labelled with eGFP.

To establish the relationship between CR<sup>+</sup>/eGFP<sup>+</sup> cells and NPY, 3 sections from 3 animals that immunoreacted with eGFP, CR, NPY and NeuN were analysed. A total of 337 (mean 112.3) and 143 (mean 47.7) eGFP-positive cells and CR<sup>+</sup>/eGFP<sup>+</sup> neurons were counted in laminae I-II, respectively. Of this, 95% (range 94.2-96.2%) of the CR<sup>+</sup>/eGFP<sup>+</sup> cells were found in lamina II. In the SDH, 236 (mean 78.7) NPY-immunoreactive cells were counted and 7% (range 2.6-

9.6%) of the CR<sup>+</sup>/eGFP<sup>+</sup> cells were labelled with NPY. Most of the time, NPY-immunoreactivity seen with CR<sup>+</sup>/eGFP<sup>+</sup> cells was invariably weak. In addition, 22% (range 15-30.2%) of the CR<sup>-</sup>/eGFP<sup>+</sup> neurons were NPY-immunoreactive and 18% (range 13-24.1%) of the NPY-positive cells were immunoreactive for eGFP in SDH.

To explore the extent of overlap between PV and CR<sup>+</sup>/eGFP<sup>+</sup> cells, a total of 547 (mean 182.3) and 165 (mean 55) of eGFP<sup>-</sup> and CR<sup>+</sup>/eGFP<sup>+</sup> cells were counted in laminae I-III, respectively. In laminae I-III, 469 (mean 149) PV-positive cells were calculated and the analysis showed that none of the CR<sup>+</sup>/eGFP<sup>+</sup> cells were labelled with PV. In addition, 1% (range 0-1.6%) and 9% (range 5.5-11.7%) of the CR<sup>-</sup>/eGFP<sup>+</sup> neurons were labelled with PV were seen in laminae I-II and LIII, respectively. About 9% (range 0-14.3%) and 4% (range 2.6-4.9%) of the PV-immunoreactive cells contained eGFP-immunoreactivity in SDH and lamina III, respectively.

**Table 4-2 Colocalization of neurochemical markers with CR and eGFP in RorB<sup>eGFP</sup> mice**

	Lamina	GFP <sup>+</sup>	CR <sup>+</sup> /GFP <sup>+</sup>	Galanin <sup>+</sup>	CR <sup>+</sup> /GFP <sup>+</sup> /Galanin <sup>+</sup>
<b>Galanin</b>	I	13.7 (10-20)	3 (2-5)	5 (4-7)	0
	II	92.3 (89-96)	42.3 (35-52)	46.3 (46-47)	0
	I-II	106.3 (100-113)	45.3 (37-57)	51.3 (50-54)	0
	Lamina	GFP <sup>+</sup>	CR <sup>+</sup> /GFP <sup>+</sup>	nNOS <sup>+</sup>	CR <sup>+</sup> /GFP <sup>+</sup> /nNOS <sup>+</sup>
<b>nNOS</b>	I	15.7 (11-24)	3.3 (2-5)	7.7 (2-12)	0
	II	97.3 (88-109)	44 (34-52)	138 (123-155)	2 (0-2)
	I-II	113 (107-120)	47.3 (39-55)	145.7 (132-167)	2 (0-2)
	Lamina	GFP <sup>+</sup>	CR <sup>+</sup> /GFP <sup>+</sup>	NPY <sup>+</sup>	CR <sup>+</sup> /GFP <sup>+</sup> /NPY <sup>+</sup>
<b>NPY</b>	I	10.3 (7-12)	2.3 (2-3)	6.7 (6-7)	0
	II	102 (97-109)	45.3 (37-50)	72 (62-82)	3.3 (1-5)
	I-II	112.3 (109-116)	47.7 (39-52)	78.7 (69-88)	3.3 (1-5)
	Lamina	GFP <sup>+</sup>	CR <sup>+</sup> /GFP <sup>+</sup>	PV <sup>+</sup>	CR <sup>+</sup> /GFP <sup>+</sup> /PV <sup>+</sup>
<b>PV</b>	I	21.3 (18-25)	4.3 (4-5)	0 (0)	0
	II	97.7 (84-106)	49 (46-52)	7.3 (6-9)	0
	III	63.3 (56-70)	1.7 (1-2)	91 (80-97)	0
	I-III	182.3 (173-197)	55 (53-58)	149 (143-157)	0

In each case, the mean values for 3 RorB<sup>eGFP</sup> mice are shown, with the range in brackets.

## 4.4 Discussion

The main findings of this part of study are that: (1) none of the CR<sup>+</sup>/eGFP<sup>+</sup> cells in either Nociceptin::eGFP or RorB<sup>eGFP</sup> mice expressed galanin or PV, while there was minimal overlap with NPY and nNOS; (2) around half of the CR<sup>+</sup>/eGFP<sup>+</sup> cells in Nociceptin::eGFP mice are labelled with sst<sub>2A</sub> antibody; and (3) in the RorB<sup>eGFP</sup> mice, eGFP-immunoreactive cells that lacked CR overlapped with the other four inhibitory markers (galanin, nNOS, NPY and PV). Tissues from both mouse lines were analysed because initially only Nociceptin::eGFP mice were available. However, later in the study, tissues from RorB<sup>eGFP</sup> mice were received and subsequently it was found that it captures more of inhibitory CR cells compared to Nociceptin::eGFP mice.

### 4.4.1 Expression of neurochemical markers for inhibitory neurons in CR<sup>+</sup>/eGFP<sup>+</sup> cells in Nociceptin::eGFP and RorB<sup>eGFP</sup>

Smith et al. (2015) reported that none of the galanin immunoreactive neurons exhibited CR labelling, however, some of the NPY- and nNOS-positive cells were CR-immunoreactive in the SDH. In their study, CR::eGFP mice were used to investigate the CR populations in the SDH. As mentioned before, the great majority (~85%) of CR cells are excitatory neurons, therefore it is difficult to assess the extent to which inhibitory CR cell populations overlap with other inhibitory neurochemical markers such as those that expressed nNOS, NPY and PV. One way to resolve this issue is to use Pax2 to distinguished inhibitory CR cells in the CR::eGFP mice. However, this could not be done since the antibodies for Pax2, galanin, nNOS, and NPY were derived from the same species (rabbit). Unfortunately, antibodies for these neuronal markers obtain from other species were found not to be reliable. Therefore, Smith and colleagues were unable to directly determine the extent of overlap between inhibitory CR (Pax2<sup>+</sup>) cells labelled with the other neuronal markers mentioned above. In the current study, the need for Pax2 antibody could be avoided by using eGFP-immunoreactivity to label inhibitory CR cells in the SDH of Nociceptin::eGFP and RorB<sup>eGFP</sup> mice, since result from previous chapter showed that ~92% of the eGFP-immunoreactive cells were labelled with Pax2 antibody in both mouse lines.

The results of this study showed that none of the CR<sup>+</sup>/eGFP<sup>+</sup> cells in either mouse lines expressed galanin, consistent with the finding of Smith et al. (2015). They also lack of PV although there was minimal (1%) overlap with nNOS in the SDH of RorB<sup>eGFP</sup> mice. In both Nociceptin::eGFP and RorB<sup>eGFP</sup> mouse lines there was limited overlap between CR<sup>+</sup>/eGFP<sup>+</sup> cells and NPY populations (8% and 7% of CR<sup>+</sup>/eGFP<sup>+</sup> cells, respectively) in the SDH. The lack of overlap between CR<sup>+</sup>/eGFP<sup>+</sup> cells with PV populations can be partially explained by their difference in laminar locations, since the majority of CR<sup>+</sup>/eGFP<sup>+</sup> neurons were found in lamina II, while the PV-expressing cells were mostly located in laminae II<sub>i</sub>-III. PV is expressed in a different population of islet cells (Hughes et al., 2012) and intriguingly both islet cell populations express Ca<sup>2+</sup> binding proteins.

Smith et al. (2015) reported that 1.6% of NPY cells in the SDH were CR-immunoreactive. As mention before that inhibitory CR cells make up 25% of all inhibitory interneurons and this current study found that 7.5% of the CR<sup>+</sup>/eGFP<sup>+</sup> cells were NPY-immunoreactive. This represent 1.875% of all inhibitory neurons in SDH. Meanwhile NPY-immunoreactive neurons account for 33% of the inhibitory interneurons in SDH (Boyle et al., 2017). Therefore, 5.7% (1.875% of/33%) of the NPY cells in the SDH were CR-immunoreactive. This prediction is higher than what was found by Smith et al. (2015). The likely explanation would be that they would have missed cells with weak NPY-immunoreactivity.

In addition to the peptide listed above, they may also be expression of endogenous opioid peptide enkephalin (ENK) that have been investigated by Huang et al. (2010) using a mouse in which the eGFP was expressed by ENK-positive cells. They reported that ~43% of CR-positive cells were eGFP-immunoreactive and ~48% of eGFP-positive neurons also contained CR-immunoreactivity. However, they did not specifically look at the inhibitory CR cells. Thus, it is possible that the entire eGFP<sup>+</sup>/CR<sup>+</sup> cells in their study falls within excitatory CR cells population.

The present findings suggested that CR<sup>+</sup>/eGFP<sup>+</sup> (inhibitory CR) neurons represent another neurochemically distinct group of inhibitory interneurons in the dorsal horn. In addition, more than 80% of CR<sup>+</sup>/eGFP<sup>+</sup> neurons were found in lamina II and this was consistent in both animals.

#### 4.4.2 Expression of the $sst_{2A}$ receptor in CR<sup>+</sup>/eGFP<sup>+</sup> neurons in Nociceptin::eGFP mice

To further examine CR<sup>+</sup>/eGFP<sup>+</sup> cells in the SDH,  $sst_{2A}$  immunostaining was applied on sections from Nociceptin::eGFP mice. Previously, several studies have used  $sst_{2A}$  as a marker to define inhibitory interneurons and it was found that virtually all  $sst_{2A}$ -positive cells were GABA-immunoreactive (Todd et al., 1998, Polgár et al., 2013a, Polgár et al., 2013b, Smith et al., 2015, Cameron et al., 2015). Studies that were carried out in both rat and mouse reported that around half of the inhibitory interneurons in laminae I and II expressed  $sst_{2A}$  (Polgár et al., 2013b, Polgár et al., 2013a).

Five ( $sst_{1-5}$ ) somatostatin receptors have been identified (Hoyer et al., 1995, Reisine and Bell, 1995) but according to the Allen Brain atlas, it appears that  $sst_2$  is the only receptor that is expressed by neurons in SDH of mouse since only  $sst_2$  mRNA is found there. Somatostatin receptor  $sst_2$  have 2 different forms,  $sst_{2A}$  and  $sst_{2B}$  made by carboxy-terminal splicing (Schulz et al., 1998a). As mention before, cells that expresses  $sst_{2A}$  is distributed mainly in laminae I-II, meanwhile  $sst_{2B}$  immunoreactivity is observed throughout the spinal gray matter but more prominent in the ventral horn. Frequently, immunostaining of  $sst_{2A}$  can be seen in the cell membrane of a small cell bodies and their dendrites, contrary  $sst_{2B}$  is seen in cell bodies of bigger neurons and their proximal dendrites (Schulz et al., 1998a).

In this current study, 48% of the CR<sup>+</sup>/eGFP<sup>+</sup> cells were labelled with  $sst_{2A}$  receptor in lamina II. This finding was similar to that of Smith et al. (2015) who estimated around half (53%) of inhibitory CR cells in lamina II expressed  $sst_{2A}$  receptor. Among the four distinct inhibitory neurochemical populations mention above, almost all galanin and nNOS expressing cells in the mouse and rat were labelled with  $sst_{2A}$  (Polgár et al., 2013b, Iwagaki et al., 2013), and galanin and nNOS accounted for 44% and 30% of the  $sst_{2A}$  cells, respectively (Iwagaki et al., 2013). However, none of the PV-immunoreactive cells were labelled with  $sst_{2A}$ . For NPY-immunoreactive cells, slightly different proportion were found in different species. Only 16% of the cells that were positive for NPY in the rat were labelled with  $sst_{2A}$  (Polgár et al., 2013b) and in the mouse, 24% of NPY-

containing neurons were labelled with  $sst_{2A}$ , slightly higher percentage than those cells that were found in the rat (Iwagaki et al., 2013).

$Sst_{2A}$  expressing cells are found mainly in laminae I and II, where they generally matched the distribution of the peptide somatostatin, which is present in both primary afferents and glutamatergic interneurons in lamina I and II (Hunt et al., 1981, Hökfelt et al., 1975). Somatostatin released from these neurons causes hyperpolarisation of those inhibitory interneurons that express  $sst_{2A}$  receptors and thus, reduces their excitability leading to disinhibition by reduction in GABA release (Yasaka et al., 2010). A study by Iwagaki et al. (2013) reported that application of CYN 154806 (a specific  $sst_2$  receptor antagonist) or tertiapin Q (a blocker of G-protein-coupled inwardly rectifying  $K^+$  channels (GIRK)), prevented somatostatin from causing membrane hyperpolarisation. These results indicate that somatostatin acts through  $sst_{2A}$  receptors and by the activation of GIRK channels (Kim et al., 2002). Recently, a study that combined chemogenetics, pharmacology and cell-specific knockout of somatostatin provided evidences that somatostatin contributes to itch by a disinhibitory mechanism at the spinal cord level (Huang et al., 2018). Huang and colleagues reported that mice that lack somatostatin in both primary afferents and dorsal horn interneurons show significantly less itch behaviour in response to several pruritogens. The pruritic effect of somatostatin was thought to involve inhibition of inhibitory dynorphin cells. Interestingly, loss of somatostatin primary afferents resulted in an increased response to noxious heat stimuli and this suggested that somatostatin released from these primary afferents suppressed nociceptive responses.

Nothing is known about the role of  $sst_{2A}$  receptor expressed by the inhibitory CR cells. However, inhibitory CR cells in the SDH are thought to be involved in presynaptic inhibition of  $C^{MrgD}$  afferents (see next chapter for details). It is possible that binding of somatostatin to  $sst_{2A}$  receptor on this cells, resulting in disinhibition of CR cells may increase response to mechanical pain. However, contrary to this prediction, Huang et al. (2018) found that deletion of somatostatin from spinal cord interneurons in fact resulting in increased sensitivity to mechanical stimuli. At present it is very difficult to explain these findings. It is likely that this reflex the action on primary afferent fibres, some

of which also express  $sst_{2A}$  receptor (Schulz et al., 1998b). Furthermore, half of the  $CR^+/eGFP^+$  cells were immunoreactive for  $sst_{2A}$ , but, so far there is no evidence to show that they are two different populations of  $CR^+/eGFP^+$  cells.

#### **4.4.3 Association of other inhibitory neurochemical markers with $CR^-/eGFP^+$ cells in $RorB^{eGFP}$ mice**

The present results showed that eGFP-cells that lack CR belong to other neurochemical populations such as those that expressed galanin, nNOS, NPY and PV. As many as 59% of the CR-negative eGFP-positive cells were labelled with galanin, followed by NPY (22%) and nNOS (17%). Despite numerous eGFP-immunoreactive cells being found in SDH, only 1% of these cells were labelled with PV. However, in lamina III, 9% of the CR-negative eGFP-positive neurons were PV-immunoreactive. Based on these numbers, the 4 neurochemical markers mentioned above accounted for ~99% of the  $CR^-/eGFP^+$  cells in SDH of  $RorB^{eGFP}$  mice.

Despite the fact that eGFP cells in the  $RorB^{eGFP}$  mice were highly concentrated in the superficial laminae and their processes form a distinct band in the middle of lamina II, nonetheless, only half of the cells belonged inhibitory CR cells population and the remaining were distributed between galanin, nNOS and NPY. The functions of RorB are not widely discussed since not many studies have been done to investigate the role of these gene in the spinal cord dorsal horn. A study by Wildner et al. (2013) reported that RorB is one of transcription factor gene that were seen mainly expressed in the superficial part of the dorsal horn of mouse. Nothing is known about the role of RorB in the cells that were immunoreactive for galanin, nNOS, NPY, PV and CR.

## **5 Synaptic connections between tdTomato<sup>+</sup> cells in RorB<sup>CreERT2</sup>; Ai9 and RorB<sup>CreERT2</sup>; Ai34 mice and non-peptidergic C-fibres**

## 5.1 Introduction

Inhibitory interneurons in the dorsal horn are activated by primary afferent fibres and descending tracts originating from the brain (Zeilhofer et al., 2012). A few early electron microscopic studies found that primary afferents which were identified by being central axons of synaptic glomeruli formed synapses onto dendrites of inhibitory interneurons revealed with immunostaining for GABA or glycine (Carlton and Hayes, 1990, Todd, 1990). Various studies using patch-clamp recordings from spinal cord slices also showed synaptic input from different types of primary afferents onto inhibitory interneurons (Lu and Perl, 2003, Heinke et al., 2004, Ganley et al., 2015, Iwagaki et al., 2016).

Meanwhile, ultrastructural studies on unmyelinated and myelinated primary afferents showed that many axonal boutons belonged to these primary afferents in the dorsal horn were postsynaptic to axon terminals or vesicle containing dendrites (Maxwell et al., 1982, Maxwell and Bannatyne, 1983, Maxwell et al., 1984). Although most synapses form by GABAergic axons are axodendritic or axosomatic, it is known that some of them form synapses onto other axons identified as axoaxonic synapses and these are thought to underlie presynaptic inhibition (Eccles et al., 1961, Gray, 1962, Eccles et al., 1962a, Eccles et al., 1962b). Historically, McLaughlin et al. (1975) showed that GAD-immunoreactive axon terminals were presynaptic to unknown axonal boutons. Later, it was found that following dorsal root rhizotomy, the unknown axonal boutons were belonged to primary afferents (Barber et al., 1978). Some of the axoaxonic synapses are found to make synaptic contacts with dendrites from other neurons that are postsynaptic to primary afferent boutons (Maxwell et al., 1982, Bannatyne et al., 1984). This arrangement is known as synaptic triad which allows the presynaptic axon terminal to mediate both presynaptic and postsynaptic inhibition of primary afferents and second order sensory neurons (Barber et al., 1978). In the ventral horn, Hughes et al. (2005) found type Ia muscle afferents received axoaxonic synapse that originated from a specific population of GABAergic neurons. Thus, it is possible that presynaptic inhibitory inputs to primary afferents in the dorsal horn originate from a specific type of GABAergic interneurons (Todd, 2010).

Preliminary work carried out by Dr David I Hughes identified a source of cells that give rise to axoaxonic synapses in type I glomeruli, and therefore presynaptically inhibit the central axons of  $C^{MrgD}$  afferents which are thought to be mechanical nociceptors. Electron microscopy study on Neurobiotin filled CR islet cells patched in a CR::eGFP mouse showed that three axonal boutons of one of the cell were presynaptic to central axon of type I glomeruli. Meanwhile, their dendrites received synapses from central boutons of these glomeruli. In chapter 3, it has been showed that tdTomato<sup>+</sup>/eGFP<sup>+</sup> cells in Nociceptin::eGFP; CR<sup>Cre</sup>; Ai9 mouse corresponds to CR islet cells. The dendritic trees of these islet cells are restricted to the IB4 plexus suggesting that they receive synaptic input from  $C^{MrgD}$  afferents and are important source of presynaptic inhibition on these primary afferents. This mouse cross was useful for the study of CR islet cells but unfortunately it has some limitation. As mentioned previously, the Nociceptin::eGFP; CR<sup>Cre</sup>; Ai9 mouse labelled most of the inhibitory cells in the SDH, thus making it very difficult to identify and patch these cells during electrophysiology experiments. Another mouse line that was used in previous chapter 3 and 4 was Nociceptin::eGFP mouse. It is a BAC transgenic mouse line, which could only be used to look at the distribution of cells and determine co-expression of neurochemical markers within the cells in the spinal cord. However, Nociceptin::eGFP mouse did not allow manipulation on the function of the cells.

In this part of the study, inducible RorB<sup>CreERT2</sup> mouse line will be used as a tool to identify CR islet cells in order to study the neurons that form axoaxonic synapses with  $C^{MrgD}$  afferents. This mouse line has two advantages over the previous alternatives. Firstly, the RorB<sup>CreERT2</sup>; Ai9 cross labelled a much more restricted population, which allows the electrophysiologist to patch the cells without having difficulty in finding the cells of interest and also allows many anatomical studies to be perform because cells are well labelled. Secondly, because this is a Cre-recombinase mouse line, it allows manipulation of the function of desired population of cells. One of the long term goal of the study would be to alter the function of these cells. For example, if inhibitory CR cells are activated or inactivated, it is predicted that this will result in decrease or increase in mechanical pain, respectively. Although this is not yet being accomplished, this remained a major goal. To achieve this goal, effectively a Cre-recombinase

provides a method for manipulation of the cells function in many different ways such as the use of toxins, optogenetics or chemogenetics as well as allowing anatomical visualisation of the cells (Roth, 2016, Bang et al., 2016, Huang et al., 2018).

The objectives of this part of the study are: 1) to validate the  $RorB^{CreERT2}$  mouse line as a useful tool to investigate further inhibitory CR cells in lamina II; and 2) to explore the excitatory input onto tdTomato cells from non-peptidergic C-nociceptors that were identified with either IB4 or PAP and also to determine whether their axons form axoaxonic synapses onto these primary afferents. To achieve the first objective of this study, the  $RorB^{CreERT2}$  mouse was crossed with a reporter mouse Ai9 (CAG-floxed tdTomato). In the early part of the study, tissues from this mouse line were reacted with Pax2 and CR antibodies to determine the percentage of inhibitory CR cells that were labelled with tdTomato. The second objective was carried out by using  $RorB^{CreERT2}; Ai9$  and  $RorB^{CreERT2}; Ai34$  mouse lines. Both of these mouse lines require treatment with tamoxifen because the activity of Cre-recombinase depends on administration of this drug due to the binding of oestrogen receptor fusion protein on Cre-recombinase.

## 5.2 Materials and methods

### 5.2.1 Tamoxifen optimization in $RorB^{CreERT2}; Ai9$

In this part of the study,  $RorB^{CreERT2}$  were crossed with two different reporter lines, Ai9 and Ai34. In these mice, either tdTomato (Ai9) or tdTomato-synaptophysin fusion protein (Ai34) with the CAG promoter is inserted into the *Gt(ROSA)26Sor* locus downstream of a *loxP*-flanked STOP cassette. Once this STOP cassette is removed by Cre-mediated excision (in  $RorB$  expressing cells) these cells will express either tdTomato or tdTomato-synaptophysin fusion protein. The tdTomato will fill the entire neuronal processes, while the tdTomato-synaptophysin fusion protein will be targeted to the axons of  $RorB$  cells. The activity of Cre- $ERT^2$  depends on the administration of tamoxifen, which leads to the entering of this Cre- $ERT^2$  into the nucleus of the cells and allowing Cre- $ERT^2$  to control gene activity in  $RorB^{CreERT2}$  mice. Both  $RorB^{CreERT2}; Ai9$  and  $RorB^{CreERT2}; Ai34$  mouse lines that were used in this part of the study

therefore require treatment with tamoxifen in order to allow expression of tdTomato.

A series of experiments were carried out to develop an effective dosage strategy for tamoxifen by giving the drug at difference postnatal ages. In one set of experiments, the animals were treated with either a single dose of 1 mg or 2 mg tamoxifen in 50  $\mu$ l corn oil at P16-P18 while in another set the same doses were given at P31-P36. In most cases administration of tamoxifen was given through intraperitoneal (IP) injection. However, in four cases, tamoxifen was delivered through gavage at P18. This was performed to determine which is the best method (IP or gavage) to achieve the maximum tdTomato expression in the spinal cord of RorB<sup>CreERT2</sup>; Ai9 mice.

### **5.2.2 Animals and tissue processing for confocal microscopy**

All of the RorB<sup>CreERT2</sup>; Ai9 mice that received difference doses of tamoxifen were subsequently deeply anaesthetised and perfused with freshly made 4% de-polymerised formaldehyde as mention previously. Lumbar spinal cord segments were dissected and post-fixed for 2 hours. Then, lumbar spinal cords were cut into 60  $\mu$ m thick transverse or parasagittal sections. Then sections were immersed in 50% ethanol for 30 minutes to enhance antibody penetration (Llewellyn-Smith and Minson, 1992). Initially, a few sections were mounted on glass slides and were viewed under the fluorescence microscope to assess the distribution and the number of tdTomato cells present per section. During the course of the study, it became apparent that animals treated with tamoxifen at P16-P18 had a far greater number of tdTomato cells from those which received tamoxifen at later stages (see below for details). Sections from some of these mice were then processed for immunocytochemistry, as described below. In all cases, sections were incubated in primary antibodies at 4°C for 5 days and overnight in secondary antibodies. Antibodies were diluted in PBS that contained 0.3% Triton-X100 and 5% normal donkey serum.

In addition, 2 RorB<sup>CreERT2</sup>; Ai34 spinal cords were obtained from Professor David Ginty from Harvard University. These mice received a single injection of 2 mg tamoxifen at P11 and were perfused in a similar way. Sections were then processed for multiple immunolabelling as described below.

### **5.2.2.1 Proportion of tdTomato cells that are CR- and Pax2-immunoreactive in the RorB<sup>CreERT2</sup>; Ai9 mouse**

To determine the relationship between inhibitory CR (Pax2<sup>+</sup>) cells and tdTomato<sup>+</sup> cells in lamina II, transverse sections from 3 young adults RorB<sup>CreERT2</sup>; Ai9 mice of either sex (17-19 g) that had received tamoxifen at P18 were incubated in rabbit anti-Pax2 and mouse anti-CR antibodies to label inhibitory CR cells. These primary antibodies were revealed with Pacific Blue and Alexa 488, respectively. The tdTomato<sup>+</sup> expression was visible without the use of antibody, due to the presence of bright native red fluorescence. Sections were mounted as described above and were viewed with a confocal microscope. Four transverse sections from each mouse were randomly selected as mentioned before. Sections were scanned through their full thickness with the 40x oil immersion lens and 1  $\mu\text{m}$  z-separation, with the aperture set to 1 Airy unit. Tile scans were used to capture the whole width of the superficial laminae of the dorsal horn. Confocal scans were analysed offline using Neurolucida for Confocal Software. The outline of the dorsal horn and the boundaries between laminae I-II were drawn. The lamina I/II boundary was drawn 20  $\mu\text{m}$  below the dorsal white matter and the ventral extent of the CR-immunoreactive cells was used to determine lamina II/III border. Neurons present in the whole depth of the sections were analysed. All cell bodies of tdTomato-positive neurons found in laminae I-II were plotted onto the Neurolucida drawing. Then, the CR channel was viewed to determine the proportion of tdTomato-positive cells that were immunoreactive for CR. Following that, the channel corresponding to Pax2 was documented for each of the selected CR<sup>+</sup>/tdTomato<sup>+</sup> neurons. In addition, to determine the proportion of the inhibitory CR (Pax2) neurons that were immunoreactive for tdTomato, cells that were immunoreactive for both CR and Pax2 were also counted before the channel representing tdTomato was viewed.

### **5.2.2.2 Contacts between IB4-binding primary afferents and tdTomato-axonal boutons in RorB<sup>CreERT2</sup>; Ai34 mice**

In order to assess the extent to which axons of the RorB cells give rise to axoaxonic on non-peptidergic C-nociceptors, transverse sections from 2 RorB<sup>CreERT2</sup>; Ai34 mice were incubated overnight in unconjugated IB4 (1:1000) at 4°C followed by incubation with goat antibody to identify IB4 and rabbit anti-VGAT to label inhibitory axonal boutons. These primary antibodies were revealed

with Pacific Blue and Alexa 488, respectively. The tdTomato was visible without the use of antibody due to the high level of native fluorescence. The binding of IB4 was used to reveal non-peptidergic C-nociceptors (Wang et al., 1994, Sakamoto et al., 1999). In the *RorB<sup>CreERT2</sup>; Ai34* mice the expression of synaptophysin-tdTomato fusion protein resulted in axonal targeting of the tdTomato in *RorB* cells.

Sections were mounted as described above and were viewed with a confocal microscope. Two sections from each mouse were randomly selected as mentioned previously. Sections were scanned with 63x oil immersion lens to produce z-series of 69 optical sections, with a z-separation of 0.3  $\mu\text{m}$  and the aperture set to 1 Airy unit. Tile scans were used to capture the IB4-axonal band that was found in the middle of lamina II across the whole mediolateral width of the dorsal horn on 1 side. It is already known that IB4-labelled primary afferents terminate mainly in the central part of lamina II (Lorenzo et al., 2008). These image stacks were analysed offline using NeuroLucida for confocal software. Eighty IB4-labelled afferent terminals were randomly selected from each section and plotted before the channel corresponding to tdTomato and VGAT were viewed. The presence or absence of tdTomato- and VGAT-positive profiles in contact with the IB4 boutons was noted.

### **5.2.2.3 Contacts between non-peptidergic primary afferents and tdTomato-positive axons and dendrites in *RorB<sup>CreERT2</sup>; Ai9* mice**

To determine the proportion of tdTomato-axonal boutons that are in contact with non-peptidergic C-nociceptors and also the proportion of the excitatory synapses on the tdTomato cells that originated from these C-nociceptors, parasagittal sections from 3 *RorB<sup>CreERT2</sup>; Ai9* young adult mice of either sex (17-21 g) that had received tamoxifen at P35 were used for this part of the study. This was reacted to reveal IB4, prostatic acid phosphatase (PAP), mCherry, and Homer. This was achieved by incubating the sections at 4°C in rabbit anti-mCherry to reveal tdTomato cells, goat anti-Homer to label glutamatergic synapses (Gutierrez-Mecinas et al., 2016b), biotinylated IB4 (IB4; 1  $\mu\text{g ml}^{-1}$ . Sigma-Aldrich, Gillingham, UK) and chicken anti-PAP. Both IB4 and the anti-PAP were used to identify non-peptidergic C-nociceptors (Zylka et al., 2008, Taylor-Blake and Zylka, 2010). Primary antibodies were revealed with Rhodamine Red,

Alexa 647, avidin-Pacific Blue and Alexa 488, respectively. Then, sections were mounted as described above. Although both IB4 and PAP antibody label non-peptidergic C-nociceptors, staining with the IB4 lectin was found to be variable in quality. The PAP antibody was therefore used to test whether it could provide an alternative to IB4 immunostaining. Two to three sections from each mouse were randomly selected and scanned with 63x oil immersion lens. Three tdTomato cells were selected from each animals and were scanned to produce z-series of 40 optical sections (z-step of 0.3- $\mu$ m and the aperture set to 1 Airy unit) to include large part of the dendritic and axonal arbors. In cases where two cells were scanned in the same section, this was sufficiently far apart, so that individual dendritic trees and axons of these cells could be analysed. The image stacks were analysed offline using NeuroLucida for Confocal software. To define the proportion of excitatory synapses on the tdTomato cells derived from IB4- or PAP-labelled central terminals, 80 dendritic spines of tdTomato cells were selected from the image stacks and labelled while only the tdTomato channel visible. The channels representing Homer, IB4 and PAP were then viewed and the presence or absence of immunostaining was recorded for each of the selected dendritic spines. During the selection of dendritic spines, the channel representing Homer was not viewed to avoid selection bias, since the presence of Homer will outline central terminal of primary afferents, which often form glomeruli. Only dendritic spines with the presence of Homer were counted in the analysis.

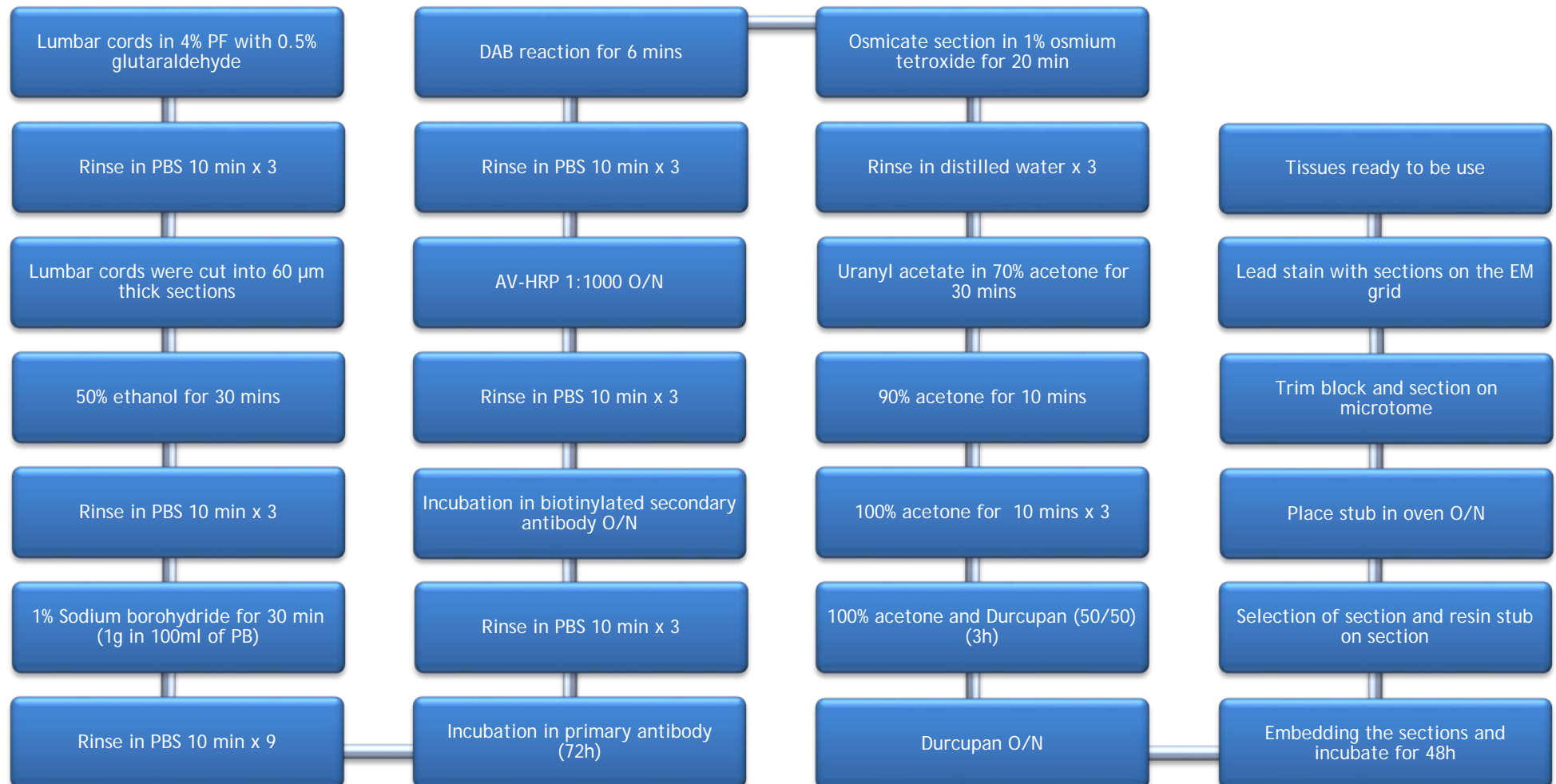
In order to determine the extent to which tdTomato-axonal boutons provide input onto IB4- or PAP-labelled primary afferents, 60 axonal boutons belonging to each tdTomato cells were identified. The channel revealing mCherry was first viewed, and boutons were plotted. The presence or absence of IB4 and/or PAP boutons in contact with the identified mCherry boutons was noted.

### **5.2.3 Animals and tissue processing for electron microscopy**

Two male RorB<sup>CreERT2</sup>; Ai9 adult mice (24-26 g) and 2 RorB<sup>CreERT2</sup>; Ai34 adult mice of either sex (21-23 g), were deeply anesthetised with pentobarbitone and perfused through the left cardiac ventricle with fixative that contained 0.2% or 0.5% glutaraldehyde and 4% freshly de-polymerised formaldehyde in PB. Lumbar spinal cord segments were dissected out from all animals and post-fixed for 2

hours with the same solution at 4°C before being transferred to PB. The lumbar segments were cut into 60 µm thick transverse sections using a vibrating blade microtome followed by immersion in 50% ethanol for 30 minutes to enhance antibody penetration (Llewellyn-Smith and Minson, 1992). They were also treated with 1% sodium borohydride for 30 minutes to reduce the damaging effects of glutaraldehyde on antigenicity (Kosaka et al., 1986). Then, the sections were rinsed extensively and incubated in mCherry anti-rabbit antibody (diluted 1:10,000 or 1:20,000 in PBS) for 72 hours, and in biotinylated donkey anti-rabbit antibody (Jackson ImmunoResearch, 1:500; 24 hours) followed by avidin conjugated to horseradish peroxidase (Sigma, 1:1000; 24 hours). The PBS used for diluting these reagents did not contain Triton because it disrupts the membrane structure. The sections then were reacted with 3,3'-diaminobenzidine (DAB) in the presence of hydrogen peroxide (Hughes et al., 2012) to reveal the HRP-labelled mCherry-immunoreactive profiles. The sections were then osmicated in 1% osmium tetroxide (OsO<sub>4</sub>) for 20 minutes, stained with uranyl acetate (in 70% acetone), dehydrated in acetone, flat embedded in Durcupan resin between acetate foils and cured for 48 hours at 70°C. A single section from each animal reacted with each antibody concentration was selected, mounted on a stub of cured resin, and trimmed to an area that included laminae I-III of the dorsal horn. Ultrathin sections (silver interference colour, ~70 nm thickness) were cut with a diamond knife, collected on Formvar-coated single slot grids and stained with lead citrate. Sections were viewed with a Philips CM100 transmission electron microscope (EM) equipped with digital camera. To investigate the relationship between tdTomato-axonal boutons and type I glomeruli in lamina II in RorB<sup>CreERT2</sup>; Ai9 and RorB<sup>CreERT2</sup>; Ai34, regions that contained numerous DAB profiles and type I glomeruli were examined with EM at high magnification. The protocol for tissue processing for EM study is shown in Figure 5-1.

**Figure 5-1 Tissue processing for Electron microscopy**



## 5.3 Results

### 5.3.1 Effects on tamoxifen dosage on tdTomato expression in RorB<sup>CreERT2</sup>; Ai9 mice

A few transverse sections from lumbar segment of RorB<sup>CreERT2</sup>; Ai9 mice that have been treated with tamoxifen at difference ages were examined with the fluorescence microscope and the cells in the SDH on each side throughout the depth of the sections were counted. In all cases, there were tdTomato cells in the dorsal horn and the plexus of processes in the middle part of lamina II with the distribution similar to that seen in RorB<sup>eGFP</sup> mice with fewer cells seen in RorB<sup>CreERT2</sup>; Ai9 mice. However, the number of tdTomato cells and the completeness of the plexus were very variable between animals. In early experiments, RorB<sup>CreERT2</sup>; Ai9 mice received a single dose of 2 mg IP tamoxifen between P34-36. Surprisingly, it was found that this resulted in very few tdTomato cells. Following this finding, a single dose of 1 mg or 2 mg tamoxifen was administered earlier, between P16-P18, and in most cases there were much higher efficiency of recombination and therefore, more tdTomato cells were labelled. Interestingly, in a few cases, relatively few tdTomato cells were visible despite early administration of tamoxifen. In four cases in which 2 mg tamoxifen was administered by gavage at P18, sparse labelling tdTomato cells were identified. This finding showed that IP injection of tamoxifen was a better method to administer this drug in RorB<sup>CreERT2</sup>; Ai9 mice. The animals were classified as having sparse labelling tdTomato cells if fewer than 5 cells were presence on one side of the superficial laminae in a per 60 µm section.

Although this was inconvenient for several of the studies to investigate these cells, it has the advantage that it provided a single cell labelling. This was used to investigate contacts between individual tdTomato cells and non-peptidergic primary afferents. In addition, the morphology of single tdTomato cells could be studied without the presence of dendrites or axons from other cells.

### 5.3.2 Inhibitory CR cells in RorB<sup>CreERT2</sup>; Ai9 mice

In this part of the study, tissues from animals with the high numbers of tdTomato cells labelling were used. Transverse sections from RorB<sup>CreERT2</sup>; Ai9 mice were examined after immunostaining for CR and Pax2 were readily

identified in these sections. The tdTomato was reasonably bright, thus for the purpose of cells counting, immunostaining with mCherry antibody to reveal tdTomato cells were not applied. The distribution of cell bodies and dendrites that were CR-immunoreactive was similar to previous findings reported in chapter 3 and 4. The general distribution of tdTomato cells in the dorsal horn was similar to RorB<sup>eGFP</sup> mice but there were fewer cells labelled in RorB<sup>CreERT2</sup>; Ai9 mice (Figure 5-2 a). The somata of tdTomato cells were highly concentrated in lamina II mainly in the band that was present in the middle of this lamina. This band was mainly formed by the dendrites of lamina II tdTomato cells. In sections that have been reacted with IB4, there was perfect overlap between this plexus of tdTomato dendrites with the IB4-labelled non-peptidergic C-nociceptors. The similar band of dendrites were also observed in RorB<sup>eGFP</sup> mice. In addition, tdTomato cells were seldom seen in lamina I and scattered cells with sparser axonal plexus seen in lamina III and in the deeper laminae. There was a clear gap between the dendritic band in lamina II and tdTomato cells and processes found in deeper laminae, which was not seen in RorB<sup>eGFP</sup> mice. This strongly suggests that the plexus of dendrites and axons in this band in lamina II is derived from tdTomato cells in the superficial laminae and not from cells in deeper laminae (Figure 5-2). This is because very rarely profiles were seen passing from ventral part into the band in lamina II.

Analysis on confocal sections on optimally labelled animals revealed that the great majority of tdTomato cells in laminae I-II were also immunoreactive for CR and Pax2. However, none of the tdTomato cells in the deeper laminae were CR-immunoreactive. Most of the cells in lamina III were Pax2-positive with higher number of excitatory tdTomato cells (Pax2 negative) seen in the deeper laminae. Generally, fewer cells were found in RorB<sup>CreERT2</sup>; Ai9 mice compared to RorB<sup>eGFP</sup> mice. A total of 189 (range 39-82, n = 3 mice) tdTomato cells were identified in lamina II and 95% (range 92.3%-97.1%) of these cells were Pax2-immunoreactive. Of this, 95% (range 92.4%-100%) of inhibitory tdTomato cells were immunoreactive for CR. In addition, 717 (range 221-263) inhibitory CR cells (Pax2<sup>+</sup>) were counted and of these only 24% (range 15.5%-28.1%) of inhibitory CR cells were tdTomato positive.



**Figure 5-2 tdTomato, CR and Pax2 immunostaining from the dorsal horn of RorB<sup>CreERT2</sup>; Ai9 that have the high numbers of tdTomato cells labelling.** a tdTomato dendritic band is seen in the middle of lamina II. A clear gap is observed between band in lamina II and tdTomato cells and processes found in deeper laminae. b,c CR- and Pax2-immunostaining are similar to the findings from the above study. d merged image. The dashed lines represent the borders between laminae I-III. Scale bar = 200  $\mu$ m.

### 5.3.3 Contacts between IB4-labelled primary afferents and RorB axonal boutons in RorB<sup>CreERT2</sup>; Ai34 mice

Four transverse sections (2 from each mouse) of RorB<sup>CreERT2</sup>; Ai34 mice were analysed after immunostaining for IB4, VGAT and mCherry were readily identified in these sections. As mentioned before, tdTomato axonal boutons were very small. In order to reveal the axons of tdTomato expressing cells, the native fluorescence was amplified by using an antibody (mCherry) which recognized tdTomato. The distribution of the IB4-labelled plexus was identical to that described in previous studies (Zylka et al., 2005, Gutierrez-Mecinas et al., 2016b). A dense band of axons that were labelled with IB4 was seen in the middle of lamina II and occasionally profiles were seen superficial or deep to this. Meanwhile, mCherry antibody labelled axon terminals and intervaricose portion of tdTomato-expressing cells. The tdTomato-positive axonal boutons were found mostly in the middle of lamina II where they formed a dense band. This band was seen to overlapped perfectly the IB4 plexus, which corresponds largely to C<sup>MrgD</sup> afferents (Zylka et al., 2003, Zylka et al., 2005). Meanwhile, a more diffused tdTomato axonal plexus was seen in laminae III-V, and this presumably originated from the deeper tdTomato cells. The axonal boutons of tdTomato cells in lamina II were very small and they were weakly immunoreactive for VGAT. In the 2 RorB<sup>CreERT2</sup>; Ai34 mice, a total of 320 (160 per mouse) IB4 terminals were identified. Of this, 80% (range 80%-81%) were in contact with axonal boutons of tdTomato cells (Figure 5-3).

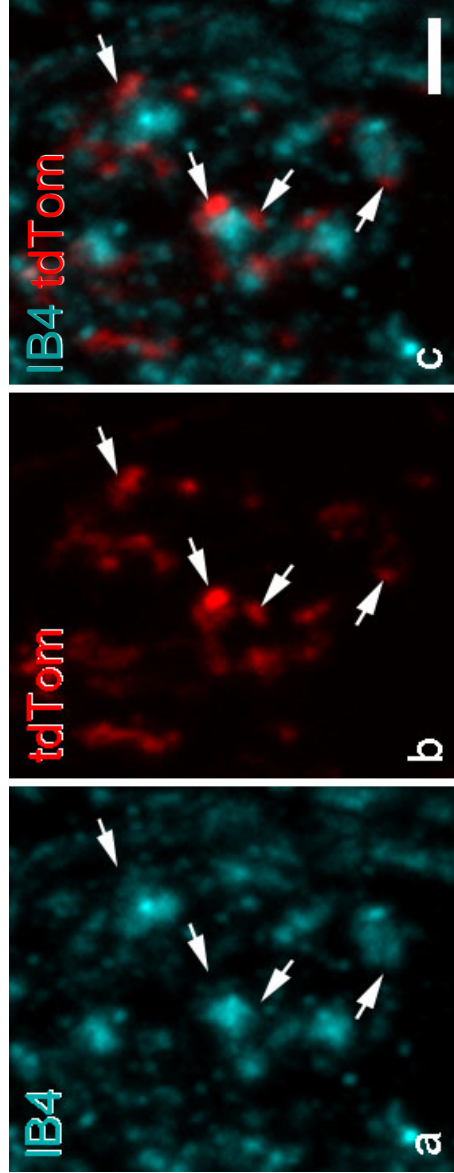


**Figure 5-3 IB4-labelled central terminals contacting tdTomato axonal boutons.** **a** About 80% of IB4-labelled boutons found in lamina II forming contacts **b** with tdTomato axonal boutons (arrow). The mCherry antibody used to immunostained RorB cells also labelled axon terminals and intervaricose portion of tdTomato-expressing cells. The tdTomato-positive axonal boutons were found mostly in the middle of lamina II where they formed a dense band. This band was seen to overlapped perfectly the IB4 plexus. **c** merged image. Scale bar = 2  $\mu$ m.

### 5.3.4 Contacts between non-peptidergic C-nociceptors and tdTomato cells in RorB<sup>CreERT2</sup>; Ai9 mice

In this part of the study, tissues from animals with sparsely labelled tdTomato cells were used. Parasagittal sections from RorB<sup>CreERT2</sup>; Ai9 mice were examined after immunostaining for IB4, PAP, Homer and mCherry were readily identified in these sections. MCherry antibody was used to amplified the native fluorescence in order to reveal tdTomato dendritic spines and axonal boutons. In sparsely labelled RorB<sup>CreERT2</sup>; Ai9 mice, individual tdTomato cells were seen mainly in lamina II, and scattered throughout deeper lamina. Individual tdTomato cell was seen in lamina II as well as in deeper laminae. In some cases, these cells were close together but more often they were sufficiently far apart that there was no overlap of the dendritic trees and axonal arbors. The dendritic trees of tdTomato cells extended rostracaudally within IB4/PAP band. The axons of these cells extended further than the dendritic trees within lamina II. The immunostaining for PAP and the distribution of the IB4-labelled plexus was identical to that seen in previous studies (Zylka et al., 2008, Taylor-Blake and Zylka, 2010, Shehab and Hughes, 2011). The plexus of PAP-labelled axonal terminals that were seen in lamina II perfectly matched the distribution of IB4 plexus. In most cases, PAP-immunoreactivity and IB4-binding were co-localized in the axon terminals. However, in some boutons that were labelled with only IB4 or PAP were seen to have multiple Homer puncta surrounding the varicosities, and this most probably correspond to type I synaptic glomeruli (Figure 5-3 and Figure 5-4). In this part of the study, only isolated lamina II tdTomato cells that did not overlap with other labelled neuron were selected for further analysis.

A total of 720 tdTomato dendritic spines were counted from 9 cells (3 cells from each animal). Among this, 595 (range 53-76) dendritic spines contained Homer and were analysed further. Around 63% (range 47.2%-76.5%) of the Homer puncta within these tdTomato-positive dendritic spines were in contact with boutons that were labelled with IB4 and/or PAP (Figure 5-4). This suggest that the majority of excitatory synapses onto dendritic spines of tdTomato cells are derived from non-peptidergic primary afferent nociceptors. During the course of this analysis, Homer puncta were also seen within the dendritic shaft of the tdTomato cells and these were in contact with IB4- and/PAP-positive boutons.

However, this was not analysed because in some cases it was difficult to be certain whether particular punctum was definitely located within dendritic shaft of the labelled cells. Of this, 47% (range 20.3%-69.1%) of the presumed primary afferent boutons were positive for both IB4 and PAP. Meanwhile 6% (range 1.5%-19.2%) and 10% (range 0%-39%) of the presumed primary afferent boutons were positive for IB4 or PAP, respectively.

To determine the proportion of tdTomato boutons that contacted IB4-/PAP-labelled primary afferent terminal, a total of 540 tdTomato axonal boutons were identified from 9 cells of *RorB<sup>CreERT2</sup>; Ai9* mice. Around 44% (range 40%-55%) of the tdTomato axonal boutons were in contact with primary afferents terminal that were positive for both IB4 and/or PAP (Figure 5-4). Within this population, 25% (range 18.3%-31.7%) of the primary afferent terminals were positive for both IB4 and PAP. Meanwhile 11.3% (range 6.7%-18.3%) and 7.6% (range 3.3%-16.7%) of the terminal axonal boutons were positive only for IB4 or PAP antibody, respectively.

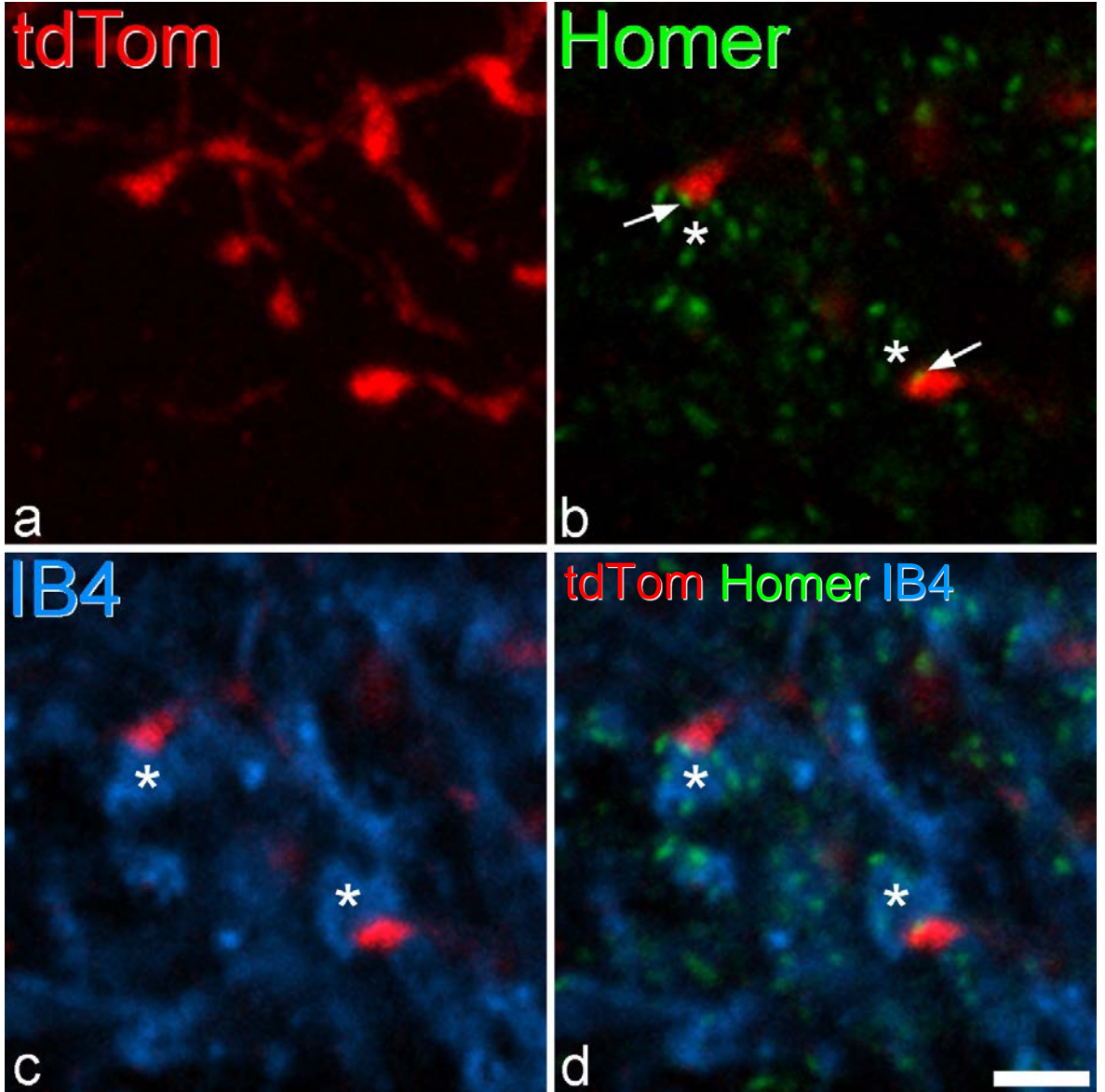


**Figure 5-4 IB4 labelled primary afferents synaptic inputs to RorB cells. a** showing dendritic spines of RorB cells, **b** that contains Homer puncta (arrow) **c** received excitatory synapse from IB4 labelled axonal boutons (asterisks). **d** a merge imaged. Scale bar = 2  $\mu$ m.

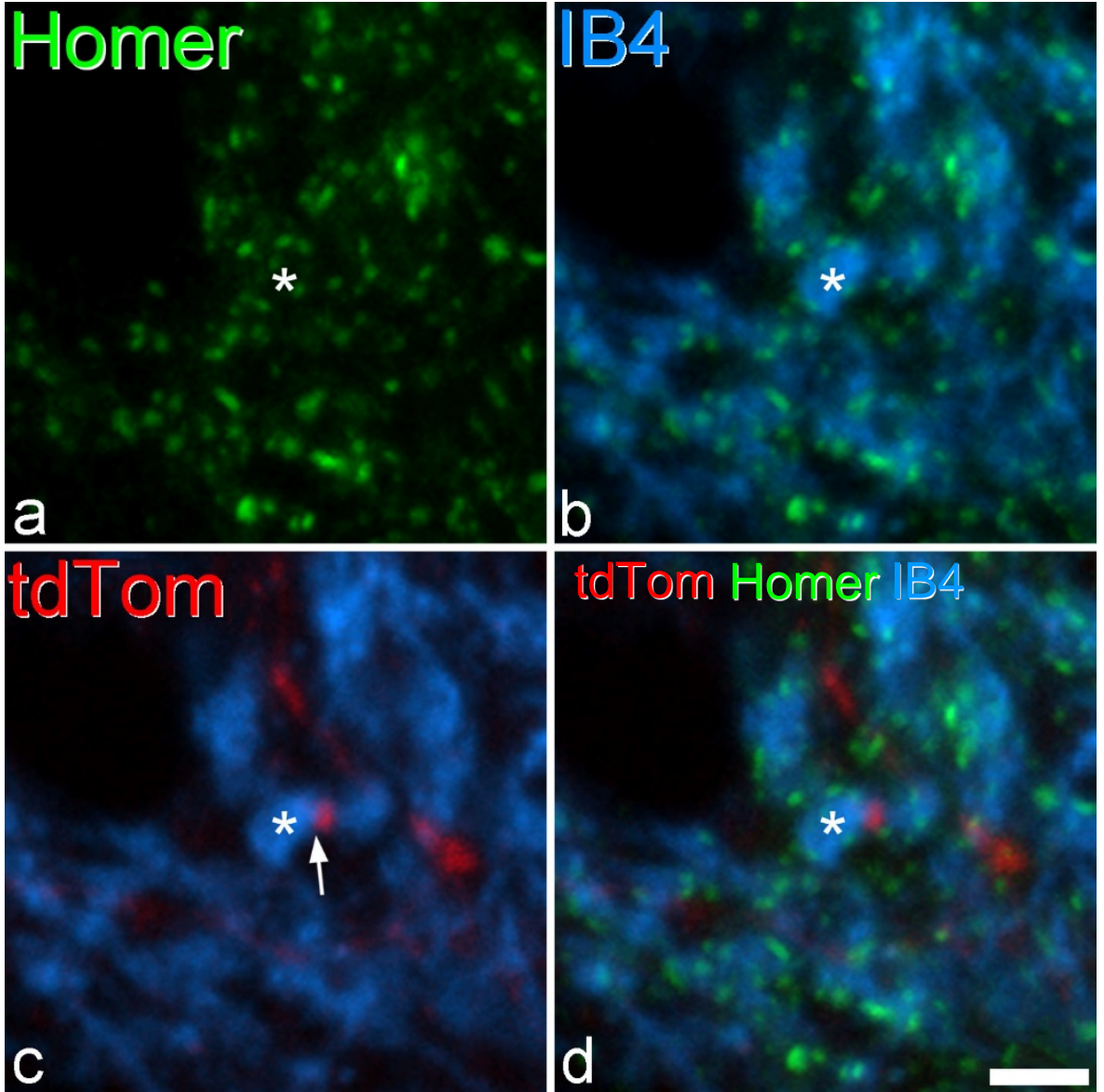


**Figure 5-5 Axoaxonic contacts formed by RorB cells.** a showing Homer, a postsynaptic marker, b surrounded the IB4 labelled central terminal, probably correspond to type I glomeruli and c received contact from RorB axons and presumably form axoaxonic synapse (asterisk). b a merge imaged. Scale bars = 2  $\mu$ m.

### 5.3.4 Electron microscopy findings

This EM was carried out on tissues from RorB<sup>CreERT2</sup>; Ai9 and RorB<sup>CreERT2</sup>; Ai34 mice to look for evidence of synapses between RorB axonal boutons and central axons of type I synaptic glomeruli, which originate from non-peptidergic C-fibres (Gerke and Plenderleith, 2004, Bailey and Ribeiro-da-Silva, 2006). Type I glomeruli were identified as structures containing a dark central axonal boutons with variable sized vesicles and few mitochondria, which formed synapses with peripheral profiles. This profiles resemble those described in several previous studies (Todd, 1996, Ribeiro-Da-Silva and Coimbra, 1982, Bailey and Ribeiro-da-Silva, 2006). Meanwhile, tdTomato-labelled axonal boutons could be recognised due to the presence of the DAB reaction product that resulted from immunostaining with mCherry antibody.

Initially this study involved tissues from the RorB<sup>CreERT2</sup>; Ai34 mice which were chosen because the immunostaining for tdTomato was largely restricted to axonal boutons (due to the present of synaptophysin fusion protein). In this tissue many DAB-labelled axonal boutons were seen intermingled among type I glomeruli and they were often in contact with them. However, it was difficult to describe the type of synaptic contact between the DAB profiles and type I glomeruli due to the intensity of the DAB product in the presynaptic terminal which made it difficult to detect whether synaptic vesicles were clustered at the presynaptic zone. Unfortunately, there were very limited tissues available for RorB<sup>CreERT2</sup>; Ai34 mice and it was not possible to repeat reaction using lower concentration of primary antibody. To overcome this problem, tissues from the RorB<sup>CreERT2</sup>; Ai9 mice were also investigated and in this case, it was repeated multiple time with difference concentration of primary antibody to ensure that DAB deposition was light. In addition, not many DAB profiles were seen due to lack of cells and axonal boutons that were labelled after injection of tamoxifen in RorB<sup>CreERT2</sup>; Ai9 mice. Although this was resulted in improved in intensity of DAB labelling in the animals that was tested, the number of cells and axons were not particularly dense. This presumably reflecting the variability in Cre mediated recombination seen in this mouse line. The great majority of DAB labelled profiles within this tissue were found to be dendritic shaft. For these reasons, the frequency of synaptic contact between RorB axonal boutons and type I glomeruli was not assessed systematically. However, in many cases, RorB-axonal

boutons were seen forming axoaxonic contacts with the central boutons of type I glomeruli (Figure 5-6).

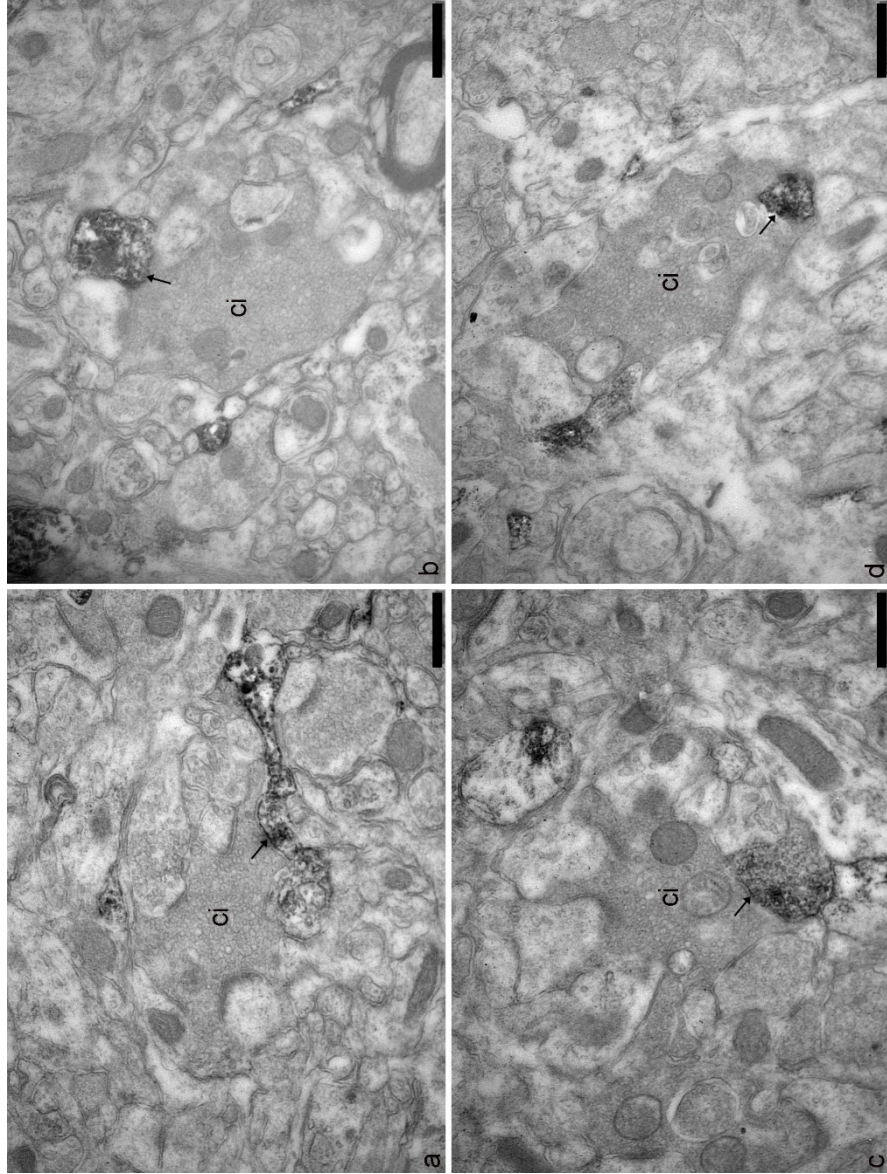


**Figure 5-6 Electron microscopic images of axoaxonic synapse on central bouton of type I glomeruli from tamoxifen treated  $RorB^{CreERT2}$ ; Ai9 mice.** **a** a dendritic spine receives a synapse from central axon of type I glomerular (Ci). **b-d** TdTomato-labelled axonal boutons could be recognised due to the presence of the DAB reaction product that resulted from immunostaining with mCherry antibody (arrow). **b-d** a bouton forming an axoaxonic synapse on Ci bouton. Scale bars: a, b, c and d = 500 nm.

## 5.4 Discussion

The main findings of this study based on crosses of  $RorB^{CreERT2}$  with either Ai9 or Ai34 are that: (1) IP injection of tamoxifen in early or later stage of postnatal life resulted in a difference level of induction of tdTomato; (2) more than 90% of tdTomato cells in the SDH are inhibitory interneurons and immunoreactive for CR; (3) under optimal conditions, only a quarter of the inhibitory CR cells in lamina II were immunoreactive for tdTomato; (4) 80% of the IB4-labelled primary afferents central terminals were in contact with axonal boutons of tdTomato cells; (5) half of the excitatory synapses on the dendritic trees of tdTomato cells were derived from IB4-labelled and PAP-immunoreactive primary afferents; (6) 44% of the tdTomato axonal boutons are in contact with non-peptidergic C-nociceptors. In addition, EM study revealed that the axons belonged to the  $RorB$  cells formed axoaxonic synapses with those primary afferents.

### 5.4.1 Tamoxifen-induced tdTomato in $RorB^{CreERT2}$ ; Ai9 mice

In the field of neuroscience, it is a very common practice to use transgenic animal models as a tool to investigate neuronal circuit; identification of functional population of cell; studying gene function; and for various other purposes (Nagy, 2000, Taniguchi et al., 2011, Häring et al., 2018, Huang et al., 2018). The Cre-LoxP recombination system is a novel method to activate or deactivate genes at a specific time point. This technology has been around for more than twenty years and was used in the field of neurology since then (Orban et al., 1992, Tsien et al., 1996). It can either remove or activate gene function by precise excision of specific region within a gene so that a functional product is not produced or Cre-recombinase could take out a STOP cassette causing activation of a gene, respectively (Feil et al., 2009). Cre-recombinase was made inducible by binding with the mutated hormone-binding domains of the oestrogen receptor (Cre-ER<sup>T</sup>). Before tamoxifen is administered, Cre-ER<sup>T</sup> is inactive and is found in the cytoplasm, bound to heat shock protein-90. Cre-ER<sup>T</sup> can be activated by the synthetic oestrogen receptor ligand 4-hydroxytamoxifen (OHT) but not by endogenous oestrogen, estradiol. The binding of OHT onto Cre-recombinase resulting in the translocation of the recombinase into the nucleus where it acts on the targets DNA (Hayashi and McMahon, 2002). In most of the studies using this Cre recombinase technology, tamoxifen is the drug of choice

for most induction protocols because it is much cheaper compared to OHT and furthermore, OHT is a metabolic product of tamoxifen. In addition, the half-life of tamoxifen is longer than 4-OHT, 12 hours and 6 hours, respectively (Robinson et al., 1991). Tamoxifen is an antagonist of the oestrogen receptor which is widely used clinically as a chemotherapeutic agent for breast cancer and is known to be relatively safe (Jordan, 1992, Bernstein et al., 1999). From published literatures, there are a variety of dosage regimens for administration of tamoxifen into any tamoxifen-inducible models (Danielian et al., 1998, Nakamura et al., 2006). There are several ways to administer tamoxifen via injection (subcutaneous or intraperitoneal) or orally by gavage (Reinert et al., 2012, Huang et al., 2018, Park et al., 2008).

Several varieties of Cre-ER<sup>T</sup> have been developed in order to reduce spontaneous translocation of this complex into the nucleus in the absence of tamoxifen and also to increase their sensitivity to tamoxifen and their recombination efficiency (Liu et al., 2010). For example, the Cre-ER<sup>TM</sup> recombinase contains the mouse oestrogen receptor ligand binding domain (ER-LBD) with a G525R mutation (Danielian et al., 1998), meanwhile Cre-ER<sup>T</sup> contains ER-LBD derived from human rather than mouse (Feil et al., 1996). Cre-ER<sup>T2</sup> is a more recent Cre-ER<sup>T</sup> variant, which was used in this study. It contains triple mutation in the human ER-LBD and is a better choice since it was found that Cre-ER<sup>T2</sup> can be induced with approximately 10 fold lower dose of OHT than Cre-ER<sup>T</sup> (Indra et al., 1999).

In this part of the study, various methods were carried out to achieve expression of tdTomato in the maximum number of cells. Administration of tamoxifen through injection in young mice (P16-18) resulted in labelling of more cells than when tamoxifen was given to older animals. However, even when injection was administered in young mice, the number of cells were variable. This probably due to some leakage of tamoxifen noted after the removal of the injection needle from the injection site, which resulted in low dose being administered (Allen C Dickie unpublished observation). Interestingly, it was found that administration of tamoxifen at later stage of postnatal life (P31-36) consistently resulted in sparse labelling of tdTomato cells. In a different study carried out in the laboratory using other Cre-ER<sup>T2</sup> (nNOS<sup>CreERT2</sup>) mouse line, it was found that treating the adult animals with tamoxifen resulted in large number of cells with

the expected distribution pattern consistent with the majority of nNOS cells being labelled (Huang et al., 2018). Probably that the RorB gene was downregulated between P18 and P36 and this resulted in fewer expression of tdTomato cells. However, this is thought not to be the case as for example that *in situ* hybridization shows large numbers of RorB mRNA positive cells in the superficial laminae of adult animals at P56 (Allen Brain Atlas). The reasons for this reduction in recombination efficiency is not known but it was seen in other Cre-ER<sup>T2</sup> lines (Professor Hanns Ulrich Zeilhofer personal communication). Two different methods of administration of 2 mg tamoxifen through gavage or IP injection method at P18 were used in this study. Findings from the experiments that was carried out on RorB<sup>CreERT2</sup>; Ai9 mice showed that IP injection was a preferable choice due to higher recombination was achieved by using this method. On the contrary, some previous studies found that tamoxifen administration in young adult or adult mice by gavage or IP injection resulted in equivalent number of labelled cells (Huh et al., 2012, Wilson et al., 2014, Rotheneichner et al., 2017).

Even in the optimal labelling experiments, although most of the tdTomato cells were immunoreactive for CR and Pax2, only a quarter of inhibitory CR (Pax2<sup>+</sup>) was labelled with tdTomato and fewer cells were found in RorB<sup>CreERT2</sup>; Ai9 mice than the RorB<sup>eGFP</sup> mouse line. Therefore, it is likely that RorB is expressed in higher number of cells than what was achieved in this study even with the best optimal labelling tissue. It is possible that to overcome this problem, tamoxifen could be given earlier than P16. However, administration of tamoxifen at earlier age could increase in mortality of the young mice due to tamoxifen toxicity and mother cannibalism (Lizen et al., 2015). Previous studies reported that induction of Cre-ER<sup>T2</sup> could be achieved successfully at early postnatal stages but the tamoxifen dosage and administration protocols were largely varied (Ganat et al., 2006, Pitulescu et al., 2010). Some studies have delivered tamoxifen intraperitoneally into pregnant mice (Boyle et al., 2008, Danielian et al., 1998). However, this technique could compromise the ability of mice to have natural birth and thus increase the mortality of both pregnant mice and new born mice as a result of difficult delivery (Boyle et al., 2008). Normally, high oestrogen level is needed to end the gestation and begin the delivery process. According to Shoda et al. (2015), tamoxifen has the ability to inhibit oestrogen level thus

explain the delivery defects. To avoid this problem, caesarean section could be performed to the tamoxifen-treated pregnant mouse at E18.5 and the pups are given to foster mothers (Lizen et al., 2015). Another downside of this technique is that foetal development could be affected due to the risk of injecting the foetuses, thus administration of tamoxifen by gavage into pregnant dam is more favoured (Lizen et al., 2015).

#### 5.4.2 The RorB<sup>CreERT2</sup> mouse line

RorB<sup>CreERT</sup> is a reliable mouse line that can be used to investigate homogenous population of inhibitory CR islet cells, which give rise to presynaptic inhibition of the central axons of the non-peptidergic C-nociceptors in type I synaptic glomeruli. At the beginning of the study, the mouse was crossed with reporter lines, Ai9 or Ai34. The RorB<sup>CreERT2</sup>; Ai9 cross labelled cell bodies and their processes (both axons and dendrites) with tdTomato, meanwhile RorB<sup>CreERT2</sup>; Ai34 crosses labelled only the axons of the cells with tdTomato due to the present of synaptophysin fusion protein. In both lines, the tdTomato labelled cells or axons were seen throughout the SDH and in the deeper laminae. In this study, it was found that 95% of tdTomato cells in superficial laminae were inhibitory (Pax2<sup>+</sup>) in RorB<sup>CreERT2</sup>; Ai9 mouse cross and 95% of these were also immunoreactive for CR. In contrast, only 42% of eGFP cells in the superficial laminae of RorB<sup>eGFP</sup> mice were CR-immunoreactive. In addition, the RorB<sup>eGFP</sup> mice also labelled other inhibitory neuronal populations such as those that expressed galanin, NPY, nNOS and PV, in the SDH. However, in this part of the study although the vast majority of tdTomato-labelled cells in RorB<sup>CreERT2</sup>; Ai9 cross showed islet morphology, even with the best treatment regime (2 mg IP injection of tamoxifen at P18), only a quarter of the inhibitory CR cells were labelled with tdTomato. In contrast, 90% of the inhibitory CR cells were labelled with eGFP in RorB<sup>eGFP</sup> mice as reported in chapter 3. An important and surprising observation was that the RorB<sup>CreERT2</sup>; Ai9 cross labelled far fewer cells than the RorB<sup>eGFP</sup> mice. It is not clear why this should be different because both RorB<sup>eGFP</sup> and RorB<sup>CreERT2</sup>; Ai9 mice are knock-in mouse lines. Thus, it will be expected that eGFP expression faithfully reflexes the expression of RorB. It is possible that the 24% that were labelled in RorB<sup>CreERT2</sup>; Ai9 cross represent a functionally distinct subset among inhibitory CR cells, although the reasons why this cells and not the other cells would be labelled in the Cre-ERT<sup>2</sup> line is not known. Alternatively, it is maybe

that another 75% showed islet morphology and give rise to axoaxonic synapses and formed presynaptic inhibitory input onto C<sup>MrgD</sup> afferents. This seems likely because it was found that all inhibitory CR cells in CR::eGFP mice that were patch clamped and filled with Neurobiotin in electrophysiology experiments showed islet cells morphology (Smith et al., 2015). However, maybe there is a sampling bias in which Smith and colleagues only recorded on larger cells during the experiments.

In a preliminary investigation we examined sections from RorB<sup>CreERT2</sup> mice that was treated with tamoxifen and had received intraspinal injections of adenoassociated virus (AAV) coding for Cre-dependent form of enhanced green fluorescent protein (eGFP) as used previously (Gutierrez-Mecinas et al., 2017). It was found that there were numerous eGFP-positive cells that were concentrating in the SDH near the injection site and this were more numerous than the cells that were tdTomato in the RorB<sup>CreERT2</sup>; Ai9 cross. In comparison these cells were far more numerous than that seen with optimal labelling of tdTomato in RorB<sup>CreERT2</sup>; Ai9 cross, and this suggest that Cre-recombinase was expressed in a larger number of cells than were detected with that other RorB<sup>CreERT2</sup> cross. An unanticipated finding was that in addition to this brightly labelled eGFP cells which were mainly inhibitory, there were also numerous weakly labelled cells at the injection site that were Pax2<sup>-</sup> and therefore presumably excitatory. This suggest that viral injection into RorB<sup>CreERT2</sup> mouse resulted in expression beyond the population of inhibitory RorB cells which would make it very difficult to interpret the finding. One of the disadvantage of incomplete labelling of inhibitory CR cells in RorB<sup>CreERT2</sup>; Ai9 cross is that it makes it difficult to determine what proportion of inhibitory axoaxonic synapses on IB4-/PAP-labelled non-peptidergic primary afferents originate from these source. In addition, in future study that would need activation or inactivation of inhibitory CR islet cells to manipulate function of these cells and test the effect on behaviour of these animals, it would be advantages if all cells belong to this population were captured.

### 5.4.3 Contacts between tdTomato-axonal boutons and non-peptidergic C-nociceptors in RorB<sup>CreERT2</sup>; Ai9 and RorB<sup>CreERT2</sup>; Ai34 mice

Analysis that was carried out on RorB<sup>CreERT2</sup>; Ai34 tissues showed that the great majority (80%) of non-peptidergic primary afferents boutons that were labelled with IB4-lectin received at least one contact from tdTomato axonal boutons. It is likely that many of these represent axoaxonic synapses from the inhibitory CR cells onto the primary afferents. In addition, non-peptidergic C-nociceptors might receive presynaptic inhibition from other sources. A study by Doyle and Maxwell (1993) reported that 37.5% of NPY boutons form axoaxonic synapses on central terminal of synaptic glomeruli. Apart from this, it is possible that non-peptidergic primary afferent boutons received axoaxonic synapses from choline acetyltransferase (ChAT)-immunoreactive neurons in which the cell bodies are mainly located in laminae III-V (Ribeiro-Da-Silva and Claudio Cuello, 1990). Meanwhile, Hughes et al. (2012) found that PV-labelled axon terminals formed axoaxonic synapse on central axons of type II glomeruli, never on type I glomeruli.

Although it is possible to determine proportion of IB4-labelled boutons that received contact from tdTomato-axons, it was challenging to carry out the reverse analysis, to work out the proportion of tdTomato-labelled axons that were in contacts with IB4-positive boutons. Effectively, it was easy to identify tdTomato axonal boutons but it is difficult to make out the structure of IB4-labelled boutons and to determine whether they represent axon terminals or intervaricose portions. Instead, this analysis was carried out in the RorB<sup>CreERT2</sup>; Ai9 mice in which there was a sparse labelling (as described below). This was partly due to suboptimal quality of IB4-labelling that was achieved in the tissues of RorB<sup>CreERT2</sup>; Ai34 mice.

In the RorB<sup>CreERT2</sup>; Ai9 mice in which there was a sparse labelling, all the tdTomato cells that were found in lamina II showed islet cell morphology. In this part of the study, IB4-lectin and PAP-antibody were used to identify non-peptidergic C-nociceptors. Previously, small diameter DRG neurons in rat were labelled using thiamine monophosphatase (TMPase), which is also known as Fluoride-Resistant Acid Phosphatase (FRAP) (Sanyal and Rustioni, 1974,

Silverman and Kruger, 1988). TMPase labelling was restricted to non-peptidergic unmyelinated neurons and a subset of peptidergic DRG neurons (Knyihár-Csillik et al., 1986). In addition, it labelled central boutons of unmyelinated primary afferents in lamina II (Hunt and Rossi, 1985). IB4 was used to distinguish different type of primary afferent and was found to label neurons that expressed TMPase. Later, IB4 became the marker of choice for non-peptidergic primary afferents since technically IB4 was easier to apply (Silverman and Kruger, 1990). More than 20 years later, it was found that in mice, TMPase is identical to transmembrane isoform of PAP (Zylka et al., 2008). PAP was discovered more than 80 years ago and has been widely used in prostate cancer studies since 1930s (Gutman and Gutman, 1938, Ostrowski and Kuciel, 1994). A study by Zylka et al. (2008) found that PAP was also expressed in nociceptive neurons. In mouse DRG cells, PAP was mainly expressed in non-peptidergic neurons that were also positive for IB4, MrgprD and P2X3 (Zylka et al., 2008). According to this paper, all MrgprD were PAP in the DRG neurons. Around 84% of IB4-labelled non-peptidergic and 15% of CGRP-positive peptidergic DRG neurons were immunoreactive for PAP (Taylor-Blake and Zylka, 2010). In the current study it was found that PAP-containing axons mainly terminated in lamina II and overlap perfectly with IB4-binding. A previous study reported that 67% of cells that bound IB4 and 10% of those that were CGRP-immunoreactive were labelled with PAP (Zylka et al., 2008). Meanwhile, there was limited overlap between PAP and CGRP in the spinal cord (Zylka et al., 2008, Taylor-Blake and Zylka, 2010). Around 19% of PAP-labelled DRG neurons were immunoreactive for capsaicin and noxious heat receptor TRPV1 (Zylka et al., 2008).

Two different types of analysis were carried out in sparsely labelled RorB<sup>CreERT2</sup>; Ai9 tissue. First, the proportion of excitatory synaptic input on individual tdTomato dendritic spines was determined and the result showed that around half of the excitatory synapses on these spines were derived from central boutons of non-peptidergic C-nociceptors that were labelled with both IB4 and PAP. Meanwhile ~6-10% of central terminals in lamina II that were labelled with IB4 or PAP were in contact with Homer puncta within tdTomato dendritic spines. However, in all cases the number of contacts between tdTomato dendritic spines and presumed primary afferent boutons that were positive for IB4 or PAP varied between individual cell. For example, some tdTomato cells had none or low

excitatory input from primary afferents that were labelled with either IB4<sup>+</sup>/PAP<sup>-</sup> or PAP<sup>+</sup>/IB4<sup>-</sup>, meanwhile in another cells, as high as ~40% of the excitatory input derived from those primary afferents. These results showed that there was a variability of contacts for each cells and this could reflect inadequate staining or penetration of the IB4 lectin or PAP antibody. However, this was not the case because the penetration and the staining of IB4 and PAP were equally good. This might represent population of primary afferents that may have slightly different function.

Next, using the same animals, the proportion of tdTomato axonal boutons that were in contact with IB4- and/or PAP-labelled central terminals of C-nociceptors was determined. The fact that the quality of staining for IB4 was better in this tissue and together with the present of Homer puncta enable the identification of primary afferent terminals more clearly than what was seen in RorB<sup>CreERT2</sup>; Ai34 mice. Around 44% tdTomato axonal boutons formed contacts with IB4- and/or PAP-labelled central terminals of C-nociceptors. This finding suggests that the most likely source of presynaptic inhibition on type I glomeruli is from RorB cells in lamina II (Gerke and Plenderleith, 2004). The contacts between the axons for individual tdTomato cells and different neurochemical types of primary afferents (IB4<sup>+</sup>/PAP<sup>+</sup> or IB4<sup>+</sup>/PAP<sup>-</sup> or PAP<sup>+</sup>/IB4<sup>-</sup>) were varied. This might reflect differences in input from different classes of C-nociceptors.

Currently, there is no ideal marker that could label individual class of C-fibres and in both cases, MrgprD is a better marker for non-peptidergic C-nociceptors because it defined the real population of these primary afferents (Zylka et al., 2005). Recent transcriptomic studies have suggested that the expression of the MrgprD defines a population of non-peptidergic C-nociceptors that largely correspond to those previously identified by the IB4-binding (Usoskin et al., 2014, Li et al., 2016). Zylka and colleagues found that both hairy and glabrous skin received innervation from MrgprD-labelled primary afferents and that they are the most abundant class of free nerve arbors that are restricted to the skin only (Zylka et al., 2005). Staining with IB4-lectin and PAP-antibody substantially overlap with non-peptidergic C-nociceptors but the relationship between axonal boutons that were labelled with IB4 and/or PAP and the expression of MrgprD is not known. Unpublished observation by Maramba Mustapa and Andrew J Todd on MrgprD-YFP mouse sections that were reacted with eGFP, IB4 and PAP revealed

that in the medial part of the L3 dorsal horn, virtually all IB4-binding axonal boutons were YFP<sup>+</sup>, whereas in the middle/lateral parts there were significant numbers of IB4-labelled axonal boutons that were not YFP. Since the medial part of the dorsal horn in this segment receives input from the glabrous skin, meanwhile the middle and lateral part from hairy skin this suggest that hairy skin is innervated by primary afferents that bind IB4 but lack MrgprD.

#### 5.4.4 Discovery from EM study

Previous studies have shown that profiles that are presynaptic to central axons of type I glomeruli were immunoreactive for GABA but not for glycine (McLaughlin et al., 1975, Barber et al., 1978, Todd, 1996). Type I synaptic glomeruli are mainly found in the middle part of lamina II and these are thought to correspond largely to axons that bind IB4 (Gerke and Plenderleith, 2004). As described previously in chapter 3, both dendrites and axons of inhibitory CR cells were perfectly overlap with IB4 plexus. Therefore, it is possible that presynaptic inhibition on central axons of type I glomeruli is mediated by axoaxonic and dendroaxonic synapses that are mostly derive from this population of cells. In this part of the study, EM was carried out to determine whether axons of RorB cells form axoaxonic synapses on the central axons of type I synaptic glomeruli. In a few cases there was clear area of contact between DAB profiles and central axons of type I glomeruli seen in the EM tissue. In all cases the DAB-immunoreaction product was rather intense which made it difficult to resolve the presence of vesicles within the DAB-labelled profiles. Although the RorB<sup>CreERT2</sup>; Ai34 cross had apparently more numerous axons, unfortunately the quality and structural preservation was less good in this tissue which made it more challenging to identify potential axoaxonic synapses. Meanwhile, the ultrastructure was better in RorB<sup>CreERT2</sup>; Ai9 tissue. However, the frequency of labelled axons was much lower which made it relatively difficult to find examples where they made contact with central axons of type I synaptic glomeruli. It is difficult to know why the axonal labelling in RorB<sup>CreERT2</sup>; Ai34 cross were more numerous than RorB<sup>CreERT2</sup>; Ai9 mice. In particular, this is because cell bodies were not reveal in RorB<sup>CreERT2</sup>; Ai34 tissue and therefore it is not possible to compare the number of labelled cells between these two different lines. It is possible that it reflexes a difference proportion of cells in which Cre-recombinase was activated and made to go into nucleus.

Alternatively, it might be that the axonal targeting due to the synaptophysin fusion protein results in more complete axonal labelling. In addition, it is possible that there are slight differences in the protocol for tamoxifen treatment may have resulted in different on axonal labelling between these two crosses. During the course of the study, another method of tissue processing was applied. The technique of freeze-thawing over liquid nitrogen (Hughes et al., 2000) was carried out in order to get a better penetration of antibody in RorB<sup>CreERT2</sup>; Ai9 tissue. However, this method was not carried out further because it did not result in increase in the number of DAB profiles.

Further research would be needed to investigate synaptic connection between axons of inhibitory CR islet cells and central axons of type I glomeruli. In future investigations, it might be possible to repeat the EM tissue processing using RorB<sup>CreERT2</sup>; Ai34 mice and vary the immunocytochemical processing to obtain optimal staining. However, the Ai34 mouse line is not currently held in the University of Glasgow. Although it will be a considerable interest to investigate axonal projections in other Cre-recombinase mouse line. However, most of other Cre mouse lines that are used in this laboratory are not Cre-ER<sup>T2</sup> and therefore crossing them with the Ai34 will resulted in axonal labelling not only in cells that permanently expressed gene of interest but also in cells that transiently expressed it, which will make it much more difficult to interpret the findings. Therefore, the Ai34 mouse line would only be a value in very limited number of cases such as RorB in which the Cre-ER<sup>T2</sup> line is available. This makes it uneconomical to carry out this experiments. An alternative approach for looking at axonal labelling would be to use intraspinal injection of AAV that code for Cre-dependent form of a fluorescence protein conjugated to synaptophysin expressing viruses into RorB<sup>CreERT2</sup> mice. However, as noted above intraspinal injection in the RorB<sup>CreERT2</sup> mouse line resulted in an unexpected pattern of expression in which both inhibitory neurons but also excitatory cells were labelled and this made it difficult to interpret.

A recent study reported that a relatively small number of substance P cells identified by either PPTA-immunoreactivity or intraspinal injections of an AAV coding for a Cre-dependent form of eGFP (AAV.flex.eGFP) into Tac1<sup>Cre</sup> mice were inhibitory (Pax2<sup>+</sup>)(Gutierrez-Mecinas et al., 2017). Gutierrez-Mecinas and colleagues found that after the AAV.flex.eGFP virus was injected into the Tac1<sup>Cre</sup>

mouse, around 11% of eGFP-labelled cells were inhibitory (Pax2<sup>+</sup>) neurons. It was found that at the rostral and caudal end of the injection site in these animals, there is a region that contains a plexus of eGFP-labelled axons in lamina II. Axons in the plexus were weakly labelled with VGAT and they are found to be closely associated with IB4-binding (Andrew J Todd unpublished observation). This suggests that inhibitory substance P cells in Tac1<sup>Cre</sup> mouse may correspond to the RorB<sup>+</sup>/CR<sup>+</sup> cell populations since tdTomato axonal boutons in RorB<sup>CreERT2</sup>; Ai34 mice were also found to be weakly labelled for VGAT. Furthermore, the majority of inhibitory substance P cells seen in Tac1<sup>Cre</sup> mouse are immunoreactive for CR (Olivia Davis unpublished data). In addition, a recent study using single cell RNA sequencing to classify spinal cord neurons in the mouse dorsal horn identified some inhibitory CR neurons contain Tac1 mRNA that correspond to GABA 9 population identified in this study (Häring et al., 2018). Häring and colleagues showed that these neurons were found mainly in lamina II and scattered in the deeper laminae. Interestingly, they also reported that these cells were activated by noxious heat. The Tac1<sup>Cre</sup> mouse line may therefore be a promising tool that can be used to investigate ultrastructure and synaptic connection between these axons and central axons of type I synaptic glomeruli.

## **6 The effect of sciatic nerve transection on inhibitory CR islet cells in RorB<sup>CreERT2</sup>; Ai9 mice**

## 6.1 Introduction

According to the International Association for the Study of Pain (IASP), pain is defined as “an unpleasant sensory and emotional experience associated with actual or potential tissue damage, or described in terms of such damage”. Various stimuli such as mechanical and thermal stimuli, including environmental and endogenous chemical irritants are detected by the nervous system. Once these stimuli become intense, they will cause acute pain. This is a very important protective reflex for the survival of both human and animal. However, in many cases adaptations of the pain pathway will lead to hypersensitivity, and when the pain persists for more than three months this condition is known as chronic pain (Basbaum et al., 2009). Chronic pain state is characterised by spontaneous pain, as well as by allodynia, where pain is perceived following a normally innocuous stimulus and hyperalgesia, where the patient experiences an increased pain intensity to noxious stimuli (Callin and Bennett, 2008). There is evidence that showed information transmitted by low threshold mechanoreceptor afferents is partly responsible for mechanical allodynia (Torsney and MacDermott, 2006, Peirs et al., 2015, Löken et al., 2017). Chronic pain represents a major clinical, social and economic problem (Phillips, 2003). More than 20% of people are affected, and every year there will be 10% of world populations that are newly diagnosed with chronic pain (Goldberg and McGee, 2011). This may represent underestimate since in the UK it was found that 43% of people suffer from chronic pain (Fayaz et al., 2016). Until now there is no standard protocol that can be used for pain management (Ashburn and Staats, 1999) and in many cases, patients do not receive adequate treatment for their pain (Elliott et al., 1999). Pharmacotherapy with commonly used drugs such as non-steroidal anti-inflammatory drugs (NSAIDs) and opiates to treat chronic pain has a limited success (Woolf and Mannion, 1999). Therefore, the mechanisms involved in the development of chronic pain need to be understood to allow for appropriate treatment for patient who suffer from this condition. The spinal cord is a potential target for pharmacological treatment for chronic pain since all primary afferent fibres, including nociceptors and the low threshold mechanoreceptor synapse here, providing sensory information conveyed to the brain. The changes that take place in the nervous system following the development of chronic pain are still not well understood.

Peripheral nerve injury (PNI) is associated with the development of chronic neuropathic pain. Unfortunately, the mechanisms through which PNI leads to neuropathic pain are still poorly understood. However, several possible changes in the spinal cord that might underlie neuropathic pain have been suggested by different research groups. An early suggestion was sprouting of afferent fibres (Woolf et al., 1992) but now it was thought not to be true (Hughes et al., 2003). Other mechanisms include central sensitization that was resulted from changes in synaptic transmission, increase excitatory circuit activity and decrease in inhibitory response within the dorsal horn (Woolf and Mannion, 1999). One example for central sensitization is long term potentiation (LTP) (Luo et al., 2014). An alternative proposed mechanism involve loss of inhibition (disinhibition) (Yaksh, 1989, Ibuki et al., 1996, Eaton et al., 1998).

One possible mechanism early on was that Woolf et al. (1992) suggested that central terminals of A $\beta$ -primary afferent fibres sprout dorsally into lamina II after peripheral axotomy. In intact peripheral nerve, CTb is transported only by myelinated afferents and this results in transganglionic labelling in deeper laminae where myelinated afferents terminate. However, following peripheral nerve injury CTb-labelling was also seen in superficial laminae (Woolf et al., 1992). Woolf and colleagues proposed that this resulted from sprouting of A $\beta$ -fibres into the SDH. In addition, they identified individual A $\beta$  primary afferents that had axons extent throughout laminae I-III in nerve injured but not in naive rats. In contrast, Yong-Guang et al. (1999) reported that CTb is taken up and transported by injured C-fibres, and that this probably accounts for the novel labelling in lamina II<sub>o</sub> seen after nerve injury. In addition, a few studies found that following PNI, there was no change in the arborisation patterns of intra-axonally labelled A $\beta$ -fibres (Hughes et al., 2003, Woodbury et al., 2008). Most probably that the axons of A $\beta$ -primary afferent fibres that was thought to sprout into lamina II (Woolf et al., 1992) are the same as myelinated nociceptors that has been shown to extent into lamina I in normal animals (Woodbury et al., 2008).

Repetitive stimulation of presynaptic fibres can lead to long term-potentiation, lasting for more than 3 hours (Luo et al., 2014). LTP is a form of long-term synaptic plasticity due to a persistent increase in the strength of synaptic

connections (Todd, 2010). It was first described in the hippocampus and is believed to be involved in learning and memory function (Bliss and Collingridge, 1993). Later studies found that there is a possibility that LTP is induced in pain pathways and contribute to hyperalgesia (Sandkühler, 2009, Sandkühler and Gruber-Schoffnegger, 2012). Spinal LTP involves presynaptic mechanisms and the opening of receptors that involve in the development of neuropathic pain such as NMDA receptors and low-threshold (T-type) voltage-gated calcium channels (Ikeda et al., 2003, Ikeda et al., 2006).

Following peripheral nerve injury, there will be changes in synaptic transmission within the spinal cord in which enhancement of excitatory and reduction of inhibitory synaptic processes occurred (Woolf, 1983, Woolf and Mannion, 1999, Kuner, 2010, Prescott et al., 2014). One of the possible causes for this altered activity results from changes in the production of voltage-gated  $K^+$  (Coull et al., 2003, Kahle et al., 2014) which will be explained further below (see discussion). According to Masuda et al. (2016), after peripheral nerve injury, adenosine triphosphate (ATP) release from dorsal horn neurons is increased due to upregulation of the vesicular nucleoside (VNUT) which normally transported cytosolic ATP into synaptic vesicles. Subsequently, ATP will stimulate purinergic receptor P2X4 which then causes the release of brain-derived neurotrophic factor (BDNF) from microglia (Trang et al., 2009). Coull et al. (2005) found that following peripheral nerve injury, BDNF release from ATP-stimulated microglia causes a depolarizing shift in the anion gradient in lamina I neurons, which reverse the ability of GABA to hyperpolarized. An interruption in the communication between BDNF and its receptor, tropomyosin receptor kinase B (TrkB) will prevent microglia-induced tactile allodynia and the shift in the anion gradient (Coull et al., 2005).

Transmission of sensory information is disturbed following nerve injury due to the less activation of GABAergic and/or glycinergic neurons in the spinal cord (Torsney et al., 2006, Prescott et al., 2014). As mention before, superficial laminae are the termination sites for nociceptors such as C- and  $A\delta$ -fibres that convey noxious information (Todd, 2010). Meanwhile, tactile and innocuous information is carried by  $A\beta$  primary afferents that terminated in laminae III-IV (Abraira et al., 2017). Normally, GABAergic and glycinergic inhibition prevent a

pre-existing excitatory communication between A $\beta$ -fibres and nociceptors (Lu et al., 2013). However, this strong feedforward inhibitory circuit is disrupted following peripheral nerve injury, thus allowing a low-threshold mechanoreceptive pathway in laminae III-IV to gain access to the nociceptive pathway in the superficial laminae. These findings explained why touch is perceived as pain in tactile allodynia (Lu et al., 2013).

In another studies, it has been suggested that one of the cause for chronic pain was a change in expression of peptides in low threshold myelinated afferents following peripheral nerve injury (Noguchi et al., 1994, Noguchi et al., 1995, Neumann et al., 1996). Normally, substance P is found in small dorsal root ganglia neurons which correspond to nociceptors. However, it was reported that peripheral axotomy resulted in increased expression of pronociceptive peptides such as CGRP and substance P in medium and large sized dorsal root ganglia neurons including some that projected into gracile nucleus (Noguchi et al., 1994). In another study by Noguchi and colleagues, they found substance P which normally contribute to pain was upregulated by affected A $\beta$ -primary afferent fibres following PNI (Noguchi et al., 1995). However, Hughes et al. (2007) reported that, following various type of nerve injury (sciatic nerve transection (SNT), spinal nerve ligation (SNL) or chronic constriction injury (CCI)), there was no expression of pronociceptive peptides such as substance P or CGRP in A $\beta$ -axon terminals in the dorsal horn. Electrical stimulation of A $\beta$  afferents in nerve injury models did not cause internalisation of NK1r in dorsal horn neurons which suggest that substance P was not released from A $\beta$ -fibres following nerve injury, therefore, this showed that this peptide does not cause allodynia in the respected models (Hughes et al., 2007).

Another mechanism that is believed to be involved in the development of chronic pain is a reduced activity in inhibitory pathway (disinhibition). Disinhibition could contribute to allodynia, hyperalgesia and spontaneous pain (Sandkühler, 2009). Torsney and MacDermott (2006) suggested that tactile allodynia could result from a loss of inhibition on excitatory interneurons that transmit LTMR inputs to lamina I projection neurons. They propose that there is polysynaptic pathway that conveys low threshold mechanoreceptor input to this lamina I cells. Subsequently this was shown to involve at least 3 different classes

of excitatory neurons; those that expressed PKC gamma as well as two morphologically defined populations, central and vertical cells (Lu et al., 2013).

Several different mechanisms were proposed to explain peripheral nerve injury and one of the proposed mechanism was a significant death of inhibitory neurons. For example, both Ibuki et al. (1996) and Eaton et al. (1998) reported that by using immunocytochemistry technique, there was a substantial loss of GABAergic neurons from the dorsal horn after CCI. Interestingly, this was seen on both sides of the spinal cord after a unilateral nerve injury even though behavioural signs of neuropathic pain were more restricted on the ipsilateral side. On the other hand, Castro-Lopes et al. (1993) showed that sciatic nerve transection causes a progressive loss of GABAergic neurons on the ipsilateral side with eventually 20% reduction in the number compared to the contralateral side.

Moore et al. (2002) also reported the presence of apoptotic neurons and provided evidence that this might be GABAergic neurons that were undergoing cell death. Sugimoto et al. (1990) proposed that increased activity of primary afferent fibres following peripheral nerve injury leading to neuronal death. Based on these findings, it has been suggested that death of inhibitory interneurons after nerve injury contributed to neuropathic pain (Whiteside and Munglani, 2001, Moore et al., 2002, Scholz et al., 2005). Despite this evidence, this finding is controversial since other studies have failed to find evidence for GABAergic neurons cells death (Polgár et al., 2003, Polgár et al., 2004, Polgár and Todd, 2008). In addition, other mechanism for disinhibition have also been proposed (see discussion).

In a preliminary study using the Nociceptin::eGFP mouse, sciatic nerve transection was performed and 4 weeks after surgery, it was found that IB4-labelled boutons had disappeared from the denervated part of lamina II. This indicated that  $C^{MrgD}$  afferents have lost their synaptic connection. It was also notice that the dense band of eGFP<sup>+</sup> dendrites that was normally present in lamina II was much reduced in the denervated sciatic nerve region. This suggest that there was a significant changes affecting the inhibitory CR cells which might be related to the fact that these cells received most of their input from  $C^{MrgD}$  afferents and axons of inhibitory CR cells form axoaxonic synapse on these afferents. A similar finding was seen in the preliminary study using  $RorB^{CreERT2}$ ;

Ai9 mouse in which a band of tdTomato cells become less dense in the denervated region in lamina II. The aim of this part of the study is to determine the effect of PNI on inhibitory CR cells in lamina II of RorB<sup>CreERT2</sup>; Ai9 mice. The hypothesis is that there is loss of these cells after PNI based on the previous studies reporting on cells death (Ibuki et al., 1996, Moore et al., 2002, Eaton et al., 1998). An additional alternative that was considered was that cells will survive but will undergo structural changes especially involving their dendritic arborisation following PNI.

## **6.2 Materials and methods**

### **6.2.1 Animals and operative procedures**

Ten young adults RorB<sup>CreERT2</sup>; Ai9 mice of either sex (15-20 g) that had received 2mg of intraperitoneal tamoxifen at P16-P18 (n=7) or P32 (n=3) were used for this part of the study. As mentioned previously, early administration of tamoxifen at P16-P18 will lead to labelling of many more cells with tdTomato. In contrast, tamoxifen treatment at P32 results in sparse labelling of tdTomato cells. The animals that were treated with tamoxifen at P16-18 were used for cell counting, while those that received tamoxifen at P32 were used for morphological analysis. Unilateral sciatic nerve transection was then performed on these mice as described in a previous study by Wall et al. (1979). The mice were anaesthetized with isoflurane. They were then placed on a heating pad in order to maintain their body temperature. Their heads were fixed in a stereotaxic frame, after which the anaesthetic was administered through a mask attached to the frame. The left sciatic nerve was exposed at mid-thigh level, proximal to the nerve trifurcation and a ligature was secured tightly around the nerve at this level. Approximately 2-3 mm of the nerve between the two ligatures was then removed to prevent the nerve from re-joining. After the nerve had been sectioned, the skin was then closed by stapling.

### **6.2.2 Tissue processing of RorB<sup>CreERT2</sup>; Ai9 mice**

After a four-week post-operative recovery period, the mice were re-anaesthetized with pentobarbitone and perfused with 4% formaldehyde as described previously. In the mouse, L3, L4 and L5 spinal nerves make up the

sciatic nerve (Rigaud et al., 2008). Therefore, for this part of the study, lumbar spinal cord segments from L3-L5 were dissected out and post-fixed for 2 hours. From the mice that were treated with tamoxifen at P16-18, each of the lumbar segments was notched on the lateral part of the ventral horn on the side contralateral to the injury in order to allow the two sides to be distinguished. Then, lumbar spinal cords were cut into 60  $\mu$ m thick transverse sections. From the mice that were treated with tamoxifen at P32, the left and right side of the spinal cord were separated and cut into 60  $\mu$ m thick parasagittal sections. In all cases, sections were then immersed in 50% ethanol for 30 minutes. Sections were then processed for immunocytochemistry, as described below. In all cases, sections were incubated in primary antibodies at 4°C for 5 days and overnight in secondary antibodies. Antibodies were diluted in PBS that contained 0.3% Triton-X100 and 5% normal donkey serum.

### **6.2.3 The number of inhibitory CR<sup>+</sup>/tdTomato<sup>+</sup> cells on the injured and intact side of the spinal cords**

To examine the effect of sciatic nerve transection on tdTomato neurons on the injured and intact side of the spinal cords, transverse sections from the L4 or L5 segments of 6 of the nerve injured RorB<sup>CreERT2</sup>; Ai9 mice that had received tamoxifen at P16-18 were used. Sections from both segments from each animal were incubated in rabbit anti-Pax2, chicken anti-PAP and mouse anti-CR antibodies. These primary antibodies were revealed with Pacific Blue, Alexa 488 and Alexa 647, respectively. The tdTomato expression was visible without the use of antibody, due to the presence of bright native red fluorescence. Sections were mounted as described above and were viewed with a confocal microscope. The PAP antibody was used to reveal non-peptidergic C-nociceptors (Zylka et al., 2008, Taylor-Blake and Zylka, 2010). Previous studies involving PNI have shown that IB4-binding was down-regulated by the primary afferents allowing the denervated area to be identified (Shehab et al., 2008, Shehab, 2014). These two markers mostly labelled the same population of non-peptidergic C-nociceptors. However, in the present study PAP antibody was used instead of IB4-lectin because it was found to give a clearer indication of the denervated region in lamina II. Between four to seven sections from each mouse were selected based on the depletion of the PAP band in lamina II (Figure 6-1). Sections in which this depletion effected at least two third of the PAP plexus on the side ipsilateral to

the injury were selected for analysis. This selection was made before the channel for tdTomato was viewed. For each section both ipsilateral and contralateral side of dorsal horn were scanned through their full thickness with the 40x oil immersion lens and 1  $\mu\text{m}$  z-separation, with the aperture set to 1 Airy unit. Tile scans were used to capture the whole width of the superficial laminae of the dorsal horn. Confocal scans were analysed offline using Neurolucida for Confocal Software. The outline of the dorsal horn and the boundaries between laminae I-II were drawn. The lamina I/II boundary was drawn 20  $\mu\text{m}$  below the dorsal white matter and the ventral extent of the CR-immunoreactive cells was used to determine lamina II/III border. The mediolateral extent of the region from which the PAP plexus was absent was delineated by drawing two parallel lines that were orthogonal to the laminar boundaries (Figure 6-2). Analysis was carried out on inhibitory CR<sup>+</sup>/tdTomato<sup>+</sup> cells that were found between the two lines, corresponding to the region from which PAP was depleted on the ipsilateral side. The equivalent region on the contralateral side was examined on the same way. All of the tdTomato cell bodies in lamina II within this region were plotted onto the Neurolucida drawing throughout the whole depth of the sections. Then, the CR and Pax2 channels were viewed to determine the proportion of tdTomato cells that were immunoreactive for either of these proteins. In addition, to determine the proportion of the inhibitory (Pax2<sup>+</sup>) CR neurons that were labelled with tdTomato, cells that were immunoreactive for both CR and Pax2 were also counted while the channel representing tdTomato was switched off. To avoid experimenter bias, the analysis was carried out blind to whether the dorsal horn was ipsilateral or contralateral to the nerve injury. This was achieved by flipping the confocal images from the ipsilateral dorsal horn so that the two sides appeared similar before the analysis was carried out.

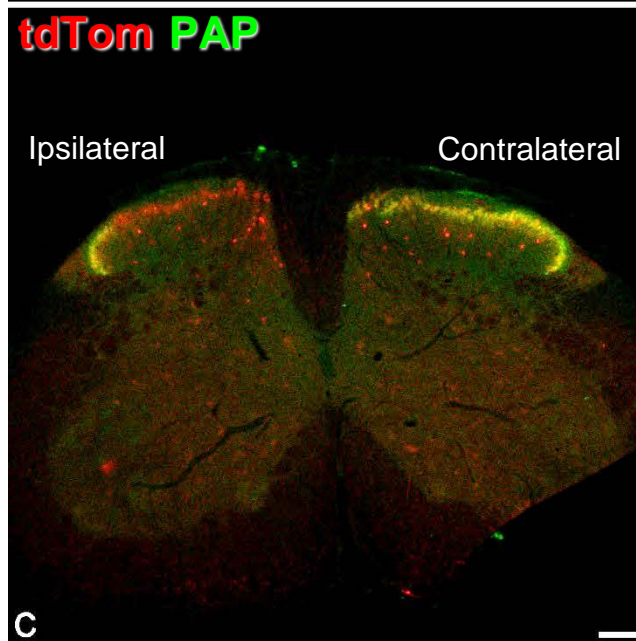
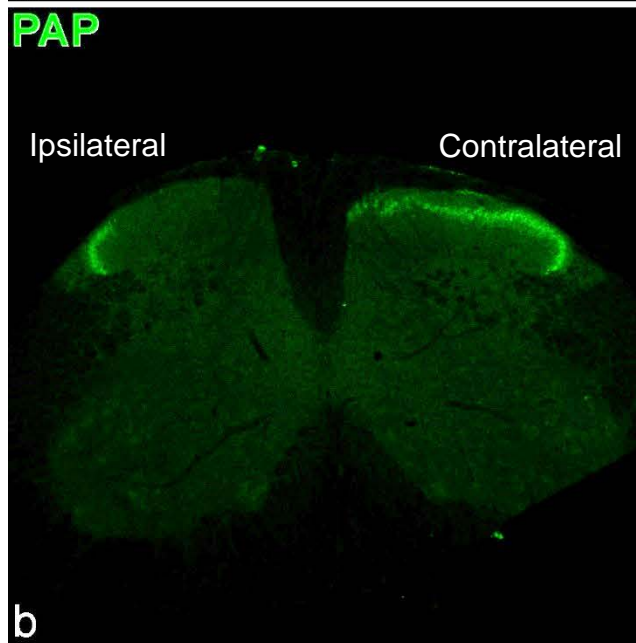
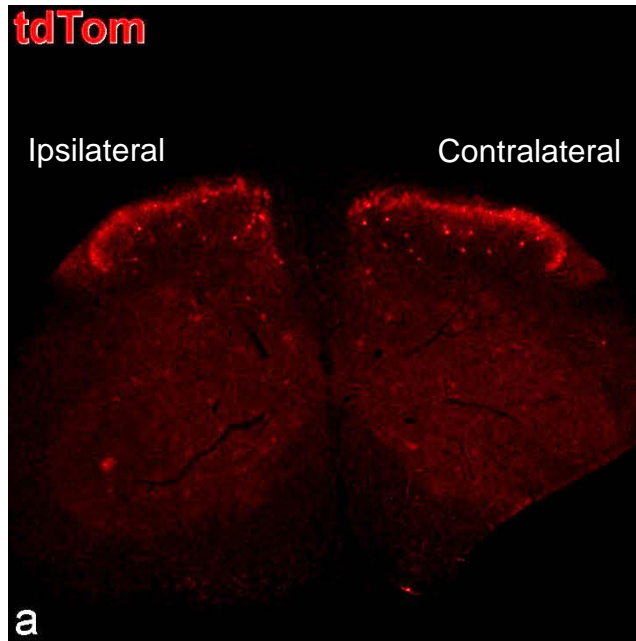


**Figure 6-1 Transverse section of RorB<sup>CreERT2</sup>; Ai9 mice that had undergone SNT on the left side. a** the density of tdTomato band was much reduced in the area where PAP depletion occur on the ipsilateral side to the nerve injury. The number of tdTomato cells seen is less than what is seen in RorB<sup>eGFP</sup> mice. However, the number of tdTomato cells on the side ipsilateral to the nerve injury is similar to the contralateral side. **b** PAP plexus is absent on the left side of the dorsal horn in which the nerve injury is performed. **c** merged image. Scale bar = 200  $\mu$ m.

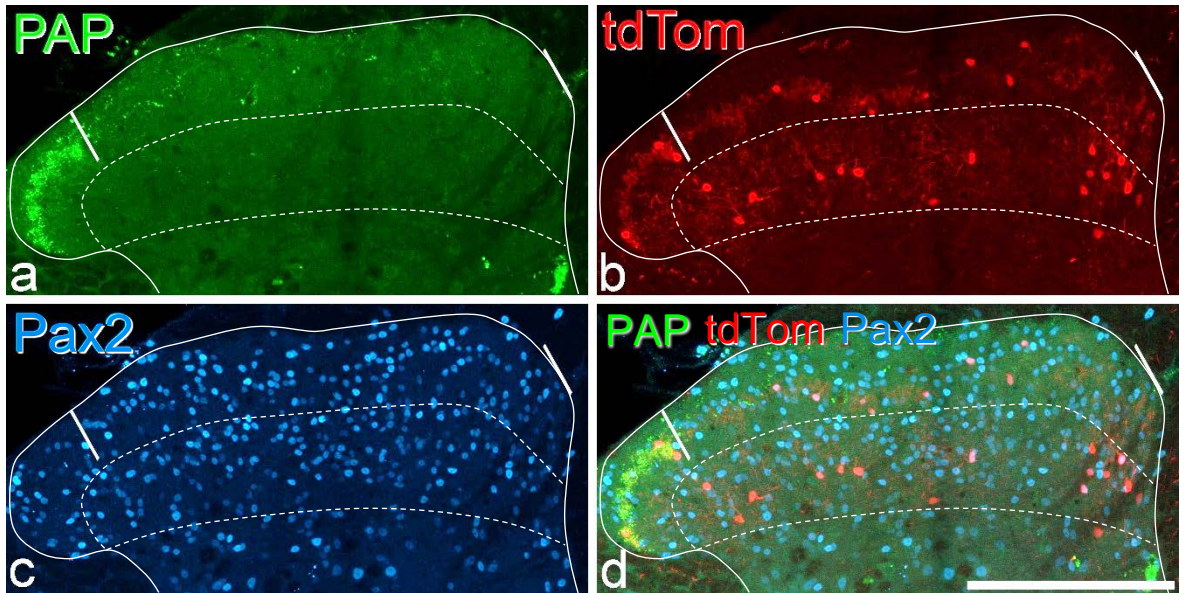


**Figure 6-2 The effect of sciatic nerve transection on the SDH neurons in RorB<sup>CreERT2</sup>; Ai9 mice.** **a** almost two third of the PAP plexus is depleted on the side ipsilateral to the nerve injury. **b** the tdTomato band is present throughout lamina II, however, the intensity of the band is reduced on the side ipsilateral to the injury. **c** Pax-immunostaining is comparable to what is seen in intact animal. **d** merged image. The dashed lines represents the dorsal and ventral borders of lamina III. Scale bar = 200  $\mu$ m.

## 6.2.4 Proportion of inhibitory CR<sup>+</sup> cells among all neurons in lamina II

TdTomato in the RorB<sup>CreERT2</sup>; Ai9 mouse does not label all inhibitory CR cells in laminae I-II even when these animals are treated with tamoxifen at P16-18. Because of this, an additional analysis using a stereological technique was carried out to determine the proportion of neurons that were inhibitory CR cells on the two side following nerve injury (Gutierrez-Mecinas et al., 2016a, Boyle et al., 2017). This analysis was carried out on a different set of sections from the animals described above and one additional animal that has undergone nerve injury. These sections have been reacted with Pax2, CR, and NeuN antibodies. The NeuN antibody was needed to reveal all neurons and DAPI to label the nuclei, thus allowing the proportion of neurons that were CR<sup>+</sup>/Pax2<sup>+</sup> to be determined. However, because these antibodies used up all of the available channel on the confocal microscope, the PAP antibody was not included in this immunoreaction protocol. In the previous set of experiment, it had been found that the depletion of the PAP plexus was greatest at the caudal half of the L4 segment. For this reason, in this part of the study sections from caudal part of L4 were chosen for analysis, based on the outline of the grey matter. The rabbit anti-Pax2, goat anti-CR and mouse anti-NeuN were revealed with Alexa 647, Alexa 488, and Rhodamine Red, respectively. Following the immunocytochemical reaction, the sections were incubated in DAPI for 10 min for nuclear staining. NeuN-immunoreactivity and tdTomato reaction were both revealed in the same channel (red fluorescence). However, this did not result in difficulty in identifying neurons that were labelled with Neun antibody since tdTomato expression was restricted in neurons.

Sections were mounted as described above and were scanned with a confocal microscope. Initially, all sections on the slide were scanned with the 5x lens to capture the entire spinal cord and allow sections from the caudal part of the L4 segment to be identified. The three most caudal sections were then selected and scanned with the 40x oil immersion lens, 1  $\mu$ m z-step and the aperture set to 1 Airy unit, to produce a z-stack of 30 optical sections. Tile scans were used to capture the whole width of laminae I-III on both sides. These scans were analysed offline using Neurolucida for Confocal Software. The outline of the dorsal horn and the boundaries between laminae I-II were drawn as described

above. All cell nuclei (identified by both Neun and DAPI) that had their bottom surface between reference and look up sections (10th and 20th optical sections, respectively) were plotted onto the NeuroLucida drawing and neurons with nuclei present in the look-up section were then excluded (Polgár et al., 2013a, Iwagaki et al., 2013). The channels corresponding to CR and Pax2 were then viewed, and the presence or absence of each type of staining on the selected cells was documented. To avoid experimenter bias, the analysis was carried out blind to whether the dorsal horn was ipsilateral or contralateral to nerve injury. This was achieved by flipping the confocal images from the ipsilateral dorsal horn so that the two sides appear similar before the analysis was carried out.

### **6.2.5 Morphology of CR<sup>+</sup>/tdTomato<sup>+</sup> cells after SNT**

To compare the morphology of CR<sup>+</sup>/tdTomato<sup>+</sup> cells on the injured and intact side of the spinal cord after SNT, parasagittal sections from 3 RorB<sup>CreERT2</sup>; Ai9 mice that had received tamoxifen at P32 were used. All the sections were incubated with rabbit anti-mCherry, goat anti-CR, and chicken anti-PAP. These primary antibodies were revealed with Rhodamine Red, Pacific Blue and Alexa 488, respectively. Sections were mounted as described above and were viewed with a confocal microscope. On the side contralateral to the nerve injury tdTomato cells within the PAP plexus were selected to ensure that they were located in lamina II. Since this plexus was not present on the nerve injured side, CR-immunoreactivity, which was found mainly in lamina II, was used as a guide to identify tdTomato cells in this lamina. A total of nine CR<sup>+</sup>/tdTomato<sup>+</sup> cells on the ipsilateral side and five CR<sup>+</sup>/tdTomato<sup>+</sup> cells on the contralateral side were scanned and analysed. Scanning was started with the 5x lens to confirm the laminar location of the cell within the section. They were then scanned through the 63x oil immersion lens at 0.5 µm z-separation with the aperture set to 1 Airy unit. In each case, tile scans were obtained in order to capture all of the labelled cells that were present in the section. The maximum intensity projection of the confocal scanned image was used to determine the RC and DV extent of the dendritic trees of the cells. Both the RC and DV length were measured using Quick Line Measure tool in NeuroLucida software.

## 6.3 Results

### 6.3.1 Quantitative analysis of the inhibitory CR<sup>+</sup>/tdTomato<sup>+</sup> cells following SNT

In this part of the study, tissues from animals that received 2mg IP tamoxifen at P16-P18 was used because early administration of tamoxifen resulted in more labelling of tdTomato cells in RorB<sup>CreERT2</sup>; Ai9 mice and to determine whether there is loss of inhibitory CR<sup>+</sup>/tdTomato<sup>+</sup> cells after SNT, it is necessary to work with animals in which numerous tdTomato cells were labelled.

On the side contralateral to nerve injury, the PAP axonal band could be seen through the mediolateral extent of lamina II, appeared similar to animals that had not undergone nerve injury (see chapter 5). Meanwhile, on the side ipsilateral to nerve injury, the PAP band was only present on the extreme lateral part of the dorsal horn and was missing from the medial part. This presumably reflex the loss of PAP correspond to the area of sciatic nerve territory. The general distribution of somata of tdTomato cells in the dorsal horn was comparable with that seen in RorB<sup>CreERT2</sup>; Ai9 mice that had not undergone SNT (see chapter 5). The dendritic and axonal band of tdTomato cells in lamina II was present on the side ipsilateral to SNT as well as on the contralateral side. However, the density of tdTomato band was much reduced in the area where PAP depletion on the side ipsilateral to nerve injury. A clear gap between the band in lamina II and tdTomato cells and processes found in deeper laminae was also seen on both side of the dorsal horn, as described previously. The distribution of cell bodies and dendrites that were CR-immunoreactive was similar to findings described in the previous chapters and reported in other studies (Albuquerque et al., 1999, Smith et al., 2015).

Quantitative analysis of tdTomato cells in RorB<sup>CreERT2</sup>; Ai9 mice that had undergone SNT was carried out between 4-7 sections per animal, and the results was shown in Table 6-1. A total of 246 (range 28-64) and 262 (range 26-61) tdTomato cells in lamina II were counted on side ipsilateral and contralateral to SNT, respectively (n = 6 mice) and this gave the mean number of cells per section of 7.48 on the side ipsilateral and 7.97 on the side contralateral to nerve injury, as shown in the table. In order to compare these animals effectively with

un-operated animals, a separate analysis was carried out on 6 intact RorB<sup>CreERT2</sup>; Ai9 mice that received tamoxifen at P16-18 (3 of these animals were previously described in chapter 5 and another additional 3 were used on this part of analysis). The number of cells per section in intact animals was estimated to be mean of 15.65 (range 9.75-20.67). One-way analysis of variance was performed followed by Holm-Sidak post-hoc for multiple-comparison test showed that number of cells in RorB<sup>CreERT2</sup>; Ai9 mice that did not undergo nerve injury were significantly different from the number of cells seen in the side ipsilateral ( $p = 0.0026$ ) and contralateral ( $p = 0.0028$ ) to the injury. However, both side ipsilateral and contralateral to SNT did not vary ( $p = 0.8064$ ).

Observations on confocal sections revealed that the great majority of tdTomato cells in the superficial laminae on both side ipsilateral and contralateral to nerve injury were also immunoreactive for CR and Pax2. This accounted for 212/246 (86.2%) and 219/262 (83.6%) on the side ipsilateral and contralateral to nerve injury, respectively. A paired t-test showed that there was no significant difference between the total number of inhibitory CR<sup>+</sup>/tdTomato<sup>+</sup> ( $p = 0.6416$ ) cells in lamina II on the side ipsilateral and contralateral to nerve injury. None of the tdTomato cells in the deeper laminae were CR-immunoreactive as seen in intact animals.

### **6.3.2 Quantitative analysis of the inhibitory CR cells following SNT**

This part of the study was carried out on tissues from RorB<sup>CreERT2</sup>; Ai9 mice that were used above together with one additional animal in order to determine whether there is loss of inhibitory CR cells in the SDH of these animals following SNT. NeuN- and Pax2-immunostaining were seen throughout the dorsal horn on the side ipsilateral and contralateral to SNT. As reported previously, numerous NeuN-immunoreactive cells were seen in the SDH (Todd et al., 1998).

Combination of NeuN antibody and DAPI was used to identify neuronal nuclei. Meanwhile, Pax2 and CR antibody were used in this part of the study to identify inhibitory CR neurons in the superficial laminae. As described previously, most of the cell bodies and dendritic plexus of CR-immunoreactive neurons were located mostly in lamina II, although occasionally cells were seen in laminae I and III. The density of CR dendritic and axonal plexus in the SDH appear the same on

both ipsilateral and contralateral side following SNT. Similar to what was seen in un-operated animals, a minority of CR cells were Pax2<sup>+</sup> in the SDH. The penetration of all antibodies could be seen throughout the full thickness of the optical sections.

Quantitative data obtain using the disector method in this part of the study are shown in Table 6-2. A total of 4378 and 4291 neurons (n=7) were analysed in laminae I-II on the side ipsilateral and contralateral of SNT, respectively. Of these, 1046 (23.9%) and 1054 (24.6%), respectively, were inhibitory interneurons as defined by the presence of immunostaining for Pax2. The total numbers of inhibitory (Pax2<sup>+</sup>) CR cells identified in laminae I-II on the side ipsilateral and contralateral to nerve injury were 246 and 240, respectively. Quantitative analysis revealed that, inhibitory (Pax2<sup>+</sup>) CR cells constituted 5.6% of neuronal populations in laminae I-II on the ipsilateral side and 5.6% of those on the contralateral side (Table 6-2). A paired t-test showed that there was no significance difference between the total number of NeuN in laminae I-II ( $p = 0.4300$ ) on the side ipsilateral and contralateral of SNT. Similarly, there was no significant difference in the proportion of all neurons that were Pax2 in laminae I-II ( $p = 0.5076$ ) on the side ipsilateral and contralateral to nerve injury. The p value for the proportion of all neurons that were inhibitory (Pax2<sup>+</sup>) CR cells in laminae I-II was not significantly different ( $p = 0.9852$ ) and this showed that the proportion of these cells among all neurons on the side ipsilateral and contralateral did not change following SNT.

### **6.3.3 Morphological analysis of CR<sup>+</sup>/tdTomato<sup>+</sup> cells**

In this part of the study, tissue from animals that had received 2mg IP tamoxifen at P32 was used because late administration of tamoxifen showed sparse labelling of tdTomato cells in RorB<sup>CreERT2</sup>; Ai9 mice. This was important because it allow the analyses of individual cell. Parasagittal sections from these animals were examined after immunostaining for mCherry, CR, and PAP were readily identified in these sections. In this part of the study, the mCherry antibody was used to amplify the native fluorescence. This was performed to reveal the finest dendritic and axonal processes. The general distribution of tdTomato cell bodies in the dorsal horn was comparable with that was seen in intact RorB<sup>CreERT2</sup>; Ai9

mice in which there was a sparse labelling of tdTomato cells, as described previously in chapter 5.

On the side ipsilateral to the nerve injury, the axonal band of PAP was absent in many sections and this correspond to the region innervated from the sciatic nerve. On this side tdTomato cells were selected from section in which the PAP band was absent. Because of the lack of PAP plexus, the distribution of CR-immunostaining which was largely restricted to lamina II, was used to identify tdTomato cells on the denervated side. On the contralateral side the PAP-band was intact and to allow for comparison, cells were chosen from sections in the medial part of the dorsal horn which can be identified by the present of white matter, dorsal to the lamina I. On initial observation of the cells, there was no obvious differences in the size of the dendritic trees of the neurons between the ipsilateral and contralateral side to the nerve injury. The distribution of cell bodies and dendrites that were CR-immunoreactive was similar with previous findings reported in the previous chapters and studies (Albuquerque et al., 1999, Smith et al., 2015). Isolated tdTomato cells that were immunoreactive for CR was chosen for neuronal reconstruction using NeuroLucida software.

The tdTomato cells in lamina II on the side ipsilateral and contralateral to the nerve injury showed islet cell morphology (Figure 6-3), confirmed by extensive rostrocaudal extension of the dendritic trees and the limited dorsoventral arborisation of the cells as described previously (Grudt and Perl, 2002, Yasaka et al., 2007, Yasaka et al., 2010). The RC and DV extent of 9 and 5 cells on the side ipsilateral and contralateral to the nerve injury, respectively, were measured. On the ipsilateral side of the injury, the RC and DV extent of the dendritic trees of these cells were  $261.1 \mu\text{m} \pm 24.19$  (mean  $\pm$  SD) and  $40.32 \mu\text{m} \pm 19.15$  (mean  $\pm$  SD), respectively. Meanwhile, on the side contralateral to the nerve injury, the values for RC and DV length were  $283.2 \mu\text{m} \pm 82.22$  (mean  $\pm$  SD) and  $34.94 \mu\text{m} \pm 14.31$  (mean  $\pm$  SD), respectively. A two sample unpaired t-test showed that there was no significant difference in either the RC ( $p = 0.4559$ ) or the DV ( $p = 0.5953$ ) extent between the cells on either side. Information on the dendritic dimensions of all cells is shown in Table 6-3.

**Table 6-1 Number of tdTomato cells counted on the side ipsilateral and contralateral to the nerve injury**

		Ipsilateral		Contralateral	
Animal	Number of sections analysed	Number of tdTomato cells	Number of cells per section	Number of tdTomato cells	Number of cells per section
1	4	45	11.25	46	11.50
2	4	28	7.00	28	7.00
3	6	29	4.83	42	7.00
4	6	51	8.50	61	10.17
5	7	29	4.14	36	5.14
6	7	64	9.14	49	7.00
Mean			<b>7.48</b>		<b>7.97</b>

The numbers represent a total number of cells counted in the side ipsilateral and contralateral to SNT.

**Table 6-2 Numbers of NeuN, Pax2 and inhibitory CR<sup>+</sup> cells in laminae I- II on the side ipsilateral and contralateral to the nerve injury**

<b>Lamina</b>	<b>Number of neurons counted</b>	<b>Pax2 cells</b>	<b>Inhibitory(Pax2<sup>+</sup>) CR<sup>+</sup> cells</b>	<b>% of neurons that were Pax2<sup>+</sup></b>	<b>% of neurons that were CR<sup>+</sup>/Pax2<sup>+</sup></b>
Ipsilateral					
I	76.1 (62-92)	21 (17-28)	2.4 (0-5)	27.6 (21.5-32.3)	3.2 (0-6.9)
II	549.3 (496-597)	128.4 (105-147)	32.7 (13-44)	23.4 (20.8-25.7)	6.0 (2.6-8.6)
I-II	625.4 (561-676)	149.4 (126-175)	35.1 (13-49)	23.9 (20.9-26.4)	5.6 (2.3-8.4)
Contralateral					
I	75.6 (62-99)	19 (15-26)	3.3 (1-6)	25.1 (20-31)	4.3 (1-6.5)
II	537.4 (444-590)	131.6 (121-144)	31 (19-44)	24.5 (21-26.2)	5.7 (3.7-7.8)
I-II	613 (519-661)	150.6 (137-170)	34.3 (20-48)	24.6 (21.4-26.8)	5.6 (3.5-7.7)

Numbers of cells counted or percentages of cells are shown in the table. Values are the mean cell counts for 7 mice with ranges in parentheses.

**Table 6-3 CR<sup>+</sup>/tdTomato<sup>+</sup> cells dendritic dimensions on the side ipsilateral and contralateral to the nerve injury**

Ipsilateral ( <i>n</i> = 9)		
Cells	RC extent (μm)	DV extent (μm)
1	280.8	51
2	227.5	44
3	266	68.2
4	291.3	42.5
5	260.1	30.2
6	277.9	14.1
7	217.3	16.8
8	264.3	31.3
9	265.1	64.8
Contralateral ( <i>n</i> = 5)		
Cells	RC extent (μm)	DV extent (μm)
1	321.2	58.3
2	300.1	38.3
3	253.3	29.4
4	380.6	22.5
5	161	26.2

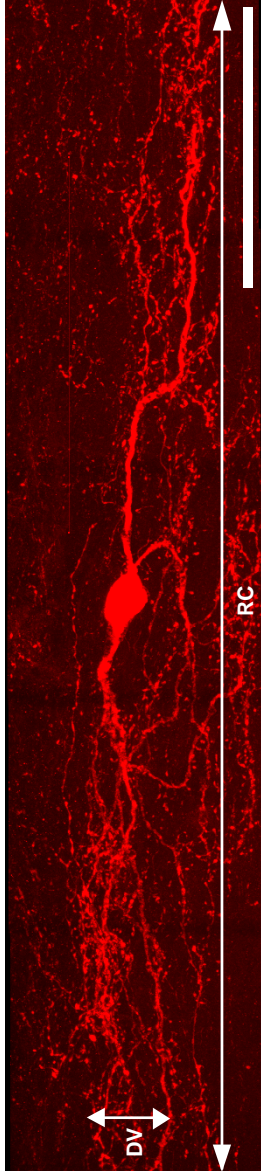


**Figure 6-3 A typical islet cell morphology of RorB cell found in the middle of lamina II on the side ipsilateral to the nerve injury.** Maximal projection of tdTomato cell shows that the rostrocaudal (RC) and dorsoventral (DV) extent of the cell appear to be normal and resemble islet cell morphology. Scale bar = 100  $\mu$ m.

## 6.4 Discussion

The main findings of this study are that following SNT: (1) there is no difference on the number of lamina II tdTomato cells that are CR<sup>+</sup> and Pax2<sup>+</sup> on the ipsilateral and contralateral side; (2) the proportion of all neurons that are CR<sup>+</sup> and Pax2<sup>+</sup> in laminae I-II do not differ on both side (3) the dendritic extent of tdTomato cells does not change in the area where PAP was depleted.

### 6.4.1 No loss of cells after PNI

Despite many evidence showed that there was cells death following peripheral nerve injury (Ibuki et al., 1996, Eaton et al., 1998, Moore et al., 2002, Yowtak et al., 2013), this current study found that there is no loss of neurons after four weeks of SNT. This is consistent with other studies that failed to see any loss of cells or alteration in the overall number of neurons that were GABA immunoreactive in laminae I-III of the rat following CCI (Polgár et al., 2003, Polgár et al., 2004). Even though they cannot rule out any cell death, the animals used in their studies showed signs of thermal hyperalgesia. In addition, it was found that no reduction in cell counts in laminae I-III after four weeks of spared nerve injury (Polgár et al., 2005). In another study using spared nerve injury model of neuropathic pain, it was reported that after 1 week of surgery, apoptosis of cells was detected using TUNEL-staining in the white and grey matter of the dorsal spinal cord on the side of the injury. However, those apoptotic cells also expressed Iba-1 and this showed that spared nerve injury affected microglia rather than neurons. In addition, a study using quantitative immunogold method found that there was no change on GABA-immunoreactivity in the inhibitory axonal boutons in laminae I-II on the ipsilateral and contralateral side of spared nerve injury (Polgár and Todd, 2008). All of these findings suggest that neuropathic pain could develop without the need for neuronal death.

Because of the lack of cell death, an alternative explanation for the loss of inhibition has been look for. A few studies have shown that there was no depletion of GABA type A receptor following peripheral nerve injury (Moore et al., 2002, Polgár and Todd, 2008). Coull et al. (2003) suggested that efficiency of GABA as the inhibitory transmitter was reduced due to the changes in the

concentration of anion across the neuronal membranes as a result of down-regulation of potassium-chloride exporter 2 (KCC2). In normal condition, KCC2 in spinal cord dorsal horn neurons maintains a low intracellular chloride ( $\text{Cl}^-$ ) concentration. A pathological reduction in functional expression of KCC2 will result in the accumulation of  $\text{Cl}^-$  within the neurons (Coull et al., 2003). The equilibrium potential for  $\text{Cl}^-$  would be less negative and this will lead to central disinhibition of GABA type A receptor and glycine receptor due to a loss of hyperpolarizing action of these receptors (Coull et al., 2003). Despite this finding, it has been reported that GABA type A receptor agonist reduce tactile allodynia and hyperalgesia in neuropathic pain model (Hwang and Yaksh, 1997, Malan et al., 2002).

Dorsal horn excitability may increase following chronic constriction injury or axotomy of the sciatic nerve (Lu et al., 2009). Several studies have shown that these animal models cause increased excitatory input to putative excitatory delay firing and transient firing neurons and decreased excitatory firing to putative inhibitory tonic firing neurons (Chen et al., 2009, Lu et al., 2009, Bailey and Ribeiro-da-Silva, 2006). Leitner et al. (2013) found that peripheral nerve injury generates  $\text{Ca}^{2+}$  dependent signalling pathways in GABAergic neurons in the spinal cord. This results in a widespread reduction of their excitatory drive. Leitner and colleagues also found that A $\delta$ - and C-fibres input on GABAergic neurons is decreased during noxious stimulation, thus weaken the normal feedforward inhibition.

Neuropathic animal models are needed to understand the process involved in chronic pain. Once the mechanism is understood, then successful pharmacotherapies for treating chronic pain could be developed. The neuropathic animal models ideally should include behavioural signs that result from allodynia, hyperalgesia and spontaneous pain. There are several different types of animal models have been developed including chronic constriction injury (Bennett and Xie, 1988); partial sciatic nerve ligation (Seltzer et al., 1990); spinal nerve ligation (Kim and Chung, 1992) and spared nerve injury (Decosterd and Woolf, 2000). Chronic constriction injury represents an entrapment neuropathy in which there is a preferential loss of large fibres. Spared nerve injury and spinal nerve ligation, both involve ligation and

transection parts of the lumbar or sciatic nerve. These were developed because the finding of partial nerve injury in human is much more likely to result in neuropathic pain than the complete nerve transection. The complete transection of sciatic nerve allowed the three branches of sciatic nerve (common peroneal, tibial and sural nerve) to have the same degree of injury (Cheng et al., 2015). This model was chosen because the effect of this type of surgery on the dorsal horn was extensive. This result in the depletion of C<sup>MrgD</sup> boutons from two thirds of the dorsal horn thus allowing a larger region in which any anatomical changes can be detected. In particular, this was needed since a relatively small number of cells expressed tdTomato in RorB<sup>CreERT2</sup>; Ai9 mice. The present finding strongly suggests that there is no loss of cells after peripheral nerve injury. However, since less extensive nerve injury is more likely to cause neuropathic pain, it is recommended to apply partial sciatic nerve injury or chronic constriction injury in order to test whether there are any changes in tdTomato cells.

#### **6.4.2 No change in the morphology of the cells**

Coderre et al. (1993) suggested there is a possibility that dorsal horn neuronal circuit reorganisation is responsible for the development of chronic pain. In the preliminary study using Nociceptin::eGFP mouse, following 4 weeks after SNT, it was found that the density of eGFP dendritic plexus in lamina II was greatly reduced in the denervated sciatic nerve territory which suggests there was a change on the morphology of the cells. It is possible that the cells were not dead but down-regulate eGFP. Meanwhile, in the present study, it was found that the density of tdTomato band was much reduced in the area where PAP depletion on the side ipsilateral to nerve injury. The reduction of the dendritic plexus of the eGFP and tdTomato cells in the region where the primary afferent terminal was depleted can either be explained by the loss of cells or alternatively by the same number of cells having less complex dendritic trees (fewer dendrites). Since we have shown that there is no loss of cells, the only reason for explanation seems to be that each cell generates less dendrites. It might, therefore, be expected that the overall dimension of the cell (RC and DV extent) would have been reduced.

However, in the current study, it was found that there were no changes in the RC and DV extent as well as RC:DV ratio of the cells in the side ipsilateral and

contralateral to the nerve injury. The possible explanation for this is that there is a genuine reduction in the dendritic extent of the cells, but this is not being detected because there is a considerable degree of variability of RC and DV extent between different cells. A lot of observations on the cells must be done in order to see this variability. This would require more extensive analysis, but unfortunately, we did not examine large enough sample. Alternatively, the cells genuinely do not show a change in their RC and DV extent but the density of dendrites within that volume that they occupied become less complex presumably due to loss of dendritic branches. Polgár et al. (2003) reported that there was no loss of cells following PNI, however, maybe there is a possibility that there is a change occur in the synaptic elements leading to loss of synaptic connections of GABAergic axon terminals. Given the very high proportion of synaptic input into the cells derived from C<sup>MrgD</sup> afferents boutons which appear to have vanished after the nerve injury, it is expected that these cells might undergo significant dendritic change and it could also be that the axonal boutons of these cells were reduced. The limitation in this part of the study was that the restructuring of the dendritic spines could not be resolved as shown by Tan et al. (2008) that found there were alteration and redistribution of dendritic spines of neurons in the spinal cord following PNI. Although the findings in this study are similar with the previous studies that were carried out in this laboratory (Polgár et al., 2003, Polgár et al., 2004, Polgár et al., 2005), the future studies should investigate dendritic spines in order to evaluate any ultrastructural reorganisation.

## **7 Concluding remarks**

The superficial laminae receive innervation from various types of primary afferents that detect noxious and pruritic stimuli. Information that is carried from peripheral tissues is modulated by internal neuronal circuits within the spinal cord before being transmitted to the brain via projection neurons. Melzack and Wall (1965) suggested that lamina II of the dorsal horn, play a major role in modulating somatosensation by inhibiting primary afferent inputs before transmitting it to the higher centre. Countless studies have been carried out to investigate the pathway on how the superficial dorsal horn neurons modulate the nociceptive input with the ultimate aim to identify novel targets for the treatment of pathological pain states.

Interneurons can be divided into excitatory and inhibitory classes and for this project, the focus was on inhibitory cells in the SDH. Most inhibitory interneurons generate postsynaptic inhibition through axodendritic synapses, but many primary afferent axons receive GABAergic presynaptic inhibition through axoaxonic synapses (Eccles et al., 1962b, Barber et al., 1978, Todd, 1996). The initial aim of this project was to characterise inhibitory CR islet cells in superficial laminae and to investigate whether these neurons are a major source of axoaxonic synapses on the  $C^{MrgD}$  afferents that formed the central axons of type I synaptic glomeruli. To achieve this aim, this study initially used various transgenic mouse lines and crosses, including those that express transgenes under control of the Nociceptin and RorB promoters. This was done in order to identify suitable mouse line that captures inhibitory CR islet cells. This is important because the majority of CR expressing cells are excitatory interneurons with only a small proportion being inhibitory (Smith et al., 2015).

To understand the morphology of inhibitory CR cells in great details, a BAC transgenic mouse line, Nociceptin::eGFP mouse was used since it was found that the great majority of inhibitory interneurons in the SDH was captured by these mice. Inhibitory CR cells formed a band of dendrites and axons that were perfectly overlap with IB4 plexus, thus showed that there were higher chances that these cells form a contact with non-peptidergic C fibres that mainly terminated in the middle of lamina II. We found that inhibitory CR cells make up a small proportion of total neuronal populations in the dorsal horn since the great majority of calretinin cells are excitatory interneurons. Grudt and Perl

(2002) found four major types of cells including islet cells that are found to be GABA-immunoreactive. Parallel to these findings, we found that inhibitory CR cells that had undergone whole cell recordings and that were labelled with Neurobiotin and subsequently reconstructed were found to have islet morphology. This finding is consistent with what was seen in a previous study by Smith et al. (2015) in which they reported that atypical (inhibitory) CR cells were mainly had islet morphology. During the course of the study, it was found that RorB<sup>eGFP</sup> mice labelled the great majority of inhibitory CR cells in SDH compared to Nociceptin::eGFP mouse line. Furthermore, the proportion of eGFP-positive cells that were labelled with both CR and Pax2 in RorB<sup>eGFP</sup> mice was much higher compared to Nociceptin::eGFP mice. Both the RorB<sup>eGFP</sup> and Nociceptin::eGFP mouse lines are trusted tools for investigating inhibitory CR cells because almost all eGFP cells in both animals were Pax2<sup>+</sup> and many inhibitory CR cells were captured. Therefore, RorB<sup>eGFP</sup> mice appeared to be a better choice for investigating the inhibitory CR cells than Nociceptin::eGFP mice. Consistent with the data reported by Smith et al. (2015) it was found that in this mice 15% of CR-immunoreactive cells in the SDH co-expressed Pax2 and this accounted for around a quarter of Pax2 positive cells.

Neuropeptides may be differentially expressed by distinct functional populations of interneurons since the laminar distribution of dorsal horn neurons that contain these different peptides varies significantly. For example, NPY-expressing cells are found in laminae I-III, galanin in lamina I and II outer and CR are mainly found in lamina II. There are many neurochemical markers available to classify interneurons in laminae I-III. However, it is unlikely that any one of these markers can be used to identify the specific functional population. One method that has been performed to identify discrete populations is by using a neurochemical marker that are expressed in non-overlapping subsets in either inhibitory or excitatory interneurons. Using this method, we found that almost none of inhibitory CR cells were positive for galanin, PV, nNOS and NPY. Only half of the inhibitory CR islet cells in the SDH were labelled with sst<sub>2A</sub> antibody. However, it is not known whether those cells that expressed sst<sub>2A</sub> were any different from the ones that do not express somatostatin receptor. Previous studies have shown that sst<sub>2A</sub> receptor is differentially distributed among inhibitory interneuron populations. Specifically, it is expressed by most galanin,

dynorphin and nNOS cells but relatively few by NPY and none by PV. Recently, Gutierrez-Mecinas et al. (2019) found that virtually all of the inhibitory Tac-1 expressing neurons co-expressed calretinin in lamina II of the dorsal horn. This finding is further supported by transcriptomic studies that identified cells that are positive for Calbindin (Calb2) among the inhibitory neurons (DI-1 and Gaba 8-9, respectively) (Häring et al., 2018, Sathyamurthy et al., 2018). The DI-1 group of cells strongly expressed Tac-1 (Sathyamurthy et al., 2018) with high level of expression seen GABA 9 cluster (Häring et al., 2018).

To investigate the synaptic connection between CR islet cells with C<sup>MrgD</sup> afferents, the RorB<sup>CreERT2</sup> mouse line with tamoxifen induction were used. A particular advantage of the Cre-recombinase transgene compare to eGFP is that it allows labelling with fluorescence reporter lines or viruses but also manipulation of the function of the cells to occur for example using optogenetics (Xu et al., 2008) or chemogenetics (Koga et al., 2017). This type of experiment will be carry out in the future. In this part of the study, RorB<sup>CreERT2</sup> mouse was crossed with the reporter lines Ai9 or Ai34. The neuronal cell bodies together with their processes were labelled with tdTomato in the RorB<sup>CreERT2</sup>; Ai9 cross, meanwhile in RorB<sup>CreERT2</sup>; Ai34 cross only the axons were labelled with tdTomato due to the expression of synaptophysin fusion protein which directs the resulting protein to axon terminal. This series of experiment began with an investigation into the optimal method for labelling cells in the RorB<sup>CreERT2</sup>; Ai9 cross. It was found that giving tamoxifen in the early postnatal age (P16-18), consistently resulted in more labelling of cells than when tamoxifen was giving at the later ages (P32-36). The reasons for this are not known since numerous RorB mRNA positive cells are seen in the superficial dorsal horn of P56 mice in Allen Brain Atlas. Presumably in some cases, this results in failure of tamoxifen to cause recombination in some cells particularly when it was given in later stages. However, almost all tdTomato cells in the SDH were immunoreactive for Pax2 and CR in this mouse cross. Thus showed that this mouse line was highly selective for inhibitory CR cells.

Although it is not possible to target all of the inhibitory CR cells in this mouse line, it was still very useful because in particular when sparse labelling was achieved (IP administration of tamoxifen at P32-36), and this allowed details

anatomical analysis of individual cells. Therefore,  $RorB^{CreERT2}; Ai9$  crosses that received IP injection of tamoxifen at P35 were then used to investigate the synaptic connection of inhibitory CR islet cells with unmyelinated primary afferents. This analysis shown that around half of the excitatory synaptic input onto the dendritic spines of tdTomato cells originated from these afferents, meanwhile some tdTomato-positive axonal boutons were seen to form contacts with these primary afferents. In a separate analysis that was carried out on  $RorB^{CreERT2}; Ai34$  mouse crosses it was found that the great majority of non-peptidergic C fibres received at least one contact from tdTomato axonal boutons. Electron microscopic study on  $RorB^{CreERT2}; Ai9$  and  $RorB^{CreERT2}; Ai34$  mice revealed that there were many contacts between DAB-labelled profiles and central axons of type I synaptic glomeruli.

In this study, SNT was carried out in  $RorB^{CreERT2}; Ai9$  mouse lines following the findings in the preliminary study that showed a reduction in the density of eGFP plexus in the sciatic nerve territory at the side ipsilateral to the nerve injury in  $Nociceptin::eGFP$  mice. Although many previous studies reported that there is loss of SDH neurons in different types of neuropathic pain models (Ibuki et al., 1996, Moore et al., 2002, Eaton et al., 1998, Yowtak et al., 2013), this has been controversial since works reported by Polgár et al. (2003, 2005 and 2008) have found no evidence of neuronal loss following various type of nerve injury. Consistent with the finding by Polgár and colleagues there was no reduction in the number of tdTomato cells between the side ipsilateral or contralateral in the nerve injured  $RorB^{CreERT2}; Ai9$  mice, suggesting that there is no loss of neurons. Since there was a reduction in the plexus, this would suggest that the dendritic trees of individual cells must have been altered. However, finding from this study showed that there was no change noted on the RC and DV extent of dendritic arbors of individual tdTomato cells on either side.

Two studies were carried out to investigate the functional role of dorsal horn CR cells in modulating nociceptive input (Duan et al., 2014, Peirs et al., 2015). The majority of CR expressing neurons are excitatory and activating these cells in lamina II caused a reduction of von Frey thresholds and guarding of the affected paw (Peirs et al., 2015). Meanwhile in another study it was found that ablation of CR expressing cells caused enhanced paw withdrawal thresholds to noxious

mechanical stimuli (Duan et al., 2014). Both of these studies suggest CR positive cells open the gate to the innocuous tactile input with nociceptive circuits and cause allodynia. In normal condition, this connection is not activated because stimulation by light touch do not cause pain. However, certain pathological condition can activate this pathway. As a conclusion, reducing or silencing the activity of CR expressing cells could resolve allodynia. Meanwhile, modifying their properties would alter responses in chronic pain states.

Although it has long been known that unmyelinated nociceptors received axoaxonic synapses from GABAergic interneurons, until now the source of these synapses is not known. The findings of the present study address this gap in knowledge. Using multiple mouse lines to investigate CR-expressing inhibitory interneurons in the SDH, we showed that these cells have islet morphology and most probably forms axoaxonic synapses on  $C^{MrgD}$  afferents that form the central axons of type I synaptic glomeruli (Figure 7-1). Intriguingly, it appears that there is a changes in these cells after nerve injury although this is not a result of loss of the cells and further investigations is needed to investigate whether it reflex changes in the dendritic arbors.

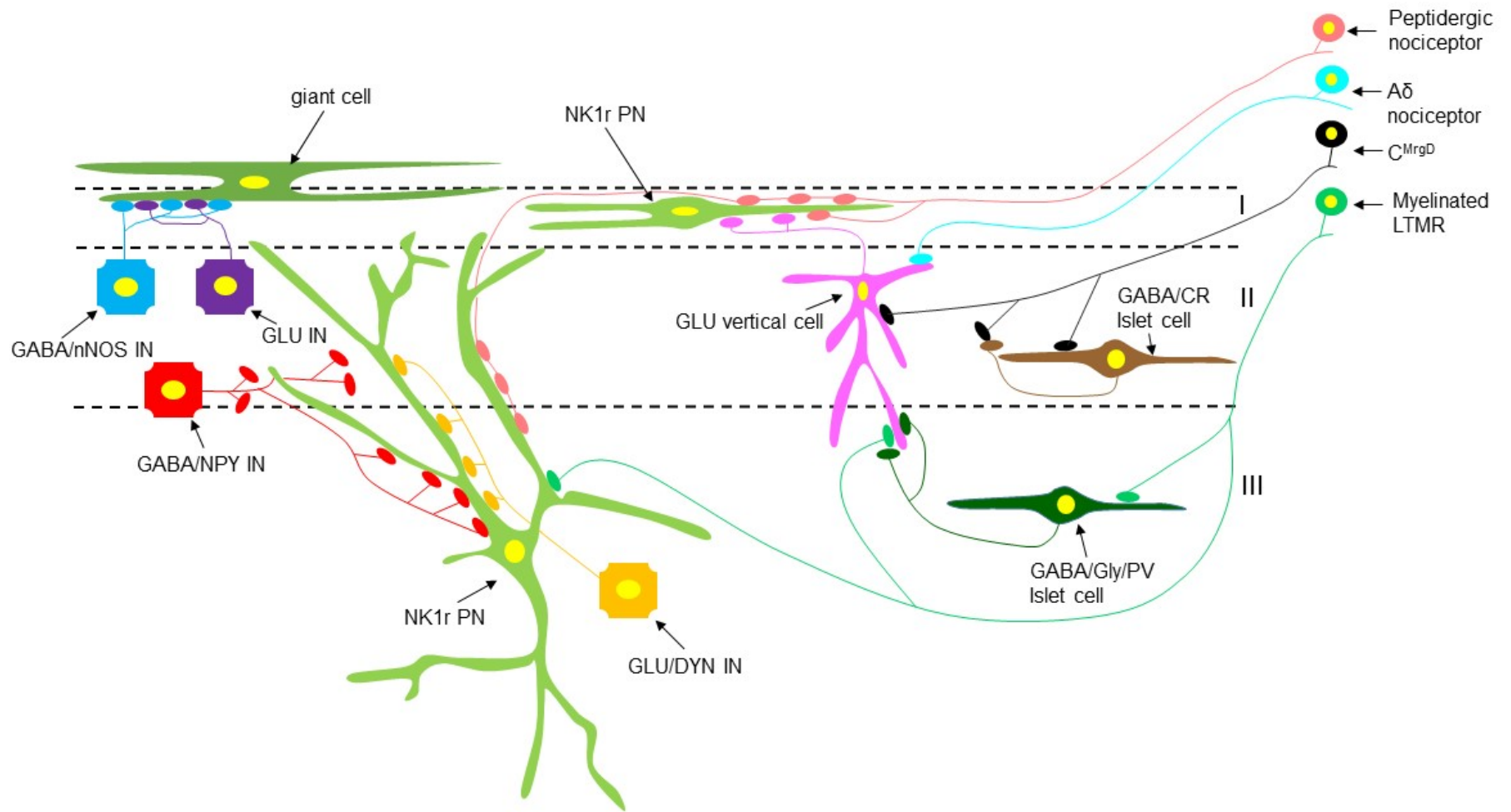


**Figure 7-1 Neuronal circuits in the dorsal horn of the spinal cord.**

A diagram showing the complexity of the identified dorsal horn synaptic circuit between primary afferents, local dorsal horn neurons and projection neurons in laminae I-III. Results from this study found that inhibitory calretinin (CR) islet cells (brown) that can be found mainly in lamina II is seen forming axoaxonic synapse with central boutons of type I glomeruli (black). The inhibitory CR cells also receive excitatory input from the same primary afferents that belonged to a group of C fibres that expressed Mas-related-G-protein coupled receptor member D (C<sup>MrgD</sup>). Modified from Todd 2010.

## 8 References

- ABRAIRA, V. E. & GINTY, D. D. 2013. The Sensory Neurons of Touch. *Neuron*, 79, 10.1016/j.neuron.2013.07.051.
- ABRAIRA, V. E., KUEHN, E. D., CHIRILA, A. M., SPRINGEL, M. W., TOLIVER, A. A., ZIMMERMAN, A. L., OREFICE, L. L., BOYLE, K. A., BAI, L., SONG, B. J., BASHISTA, K. A., O'NEILL, T. G., ZHUO, J., TSAN, C., HOYNOSKI, J., RUTLIN, M., KUS, L., NIEDERKOFER, V., WATANABE, M., DYMECKI, S. M., NELSON, S. B., HEINTZ, N., HUGHES, D. I. & GINTY, D. D. 2017. The Cellular and Synaptic Architecture of the Mechanosensory Dorsal Horn. *Cell*, 168, 295-310.e19.
- AFIFI, A. K. & BERGMAN, R. A. 1986. *Spinal Cord. Basic neuroscience: a structural and functional approach*. Baltimore: Urban & Schwarzenberg.
- AL-KHATER, K. M., KERR, R. & TODD, A. J. 2008. A quantitative study of spinothalamic neurons in laminae I, III, and IV in lumbar and cervical segments of the rat spinal cord. *The Journal of Comparative Neurology*, 511, 1-18.
- AL-KHATER, K. M. & TODD, A. J. 2009. Collateral projections of neurons in laminae I, III, and IV of rat spinal cord to thalamus, periaqueductal gray matter, and lateral parabrachial area. *J Comp Neurol*, 515, 629-46.
- AL GHAMDI, K. S., POLGÁR, E. & TODD, A. J. 2009. Soma size distinguishes projection neurons from neurokinin 1 receptor-expressing interneurons in lamina I of the rat lumbar spinal dorsal horn. *Neuroscience*, 164, 1794-1804.
- ALBUQUERQUE, C., LEE, C. J., JACKSON, A. C. & MACDERMOTT, A. B. 1999. Subpopulations of GABAergic and non-GABAergic rat dorsal horn neurons express Ca<sup>2+</sup>-permeable AMPA receptors. *European Journal of Neuroscience*, 11, 2758-2766.
- ALMARESTANI, L., WATERS, S. M., KRAUSE, J. E., BENNETT, G. J. & RIBEIRO-DA-SILVA, A. 2007. Morphological characterization of spinal cord dorsal horn lamina I neurons projecting to the parabrachial nucleus in the rat. *J Comp Neurol*, 504, 287-97.
- ANELLI, R. & HECKMAN, C. J. 2005. The calcium binding proteins calbindin, parvalbumin, and calretinin have specific patterns of expression in the gray matter of cat spinal cord. *Journal of Neurocytology*, 34, 369-385.
- ANTAL, M., FREUND, T. F. & POLGÁR, E. 1990. Calcium-binding proteins, parvalbumin- and calbindin-D 28k-immunoreactive neurons in the rat spinal cord and dorsal root ganglia: A light and electron microscopic study. *The Journal of Comparative Neurology*, 295, 467-484.
- ANTAL, M., POLGÁR, E., CHALMERS, J., MINSON, J. B., LLEWELLYN-SMITH, I., HEIZMANN, C. W. & SOMOGYI, P. 1991. Different populations of parvalbumin- and calbindin-D28k-immunoreactive neurons contain GABA and accumulate 3H-D-aspartate in the dorsal horn of the rat spinal cord. *The Journal of Comparative Neurology*, 314, 114-124.

- ASHBURN, M. A. & STAATS, P. S. 1999. Management of chronic pain. *The Lancet*, 353, 1865-1869.
- AVERILL, S., MCMAHON, S. B., CLARY, D. O., REICHARDT, L. F. & PRIESTLEY, J. V. 1995. Immunocytochemical Localization of trkA Receptors in Chemically Identified Subgroups of Adult Rat Sensory Neurons. *The European journal of neuroscience*, 7, 1484-1494.
- BAILEY, A. L. & RIBEIRO-DA-SILVA, A. 2006. Transient loss of terminals from non-peptidergic nociceptive fibers in the substantia gelatinosa of spinal cord following chronic constriction injury of the sciatic nerve. *Neuroscience*, 138, 675-690.
- BANG, J., KIM, H. Y. & LEE, H. 2016. Optogenetic and Chemogenetic Approaches for Studying Astrocytes and Gliotransmitters. *Experimental Neurobiology*, 25, 205-221.
- BANNATYNE, B. A., MAXWELL, D. J., FYFFE, R. E. W. & BROWN, A. G. 1984. FINE STRUCTURE OF PRIMARY AFFERENT AXON TERMINALS OF SLOWLY ADAPTING CUTANEOUS RECEPTORS IN THE CAT. *Quarterly Journal of Experimental Physiology*, 69, 547-557.
- BARBER, R. P., VAUGHN, J. E., SAITO, K., MCLAUGHLIN, B. J. & ROBERTS, E. 1978. GABAergic terminals are presynaptic to primary afferent terminals in the substantia gelatinosa of the rat spinal cord. *Brain Research*, 141, 35-55.
- BARDONI, R. 2013. Role of Presynaptic Glutamate Receptors in Pain Transmission at the Spinal Cord Level. *Current Neuropharmacology*, 11, 477-483.
- BASBAUM, A. I., BAUTISTA, D. M., SCHERRER, G. & JULIUS, D. 2009. Cellular and Molecular Mechanisms of Pain. *Cell*, 139, 267-284.
- BASEER, N., AL-BALOUSHI, A. S., WATANABE, M., SHEHAB, S. A. & TODD, A. J. 2014. Selective innervation of NK1 receptor-lacking lamina I spinoparabrachial neurons by presumed nonpeptidergic Adelta nociceptors in the rat. *Pain*, 155, 2291-300.
- BASEER, N., POLGÁR, E., WATANABE, M., FURUTA, T., KANEKO, T. & TODD, A. J. 2012. Projection Neurons in Lamina III of the Rat Spinal Cord Are Selectively Innervated by Local Dynorphin-Containing Excitatory Neurons. *The Journal of Neuroscience*, 32, 11854-11863.
- BELL, A. M., GUTIERREZ-MECINAS, M., POLGÁR, E. & TODD, A. J. 2016. Spinal neurons that contain gastrin-releasing peptide seldom express Fos or phosphorylate extracellular signal-regulated kinases in response to intradermal chloroquine. *Molecular Pain*, 12, 1744806916649602.
- BENNETT, D. L. H., DMIETRIEVA, N., PRIESTLEY, J. V., CLARY, D. & MCMAHON, S. B. 1996. trkA, CGRP and IB4 expression in retrogradely labelled cutaneous and visceral primary sensory neurones in the rat. *Neuroscience Letters*, 206, 33-36.

- BENNETT, D. L. H., MICHAEL, G. J., RAMACHANDRAN, N., MUNSON, J. B., AVERILL, S., YAN, Q., MCMAHON, S. B. & PRIESTLEY, J. V. 1998. A Distinct Subgroup of Small DRG Cells Express GDNF Receptor Components and GDNF Is Protective for These Neurons after Nerve Injury. *The Journal of Neuroscience*, 18, 3059-3072.
- BENNETT, G. J., NISHIKAWA, N., LU, G.-W., HOFFERT, M. J. & DUBNER, R. 1984. The morphology of dorsal column postsynaptic spinomedullary neurons in the cat. 224, 568-578.
- BENNETT, G. J., SELTZER, Z. E., LU, G.-W., NISHIKAWA, N. & DUBNER, R. 1983. The Cells of Origin of the Dorsal Column Postsynaptic Projection in the Lumbosacral Enlargements of Cats and Monkeys. *Somatosensory Research*, 1, 131-149.
- BENNETT, G. J. & XIE, Y. K. 1988. A peripheral mononeuropathy in rat that produces disorders of pain sensation like those seen in man. *Pain*, 33, 87-107.
- BERKLEY, K. J., BLOMQUIST, A., PELT, A. & FLINK, R. 1980. Differences in the collateralization of neuronal projections from the dorsal column nuclei and lateral cervical nucleus to the thalamus and tectum in the cat: An anatomical study using two different double-labeling techniques. *Brain Research*, 202, 273-290.
- BERNSTEIN, L., DEAPEN, D., CERHAN, J. R., SCHWARTZ, S. M., LIFF, J., MCGANN-MALONEY, E., PERLMAN, J. A. & FORD, L. 1999. Tamoxifen Therapy for Breast Cancer and Endometrial Cancer Risk. *JNCI: Journal of the National Cancer Institute*, 91, 1654-1662.
- BESSOU, P., BURGESS, P. R., PERL, E. R. & TAYLOR, C. B. 1971. Dynamic properties of mechanoreceptors with unmyelinated (C) fibers. *Journal of Neurophysiology*, 34, 116-131.
- BESSOU, P. & PERL, E. R. 1969. Response of cutaneous sensory units with unmyelinated fibers to noxious stimuli. *Journal of Neurophysiology*, 32, 1025-1043.
- BJUGN, R. 1993. The use of the optical disector to estimate the number of neurons, glial and endothelial cells in the spinal cord of the mouse — with a comparative note on the rat spinal cord. *Brain Research*, 627, 25-33.
- BLISS, T. V. P. & COLLINGRIDGE, G. L. 1993. A synaptic model of memory: long-term potentiation in the hippocampus. *Nature*, 361, 31.
- BOYLE, K. A., GUTIERREZ-MECINAS, M., POLGÁR, E., MOONEY, N., O'CONNOR, E., FURUTA, T., WATANABE, M. & TODD, A. J. 2017. A quantitative study of neurochemically defined populations of inhibitory interneurons in the superficial dorsal horn of the mouse spinal cord. *Neuroscience*, 363, 120-133.
- BOYLE, S., MISFELDT, A., CHANDLER, K. J., DEAL, K. K., SOUTHARD-SMITH, E. M., MORTLOCK, D. P., BALDWIN, H. S. & DE CAESTECKER, M. 2008.

Fate mapping using Cited1-CreER(T2) mice demonstrates that the cap mesenchyme contains self-renewing progenitor cells and gives rise exclusively to nephronic epithelia. *Developmental biology*, 313, 234-245.

- BROMAN, J., ANDERSON, S. & OTTERSEN, O. P. 1993. Enrichment of Glutamate-like Immunoreactivity in Primary Afferent Terminals Throughout the Spinal Cord Dorsal Horn. *European Journal of Neuroscience*, 5, 1050-1061.
- BROWN, A. G. & FYFFE, R. E. 1981. Form and function of dorsal horn neurones with axons ascending the dorsal columns in cat. *The Journal of Physiology*, 321, 31-47.
- BROWN, A. G., FYFFE, R. E., ROSE, P. K. & SNOW, P. J. 1981. Spinal cord collaterals from axons of type II slowly adapting units in the cat. *The Journal of Physiology*, 316, 469-480.
- BRUMOVSKY, P., SHI, T. S., LANDRY, M., VILLAR, M. J. & HÖKFELT, T. 2007. Neuropeptide tyrosine and pain. *Trends in Pharmacological Sciences*, 28, 93-102.
- BURGESS, P. R. & PERL, E. R. 1967. Myelinated afferent fibres responding specifically to noxious stimulation of the skin. *The Journal of Physiology*, 190, 541-562.
- BURGESS, P. R., PETIT, D. & WARREN, R. M. 1968. Receptor types in cat hairy skin supplied by myelinated fibers. *Journal of Neurophysiology*, 31, 833-848.
- BURSTEIN, R., DADO, R. J. & GIESLER, G. J., JR. 1990. The cells of origin of the spinothalamic tract of the rat: a quantitative reexamination. *Brain Res*, 511, 329-37.
- BUXTON, D. F. & GOODMAN, D. C. 1967. Motor function and the corticospinal tracts in the dog and raccoon. *The Journal of Comparative Neurology*, 129, 341-360.
- CAIN, D. M., KHASABOV, S. G. & SIMONE, D. A. 2001. Response Properties of Mechanoreceptors and Nociceptors in Mouse Glabrous Skin: An In Vivo Study. *Journal of Neurophysiology*, 85, 1561-1574.
- CALLIN, S. & BENNETT, M. I. 2008. Assessment of neuropathic pain. *Continuing Education in Anaesthesia Critical Care & Pain*, 8, 210-213.
- CAMERON, D., POLGÁR, E., GUTIERREZ-MECINAS, M., GOMEZ-LIMA, M., WATANABE, M. & TODD, A. J. 2015. The organisation of spinoparabrachial neurons in the mouse. *Pain*, 156, 2061-2071.
- CAMILLO, D., LEVELT, C. N. & HEIMEL, J. A. 2014. Lack of functional specialization of neurons in the mouse primary visual cortex that have expressed calretinin. *Frontiers in Neuroanatomy*, 8, 89.

- CAO, Y. Q., MANTYH, P. W., CARLSON, E. J., GILLESPIE, A.-M., EPSTEIN, C. J. & BASBAUM, A. I. 1998. Primary afferent tachykinins are required to experience moderate to intense pain. *Nature*, 392, 390-394.
- CARLTON, S. M. & HAYES, E. S. 1990. Light microscopic and ultrastructural analysis of GABA-immunoreactive profiles in the monkey spinal cord. *The Journal of Comparative Neurology*, 300, 162-182.
- CASTRO-LOPES, J., TAVARES, I. & COIMBRA, A. 1993. GABA decreases in the spinal cord dorsal horn after peripheral neurectomy. *Brain Research*, 620, 287-291.
- CATERINA, M. J. & JULIUS, D. 2001. The Vanilloid Receptor: A Molecular Gateway to the Pain Pathway. *Annual Review of Neuroscience*, 24, 487-517.
- CATERINA, M. J., LEFFLER, A., MALMBERG, A. B., MARTIN, W. J., TRAFTON, J., PETERSEN-ZEITZ, K. R., KOLTZENBURG, M., BASBAUM, A. I. & JULIUS, D. 2000. Impaired Nociception and Pain Sensation in Mice Lacking the Capsaicin Receptor. *Science*, 288, 306-313.
- CATERINA, M. J., SCHUMACHER, M. A., TOMINAGA, M., ROSEN, T. A., LEVINE, J. D. & JULIUS, D. 1997. The capsaicin receptor: a heat-activated ion channel in the pain pathway. *Nature*, 389, 816.
- CAVANAUGH, D. J., CHESLER, A. T., BRÁZ, J. M., SHAH, N. M., JULIUS, D. & BASBAUM, A. I. 2011. Restriction of Transient Receptor Potential Vanilloid-1 to the Peptidergic Subset of Primary Afferent Neurons Follows Its Developmental Downregulation in Nonpeptidergic Neurons. *The Journal of Neuroscience*, 31, 10119-10127.
- CAVANAUGH, D. J., LEE, H., LO, L., SHIELDS, S. D., ZYLKA, M. J., BASBAUM, A. I. & ANDERSON, D. J. 2009. Distinct subsets of unmyelinated primary sensory fibers mediate behavioral responses to noxious thermal and mechanical stimuli. *Proceedings of the National Academy of Sciences*, 106, 9075-9080.
- CHEN, Y., BALASUBRAMANYAN, S., LAI, A. Y., TODD, K. G. & SMITH, P. A. 2009. Effects of Sciatic Nerve Axotomy on Excitatory Synaptic Transmission in Rat Substantia Gelatinosa. 102, 3203-3215.
- CHENG, L., ARATA, A., MIZUGUCHI, R., QIAN, Y., KARUNARATNE, A., GRAY, P. A., ARATA, S., SHIRASAWA, S., BOUCHARD, M., LUO, P., CHEN, C.-L., BUSSLINGER, M., GOULDING, M., ONIMARU, H. & MA, Q. 2004. Tlx3 and Tlx1 are post-mitotic selector genes determining glutamatergic over GABAergic cell fates. *Nat Neurosci*, 7, 510-517.
- CHENG, X.-L., WANG, P., SUN, B., LIU, S.-B., GAO, Y.-F., HE, X.-Z. & YU, C.-Y. 2015. The longitudinal epineural incision and complete nerve transection method for modeling sciatic nerve injury. *Neural Regeneration Research*, 10, 1663-1668.

- CHÉRY, N. & DE KONINCK, Y. 1999. Junctional versus Extrajunctional Glycine and GABA<sub>A</sub> Receptor-Mediated IPSCs in Identified Lamina I Neurons of the Adult Rat Spinal Cord. *The Journal of Neuroscience*, 19, 7342-7355.
- CLAPHAM, D. E. 2003. TRP channels as cellular sensors. *Nature*, 426, 517.
- CODERRE, T. J., KATZ, J., VACCARINO, A. L. & MELZACK, R. 1993. Contribution of central neuroplasticity to pathological pain: review of clinical and experimental evidence. *PAIN*, 52, 259-285.
- COIMBRA, A., SODRÉ-BORGES, B. P. & MAGALHÃES, M. M. 1974. The substantia gelatinosa Rolandi of the rat. Fine structure, cytochemistry (acid phosphatase) and changes after dorsal root section. *Journal of Neurocytology*, 3, 199-217.
- COULL, J. A. M., BEGGS, S., BOUDREAU, D., BOIVIN, D., TSUDA, M., INOUE, K., GRAVEL, C., SALTER, M. W. & DE KONINCK, Y. 2005. BDNF from microglia causes the shift in neuronal anion gradient underlying neuropathic pain. *Nature*, 438, 1017.
- COULL, J. A. M., BOUDREAU, D., BACHAND, K., PRESCOTT, S. A., NAULT, F., SÍK, A., KONINCK, P. D. & KONINCK, Y. D. 2003. Trans-synaptic shift in anion gradient in spinal lamina I neurons as a mechanism of neuropathic pain. *Nature*, 424, 938.
- CUELLO, A. C., JESSELL, T. M., KANAZAWA, I. & IVERSEN, L. L. 1977. Substance P: localization in synaptic vesicles in rat central nervous system. *Journal of Neurochemistry*, 29, 747-751.
- DANIELIAN, P. S., MUCCINO, D., ROWITCH, D. H., MICHAEL, S. K. & MCMAHON, A. P. 1998. Modification of gene activity in mouse embryos in utero by a tamoxifen-inducible form of Cre recombinase. *Current Biology*, 8, 1323-1326.
- DE BIASI, S. & RUSTIONI, A. 1988. Glutamate and substance P coexist in primary afferent terminals in the superficial laminae of spinal cord. *Proceedings of the National Academy of Sciences of the United States of America*, 85, 7820-7824.
- DE FELIPE, C., HERRERO, J. F., O'BRIEN, J. A., PALMER, J. A., DOYLE, C. A., SMITH, A. J. H., LAIRD, J. M. A., BELMONTE, C., CERVERO, F. & HUNT, S. P. 1998. Altered nociception, analgesia and aggression in mice lacking the receptor for substance P. *Nature*, 392, 394-397.
- DECOSTERD, I. & WOOLF, C. J. 2000. Spared nerve injury: an animal model of persistent peripheral neuropathic pain. *Pain*, 87, 149-158.
- DHAKA, A., EARLEY, T. J., WATSON, J. & PATAPOUTIAN, A. 2008. Visualizing Cold Spots: TRPM8-Expressing Sensory Neurons and Their Projections. *The Journal of Neuroscience*, 28, 566-575.

- DHAKA, A., MURRAY, A. N., MATHUR, J., EARLEY, T. J., PETRUS, M. J. & PATAPOUTIAN, A. 2007. TRPM8 Is Required for Cold Sensation in Mice. *Neuron*, 54, 371-378.
- DJOUHRI, L. & LAWSON, S. N. 2004. A $\beta$ -fiber nociceptive primary afferent neurons: a review of incidence and properties in relation to other afferent A-fiber neurons in mammals. *Brain Research Reviews*, 46, 131-145.
- DONG, X., HAN, S.-K., ZYLKA, M. J., SIMON, M. I. & ANDERSON, D. J. 2001. A Diverse Family of GPCRs Expressed in Specific Subsets of Nociceptive Sensory Neurons. *Cell*, 106, 619-632.
- DOUGLAS, S. D. & LEEMAN, S. E. 2011. Neurokinin-1 receptor: functional significance in the immune system in reference to selected infections and inflammation. *Annals of the New York Academy of Sciences*, 1217, 83-95.
- DOYLE, C. A. & MAXWELL, D. J. 1993. Neuropeptide Y-immunoreactive terminals form axo-axonic synaptic arrangements in the substantia gelatinosa (lamina II) of the cat spinal dorsal horn. *Brain Research*, 603, 157-161.
- DRESSLER, G. R. & DOUGLASS, E. C. 1992. Pax-2 is a DNA-binding protein expressed in embryonic kidney and Wilms tumor. *Proceedings of the National Academy of Sciences of the United States of America*, 89, 1179-1183.
- DU BEAU, A., SHAKYA SHRESTHA, S., BANNATYNE, B. A., JALICY, S. M., LINNEN, S. & MAXWELL, D. J. 2012. Neurotransmitter phenotypes of descending systems in the rat lumbar spinal cord. *Neuroscience*, 227, 67-79.
- DUAN, B., CHENG, L., BOURANE, S., BRITZ, O., PADILLA, C., GARCIA-CAMPANY, L., KRASHES, M., KNOWLTON, W., VELASQUEZ, T., REN, X., ROSS, SARAH E., LOWELL, BRADFORD B., WANG, Y., GOULDING, M. & MA, Q. 2014. Identification of Spinal Circuits Transmitting and Gating Mechanical Pain. *Cell*, 159, 1417-1432.
- DUGGAN, A., HOPE, P. J. & LANG, C. W. 1991. Microinjection of neuropeptide y into the superficial dorsal horn reduces stimulus-evoked release of immunoreactive substance p in the anaesthetized cat. *Neuroscience*, 44, 733-740.
- DUSSOR, G., ZYLKA, M. J., ANDERSON, D. J. & MCCLESKEY, E. W. 2008. Cutaneous Sensory Neurons Expressing the Mrgprd Receptor Sense Extracellular ATP and Are Putative Nociceptors. *Journal of neurophysiology*, 99, 1581-1589.
- EATON, M. J., PLUNKETT, J. A., KARMALLY, S., MARTINEZ, M. A. & MONTANEZ, K. 1998. Changes in GAD- and GABA- immunoreactivity in the spinal dorsal horn after peripheral nerve injury and promotion of recovery by lumbar transplant of immortalized serotonergic precursors. *Journal of Chemical Neuroanatomy*, 16, 57-72.

- ECCLES, J. C., ECCLES, R. M. & MAGNI, F. 1961. Central inhibitory action attributable to presynaptic depolarization produced by muscle afferent volleys. *The Journal of Physiology*, 159, 147-166.
- ECCLES, J. C., KOSTYUK, P. G. & SCHMIDT, R. F. 1962a. Central pathways responsible for depolarization of primary afferent fibres. *The Journal of Physiology*, 161, 237-257.
- ECCLES, J. C., SCHMIDT, R. F. & WILLIS, W. D. 1962b. Presynaptic inhibition of the spinal monosynaptic reflex pathway. *The Journal of Physiology*, 161, 282-297.
- ELLIOTT, A. M., SMITH, B. H., PENNY, K. I., CAIRNS SMITH, W. & ALASTAIR CHAMBERS, W. 1999. The epidemiology of chronic pain in the community. *The Lancet*, 354, 1248-1252.
- FAYAZ, A., CROFT, P., LANGFORD, R. M., DONALDSON, L. J. & JONES, G. T. 2016. Prevalence of chronic pain in the UK: a systematic review and meta-analysis of population studies. *BMJ Open*, 6.
- FEIL, R., BROCARD, J., MASCREZ, B., LEMEUR, M., METZGER, D. & CHAMBON, P. 1996. Ligand-activated site-specific recombination in mice. *Proceedings of the National Academy of Sciences of the United States of America*, 93, 10887-10890.
- FEIL, S., VALTCHEVA, N. & FEIL, R. 2009. Inducible Cre Mice. In: WURST, W. & KÜHN, R. (eds.) *Gene Knockout Protocols: Second Edition*. Totowa, NJ: Humana Press.
- FREMEAU, R. T., BURMAN, J., QURESHI, T., TRAN, C. H., PROCTOR, J., JOHNSON, J., ZHANG, H., SULZER, D., COPENHAGEN, D. R., STORM-MATHISEN, J., REIMER, R. J., CHAUDHRY, F. A. & EDWARDS, R. H. 2002. The identification of vesicular glutamate transporter 3 suggests novel modes of signaling by glutamate. *Proceedings of the National Academy of Sciences*, 99, 14488-14493.
- FUKUOKA, T., TOKUNAGA, A., KONDO, E., MIKI, K., TACHIBANA, T. & NOGUCHI, K. 1998. Change in mRNAs for neuropeptides and the GABAA receptor in dorsal root ganglion neurons in a rat experimental neuropathic pain model. *Pain*, 78, 13-26.
- GANAT, Y. M., SILBEREIS, J., CAVE, C., NGU, H., ANDERSON, G. M., OHKUBO, Y., MENT, L. R. & VACCARINO, F. M. 2006. Early Postnatal Astroglial Cells Produce Multilineage Precursors and Neural Stem Cells *In Vivo*. *The Journal of Neuroscience*, 26, 8609-8621.
- GANLEY, R. P., IWAGAKI, N., DEL RIO, P., BASEER, N., DICKIE, A. C., BOYLE, K. A., POLGÁR, E., WATANABE, M., ABRAIRA, V. E., ZIMMERMAN, A., RIDDELL, J. S. & TODD, A. J. 2015. Inhibitory Interneurons That Express GFP in the PrP-GFP Mouse Spinal Cord Are Morphologically Heterogeneous, Innervated by Several Classes of Primary Afferent and Include Lamina I Projection Neurons among Their Postsynaptic Targets. *The Journal of Neuroscience*, 35, 7626-7642.

- GAO, Y.-J. & JI, R.-R. 2009. c-Fos and pERK, which is a better marker for neuronal activation and central sensitization after noxious stimulation and tissue injury? *The open pain journal*, 2, 11-17.
- GAURIAU, C. & BERNARD, J.-F. 2002. Pain Pathways and Parabrachial Circuits in the Rat. 87, 251-258.
- GAURIAU, C. & BERNARD, J. F. 2004. A comparative reappraisal of projections from the superficial laminae of the dorsal horn in the rat: the forebrain. *J Comp Neurol*, 468, 24-56.
- GERKE, M. B. & PLENDERLEITH, M. B. 2004. Ultrastructural analysis of the central terminals of primary sensory neurones labelled by transganglionic transport of *bandeiraea simplicifolia* i-isolectin B4. *Neuroscience*, 127, 165-175.
- GIBBINS, I. L., FURNESS, J. B., COSTA, M., MACINTYRE, I., HILLYARD, C. J. & GIRGIS, S. 1985. Co-localization of calcitonin gene-related peptide-like immunoreactivity with substance P in cutaneous, vascular and visceral sensory neurons of guinea pigs. *Neuroscience Letters*, 57, 125-130.
- GIESLER, G. J. & D. CLIFFER, K. 1985. Postsynaptic dorsal column pathway of the rat. II. Evidence against an important role in nociception. *Brain Research*, 326, 347-356.
- GILBERT, R. F. T., EMSON, P. C., HUNT, S. P., BENNETT, G. W., MARSDEN, C. A., SANDBERG, B. E. B., STEINBUSCH, H. W. M. & VERHOFSTAD, A. A. J. 1982. The effects of monoamine neurotoxins on peptides in the rat spinal cord. *Neuroscience*, 7, 69-87.
- GOBEL, S. 1975. Golgi studies of the substantia gelatinosa neurons in the spinal trigeminal nucleus. *The Journal of Comparative Neurology*, 162, 397-415.
- GOBEL, S. 1978. Golgi studies of the neurons in layer II of the dorsal horn of the medulla (trigeminal nucleus caudalis). *The Journal of Comparative Neurology*, 180, 395-413.
- GOBEL, S., FALLS, W. M., BENNETT, G. J., ABDELMOUMENE, M., HAYASHI, H. & HUMPHREY, E. 1980. An EM analysis of the synaptic connections of horseradish peroxidase-filled stalked cells and islet cells in the substantia gelatinosa of adult cat spinal cord. *Journal of Comparative Neurology*, 194, 781-807.
- GOLDBERG, D. S. & MCGEE, S. J. 2011. Pain as a global public health priority. *BMC Public Health*, 11, 770-770.
- GRAHAM, B. A., BRICHTA, A. M. & CALLISTER, R. J. 2007. Moving From an Averaged to Specific View of Spinal Cord Pain Processing Circuits. *Journal of Neurophysiology*, 98, 1057-1063.
- GRAY, E. G. 1962. A Morphological Basis for Pre-synaptic Inhibition? *Nature*, 193, 82.

- GRUDT, T. J. & PERL, E. R. 2002. Correlations between neuronal morphology and electrophysiological features in the rodent superficial dorsal horn. *The Journal of Physiology*, 540, 189-207.
- GUAN, Y., YASTER, M., RAJA, S. N. & TAO, Y.-X. 2007. Genetic knockout and pharmacologic inhibition of neuronal nitric oxide synthase attenuate nerve injury-induced mechanical hypersensitivity in mice. *Molecular Pain*, 3, 29-29.
- GUTIERREZ-MECINAS, M., BELL, A. M., MARIN, A., TAYLOR, R., BOYLE, K. A., FURUTA, T., WATANABE, M., POLGÁR, E. & TODD, A. J. 2017. Preprotachykinin A is expressed by a distinct population of excitatory neurons in the mouse superficial spinal dorsal horn including cells that respond to noxious and pruritic stimuli. *Pain*, 158, 440-456.
- GUTIERREZ-MECINAS, M., DAVIS, O., POLGÁR, E., SHAHZAD, M., NAVARRO-BATISTA, K., FURUTA, T., WATANABE, M., HUGHES, D. I. & TODD, A. J. 2019. Expression of Calretinin Among Different Neurochemical Classes of Interneuron in the Superficial Dorsal Horn of the Mouse Spinal Cord. *Neuroscience*, 398, 171-181.
- GUTIERREZ-MECINAS, M., FURUTA, T., WATANABE, M. & TODD, A. J. 2016a. A quantitative study of neurochemically defined excitatory interneuron populations in laminae I–III of the mouse spinal cord. *Molecular Pain*, 12, 1744806916629065.
- GUTIERREZ-MECINAS, M., KUEHN, E. D., ABRAIRA, V. E., POLGÁR, E., WATANABE, M. & TODD, A. J. 2016b. Immunostaining for Homer reveals the majority of excitatory synapses in laminae I–III of the mouse spinal dorsal horn. *Neuroscience*, 329, 171-181.
- GUTIERREZ-MECINAS, M., WATANABE, M. & TODD, A. J. 2014. Expression of gastrin-releasing peptide by excitatory interneurons in the mouse superficial dorsal horn. *Mol Pain*, 10, 79.
- GUTMAN, A. B. & GUTMAN, E. B. 1938. AN " ACID " PHOSPHATASE OCCURRING IN THE SERUM OF PATIENTS WITH METASTASIZING CARCINOMA OF THE PROSTATE GLAND. *Journal of Clinical Investigation*, 17, 473-478.
- HABIG, K., SCHÄNZER, A., SCHIRNER, W., LAUTENSCHLÄGER, G., DASSINGER, B., OLAUSSON, H., BIRKLEIN, F., GIZEWSKI, E. R. & KRÄMER, H. H. 2017. Low threshold unmyelinated mechanoafferents can modulate pain. *BMC Neurology*, 17, 184.
- HAN, Z. S., ZHANG, E. T. & CRAIG, A. D. 1998. Nociceptive and thermoreceptive lamina I neurons are anatomically distinct. *Nature Neuroscience*, 1, 218-225.
- HANTMAN, A. W., VAN DEN POL, A. N. & PERL, E. R. 2004. Morphological and Physiological Features of a Set of Spinal Substantia Gelatinosa Neurons Defined by Green Fluorescent Protein Expression. *The Journal of Neuroscience*, 24, 836-842.

- HÄRING, M., ZEISEL, A., HOCHGERNER, H., RINWA, P., JAKOBSSON, J. E. T., LÖNNERBERG, P., LA MANNO, G., SHARMA, N., BORGIUS, L., KIEHN, O., LAGERSTRÖM, M. C., LINNARSSON, S. & ERNFORS, P. 2018. Neuronal atlas of the dorsal horn defines its architecture and links sensory input to transcriptional cell types. *Nature Neuroscience*.
- HAYASHI, S. & MCMAHON, A. P. 2002. Efficient Recombination in Diverse Tissues by a Tamoxifen-Inducible Form of Cre: A Tool for Temporally Regulated Gene Activation/Inactivation in the Mouse. *Developmental Biology*, 244, 305-318.
- HEINKE, B., RUSCHEWEYH, R., FORSTHUBER, L., WUNDERBALDINGER, G. & SANDKÜHLER, J. 2004. Physiological, neurochemical and morphological properties of a subgroup of GABAergic spinal lamina II neurones identified by expression of green fluorescent protein in mice. *The Journal of Physiology*, 560, 249-266.
- HERBISON, A. E., SIMONIAN, S. X., NORRIS, P. J. & EMSON, P. C. 1996. Relationship of Neuronal Nitric Oxide Synthase Immunoreactivity to GnRH Neurons in the Ovariectomized and Intact Female Rat. *Journal of Neuroendocrinology*, 8, 73-82.
- HÖKFELT, T., ELDE, R., JOHANSSON, O., LUFT, R. & ARIMURA, A. 1975. Immunohistochemical evidence for the presence of somatostatin, a powerful inhibitory peptide, in some primary sensory neurons. *Neuroscience Letters*, 1, 231-235.
- HÖKFELT, T., LJUNGDAHL, Å., STEINBUSCH, H., VERHOFSTAD, A., NILSSON, G., BRODIN, E., PERNOW, B. & GOLDSTEIN, M. 1978. Immunohistochemical evidence of substance P-like immunoreactivity in some 5-hydroxytryptamine-containing neurons in the rat central nervous system. *Neuroscience*, 3, 517-538.
- HÖKFELT, T., ZHANG, X. & WIESENFELD-HALLIN, Z. 1994. Messenger plasticity in primary sensory neurons following axotomy and its functional implications. *Trends in Neurosciences*, 17, 22-30.
- HOLZER, P. 1991. Capsaicin: cellular targets, mechanisms of action, and selectivity for thin sensory neurons. *Pharmacological Reviews*, 43, 143-201.
- HORCH, K. W., TUCKETT, R. P. & BURGESS, P. R. 1977. A KEY TO THE CLASSIFICATION OF CUTANEOUS MECHANORECEPTORS. *Journal of Investigative Dermatology*, 69, 75-82.
- HOSSAINI, M., FRENCH, P. J. & HOLSTEGE, J. C. 2007. Distribution of glycinergic neuronal somata in the rat spinal cord. *Brain research*, 1142, 61-69.
- HOYER, D., BELL, G. I., BERELOWITZ, M., EPELBAUM, J., FENIUK, W., HUMPHREY, P. P. A., O'CARROLL, A. M., PATEL, Y. C., SCHONBRUNN, A., TAYLOR, J. E. & REISINE, T. 1995. Classification and nomenclature of somatostatin receptors. *Trends in Pharmacological Sciences*, 16, 86-88.

- HUANG, H.-Y., CHENG, J.-K., SHIH, Y.-H., CHEN, P.-H., WANG, C.-L. & TSAUR, M.-L. 2005. Expression of A-type K<sup>+</sup> channel  $\alpha$  subunits Kv4.2 and Kv4.3 in rat spinal lamina II excitatory interneurons and colocalization with pain-modulating molecules. *European Journal of Neuroscience*, 22, 1149-1157.
- HUANG, J., CHEN, J., WANG, W., WANG, W., KOSHIMIZU, Y., WEI, Y.-Y., KANEKO, T., LI, Y.-Q. & WU, S.-X. 2010. Neurochemical properties of enkephalinergic neurons in lumbar spinal dorsal horn revealed by preproenkephalin–green fluorescent protein transgenic mice. *Journal of Neurochemistry*, 113, 1555-1564.
- HUANG, J., POLGÁR, E., SOLINSKI, H. J., MISHRA, S. K., TSENG, P.-Y., IWAGAKI, N., BOYLE, K. A., DICKIE, A. C., KRIEGBAUM, M. C., WILDNER, H., ZEILHOFER, H. U., WATANABE, M., RIDDELL, J. S., TODD, A. J. & HOON, M. A. 2018. Circuit dissection of the role of somatostatin in itch and pain. *Nature Neuroscience*.
- HUANG, M., HUANG, T., XIANG, Y., XIE, Z., CHEN, Y., YAN, R., XU, J. & CHENG, L. 2008. Ptf1a, Lbx1 and Pax2 coordinate glycinergic and peptidergic transmitter phenotypes in dorsal spinal inhibitory neurons. *Developmental Biology*, 322, 394-405.
- HUGHES, D. I., BANNISTER, A. P., PAWELZIK, H. & THOMSON, A. M. 2000. Double immunofluorescence, peroxidase labelling and ultrastructural analysis of interneurons following prolonged electrophysiological recordings in vitro. *Journal of Neuroscience Methods*, 101, 107-116.
- HUGHES, D. I., MACKIE, M., NAGY, G. G., RIDDELL, J. S., MAXWELL, D. J., SZABÓ, G., ERDÉLYI, F., VERESS, G., SZÚCS, P., ANTAL, M. & TODD, A. J. 2005. P boutons in lamina IX of the rodent spinal cord express high levels of glutamic acid decarboxylase-65 and originate from cells in deep medial dorsal horn. *Proceedings of the National Academy of Sciences of the United States of America*, 102, 9038-9043.
- HUGHES, D. I., SCOTT, D. T., RIDDELL, J. S. & TODD, A. J. 2007. Upregulation of Substance P in Low-Threshold Myelinated Afferents Is Not Required for Tactile Allodynia in the Chronic Constriction Injury and Spinal Nerve Ligation Models. *The Journal of Neuroscience*, 27, 2035-2044.
- HUGHES, D. I., SCOTT, D. T., TODD, A. J. & RIDDELL, J. S. 2003. Lack of Evidence for Sprouting of A $\beta$  Afferents into the Superficial Laminas of the Spinal Cord Dorsal Horn after Nerve Section. *The Journal of Neuroscience*, 23, 9491-9499.
- HUGHES, D. I., SIKANDER, S., KINNON, C. M., BOYLE, K. A., WATANABE, M., CALLISTER, R. J. & GRAHAM, B. A. 2012. Morphological, neurochemical and electrophysiological features of parvalbumin-expressing cells: a likely source of axo-axonic inputs in the mouse spinal dorsal horn. *The Journal of Physiology*, 590, 3927-3951.
- HUH, W. J., KHURANA, S. S., GEAHLEN, J. H., KOHLI, K., WALLER, R. A. & MILLS, J. C. 2012. Tamoxifen Induces Rapid, Reversible Atrophy, and Metaplasia in Mouse Stomach. *Gastroenterology*, 142, 21-24.e7.

- HUNT, S. P., KELLY, J. S., EMSON, P. C., KIMMEL, J. R., MILLER, R. J. & WU, J. Y. 1981. An immunohistochemical study of neuronal populations containing neuropeptides or  $\gamma$ -aminobutyrate within the superficial layers of the rat dorsal horn. *Neuroscience*, 6, 1883-1898.
- HUNT, S. P. & ROSSI, J. 1985. Peptide- and non-peptide-containing unmyelinated primary afferents: the parallel processing of nociceptive information. *Philosophical Transactions of the Royal Society of London. B, Biological Sciences*, 308, 283-289.
- HWANG, J. H. & YAKSH, T. L. 1997. The effect of spinal GABA receptor agonists on tactile allodynia in a surgically-induced neuropathic pain model in the rat. *Pain*, 70, 15-22.
- HYLDEN, J. L. K., ANTON, F. & NAHIN, R. L. 1989. Spinal lamina I projection neurons in the rat: Collateral innervation of parabrachial area and thalamus. *Neuroscience*, 28, 27-37.
- IBUKI, T., HAMA, A. T., WANG, X. T., PAPPAS, G. D. & SAGEN, J. 1996. Loss of GABA-immunoreactivity in the spinal dorsal horn of rats with peripheral nerve injury and promotion of recovery by adrenal medullary grafts. *Neuroscience*, 76, 845-858.
- IKEDA, H., HEINKE, B., RUSCHEWEYH, R. & SANDKÜHLER, J. 2003. Synaptic Plasticity in Spinal Lamina I Projection Neurons That Mediate Hyperalgesia. *Science*, 299, 1237-1240.
- IKEDA, H., STARK, J., FISCHER, H., WAGNER, M., DRDLA, R., JÄGER, T. & SANDKÜHLER, J. 2006. Synaptic Amplifier of Inflammatory Pain in the Spinal Dorsal Horn. 312, 1659-1662.
- IKEDA, K., WATANABE, M., ICHIKAWA, T., KOBAYASHI, T., YANO, R. & KUMANISHI, T. 1998. Distribution of prepro-nociceptin/ orphanin FQ mRNA and its receptor mRNA in developing and adult mouse central nervous systems. *Journal of Comparative Neurology*, 399, 139-151.
- INDRA, A. K., WAROT, X., BROCARD, J., BORNERT, J. M., XIAO, J. H., CHAMBON, P. & METZGER, D. 1999. Temporally-controlled site-specific mutagenesis in the basal layer of the epidermis: comparison of the recombinase activity of the tamoxifen-inducible Cre-ER(T) and Cre-ER(T2) recombinases. *Nucleic Acids Research*, 27, 4324-4327.
- IWAGAKI, N., GANLEY, R. P., DICKIE, A. C., POLGÁR, E., HUGHES, D. I., DEL RIO, P., REVINA, Y., WATANABE, M., TODD, A. J. & RIDDELL, J. S. 2016. A combined electrophysiological and morphological study of neuropeptide Y-expressing inhibitory interneurons in the spinal dorsal horn of the mouse. *PAIN*, 157, 598-612.
- IWAGAKI, N., GARZILLO, F., POLGAR, E., RIDDELL, J. & TODD, A. 2013. Neurochemical characterisation of lamina II inhibitory interneurons that express GFP in the PrP-GFP mouse. *Molecular Pain*, 9, 56.

- JI, R.-R., BABA, H., BRENNER, G. J. & WOOLF, C. J. 1999. Nociceptive-specific activation of ERK in spinal neurons contributes to pain hypersensitivity. *Nat Neurosci*, 2, 1114-1119.
- JORDAN, V. C. 1992. The strategic use of antiestrogens to control the development and growth of breast cancer. *Cancer*, 70, 977-982.
- JU, G., HÖKFELT, T., BRODIN, E., FAHRENKRUG, J., FISCHER, J. A., FREY, P., ELDE, R. P. & BROWN, J. C. 1987. Primary sensory neurons of the rat showing calcitonin gene-related peptide immunoreactivity and their relation to substance P-, somatostatin-, galanin-, vasoactive intestinal polypeptide- and cholecystokinin-immunoreactive ganglion cells. *Cell and Tissue Research*, 247, 417-431.
- JULIUS, D. & BASBAUM, A. I. 2001. Molecular mechanisms of nociception. *Nature*, 413, 203-210.
- KAHLE, K. T., KHANNA, A., CLAPHAM, D. E. & WOOLF, C. J. 2014. Therapeutic restoration of spinal inhibition via druggable enhancement of potassium-chloride cotransporter KCC2-mediated chloride extrusion in peripheral neuropathic pain. *JAMA neurology*, 71, 640-645.
- KANEKO, T., MURASHIMA, M., LEE, T. & MIZUNO, N. 1998. Characterization of neocortical non-pyramidal neurons expressing preprotachykinins A and B: a double immunofluorescence study in the rat. *Neuroscience*, 86, 765-781.
- KANTNER, R. M., KIRBY, M. L. & GOLDSTEIN, B. D. 1985. Increase in substance P in the dorsal horn during a chemogenic nociceptive stimulus. *Brain Research*, 338, 196-199.
- KARDON, ADAM P., POLGÁR, E., HACHISUKA, J., SNYDER, LINDSEY M., CAMERON, D., SAVAGE, S., CAI, X., KARNUP, S., FAN, CHRISTOPHER R., HEMENWAY, GREGORY M., BERNARD, CARCHA S., SCHWARTZ, ERICA S., NAGASE, H., SCHWARZER, C., WATANABE, M., FURUTA, T., KANEKO, T., KOERBER, H. R., TODD, ANDREW J. & ROSS, SARAH E. 2014. Dynorphin Acts as a Neuromodulator to Inhibit Itch in the Dorsal Horn of the Spinal Cord. *Neuron*, 82, 573-586.
- KIM, S. H. & CHUNG, J. M. 1992. An experimental model for peripheral neuropathy produced by segmental spinal nerve ligation in the rat. *PAIN*, 50, 355-363.
- KIM, S. J., CHUNG, W. H., RHIM, H., EUN, S. Y., JUNG, S. J. & KIM, J. 2002. Postsynaptic action mechanism of somatostatin on the membrane excitability in spinal substantia gelatinosa neurons of juvenile rats. *Neuroscience*, 114, 1139-1148.
- KNYIHÁR-CSILLIK, E., BEZZEGH, A., BÖTI, S. & CSILLIK, B. 1986. Thiamine monophosphatase: a genuine marker for transganglionic regulation of primary sensory neurons. *Journal of Histochemistry & Cytochemistry*, 34, 363-371.

- KOBAYASHI, K., FUKUOKA, T., OBATA, K., YAMANAKA, H., DAI, Y., TOKUNAGA, A. & NOGUCHI, K. 2005. Distinct expression of TRPM8, TRPA1, and TRPV1 mRNAs in rat primary afferent neurons with a $\delta$ /c-fibers and colocalization with trk receptors. *The Journal of Comparative Neurology*, 493, 596-606.
- KOGA, K., KANEHISA, K., KOHRO, Y., SHIRATORI-HAYASHI, M., TOZAKI-SAITOH, H., INOUE, K., FURUE, H. & TSUDA, M. 2017. Chemogenetic silencing of GABAergic dorsal horn interneurons induces morphine-resistant spontaneous nocifensive behaviours. *Scientific Reports*, 7, 4739.
- KOSAKA, T., NAGATSU, I., WU, J. Y. & HAMA, K. 1986. Use of high concentrations of glutaraldehyde for immunocytochemistry of transmitter-synthesizing enzymes in the central nervous system. *Neuroscience*, 18, 975-990.
- KUNER, R. 2010. Central mechanisms of pathological pain. *Nature Medicine*, 16, 1258.
- LABORATORY, T. J. 2015. Available: <https://www.jax.org/strain/013730> [Accessed 22 January 2018].
- LAING, I., TODD, A. J., HEIZMANN, C. W. & SCHMIDT, H. H. H. W. 1994. Subpopulations of gabaergic neurons in laminae i–iii of rat spinal dorsal horn defined by coexistence with classical transmitters, peptides, nitric oxide synthase or parvalbumin. *Neuroscience*, 61, 123-132.
- LAM, H. H. D., HANLEY, D. F., TRAPP, B. D., SAITO, S., RAJA, S., DAWSON, T. M. & YAMAGUCHI, H. 1996. Induction of spinal cord neuronal nitric oxide synthase (NOS) after formalin injection in the rat hind paw. *Neuroscience Letters*, 210, 201-204.
- LAMOTTE, C. C., KAPADIA, S. E. & SHAPIRO, C. M. 1991. Central projections of the sciatic, saphenous, median, and ulnar nerves of the rat demonstrated by transganglionic transport of cholera toxin B-subunit (B-HRP) and wheat germ agglutinin-HRP (WGA-HRP). *The Journal of Comparative Neurology*, 311, 546-562.
- LARSSON, M. 2017a. Non-canonical heterogeneous cellular distribution and colocalization of CaMKII $\alpha$  and CaMKII $\beta$  in the spinal superficial dorsal horn. *Brain Structure and Function*.
- LARSSON, M. 2017b. Pax2 is persistently expressed by GABAergic neurons throughout the adult rat dorsal horn. *Neuroscience Letters*, 638, 96-101.
- LAWSON, S. N., CREPPS, B. & PERL, E. R. 2002. Calcitonin gene-related peptide immunoreactivity and afferent receptive properties of dorsal root ganglion neurones in guinea-pigs. *The Journal of Physiology*, 540, 989-1002.
- LAWSON, S. N., CREPPS, B. A. & PERL, E. R. 1997. Relationship of substance P to afferent characteristics of dorsal root ganglion neurones in guinea-pig. *The Journal of Physiology*, 505, 177-191.

- LEE, Y., TAKAMI, K., KAWAI, Y., GIRGIS, S., HILLYARD, C. J., MACINTYRE, I., EMSON, P. C. & TOHYAMA, M. 1985. Distribution of calcitonin gene-related peptide in the rat peripheral nervous system with reference to its coexistence with substance P. *Neuroscience*, 15, 1227-1237.
- LEITNER, J., WESTERHOLZ, S., HEINKE, B., FORSTHUBER, L., WUNDERBALDINGER, G., JÄGER, T., GRUBER-SCHOFFNEGGER, D., BRAUN, K. & SANDKÜHLER, J. 2013. Impaired excitatory drive to spinal GABAergic neurons of neuropathic mice. *PLoS one*, 8, e73370-e73370.
- LI, C.-L., LI, K.-C., WU, D., CHEN, Y., LUO, H., ZHAO, J.-R., WANG, S.-S., SUN, M.-M., LU, Y.-J., ZHONG, Y.-Q., HU, X.-Y., HOU, R., ZHOU, B.-B., BAO, L., XIAO, H.-S. & ZHANG, X. 2016. Somatosensory neuron types identified by high-coverage single-cell RNA-sequencing and functional heterogeneity. *Cell Research*, 26, 83-102.
- LI, L., RUTLIN, M., ABRAIRA, VICTORIA E., CASSIDY, C., KUS, L., GONG, S., JANKOWSKI, MICHAEL P., LUO, W., HEINTZ, N., KOERBER, H. R., WOODBURY, C. J. & GINTY, DAVID D. 2011. The Functional Organization of Cutaneous Low-Threshold Mechanosensory Neurons. *Cell*, 147, 1615-1627.
- LIGHT, A. R. & PERL, E. R. 1979. Spinal termination of functionally identified primary afferent neurons with slowly conducting myelinated fibers. *The Journal of Comparative Neurology*, 186, 133-150.
- LIGHT, A. R., PERL, E. R. & RÉTHELYI, M. 1982. Synaptic complexes formed by functionally defined primary afferent units with fine myelinated fibers. *The Journal of Comparative Neurology*, 207, 381-393.
- LIMA, D. & COIMBRA, A. 1986. A Golgi study of the neuronal population of the marginal zone (lamina I) of the rat spinal cord. *The Journal of Comparative Neurology*, 244, 53-71.
- LIMA, D. & COIMBRA, A. 1988. The spinothalamic system of the rat: structural types of retrogradely labelled neurons in the marginal zone (lamina I). *Neuroscience*, 27, 215-30.
- LIMA, D., MENDES-RIBEIRO, J. A. & COIMBRA, A. 1991. The spino-latero-reticular system of the rat: projections from the superficial dorsal horn and structural characterization of marginal neurons involved. *Neuroscience*, 45, 137-52.
- LIU, C. N. & CHAMBERS, W. W. 1964. An Experimental study of the cortico-spinal system in the monkey (*Macaca mulatta*). The spinal pathways and preterminal distribution of degenerating fibers following discrete lesions of the pre- and postcentral gyri and bulbar pyramid. *The Journal of Comparative Neurology*, 123, 257-283.
- LIU, H., KIM, S.-Y., FU, Y., WU, X., NG, L., SWAROOP, A. & FORREST, D. 2013. An isoform of retinoid-related orphan receptor  $\beta$  directs differentiation of retinal amacrine and horizontal interneurons. *Nature communications*, 4, 1813-1813.

- LIU, P., JENKINS, N. A. & COPELAND, N. G. 2003. A Highly Efficient Recombineering-Based Method for Generating Conditional Knockout Mutations. *Genome Research*, 13, 476-484.
- LIU, Q., VRONTOU, S., RICE, F. L., ZYLKA, M. J., DONG, X. & ANDERSON, D. J. 2007. Molecular genetic visualization of a rare subset of unmyelinated sensory neurons that may detect gentle touch. *Nature Neuroscience*, 10, 946.
- LIU, Y., SUCKALE, J., MASJKUR, J., MAGRO, M. G., STEFFEN, A., ANASTASSIADIS, K. & SOLIMENA, M. 2010. Tamoxifen-Independent Recombination in the RIP-CreER Mouse. *PLoS ONE*, 5, e13533.
- LIZEN, B., CLAUS, M., JEANNOTTE, L., RIJLI, F. M. & GOFFLOT, F. 2015. Perinatal induction of Cre recombination with tamoxifen. *Transgenic Research*, 24, 1065-1077.
- LLEWELLYN-SMITH, I. J. & MINSON, J. B. 1992. Complete penetration of antibodies into vibratome sections after glutaraldehyde fixation and ethanol treatment: light and electron microscopy for neuropeptides. *Journal of Histochemistry & Cytochemistry*, 40, 1741-1749.
- LÖKEN, L. S., DUFF, E. P. & TRACEY, I. 2017. Low-threshold mechanoreceptors play a frequency-dependent dual role in subjective ratings of mechanical allodynia. *Journal of Neurophysiology*, 118, 3360-3369.
- LÖKEN, L. S., WESSBERG, J., MORRISON, I., MCGLONE, F. & OLAUSSON, H. 2009. Coding of pleasant touch by unmyelinated afferents in humans. *Nature Neuroscience*, 12, 547.
- LORENZO, L. E., RAMIEN, M., LOUIS, M. S., KONINCK, Y. D. & RIBEIRO-DA-SILVA, A. 2008. Postnatal changes in the Rexed lamination and markers of nociceptive afferents in the superficial dorsal horn of the rat. *Journal of Comparative Neurology*, 508, 592-604.
- LU, V. B., BIGGS, J. E., STEBBING, M. J., BALASUBRAMANYAN, S., TODD, K. G., LAI, A. Y., COLMERS, W. F., DAWBARN, D., BALLANYI, K. & SMITH, P. A. 2009. Brain-derived neurotrophic factor drives the changes in excitatory synaptic transmission in the rat superficial dorsal horn that follow sciatic nerve injury. *The Journal of physiology*, 587, 1013-1032.
- LU, Y., DONG, H., GAO, Y., GONG, Y., REN, Y., GU, N., ZHOU, S., XIA, N., SUN, Y.-Y., JI, R.-R. & XIONG, L. 2013. A feed-forward spinal cord glycinergic neural circuit gates mechanical allodynia. *The Journal of Clinical Investigation*, 123, 4050-4062.
- LU, Y. & PERL, E. R. 2003. A Specific Inhibitory Pathway between Substantia Gelatinosa Neurons Receiving Direct C-Fiber Input. *The Journal of Neuroscience*, 23, 8752-8758.
- LU, Y. & PERL, E. R. 2005. Modular Organization of Excitatory Circuits between Neurons of the Spinal Superficial Dorsal Horn (Laminae I and II). *The Journal of Neuroscience*, 25, 3900-3907.

- LUO, C., KUMAMOTO, E., FURUE, H., CHEN, J. & YOSHIMURA, M. 2002. Nociceptin inhibits excitatory but not inhibitory transmission to substantia gelatinosa neurones of adult rat spinal cord. *Neuroscience*, 109, 349-358.
- LUO, C., KUNER, T. & KUNER, R. 2014. Synaptic plasticity in pathological pain. *Trends in Neurosciences*, 37, 343-355.
- MACKIE, M., HUGHES, D. I., MAXWELL, D. J., TILLAKARATNE, N. J. K. & TODD, A. J. 2003. Distribution and colocalisation of glutamate decarboxylase isoforms in the rat spinal cord. *Neuroscience*, 119, 461-472.
- MADISEN, L., MAO, T., KOCH, H., ZHUO, J.-M., BERENYI, A., FUJISAWA, S., HSU, Y.-W. A., GARCIA, A. J., GU, X., ZANELLA, S., KIDNEY, J., GU, H., MAO, Y., HOOKS, B. M., BOYDEN, E. S., BUZSÁKI, G., RAMIREZ, J. M., JONES, A. R., SVOBODA, K., HAN, X., TURNER, E. E. & ZENG, H. 2012. A toolbox of Cre-dependent optogenetic transgenic mice for light-induced activation and silencing. *Nature neuroscience*, 15, 793-802.
- MADISEN, L., ZWINGMAN, T. A., SUNKIN, S. M., OH, S. W., ZARIWALA, H. A., GU, H., NG, L. L., PALMITER, R. D., HAWRYLYCZ, M. J., JONES, A. R., LEIN, E. S. & ZENG, H. 2010. A robust and high-throughput Cre reporting and characterization system for the whole mouse brain. *Nature neuroscience*, 13, 133-140.
- MAGGI, C. A. 1995. The mammalian tachykinin receptors. *General Pharmacology: The Vascular System*, 26, 911-944.
- MAGOUL, R., ONTENIENTE, B., GEFFARD, M. & CALAS, A. 1987. Anatomical distribution and ultrastructural organization of the gabaergic system in the rat spinal cord. An immunocytochemical study using anti-GABA antibodies. *Neuroscience*, 20, 1001-1009.
- MAKWANA, M., WERNER, A., ACOSTA-SALTOS, A., GONITEL, R., PARARAJASINGAM, A., RUFF, C., RUMAJOGEE, P., CUTHILL, D., GALIANO, M., BOHATSCHKEK, M., WALLACE, A. S., ANDERSON, P. N., MAYER, U., BEHRENS, A. & RAIVICH, G. 2010. Peripheral facial nerve axotomy in mice causes sprouting of motor axons into perineuronal central white matter: time course and molecular characterization. *J Comp Neurol*, 518, 699-721.
- MALAN, T. P., MATA, H. P. & PORRECA, F. 2002. Spinal GABAA and GABAB Receptor Pharmacology in a Rat Model of Neuropathic Pain. *Anesthesiology*, 96, 1161-1167.
- MALMBERG, A. B., CHEN, C., TONEGAWA, S. & BASBAUM, A. I. 1997. Preserved Acute Pain and Reduced Neuropathic Pain in Mice Lacking PKC $\gamma$ . *Science*, 278, 279-283.
- MANTYH, P. W., ROGERS, S. D., HONORE, P., ALLEN, B. J., GHILARDI, J. R., LI, J., DAUGHTERS, R. S., LAPPI, D. A., WILEY, R. G. & SIMONE, D. A. 1997. Inhibition of Hyperalgesia by Ablation of Lamina I Spinal Neurons Expressing the Substance P Receptor. *Science*, 278, 275-279.

- MARCHAND, J. E., WURM, W. H., KATO, T. & KREAM, R. M. 1994. Altered tachykinin expression by dorsal root ganglion neurons in a rat model of neuropathic pain. *Pain*, 58, 219-231.
- MARICICH, S. M. & HERRUP, K. 1999. Pax-2 expression defines a subset of GABAergic interneurons and their precursors in the developing murine cerebellum. *Journal of Neurobiology*, 41, 281-294.
- MARSHALL, G. E., SHEHAB, S. A. S., SPIKE, R. C. & TODD, A. J. 1996. Neurokinin-1 receptors on lumbar spinothalamic neurons in the rat. *Neuroscience*, 72, 255-263.
- MARTIN, R. J., APKARIAN, A. V. & C. J. HODGE, J. 1990. Ventrolateral and dorsolateral ascending spinal cord pathway influence on thalamic nociception in cat. 64, 1400-1412.
- MASUDA, T., OZONO, Y., MIKURIYA, S., KOHRO, Y., TOZAKI-SAITOH, H., IWATSUKI, K., UNEYAMA, H., ICHIKAWA, R., SALTER, M. W., TSUDA, M. & INOUE, K. 2016. Dorsal horn neurons release extracellular ATP in a VNUT-dependent manner that underlies neuropathic pain. *Nature Communications*, 7, 12529.
- MAXWELL, D. J. & BANNATYNE, B. A. 1983. Ultrastructure of muscle spindle afferent terminations in lamina VI of the cat spinal cord. *Brain Research*, 288, 297-301.
- MAXWELL, D. J., BANNATYNE, B. A., BROWN, A. G. & FYFFE, R. E. W. 1984. FINE STRUCTURE OF PRIMARY AFFERENT AXON TERMINALS PROJECTING FROM RAPIDLY ADAPTING MECHANORECEPTORS OF THE TOE AND FOOT PADS OF THE CAT. *Quarterly Journal of Experimental Physiology*, 69, 381-392.
- MAXWELL, D. J., BANNATYNE, B. A., FYFFE, R. E. W. & BROWN, A. G. 1982. Ultrastructure of hair follicle afferent fibre terminations in the spinal cord of the cat. *Journal of Neurocytology*, 11, 571-582.
- MAXWELL, D. J., BELLE, M. D., CHEUNSUANG, O., STEWART, A. & MORRIS, R. 2007. Morphology of inhibitory and excitatory interneurons in superficial laminae of the rat dorsal horn. *J Physiol*, 584, 521-33.
- MAXWELL, D. J., CHRISTIE, W. M., SHORT, A. D., STORM-MATHISEN, J. & OTTERSEN, O. P. 1990. Central boutons of glomeruli in the spinal cord of the cat are enriched with l-glutamate-like immunoreactivity. *Neuroscience*, 36, 83-104.
- MAXWELL, D. J. & NOBLE, R. 1987. Relationships between hair-follicle afferent terminations and glutamic acid decarboxylase-containing boutons in the cat's spinal cord. *Brain Research*, 408, 308-312.
- MCCOY, E. S., TAYLOR-BLAKE, B., STREET, S. E., PRIBISKO, A. L., ZHENG, J. & ZYLKA, M. J. 2013. Peptidergic CGRP $\alpha$  primary sensory neurons encode heat and itch and tonically suppress sensitivity to cold. *Neuron*, 78, 138-151.

- MCKEMY, D. D., NEUHAUSSER, W. M. & JULIUS, D. 2002. Identification of a cold receptor reveals a general role for TRP channels in thermosensation. *Nature*, 416, 52.
- MCLAUGHLIN, B. J., BARBER, R., SAITO, K., ROBERTS, E. & WU, J. Y. 1975. Immunocytochemical localization of glutamate decarboxylase in rat spinal cord. *Journal of Comparative Neurology*, 164, 305-321.
- MELNICK, I. 2008. Morphophysiological properties of islet cells in substantia gelatinosa of the rat spinal cord. *Neuroscience Letters*, 446, 65-69.
- MELZACK, R. & WALL, P. D. 1965. Pain Mechanisms: A New Theory. *Science*, 150, 971-979.
- MEUNIER, J.-C., MOLLEREAU, C., TOLL, L., SUAUDEAU, C., MOISAND, C., ALVINERIE, P., BUTOUR, J.-L., GUILLEMOT, J.-C., FERRARA, P., MONSARRAT, B., MAZARGUIL, H., VASSART, G., PARMENTIER, M. & COSTENTIN, J. 1995. Isolation and structure of the endogenous agonist of opioid receptor-like ORL1 receptor. *Nature*, 377, 532-535.
- MICHAEL, S. F., DANIEL, R., SEUNG BAEK, H., JIANYUAN, Z., YOUNG-JIN, S. & WENQIN, L. 2012. The Majority of Dorsal Spinal Cord Gastrin Releasing Peptide is Synthesized Locally Whereas Neuromedin B is Highly Expressed in Pain- and Itch-Sensing Somatosensory Neurons. *Molecular Pain*, 8, 1744-8069-8-52.
- MINKE, B. 1977. *Drosophila* mutant with a transducer defect. *Biophys Struct Mech* 3:59-64.
- MOLANDER, C., XU, Q., RIVERO-MELIAN, C. & GRANT, G. 1989. Cytoarchitectonic organization of the spinal cord in the rat: II. The cervical and upper thoracic cord. *The Journal of Comparative Neurology*, 289, 375-385.
- MONTELL, C., BIRNBAUMER, L., FLOCKERZI, V., BINDELS, R. J., BRUFORD, E. A., CATERINA, M. J., CLAPHAM, D. E., HARTENECK, C., HELLER, S., JULIUS, D., KOJIMA, I., MORI, Y., PENNER, R., PRAWITT, D., SCHARENBERG, A. M., SCHULTZ, G., SHIMIZU, N. & ZHU, M. X. 2002. A Unified Nomenclature for the Superfamily of TRP Cation Channels. *Molecular Cell*, 9, 229-231.
- MOORE, K. A., KOHNO, T., KARCHEWSKI, L. A., SCHOLZ, J., BABA, H. & WOOLF, C. J. 2002. Partial peripheral nerve injury promotes a selective loss of GABAergic inhibition in the superficial dorsal horn of the spinal cord. *J Neurosci*, 22, 6724-31.
- MORAN, M. M., XU, H. & CLAPHAM, D. E. 2004. TRP ion channels in the nervous system. *Current Opinion in Neurobiology*, 14, 362-369.
- MULLEN, R. J., BUCK, C. R. & SMITH, A. M. 1992. NeuN, a neuronal specific nuclear protein in vertebrates. *Development*, 116, 201-211.

- NAGY, A. 2000. Cre recombinase: The universal reagent for genome tailoring. *genesis*, 26, 99-109.
- NAKAMURA, E., NGUYEN, M. T. & MACKEM, S. 2006. Kinetics of tamoxifen-regulated Cre activity in mice using a cartilage-specific CreERT to assay temporal activity windows along the proximodistal limb skeleton. *Developmental Dynamics*, 235, 2603-2612.
- NAKAMURA, M., SATO, K., FUKAYA, M., ARAISHI, K., AIBA, A., KANO, M. & WATANABE, M. 2004. Signaling complex formation of phospholipase C $\beta$ 4 with metabotropic glutamate receptor type 1 $\alpha$  and 1,4,5-trisphosphate receptor at the perisynapse and endoplasmic reticulum in the mouse brain. *European Journal of Neuroscience*, 20, 2929-2944.
- NEAL, C. R., MANSOUR, A., REINSCHIED, R., NOTHACKER, H. P., CIVELLI, O. & WATSON, S. J. 1999. Localization of orphanin FQ (nociceptin) peptide and messenger RNA in the central nervous system of the rat. *Journal of Comparative Neurology*, 406, 503-547.
- NEUMANN, S., DOUBELL, T. P., LESLIE, T. & WOOLF, C. J. 1996. Inflammatory pain hypersensitivity mediated by phenotypic switch in myelinated primary sensory neurons. *Nature*, 384, 360.
- NICHOLS, M. L., ALLEN, B. J., ROGERS, S. D., GHILARDI, J. R., HONORE, P., LUGER, N. M., FINKE, M. P., LI, J., LAPPI, D. A., SIMONE, D. A. & MANTYH, P. W. 1999. Transmission of Chronic Nociception by Spinal Neurons Expressing the Substance P Receptor. *Science*, 286, 1558-1561.
- NOGUCHI, K., DUBNER, R., DE LEON, M., SENBA, E. & RUDA, M. A. 1994. Axotomy induces preprotachykinin gene expression in a subpopulation of dorsal root ganglion neurons. *Journal of Neuroscience Research*, 37, 596-603.
- NOGUCHI, K., KAWAI, Y., FUKUOKA, T., SENBA, E. & MIKI, K. 1995. Substance P induced by peripheral nerve injury in primary afferent sensory neurons and its effect on dorsal column nucleus neurons. *The Journal of Neuroscience*, 15, 7633-7643.
- NOGUCHI, K., SENBA, E., MORITA, Y., SATO, M. & TOHYAMA, M. 1990. Co-expression of alpha-CGRP and beta-CGRP mRNAs in the rat dorsal root ganglion cells. *Neuroscience letters*, 108, 1-5.
- OGAWA, T., KANAZAWA, I. & KIMURA, S. 1985. Regional distribution of substance P, neurokinin  $\alpha$  and neurokinin  $\beta$  in rat spinal cord, nerve roots and dorsal root ganglia, and the effects of dorsal root section or spinal transection. *Brain Research*, 359, 152-157.
- OLAUSSON, H., LAMARRE, Y., BACKLUND, H., MORIN, C., WALLIN, B. G., STARCK, G., EKHOLM, S., STRIGO, I., WORSLEY, K., VALLBO, Å. B. & BUSHNELL, M. C. 2002. Unmyelinated tactile afferents signal touch and project to insular cortex. *Nature Neuroscience*, 5, 900.

- ORBAN, P. C., CHUI, D. & MARTH, J. D. 1992. Tissue- and site-specific DNA recombination in transgenic mice. *Proceedings of the National Academy of Sciences of the United States of America*, 89, 6861-6865.
- OSTROWSKI, W. S. & KUCIEL, R. 1994. Human prostatic acid phosphatase: Selected properties and practical applications. *Clinica Chimica Acta*, 226, 121-129.
- PARK, E. J., SUN, X., NICHOL, P., SAIJOH, Y., MARTIN, J. F. & MOON, A. M. 2008. System for tamoxifen-inducible expression of cre-recombinase from the Foxa2 locus in mice. *Developmental Dynamics*, 237, 447-453.
- PEIER, A. M., MOQRICH, A., HERGARDEN, A. C., REEVE, A. J., ANDERSSON, D. A., STORY, G. M., EARLEY, T. J., DRAGONI, I., MCINTYRE, P., BEVAN, S. & PATAPOUTIAN, A. 2002. A TRP Channel that Senses Cold Stimuli and Menthol. *Cell*, 108, 705-715.
- PEIRS, C., WILLIAMS, S.-PAUL G., ZHAO, X., WALSH, CLAIRE E., GEDEON, JEREMY Y., CAGLE, NATALIE E., GOLDRING, ADAM C., HIOKI, H., LIU, Z., MARELL, PAULINA S. & SEAL, REBECCA P. 2015. Dorsal Horn Circuits for Persistent Mechanical Pain. *Neuron*, 87, 797-812.
- PERL, E. R. 1968. Myelinated afferent fibres innervating the primate skin and their response to noxious stimuli. *The Journal of Physiology*, 197, 593-615.
- PERL, E. R. 1996. Chapter 2. Cutaneous polymodal receptors: characteristics and plasticity. In: KUMAZAWA, T., KRUGER, L. & MIZUMURA, K. (eds.) *Progress in Brain Research*. Elsevier.
- PETITJEAN, H., PAWLOWSKI, S. A., FRAINE, S. L., SHARIF, B., HAMAD, D., FATIMA, T., BERG, J., BROWN, C. M., JAN, L.-Y., RIBEIRO-DA-SILVA, A., BRAZ, J. M., BASBAUM, A. I. & SHARIF-NAEINI, R. 2015. Dorsal Horn Parvalbumin Neurons Are Gate-Keepers of Touch-Evoked Pain after Nerve Injury. *Cell Reports*, 13, 1246-1257.
- PHILLIPS, C. J. 2003. [Pain management: health economics and quality of life considerations]. *Drugs*, 63 Spec No 2, 47-50.
- PITULESCU, M. E., SCHMIDT, I., BENEDITO, R. & ADAMS, R. H. 2010. Inducible gene targeting in the neonatal vasculature and analysis of retinal angiogenesis in mice. *Nature Protocols*, 5, 1518.
- PLENDERLEITH, M. B., HALLER, C. J. & SNOW, P. J. 1990. Peptide coexistence in axon terminals within the superficial dorsal horn of the rat spinal cord. *Synapse*, 6, 344-350.
- POLGÁR, E., AL-KHATER, K. M., SHEHAB, S., WATANABE, M. & TODD, A. J. 2008. Large Projection Neurons in Lamina I of the Rat Spinal Cord That Lack the Neurokinin 1 Receptor Are Densely Innervated by VGLUT2-Containing Axons and Possess GluR4-Containing AMPA Receptors. *The Journal of Neuroscience*, 28, 13150-13160.

- POLGÁR, E., CAMPBELL, A. D., MACINTYRE, L. M., WATANABE, M. & TODD, A. J. 2007. Phosphorylation of ERK in neurokinin 1 receptor-expressing neurons in laminae III and IV of the rat spinal dorsal horn following noxious stimulation. *Molecular Pain*, 3, 4-4.
- POLGÁR, E., DURRIEUX, C., HUGHES, D. I. & TODD, A. J. 2013a. A Quantitative Study of Inhibitory Interneurons in Laminae I-III of the Mouse Spinal Dorsal Horn. *PLOS ONE*, 8, e78309.
- POLGAR, E., FOWLER, J. H., MCGILL, M. M. & TODD, A. J. 1999. The types of neuron which contain protein kinase C gamma in rat spinal cord. *Brain Res*, 833, 71-80.
- POLGÁR, E., FURUTA, T., KANEKO, T. & TODD, A. 2006. Characterization of neurons that express preprotachykinin B in the dorsal horn of the rat spinal cord. *Neuroscience*, 139, 687-697.
- POLGÁR, E., GRAY, S., RIDDELL, J. S. & TODD, A. J. 2004. Lack of evidence for significant neuronal loss in laminae I-III of the spinal dorsal horn of the rat in the chronic constriction injury model. *Pain*, 111, 144-150.
- POLGÁR, E., HUGHES, D. I., ARHAM, A. Z. & TODD, A. J. 2005. Loss of Neurons from Laminas I-III of the Spinal Dorsal Horn Is Not Required for Development of Tactile Allodynia in the Spared Nerve Injury Model of Neuropathic Pain. *The Journal of Neuroscience*, 25, 6658-6666.
- POLGÁR, E., HUGHES, D. I., RIDDELL, J. S., MAXWELL, D. J., PUSKÁR, Z. & TODD, A. J. 2003. Selective loss of spinal GABAergic or glycinergic neurons is not necessary for development of thermal hyperalgesia in the chronic constriction injury model of neuropathic pain. *Pain*, 104, 229-239.
- POLGÁR, E., SARDELLA, T. C. P., TIONG, S. Y. X., LOCKE, S., WATANABE, M. & TODD, A. J. 2013b. Functional differences between neurochemically defined populations of inhibitory interneurons in the rat spinal dorsal horn. *PAIN®*, 154, 2606-2615.
- POLGÁR, E., SARDELLA, T. C. P., WATANABE, M. & TODD, A. J. 2011. Quantitative study of NPY-expressing GABAergic neurons and axons in rat spinal dorsal horn. *The Journal of Comparative Neurology*, 519, 1007-1023.
- POLGÁR, E., SHEHAB, S. A. S., WATT, C. & TODD, A. J. 1999. GABAergic Neurons that Contain Neuropeptide Y Selectively Target Cells with the Neurokinin 1 Receptor in Laminae III and IV of the Rat Spinal Cord. *The Journal of Neuroscience*, 19, 2637-2646.
- POLGÁR, E. & TODD, A. J. 2008. Tactile allodynia can occur in the spared nerve injury model in the rat without selective loss of GABA or GABA(A) receptors from synapses in laminae I-II of the ipsilateral spinal dorsal horn. *Neuroscience*, 156, 193-202.
- PRESCOTT, S. A. & KONINCK, Y. D. 2002. Four cell types with distinctive membrane properties and morphologies in lamina I of the spinal dorsal horn of the adult rat. *The Journal of Physiology*, 539, 817-836.

- PRESCOTT, S. A., MA, Q. & DE KONINCK, Y. 2014. Normal and abnormal coding of somatosensory stimuli causing pain. *Nature Neuroscience*, 17, 183.
- PROUDLOCK, F., SPIKE, R. C. & TODD, A. J. 1993. Immunocytochemical study of somatostatin, neurotensin, GABA, and glycine in rat spinal dorsal horn. *Journal of Comparative Neurology*, 327, 289-297.
- PUNNAKKAL, P., VON SCHOULTZ, C., HAENRAETS, K., WILDNER, H. & ZEILHOFER, H. U. 2014. Morphological, biophysical and synaptic properties of glutamatergic neurons of the mouse spinal dorsal horn. *The Journal of Physiology*, 592, 759-776.
- PUSKÁR, Z., POLGÁR, E. & TODD, A. J. 2001. A population of large lamina I projection neurons with selective inhibitory input in rat spinal cord. *Neuroscience*, 102, 167-176.
- RAU, K. K., MCILWRATH, S. L., WANG, H., LAWSON, J. J., JANKOWSKI, M. P., ZYLKA, M. J., ANDERSON, D. J. & KOERBER, H. R. 2009. Mrgprd Enhances Excitability in Specific Populations of Cutaneous Murine Polymodal Nociceptors. *The Journal of Neuroscience*, 29, 8612-8619.
- REINERT, R. B., KANTZ, J., MISFELDT, A. A., POFFENBERGER, G., GANNON, M., BRISSOVA, M. & POWERS, A. C. 2012. Tamoxifen-Induced Cre-loxP Recombination Is Prolonged in Pancreatic Islets of Adult Mice. *PLoS ONE*, 7, e33529.
- REINSCHIED, R. K., NOTHACKER, H.-P., BOURSON, A., ARDATI, A., HENNINGSEN, R. A., BUNZOW, J. R., GRANDY, D. K., LANGEN, H., MONSMA, F. J. & CIVELLI, O. 1995. Orphanin FQ: A Neuropeptide That Activates an Opioidlike G Protein-Coupled Receptor. *Science*, 270, 792-794.
- REISINE, T. & BELL, G. I. 1995. Molecular properties of somatostatin receptors. *Neuroscience*, 67, 777-790.
- REN, K., RUDA, M. A. & JACOBOWITZ, D. M. 1993. Immunohistochemical localization of calretinin in the dorsal root ganglion and spinal cord of the rat. *Brain Research Bulletin*, 31, 13-22.
- REXED, B. 1952. The cytoarchitectonic organization of the spinal cord in the cat. *J Comp Neurol*, 96, 414-95.
- RIBEIRO-DA-SILVA, A. & COIMBRA, A. 1982. Two types of synaptic glomeruli and their distribution in laminae I-III of the rat spinal cord. *The Journal of Comparative Neurology*, 209, 176-186.
- RIBEIRO-DA-SILVA, A. & COIMBRA, A. 1984. Capsaicin causes selective damage to type I synaptic glomeruli in rat substantia gelatinosa. *Brain Research*, 290, 380-383.
- RIBEIRO-DA-SILVA, A., TAGARI, P. & CUELLO, A. C. 1989. Morphological characterization of substance P-like immunoreactive glomeruli in the

superficial dorsal horn of the rat spinal cord and trigeminal subnucleus caudalis: A quantitative study. *The Journal of Comparative Neurology*, 281, 497-515.

- RIBEIRO-DA-SILVA, A. & CLAUDIO CUELLO, A. 1990. Choline acetyltransferase-immunoreactive profiles are presynaptic to primary sensory fibers in the rat superficial dorsal horn. *Journal of Comparative Neurology*, 295, 370-384.
- RIGAUD, M., GEMES, G., BARABAS, M.-E., CHERNOFF, D. I., ABRAM, S. E., STUCKY, C. L. & HOGAN, Q. H. 2008. Species and strain differences in rodent sciatic nerve anatomy: Implications for studies of neuropathic pain. *Pain*, 136, 188-201.
- RINGKAMP, M., PENG, Y. B., WU, G., HARTKE, T. V., CAMPBELL, J. N. & MEYER, R. A. 2001. Capsaicin Responses in Heat-Sensitive and Heat-Insensitive A-Fiber Nociceptors. *The Journal of Neuroscience*, 21, 4460-4468.
- ROBINSON, S. P., LANGAN-FAHEY, S. M., JOHNSON, D. A. & JORDAN, V. C. 1991. Metabolites, pharmacodynamics, and pharmacokinetics of tamoxifen in rats and mice compared to the breast cancer patient. *Drug Metabolism and Disposition*, 19, 36-43.
- ROGERS, J. H. 1987. Calretinin: a gene for a novel calcium-binding protein expressed principally in neurons. *The Journal of Cell Biology*, 105, 1343-1353.
- ROSS, S. E., MARDINLY, A. R., MCCORD, A. E., ZURAWSKI, J., COHEN, S., JUNG, C., HU, L., MOK, S. I., SHAH, A., SAVNER, E. M., TOLIAS, C., CORFAS, R., CHEN, S., INQUIMBERT, P., XU, Y., MCINNES, R. R., RICE, F. L., CORFAS, G., MA, Q., WOOLF, C. J. & GREENBERG, M. E. 2010. Loss of Inhibitory Interneurons in the Dorsal Spinal Cord and Elevated Itch in Bhlhb5 Mutant Mice. *Neuron*, 65, 886-898.
- ROTH, B. L. 2016. DREADDs for Neuroscientists. *Neuron*, 89, 683-694.
- ROTHENEICHER, P., ROMANELLI, P., BIELER, L., PAGITSCH, S., ZAUNMAIR, P., KREUTZER, C., KÖNIG, R., MARSCHALLINGER, J., AIGNER, L. & COUILLARD-DESPRÉS, S. 2017. Tamoxifen Activation of Cre-Recombinase Has No Persisting Effects on Adult Neurogenesis or Learning and Anxiety. *Frontiers in Neuroscience*, 11.
- ROWAN, S., TODD, A. J. & SPIKE, R. C. 1993. Evidence that neuropeptide Y is present in gabaergic neurons in the superficial dorsal horn of the rat spinal cord. *Neuroscience*, 53, 537-545.
- RUSCHEWEYH, R. & SANDKÜHLER, J. 2002. Lamina-specific membrane and discharge properties of rat spinal dorsal horn neurones in vitro. *The Journal of Physiology*, 541, 231-244.
- SAKAMOTO, H., SPIKE, R. C. & TODD, A. J. 1999. Neurons in laminae III and IV of the rat spinal cord with the neurokinin-1 receptor receive few contacts

from unmyelinated primary afferents which do not contain substance P. *Neuroscience*, 94, 903-908.

- SALTER, M. W. & HENRY, J. L. 1991. Responses of functionally identified neurones in the dorsal horn of the cat spinal cord to substance P, neurokinin A and physalaemin. *Neuroscience*, 43, 601-610.
- SANDKÜHLER, J. 2009. Models and Mechanisms of Hyperalgesia and Allodynia. *Physiological Reviews*, 89, 707-758.
- SANDKÜHLER, J. & GRUBER-SCHOFFNEGGER, D. 2012. Hyperalgesia by synaptic long-term potentiation (LTP): an update. *Current opinion in pharmacology*, 12, 18-27.
- SANYAL, S. & RUSTIONI, A. 1974. Phosphatases in the substantia gelatinosa and motoneurons: a comparative histochemical study. *Brain Research*, 76, 161-166.
- SARDELLA, T., POLGAR, E., GARZILLO, F., FURUTA, T., KANEKO, T., WATANABE, M. & TODD, A. 2011a. Dynorphin is expressed primarily by GABAergic neurons that contain galanin in the rat dorsal horn. *Molecular Pain*, 7, 76.
- SARDELLA, T. C. P., POLGÁR, E., WATANABE, M. & TODD, A. J. 2011b. A quantitative study of neuronal nitric oxide synthase expression in laminae I–III of the rat spinal dorsal horn. *Neuroscience*, 192, 708-720.
- SATHYAMURTHY, A., JOHNSON, K. R., MATSON, K. J. E., DOBROTT, C. I., LI, L., RYBA, A. R., BERGMAN, T. B., KELLY, M. C., KELLEY, M. W. & LEVINE, A. J. 2018. Massively Parallel Single Nucleus Transcriptional Profiling Defines Spinal Cord Neurons and Their Activity during Behavior. *Cell Reports*, 22, 2216-2225.
- SCHOENEN, J. 1982. The dendritic organization of the human spinal cord: The dorsal horn. *Neuroscience*, 7, 2057-2087.
- SCHOENEN, J. & FAULL, R. L. M. 2004. CHAPTER 7 - Spinal Cord: Cyto- and Chemoarchitecture A2 - PAXINOS, GEORGE. In: MAI, J. K. (ed.) *The Human Nervous System (Second Edition)*. San Diego: Academic Press.
- SCHOLZ, J., BROOM, D. C., YOUN, D.-H., MILLS, C. D., KOHNO, T., SUTER, M. R., MOORE, K. A., DECOSTERD, I., COGGESHALL, R. E. & WOOLF, C. J. 2005. Blocking Caspase Activity Prevents Transsynaptic Neuronal Apoptosis and the Loss of Inhibition in Lamina II of the Dorsal Horn after Peripheral Nerve Injury. *The Journal of Neuroscience*, 25, 7317-7323.
- SCHULZ, S., SCHMIDT, H., HÄNDEL, M., SCHREFF, M. & HÖLLT, V. 1998a. Differential distribution of alternatively spliced somatostatin receptor 2 isoforms (sst2A and sst2B) in rat spinal cord. *Neuroscience Letters*, 257, 37-40.
- SCHULZ, S., SCHREFF, M., SCHMIDT, H., HÄNDEL, M., PRZEWLOCKI, R. & HÖLLT, V. 1998b. Immunocytochemical localization of somatostatin

- receptor sst2A in the rat spinal cord and dorsal root ganglia. *European Journal of Neuroscience*, 10, 3700-3708.
- SEAL, R. P., WANG, X., GUAN, Y., RAJA, S. N., WOODBURY, C. J., BASBAUM, A. I. & EDWARDS, R. H. 2009. Injury-induced mechanical hypersensitivity requires C-low threshold mechanoreceptors. *Nature*, 462, 651-655.
- SELTZER, Z. E., DUBNER, R. & SHIR, Y. 1990. A novel behavioral model of neuropathic pain disorders produced in rats by partial sciatic nerve injury. *Pain*, 43, 205-218.
- SENGUL, G. & WATSON, C. 2012. Chapter 13 - Spinal Cord. *The Mouse Nervous System*. San Diego: Academic Press.
- SHEHAB, S. A.-D. S. 2014. Fifth lumbar spinal nerve injury causes neurochemical changes in corresponding as well as adjacent spinal segments: A possible mechanism underlying neuropathic pain. *Journal of Chemical Neuroanatomy*, 55, 38-50.
- SHEHAB, S. A. S., AL-MARASHDA, K., AL-ZAHMI, A., ABDUL-KAREEM, A. & AL-SULTAN, M. A. H. 2008. Unmyelinated primary afferents from adjacent spinal nerves intermingle in the spinal dorsal horn: A possible mechanism contributing to neuropathic pain. *Brain Research*, 1208, 111-119.
- SHEHAB, S. A. S. & HUGHES, D. I. 2011. Simultaneous identification of unmyelinated and myelinated primary somatic afferents by co-injection of isolectin B4 and Cholera toxin subunit B into the sciatic nerve of the rat. *Journal of Neuroscience Methods*, 198, 213-221.
- SHI, T.-J. S., XIANG, Q., ZHANG, M.-D., BARDE, S., KAI-LARSEN, Y., FRIED, K., JOSEPHSON, A., GLÜCK, L., DEYEV, S. M., ZVYAGIN, A. V., SCHULZ, S. & HÖKFELT, T. 2014. Somatostatin and its 2A receptor in dorsal root ganglia and dorsal horn of mouse and human: expression, trafficking and possible role in pain. *Molecular Pain*, 10, 12-12.
- SHODA, T., KATO, M., HARADA, R., FUJISATO, T., OKUHIRA, K., DEMIZU, Y., INOUE, H., NAITO, M. & KURIHARA, M. 2015. Synthesis and evaluation of tamoxifen derivatives with a long alkyl side chain as selective estrogen receptor down-regulators. *Bioorganic & Medicinal Chemistry*, 23, 3091-3096.
- SIDMAN, R. L., ANGEVINE, J. & PIERCE, E. 1971. *Atlas of the Mouse Brain and Spinal Cord*, Harvard University Press, Cambridge.
- SILVERMAN, J. D. & KRUGER, L. 1988. Acid Phosphatase as a Selective Marker for a Class of Small Sensory Ganglion Cells in Several Mammals: Spinal Cord Distribution, Histochemical Properties, and Relation to Fluoride-Resistant Acid Phosphatase (FRAP) of Rodents. *Somatosensory Research*, 5, 219-246.
- SILVERMAN, J. D. & KRUGER, L. 1990. Selective neuronal glycoconjugate expression in sensory and autonomic ganglia: relation of lectin reactivity to peptide and enzyme markers. *Journal of Neurocytology*, 19, 789-801.

- SIMMONS, D. R., SPIKE, R. C. & TODD, A. J. 1995. Galanin is contained in GABAergic neurons in the rat spinal dorsal horn. *Neuroscience Letters*, 187, 119-122.
- SIVILOTTI, L. & WOOLF, C. J. 1994. The contribution of GABAA and glycine receptors to central sensitization: disinhibition and touch-evoked allodynia in the spinal cord. *J Neurophysiol*, 72, 169-79.
- SLOVITER, R. S., ALI-AKBARIAN, L., HORVATH, K. D. & MENKENS, K. A. 2001. Substance P receptor expression by inhibitory interneurons of the rat hippocampus: Enhanced detection using improved immunocytochemical methods for the preservation and colocalization of GABA and other neuronal markers. *Journal of Comparative Neurology*, 430, 283-305.
- SLUGG, R. M., MEYER, R. A. & CAMPBELL, J. N. 2000. Response of Cutaneous A- and C-Fiber Nociceptors in the Monkey to Controlled-Force Stimuli. *Journal of Neurophysiology*, 83, 2179-2191.
- SMITH, K. M., BOYLE, K. A., MADDEN, J. F., DICKINSON, S. A., JOBLING, P., CALLISTER, R. J., HUGHES, D. I. & GRAHAM, B. A. 2015. Functional heterogeneity of calretinin-expressing neurons in the mouse superficial dorsal horn: implications for spinal pain processing. *The Journal of Physiology*, 593, 4319-4339.
- SMITH, K. M., BOYLE, K. A., MUSTAPA, M., JOBLING, P., CALLISTER, R. J., HUGHES, D. I. & GRAHAM, B. A. 2016. Distinct forms of synaptic inhibition and neuromodulation regulate calretinin-positive neuron excitability in the spinal cord dorsal horn. *Neuroscience*, 326, 10-21.
- SNIDER, W. D. & MCMAHON, S. B. 1998. Tackling Pain at the Source: New Ideas about Nociceptors. *Neuron*, 20, 629-632.
- SOLORZANO, C., VILLAFUERTE, D., MEDA, K., CEVIKBAS, F., BRÁZ, J., SHARIF-NAEINI, R., JUAREZ-SALINAS, D., LLEWELLYN-SMITH, I. J., GUAN, Z. & BASBAUM, A. I. 2015. Primary Afferent and Spinal Cord Expression of Gastrin-Releasing Peptide: Message, Protein, and Antibody Concerns. *The Journal of Neuroscience*, 35, 648-657.
- SPIKE, R. C., PUSKÁR, Z., ANDREW, D. & TODD, A. J. 2003. A quantitative and morphological study of projection neurons in lamina I of the rat lumbar spinal cord. *European Journal of Neuroscience*, 18, 2433-2448.
- STORY, G. M., PEIER, A. M., REEVE, A. J., EID, S. R., MOSBACHER, J., HRICIK, T. R., EARLEY, T. J., HERGARDEN, A. C., ANDERSSON, D. A., HWANG, S. W., MCINTYRE, P., JEGLA, T., BEVAN, S. & PATAPOUTIAN, A. 2003. ANKTM1, a TRP-like Channel Expressed in Nociceptive Neurons, Is Activated by Cold Temperatures. *Cell*, 112, 819-829.
- SUGIMOTO, T., BENNETT, G. J. & KAJANDER, K. C. 1990. Transsynaptic degeneration in the superficial dorsal horn after sciatic nerve injury: effects of a chronic constriction injury, transection, and strychnine. *Pain*, 42, 205-213.

- SUN, Y.-G. & CHEN, Z.-F. 2007. A gastrin-releasing peptide receptor mediates the itch sensation in the spinal cord. *Nature*, 448, 700.
- SUN, Y.-G., ZHAO, Z.-Q., MENG, X.-L., YIN, J., LIU, X.-Y. & CHEN, Z.-F. 2009. Cellular Basis of Itch Sensation. *Science*, 325, 1531-1534.
- TAKAMORI, S. 2006. VGLUTs: 'Exciting' times for glutamatergic research? *Neuroscience Research*, 55, 343-351.
- TAKAMORI, S., RIEDEL, D. & JAHN, R. 2000. Immunoprecipitation of GABA-Specific Synaptic Vesicles Defines a Functionally Distinct Subset of Synaptic Vesicles. *The Journal of Neuroscience*, 20, 4904-4911.
- TAKANAMI, K., SAKAMOTO, H., MATSUDA, K. I., SATOH, K., TANIDA, T., YAMADA, S., INOUE, K., OTI, T., SAKAMOTO, T. & KAWATA, M. 2014. Distribution of gastrin-releasing peptide in the rat trigeminal and spinal somatosensory systems. *Journal of Comparative Neurology*, 522, 1858-1873.
- TAN, A. M., STAMBOULIAN, S., CHANG, Y. W., ZHAO, P., HAINS, A. B., WAXMAN, S. G. & HAINS, B. C. 2008. Neuropathic Pain Memory Is Maintained by Rac1-Regulated Dendritic Spine Remodeling after Spinal Cord Injury. *The Journal of Neuroscience*, 28, 13173-13183.
- TANIGUCHI, H., HE, M., WU, P., KIM, S., PAIK, R., SUGINO, K., KVITSANI, D., FU, Y., LU, J., LIN, Y., MIYOSHI, G., SHIMA, Y., FISHELL, G., NELSON, S. B. & HUANG, Z. J. 2011. A Resource of Cre Driver Lines for Genetic Targeting of GABAergic Neurons in Cerebral Cortex. *Neuron*, 71, 995-1013.
- TAO, Y.-X., GU, J. & STEPHENS, R. L. 2005. Role of spinal cord glutamate transporter during normal sensory transmission and pathological pain states. *Molecular Pain*, 1, 30-30.
- TAYLOR-BLAKE, B. & ZYLKA, M. J. 2010. Prostatic Acid Phosphatase Is Expressed in Peptidergic and Nonpeptidergic Nociceptive Neurons of Mice and Rats. *PLoS ONE*, 5, e8674.
- TAYLOR, A. M. W., PELESHOK, J. C. & RIBEIRO-DA-SILVA, A. 2009. Distribution of P2X3-immunoreactive fibers in hairy and glabrous skin of the rat. *The Journal of Comparative Neurology*, 514, 555-566.
- TIONG, S., POLGAR, E., VAN KRALINGEN, J., WATANABE, M. & TODD, A. 2011. Galanin-immunoreactivity identifies a distinct population of inhibitory interneurons in laminae I-III of the rat spinal cord. *Molecular Pain*, 7, 36.
- TODD, A., SPIKE, R., PRICE, R. & NEILSON, M. 1994. Immunocytochemical evidence that neurotensin is present in glutamatergic neurons in the superficial dorsal horn of the rat. *The Journal of Neuroscience*, 14, 774-784.
- TODD, A. J. 1990. An electron microscope study of glycine-like immunoreactivity in laminae I-III of the spinal dorsal horn of the rat. *Neuroscience*, 39, 387-394.

- TODD, A. J. 1996. GABA and Glycine in Synaptic Glomeruli of the Rat Spinal Dorsal Horn. *European Journal of Neuroscience*, 8, 2492-2498.
- TODD, A. J. 2010. Neuronal circuitry for pain processing in the dorsal horn. *Nat Rev Neurosci*, 11, 823-836.
- TODD, A. J. 2017. Identifying functional populations among the interneurons in laminae I-III of the spinal dorsal horn. *Molecular Pain*, 13, 1744806917693003.
- TODD, A. J., HUGHES, D. I., POLGAR, E., NAGY, G. G., MACKIE, M., OTTERSEN, O. P. & MAXWELL, D. J. 2003. The expression of vesicular glutamate transporters VGLUT1 and VGLUT2 in neurochemically defined axonal populations in the rat spinal cord with emphasis on the dorsal horn. *Eur J Neurosci*, 17, 13-27.
- TODD, A. J. & LEWIS, S. G. 1986. The morphology of Golgi-stained neurons in lamina II of the rat spinal cord. *Journal of Anatomy*, 149, 113-119.
- TODD, A. J., MAXWELL, D. J. & BROWN, A. G. 1991. Relationships between hair-follicle afferent axons and glycine-immunoreactive profiles in cat spinal dorsal horn. *Brain Research*, 564, 132-137.
- TODD, A. J., MCGILL, M. M. & SHEHAB, S. A. 2000. Neurokinin 1 receptor expression by neurons in laminae I, III and IV of the rat spinal dorsal horn that project to the brainstem. *Eur J Neurosci*, 12, 689-700.
- TODD, A. J. & MCKENZIE, J. 1989. GABA-immunoreactive neurons in the dorsal horn of the rat spinal cord. *Neuroscience*, 31, 799-806.
- TODD, A. J., PUSKÁR, Z., SPIKE, R. C., HUGHES, C., WATT, C. & FORREST, L. 2002. Projection Neurons in Lamina I of Rat Spinal Cord with the Neurokinin 1 Receptor Are Selectively Innervated by Substance P-Containing Afferents and Respond to Noxious Stimulation. *The Journal of Neuroscience*, 22, 4103-4113.
- TODD, A. J. & SPIKE, R. C. 1992. Co-localization of Met-enkephalin and somatostatin in the spinal cord of the rat. *Neuroscience Letters*, 145, 71-74.
- TODD, A. J. & SPIKE, R. C. 1993. The localization of classical transmitters and neuropeptides within neurons in laminae I-III of the mammalian spinal dorsal horn. *Prog Neurobiol*, 41, 609-45.
- TODD, A. J., SPIKE, R. C. & POLGÁR, E. 1998. A quantitative study of neurons which express neurokinin-1 or somatostatin sst2a receptor in rat spinal dorsal horn. *Neuroscience*, 85, 459-473.
- TODD, A. J., SPIKE, R. C., RUSSELL, G. & JOHNSTON, H. M. 1992. Immunohistochemical evidence that Met-enkephalin and GABA coexist in some neurones in rat dorsal horn. *Brain Research*, 584, 149-156.

- TODD, A. J. & SULLIVAN, A. C. 1990. Light microscope study of the coexistence of GABA-like and glycine-like immunoreactivities in the spinal cord of the rat. *The Journal of Comparative Neurology*, 296, 496-505.
- TOMINAGA, M., CATERINA, M. J., MALMBERG, A. B., ROSEN, T. A., GILBERT, H., SKINNER, K., RAUMANN, B. E., BASBAUM, A. I. & JULIUS, D. 1998. The Cloned Capsaicin Receptor Integrates Multiple Pain-Producing Stimuli. *Neuron*, 21, 531-543.
- TORSNEY, C., ANDERSON, R. L., RYCE-PAUL, K.-A. G. & MACDERMOTT, A. B. 2006. Characterization of sensory neuron subpopulations selectively expressing green fluorescent protein in phosphodiesterase 1C BAC transgenic mice. *Molecular Pain*, 2, 17-17.
- TORSNEY, C. & MACDERMOTT, A. B. 2006. Disinhibition Opens the Gate to Pathological Pain Signaling in Superficial Neurokinin 1 Receptor-Expressing Neurons in Rat Spinal Cord. *The Journal of Neuroscience*, 26, 1833-1843.
- TRANG, T., BEGGS, S., WAN, X. & SALTER, M. W. 2009. P2X4-receptor-mediated synthesis and release of brain-derived neurotrophic factor in microglia is dependent on calcium and p38-mitogen-activated protein kinase activation. *The Journal of neuroscience : the official journal of the Society for Neuroscience*, 29, 3518-3528.
- TRAUB, R. J. & MENDELL, L. M. 1988. The spinal projection of individual identified A-delta- and C-fibers. *Journal of Neurophysiology*, 59, 41-55.
- TRAUB, R. J., SEDIVEC, M. J. & MENDELL, L. M. 1986. The rostral projection of small diameter primary afferents in Lissauer's tract. *Brain Research*, 399, 185-189.
- TREEDE, R.-D., MEYER, R. A. & CAMPBELL, J. N. 1998. Myelinated Mechanically Insensitive Afferents From Monkey Hairy Skin: Heat-Response Properties. *Journal of Neurophysiology*, 80, 1082-1093.
- TREEDE, R. D., MEYER, R. A., RAJA, S. N. & CAMPBELL, J. N. 1995. Evidence for two different heat transduction mechanisms in nociceptive primary afferents innervating monkey skin. *The Journal of Physiology*, 483, 747-758.
- TSIEN, J. Z., CHEN, D. F., GERBER, D., TOM, C., MERCER, E. H., ANDERSON, D. J., MAYFORD, M., KANDEL, E. R. & TONEGAWA, S. 1996. Subregion- and Cell Type-Restricted Gene Knockout in Mouse Brain. *Cell*, 87, 1317-1326.
- USOSKIN, D., FURLAN, A., ISLAM, S., ABDO, H., LÖNNERBERG, P., LOU, D., HJERLING-LEFFLER, J., HAEGGSTRÖM, J., KHARCHENKO, O., KHARCHENKO, P. V., LINNARSSON, S. & ERNFORS, P. 2014. Unbiased classification of sensory neuron types by large-scale single-cell RNA sequencing. *Nature Neuroscience*, 18, 145.

- VAN EWIJK, W., COFFMAN, R. C. & WEISSMAN, I. L. 1980. Immunoelectron microscopy of cell surface antigens: a quantitative analysis of antibody binding after different fixation protocols. *The Histochemical Journal*, 12, 349-361.
- VRONTOU, S., WONG, A. M., RAU, K. K., KOERBER, H. R. & ANDERSON, D. J. 2013. Genetic identification of C fibres that detect massage-like stroking of hairy skin in vivo. *Nature*, 493, 669.
- WALL, P. D., DEVOR, M., INBAL, R., SCADDING, J. W., SCHONFELD, D., SELTZER, Z. & TOMKIEWICZ, M. M. 1979. Autotomy following peripheral nerve lesions: experimental anesthesia dolorosa. *Pain*, 7, 103-113.
- WANG, H., RIVERO-MELIÁN, C., ROBERTSON, B. & GRANT, G. 1994. transganglionic transport and binding of the isolectin B4 from *Griffonia simplicifolia* I in rat primary sensory neurons. *Neuroscience*, 62, 539-551.
- WANG, H. & ZYLKA, M. J. 2009. Mrgprd Expressing Polymodal Nociceptive Neurons Innervate Most Known Classes of Substantia Gelatinosa Neurons. *The Journal of Neuroscience*, 29, 13202-13209.
- WATSON, A. H. D., HUGHES, D. I. & BAZZAZ, A. A. 2002. Synaptic relationships between hair follicle afferents and neurones expressing GABA and glycine-like immunoreactivity in the spinal cord of the rat. *The Journal of Comparative Neurology*, 452, 367-380.
- WHITESIDE, G. T. & MUNGLANI, R. 2001. Cell death in the superficial dorsal horn in a model of neuropathic pain. *Journal of Neuroscience Research*, 64, 168-173.
- WIESENFELD-HALLIN, Z., HÖKFELT, T., LUNDBERG, J. M., FORSSMANN, W. G., REINECKE, M., TSCHOPP, F. A. & FISCHER, J. A. 1984. Immunoreactive calcitonin gene-related peptide and substance P coexist in sensory neurons to the spinal cord and interact in spinal behavioral responses of the rat. *Neuroscience Letters*, 52, 199-204.
- WIESENFELD-HALLIN, Z. & XU, X.-J. 1998. Galanin in Somatosensory Function a. *Annals of the New York Academy of Sciences*, 863, 383-389.
- WILDNER, H., DAS GUPTA, R., BRÖHL, D., HEPPENSTALL, P. A., ZEILHOFER, H. U. & BIRCHMEIER, C. 2013. Genome-Wide Expression Analysis of Ptf1a and Ascl1-Deficient Mice Reveals New Markers for Distinct Dorsal Horn Interneuron Populations Contributing to Nociceptive Reflex Plasticity. *The Journal of Neuroscience*, 33, 7299-7307.
- WILLIS, W. D. & COGGESHALL, R. E. 2004. *Sensory Mechanisms of The Spinal Cord* New York, Kluwer Academic.
- WILSON, C. H., GAMPER, I., PERFETTO, A., AUW, J., LITTLEWOOD, T. D. & EVAN, G. I. 2014. The kinetics of ER fusion protein activation in vivo. *Oncogene*, 33, 4877-4880.

- WOODBURY, C. J. & KOERBER, H. R. 2007. Central and peripheral anatomy of slowly adapting type I low-threshold mechanoreceptors innervating trunk skin of neonatal mice. *The Journal of Comparative Neurology*, 505, 547-561.
- WOODBURY, C. J., KULLMANN, F. A., MCILWRATH, S. L. & KOERBER, H. R. 2008. Identity of myelinated cutaneous sensory neurons projecting to nociceptive laminae following nerve injury in adult mice. *Journal of Comparative Neurology*, 508, 500-509.
- WOODBURY, C. J., RITTER, A. M. & KOERBER, H. R. 2000. On the problem of lamination in the superficial dorsal horn of mammals: A reappraisal of the substantia gelatinosa in postnatal life. *The Journal of Comparative Neurology*, 417, 88-102.
- WOODBURY, C. J., RITTER, A. M. & KOERBER, H. R. 2001. Central anatomy of individual rapidly adapting low-threshold mechanoreceptors innervating the "hairy" skin of newborn mice: Early maturation of hair follicle afferents. *The Journal of Comparative Neurology*, 436, 304-323.
- WOOLF, C. J. 1983. Evidence for a central component of post-injury pain hypersensitivity. *Nature*, 306, 686.
- WOOLF, C. J. 1987. Central terminations of cutaneous mechanoreceptive afferents in the rat lumbar spinal cord. *The Journal of Comparative Neurology*, 261, 105-119.
- WOOLF, C. J. & MANNION, R. J. 1999. Neuropathic pain: aetiology, symptoms, mechanisms, and management. *The Lancet*, 353, 1959-1964.
- WOOLF, C. J., SHORTLAND, P. & COGGESHALL, R. E. 1992. Peripheral nerve injury triggers central sprouting of myelinated afferents. *Nature*, 355, 75.
- XU, Y., LOPES, C., QIAN, Y., LIU, Y., CHENG, L., GOULDING, M., TURNER, E. E., LIMA, D. & MA, Q. 2008. Tlx1 and Tlx3 Coordinate Specification of Dorsal Horn Pain-Modulatory Peptidergic Neurons. *The Journal of Neuroscience*, 28, 4037-4046.
- YAKSH, T. L. 1989. Behavioral and autonomic correlates of the tactile evoked allodynia produced by spinal glycine inhibition: effects of modulatory receptor systems and excitatory amino acid antagonists. *Pain*, 37, 111-123.
- YAMAMOTO, T., CARR, P. A., BAIMBRIDGE, K. G. & NAGY, J. I. 1989. Parvalbumin- and calbindin D28k-immunoreactive neurons in the superficial layers of the spinal cord dorsal horn of rat. *Brain Research Bulletin*, 23, 493-508.
- YANG, X. W., MODEL, P. & HEINTZ, N. 1997. Homologous recombination based modification in *Escherichia coli* and germline transmission in transgenic mice of a bacterial artificial chromosome. *Nat Biotech*, 15, 859-865.
- YASAKA, T., KATO, G., FURUE, H., RASHID, M. H., SONOHATA, M., TAMAE, A., MURATA, Y., MASUKO, S. & YOSHIMURA, M. 2007. Cell-type-specific

excitatory and inhibitory circuits involving primary afferents in the substantia gelatinosa of the rat spinal dorsal horn in vitro. *The Journal of Physiology*, 581, 603-618.

- YASAKA, T., TIONG, S. Y. X., HUGHES, D. I., RIDDELL, J. S. & TODD, A. J. 2010. Populations of inhibitory and excitatory interneurons in lamina II of the adult rat spinal dorsal horn revealed by a combined electrophysiological and anatomical approach. *PAIN®*, 151, 475-488.
- YONG-GUANG, T., FREDRIK, W. H., GONG, J., GUNNAR, G., TOMAS, H. & XU, Z. 1999. Increased uptake and transport of cholera toxin B-subunit in dorsal root ganglion neurons after peripheral axotomy: Possible implications for sensory sprouting. *Journal of Comparative Neurology*, 404, 143-158.
- YOWTAK, J., WANG, J., KIM, H. Y., LU, Y., CHUNG, K. & CHUNG, J. M. 2013. Effect of antioxidant treatment on spinal GABA neurons in a neuropathic pain model in the mouse. *PAIN®*, 154, 2469-2476.
- ZEILHOFER, H. U. & CALÒ, G. 2003. Nociceptin/Orphanin FQ and Its Receptor—Potential Targets for Pain Therapy? *Journal of Pharmacology and Experimental Therapeutics*, 306, 423-429.
- ZEILHOFER, H. U., KEIST, R., ARABADZISZ, D., FRITSCHY, J. M., RLIKE, T., RUDOLPH, U. & MÖHLER, H. BAC transgenic mice expressing eGFP in nociceptin/orphanin FQ positive neurons. Neuroscience 2002 Orlando, FL.
- ZEILHOFER, H. U., STUDLER, B., ARABADZISZ, D., SCHWEIZER, C., AHMADI, S., LAYH, B., BÖSL, M. R. & FRITSCHY, J.-M. 2005. Glycinergic neurons expressing enhanced green fluorescent protein in bacterial artificial chromosome transgenic mice. *The Journal of Comparative Neurology*, 482, 123-141.
- ZEILHOFER, H. U., WILDNER, H. & YEVENES, G. E. 2012. Fast Synaptic Inhibition in Spinal Sensory Processing and Pain Control. *Physiological reviews*, 92, 193-235.
- ZHANG, L., JIANG, G.-Y., SONG, N.-J., HUANG, Y., CHEN, J.-Y., WANG, Q.-X. & DING, Y.-Q. 2014. Extracellular signal-regulated kinase (ERK) activation is required for itch sensation in the spinal cord. *Molecular Brain*, 7, 25-25.
- ZOTTERMAN, Y. 1939. Touch, pain and tickling: an electro-physiological investigation on cutaneous sensory nerves. *The Journal of Physiology*, 95, 1-28.
- ZYLKA, M. J., DONG, X., SOUTHWELL, A. L. & ANDERSON, D. J. 2003. Atypical expansion in mice of the sensory neuron-specific Mrg G protein-coupled receptor family. *Proceedings of the National Academy of Sciences*, 100, 10043-10048.
- ZYLKA, M. J., RICE, F. L. & ANDERSON, D. J. 2005. Topographically Distinct Epidermal Nociceptive Circuits Revealed by Axonal Tracers Targeted to Mrgprd. *Neuron*, 45, 17-25.

ZYLKA, M. J., SOWA, N. A., TAYLOR-BLAKE, B., TWOMEY, M. A., HERRALA, A., VOIKAR, V. & VIHKO, P. 2008. Prostatic Acid Phosphatase Is an Ectonucleotidase and Suppresses Pain by Generating Adenosine. *Neuron*, 60, 111-122.

## 9 Publication

SMITH, K. M., BOYLE, K. A., MUSTAPA, M., JOBLING, P., CALLISTER, R. J., HUGHES, D. I. & GRAHAM, B. A. 2016. Distinct forms of synaptic inhibition and neuromodulation regulate calretinin-positive neuron excitability in the spinal cord dorsal horn. *Neuroscience*, 326, 10-21.